Universitat Autònoma de Barcelona

Life History and Ecology of Late Miocene Hipparionins from the Circum-Mediterranean Area

Guillermo Orlandi Oliveras

PhD Thesis
Doctorate in Biodiversity

Life History and Ecology of Late Miocene Hipparionins from the Circum-Mediterranean Area

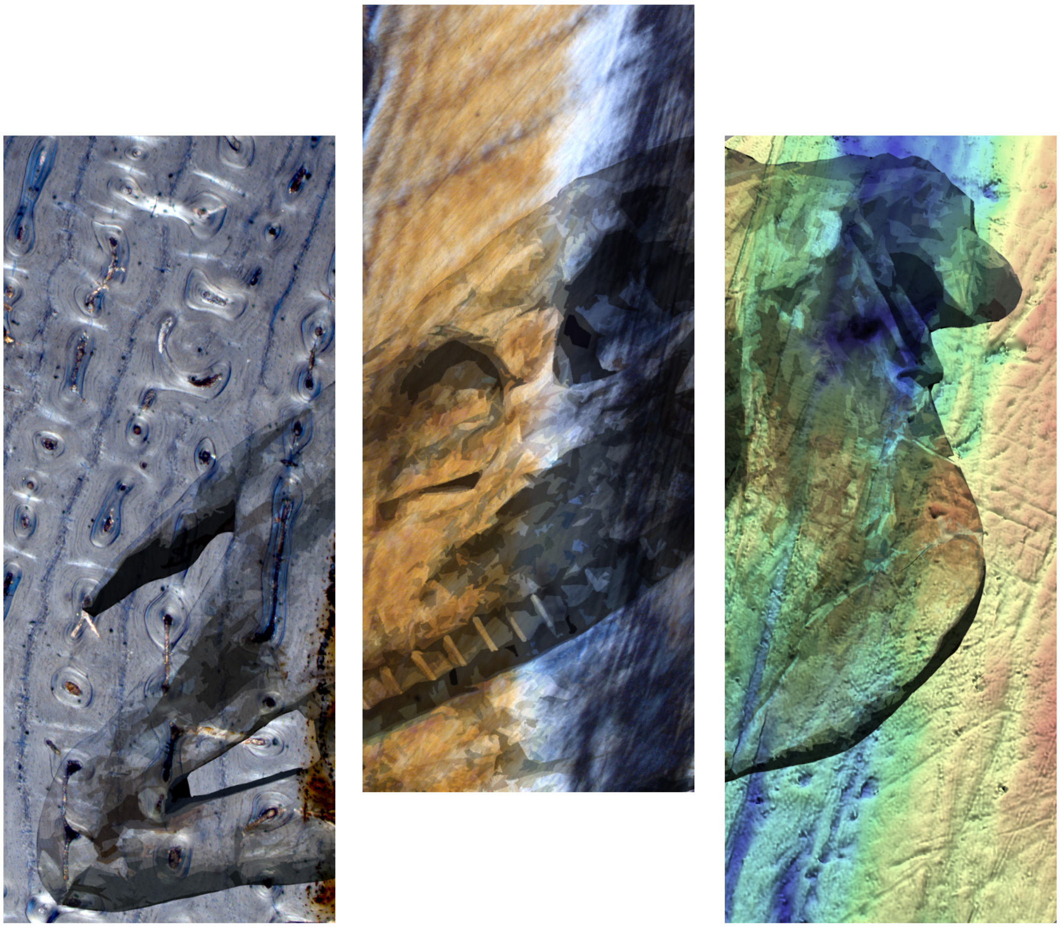

Guillermo Orlandi Oliveras

Supervisor
Dra. Meike Köhler

Institut Català de Paleontologia Miquel Crusafont
Universitat Autònoma de Barcelona
2019

Institut Català de Paleontologia
Miquel Crusafont

PhD Thesis – 2019

Universitat Autònoma de Barcelona

Life History and Ecology of Late Miocene Hipparionins from the Circum-Mediterranean Area

Guillermo Orlandi Oliveras

Dissertation presented by Guillermo Orlandi Oliveras in fulfillment of the requirements for the degree of Doctor in the Universitat Autònoma de Barcelona, doctorate program in Biodiversity of the Departament de Biologia Animal, Biologia Vegetal i d'Ecologia. Under the supervision of:

- Dra. Meike Köhler, ICREA at Institut Català de Palaeontologia Miquel Crusafont and teacher of the Departament de Biologia Animal, Biologia Vegetal i d'Ecologia at Universitat Autònoma de Barcelona.

Doctoral candidate
Guillermo Orlandi Oliveras

Supervisor
Dra. Meike Köhler

Abstract

Hipparionins are a clade of tridactyl equids that greatly diversified during the late Miocene throughout the circum-Mediterranean area, with some taxa undergoing dwarfing. Due to their abundance, they have been the subject of several paleoecological studies and constitute a key mammalian group for exploring evolutionary patterns, although more research is necessary to better understand their ecology. One central aspect of an organism's biology is its life history, which can be inferred from the analysis of bone and dental microstructure. In addition, since a species' life history evolves relative to ecological conditions, its study can provide environmental information. Feeding ecology, another feature of an organism's biology and an important link to its environment, can be inferred from dental microwear. With this in mind, the central aim of this thesis is to elucidate the ecological conditions and mechanisms that accompanied dwarfing in western and eastern Mediterranean hipparionins. Therefore, I (i) reconstruct the growth patterns of metapodials and molars in different-sized hipparionins using bone and dental histology, (ii) make inferences regarding their life histories, and (iii) examine their diets by studying dental microwear textures to test the ecological inferences obtained from life history analyses.

Metapodial histology confirms the usefulness of metapodials for reconstructing the entire ontogenetic growth and establishing a relative maturity attainment. Therefore, the identification of different timings of metapodial growth cessation demonstrate distinct growth strategies within the hipparionins analyzed. For the first time among ungulates, the analysis of daily enamel laminations reveals higher growth rates in first/second molars compared to later-formed third molars, which suggests a link between dental development and somatic growth. Thus, the slower dental growth rates and the relatively late eruption timings (correlated with life history traits) in hipparionins indicate slower paces of life compared to *Equus*. This challenges previous assumptions that hipparionins have faster life histories due to their generally smaller body size. Western dwarf hipparionins, moreover, show an even slower dental development than larger forms, and a relatively late skeletal maturity, pointing to a slower life history than expected for their size. Conforming with life history theory, this evidences that dwarfing in these western hipparionins was led by lower resource availability. Conversely, the eastern small-sized form shows an advanced relative maturity, which indicates that its size decrease was triggered by higher extrinsic mortalities (predation). This scheme suggests that paleoenvironmental differences accounted for the distinct ecological pressures inferred: forested habitats in the western Mediterranean likely provided increased cover against predation but less resources for the hipparionins, while the more open habitats further east were riskier, but richer in resources.

Dietary reconstructions reveal mixed-feeding diets and opportunistic feeding behaviors in most hipparionins, although some western large-sized forms were grazers. Dental microwear textures of western hipparionins, therefore, provide evidence of distinct diets between the size classes. In this case, dwarfs had broader browse-dominated feeding spectra supporting the idea that they dwelt in more forested habitats and/or that their resources were more limited. Conversely, eastern hipparionins do not show significantly different microwear textures, thus indicating similar dietary preferences in a resource-rich environment that precluded resource partitioning. Contrary to expectations for more open habitats, eastern hipparionins seem to have included less grass in their diets than western forms, which could be related to a higher consumption of browse during droughts and/or the presence of grit affecting microwear texture.

In summary, this thesis provides evidence that the dwarfing process and the mechanisms behind it are not uniform, but that they depend on the specific ecological context. The results represent a further step toward the understanding of the life histories and ecologies of extinct equids.

Resum

Els hipparionins eren uns èquids tridàctils molt diversificats durant el Miocè superior a l'àrea circummediterrània, on alguns van esdevenir nans. Per la seva abundància, aquests són un grup clau en la recerca paleoecològica i l'anàlisi de patrons evolutius, tot i que encara cal conèixer millor la seva ecologia. Un dels aspectes més importants de la biologia d'un organisme és la seva història de vida, la qual pot ser reconstruïda a partir de la microestructura òssia i dental, i ens proporciona informació sobre el context ambiental. Així mateix, la dieta, una altra característica de la biologia d'un organisme i un important vincle amb l'ambient, es pot inferir a través del microdesgast dental. En aquesta tesi, l'objectiu principal és dilucidar les condicions ecològiques i els mecanismes relacionats amb la disminució de mida que van patir alguns hipparionins de l'est i oest del Mediterrani. Amb aquesta finalitat, es (i) reconstrueixen els patrons de creixement de metàpodes i molars d'hipparionins de diferent mida, (ii) s'infereixen les seves històries de vida, i (iii) s'exploren les seves dietes a través del microdesgast per testar les inferències ecològiques obtingudes de l'anàlisi de les històries vitals.

L'estudi de la histologia dels metàpodes permet reconstruir el creixement ontogenètic i establir l'assoliment d'una maduresa relativa. La identificació de diferents edats de maduració, doncs, evidencia diferents estratègies de creixement en els hipparionins analitzats. L'estudi de laminacions diàries en l'esmalt revela, per primer cop en ungulats, taxes de creixement en primeres/segones molars més elevades que en terceres molars de formació més tardana, suggerint un vincle entre el desenvolupament dental i el somàtic. Així, les taxes de creixement dental més lentes i les erupcions relativament posteriors (correlacionades amb trets d'història de vida) indiquen ritmes de creixement més lents en hipparionins comparat amb *Equus*. Això contrasta amb la idea d'històries de vida ràpides en hipparionins pel fet de ser generalment més petits. A més, els hipparionins nans occidentals mostren un desenvolupament dental més lent que el de les formes grans i una maduresa relativament tardana, indicant també una història vital més lenta de l'esperada per la seva mida. D'acord amb la teoria de les històries de vida, això assenyala que la menor disponibilitat de recursos és la causa del nanisme en aquests hipparionins. Per contra, les formes petites orientals mostren una maduresa relativa avançada, el que suggereix que la disminució de mida va ser causada per una major mortalitat extrínseca (depredació). Diferències paleoambientals explicarien les pressions ecològiques contraposades: ambients més tancats a l'oest del Mediterrani proporcionaven més cobertura contra la depredació però menys recursos pels hipparionins, mentre a l'est els hàbitats més oberts eren arriscats però rics en recursos.

L'anàlisi del microdesgast dental indica un tipus d'alimentació mixta i oportunista en la majoria dels hipparionins, encara que algunes formes occidentals grans pasturaven. D'altra banda, els hipparionins occidentals nans tenien espectres tròfics més amplis i brostejaven, el que avala que habitessin ambients més boscosos i/o tinguessin recursos més limitats. En canvi, els hipparionins orientals petits no difereixen dels grans en les seves textures de microdesgast, suggerint dietes similars en un entorn ric en recursos que evitaria la necessitat del seu repartiment. Contràriament al que s'esperaria en ambients més oberts, els hipparionins orientals menjaven menys gramínies que els occidentals, cosa que es podria relacionar amb canvis de dieta durant sequeres i/o la presència de sorra alterant la textura del microdesgast.

En resum, aquesta tesi proporciona evidències que els processos de disminució de mida i els mecanismes infrajacents no són uniformes sinó que depenen del context ecològic. Els resultats presentats suposen un pas més per entendre les històries de vida i ecologies d'èquids extints.

Index

Chapter 1. Introduction 9

Abbreviations

Asfc – Area-scale fractal complexity
CDS – Crown developmental stage
CFT – Crown formation time
CGM – Cyclical growth mark
DSR – Daily secretion rate
DMT(A) – Dental microwear texture (analysis)
EDJ – Enamel dentine junction
EER – Enamel extension rate
EFS – External fundamental system
epLsar – Exact proportion of length-scale anisotropy of relief
FLC – Fibrolamellar complex
GR – Growth rate
HAsfc – Heterogeneity of area-scale fractal complexity
HS – Haversian systems
ka – Kilo-annum (10^3 years ago)
LH – Life history
LHT – Life history theory
Ma – Mega-annum (10^6 years ago)
MN – Mammal Neogene zones following Mein (1990)
Myr – Million years (period of time)
PFB – Parallel-fibered bone
RC – Resorption cavities
RGR – Relative growth rate
SSFA – Scale-sensitive fractal analysis
Tfv – Textural fill volume

Conventions

The term "hipparionin" is used here instead of "hipparionine" to formally designate those members of the Hipparionini tribe. Informal grade-level terms (e.g., merychippine) are written here between quotation marks.

In this thesis, I used the broad sense of the genus *Hipparion*. This decision follows previous work from other authors who focused on taxonomy and worked on material from the Iberian and the Balkan peninsulas (Pirlot, 1956; Sondaar, 1961; Forsten, 1968; Koufos, 1987; Alberdi, 1989; Pesquero, 2003; Vlachou, 2013), where most of my samples come from. I agree on the unlikely existence of only a single genus (i.e., *Hipparion*) during the 10 Myr that hipparionin horses were present in the Old World (Bernor et al., 1996). However, the lack of complete cranial material for some of the main taxa analyzed herein, precludes an unequivocal assignation to the supraspecific groupings to the date proposed (Bernor et al., 1990b, 1996). Therefore, rather than ambiguously assigning taxa to determinate genera—which are mainly defined based on cranial morphology (Woodburne and Bernor, 1980; Bernor et al., 1996)—I chose to refer them to the *Hipparion* genus sensu lato.

Finally, because this thesis is focused on Eurasian hipparionin faunas, the circum-Mediterranean area here only refers to its northern portion.

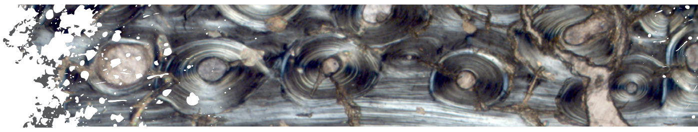

Chapter 1

Introduction

Chapter 1

Introduction

1.1. The Equidae Evolutionary History

The family Equidae is included within the order of odd-toed ungulates Perissodactyla together with the extant families Tapiridae and Rhinoceratidae (Steiner and Ryder, 2011), and other extinct groups (e.g., Chalicotheriidae). Equids are an evolutionary paradigm, primarily because of their rich fossil record, which provides evidence of the many transitions from primitive forms to the extant taxa (MacFadden, 1992, 2005; Janis, 2007). Horse evolution was first interpreted during the second half of the 19th century as a gradual linear progression from a multi-toed equid with low-crowned teeth, toward a monodactyl horse with high-crowned teeth (MacFadden, 1992; Janis, 2007). This orthogenetic trend was clearly depicted by Marsh (1879), and remains in the public perception due to its simplicity and constant presence in textbooks (Gould, 1987; MacFadden, 1992). During the 20th century, however, further fossil discoveries, and a deeper understanding of equid diversity, advocated for a more complex branching scheme within the horse's evolutionary history (Simpson, 1951; Woodburne and MacFadden, 1982; MacFadden and Hulbert, 1988).

The earliest equid representatives were the "hyracotheres", which inhabited the Holarctic realm during the early Eocene (55 Ma) (MacFadden, 1992; Froehlich, 2002). These primitive equids had small hooves and low-crowned teeth (Franzen, 2010) that they used for browsing fruits and soft leaves in dense forests (Mihlbachler et al., 2011; Semprebon et al., 2016). Much of the radiation of this group took place in North America (Froehlich, 2002), similar to many other equid clades (Woodburne and MacFadden, 1982; MacFadden, 1992). Due to the high diversity of equids within North America, this region is considered to be the center of their evolutionary history and the focus of different migratory events toward the Old World (Forsten, 1989; MacFadden, 1992; Janis, 2007; Orlando, 2015). Indeed, during the North American late Eocene, the first anchitheriine horses appeared, which were characterized by more specialized teeth and hooves than their "hyracotheriine" ancestors (Janis, 2007). After a lapse of relatively low equid diversity during most part of the Eocene up to the late Oligocene, the Equidae family experienced considerable diversification (MacFadden, 1992; Shoemaker and Clauset, 2014; Orlando, 2015). Thus, at the beginning of the early Miocene, various anchitheriine lineages were present throughout North America, and the genus *Anchitherium* began to disperse from there across Eurasia (Janis, 2007). Most of these anchitheriine horses were mainly browsing taxa with low-crowned teeth (Mihlbachler et al., 2011). However, the more derived forms showed an incipient increase in tooth height (Damuth and Janis, 2011) related to the incorporation of higher quantities of fibrous food in their diet (Semprebon et al., 2016). The major explosion in equid diversity occurred in North America during the later early Miocene (ca. 17 Ma), when the first hypsodont forms included within the "merychippine" grade underwent explosive adaptive radiation (MacFadden and Hulbert, 1988; Hulbert and MacFadden, 1991). During this time, the two tribes included in the subfamily Equinae (i.e., Hipparionini and Equini) differentiated from various lineages pertaining to the "merychippine" group (MacFadden, 1992).

The Hipparionini and the Equini are mainly distinguishable by the autopodium and dental morphology (Hulbert and MacFadden, 1991; MacFadden, 1992; Janis, 2007). The first occurrence of hipparionin horses is dated at 15 Ma in some localities from Texas, North America (MacFadden and Skinner, 1981). The members of this tribe, together with earlier representatives of the Equini, were abundant in North America from approximately 15 to 8 Ma, when they exemplified the maximum taxonomical diversity within the evolutionary history of the Equidae (MacFadden, 1984, 1992; Hulbert, 1988).

During the late Miocene, around 11 Ma, hipparionins underwent a significant dispersal across the Old World (Bernor et al., 1988; Forsten, 1989; Garcés et al., 1997), followed by an adaptive radiation that led to the appearance of different lineages (Woodburne and Bernor, 1980; Bernor et al., 1996). After this extensive and arguably isochronous dispersal (Sen, 1990; Garcés et al., 1996; Woodburne, 2009), hipparionins became a dominant element within the Eurasian and African faunal assemblages (Alberdi, 1989; Bernor and Lipscomb, 1995) representing the first equids to inhabit the African continent (Forsten, 1989). From the Pliocene onwards, Equidae diversity was comparably lower in both the Old and the New World (Alberdi, 1986; Eisenmann and Sondaar, 1989; MacFadden, 1992). It was during this epoch, about 4.5 to 4 Ma, that the first members of the genus *Equus* likely appeared in North America (Orlando et al., 2013); being initially only represented by one species (Lindsay et al., 1980; Azzaroli, 1992; MacFadden, 1992). Posteriorly, this genus flourished and dispersed over South America and the Old World during the end of the Pliocene [≈ 2.6 Ma (Lindsay et al., 1980)] (Forsten, 1989; Orlando, 2015). By that time, there were few hipparionin horses of Asian origin present in Europe (Alberdi, 1989; Bernor and Sun, 2015). Both groups arguably coexisted in Europe for a short period of time (Alberdi, 1989;

Bernor and Lipscomb, 1991; Pueyo et al., 2016; Rook et al., 2017; Athanassiou, 2018), but they mainly coexisted in Asia and Africa, where hipparionin horses remained present until less than 1 Myr ago (Eisenmann, 1985; Qiu et al., 1987).

Within the extant *Equus* genus, "caballine" (*Equus ferus*) and "non-caballine" equids (zebras and asses) are differentiated based on their genetic material (Oakenfull et al., 2000; Jónsson et al., 2014). A similar division can be established morphologically by considering the enamel pattern of the lower teeth, separating the more primitive linguaflexid fold of "stenonoid" forms—which include some Plio-Pleistocene *Equus* species and extant asses and zebras—from the more derived pattern of "caballoids", which are currently only represented by the horse (Forsten, 1988; Alberdi et al., 1998). During the first *Equus* migration wave, the "stenonoid" ancestor of the extant "non-caballine" taxa dispersed to the Old World (Lindsay et al., 1980; Alberdi et al., 1998), subsequently radiating (Azzaroli, 1992) and reaching the African continent at least twice (Orlando, 2015). "Caballine" horses appeared in the Old World after a second dispersal event during the Middle Pleistocene, replacing nearly all "stenonoid" equids of Eurasia and confining most of the "non-caballine" forms to Africa (Forsten, 1988, 1989; Alberdi et al., 1998; Orlando, 2015). As with the case of other large Pleistocene mammals, *Equus* disappeared in many areas of its distribution range approximately 8–10 ka, probably due to multiple factors such as climate change or over-killing (MacFadden, 1992; Janis, 2007; Lorenzen et al., 2011). Nowadays, all extant wild equids are comprised in one single genus with seven recognized species: the horse (*Equus ferus*), three zebra species (*Equus quagga, Equus zebra,* and *Equus grevyi*), and three species of ass (*Equus africanus*, *Equus hemionus,* and *Equus kiang*) (Orlando, 2015). Hence, the equid family today only represents a small fraction of its past diversity, which has included more than 200 species distributed across more than three dozen different genera over the course of its 55 Myr of evolutionary history (MacFadden, 1992, 2005).

1.1.1. Evolution of Body Size Within the Family Equidae

Body size is a fundamental trait in an animal as it is intimately related to many ecological and physiological parameters (Peters, 1983; Calder, 1984; McNab, 1990). Because of this, determining and understanding body size shifts has been of key importance in Paleobiology (Damuth and MacFadden, 1990). Body mass, a good proxy of body size (Damuth and MacFadden, 1990), ranged over two orders of magnitude (10–1000 kg) during the evolutionary history of equids (MacFadden, 1986, 1992; Eisenmann, 2003). When comparing the smaller-sized Paleogene equids (MacFadden, 1986) with the wild extant equids that weigh 275 kg on average (Tacutu et al., 2018), a tendency toward a larger body size can be seen. For this reason, the family Equidae has long been used as an example of a progressive size increase trend over time (Matthew, 1926) (i.e., Cope's Rule, see

Stanley, 1973), a generalization based on the idea that a larger body size is an adaptive trait that favors survival (Kurtén, 1953; Simpson, 1953; Gould, 1966).

In fact, equids have experienced significant variations in size during their evolutionary history (Simpson, 1953; MacFadden, 1986; Shoemaker and Clauset, 2014; Cantalapiedra et al., 2017). However, instead of a linear and progressive trend toward larger sizes, body size evolution within this family is complex, and has comprised periods of relative stasis as well as the presence of lineages that gradually decreased in size (MacFadden, 1986; Gould and MacFadden, 2004). For more than half of the equids' history (early Eocene to latest Oligocene), there were no significant shifts in body mass, which typically ranged from 5 to 50 kg (MacFadden, 1986, 1992; Gould and MacFadden, 2004). During the Miocene, there was a huge taxonomic and body size diversification (MacFadden, 1986; Shoemaker and Clauset, 2014), which has usually been interpreted as a result of adaptations to the spread of grassland ecosystems (MacFadden, 1986; Hulbert, 1993). This diversification has also been linked to the effect of external factors that promoted speciation (e.g., higher ecosystems productivity or increased provincialism) rather than ecomorphological differentiation (Cantalapiedra et al., 2017). Although some studies have related some of the equids' body size shifts to temperature changes (Secord et al., 2012; D'Ambrosia et al., 2017), the general size variations within the clade do not seem to be correlated with global temperature changes (Shoemaker and Clauset, 2014).

Body size decrease trends in discrete equid lineages were almost as common as giantism processes (Gould and MacFadden, 2004). Indeed, dwarfing took place multiple times in different branches of the Old World and New World equids, such as in the North American genera *Archaeohippus*, *Pseudhipparion* and *Calippus* (MacFadden, 1986, 1992). The most recent examples of size decrease trends are those independently experienced by some *Equus* lineages during the Pleistocene (Forsten, 1991; Alberdi et al., 1995, 1998; Guthrie, 2003). In Europe, both "stenonoid" (Alberdi et al., 1995, 1998) and "caballoid" equids (Forsten, 1991; Alberdi et al., 1995) decreased in mean body size, which also occurred in North America just prior to the local extinction of the genus (Guthrie, 2003). Different scenarios have been proposed as causes that underlay these shifts, such as a reduction in resource availability (Forsten, 1991; Guthrie, 2003) or environmental changes leading to a warmer climate and more forested biomes (Alberdi et al., 1995, 1998).

Some hipparionin lineages also underwent significant size decrease trends (MacFadden, 1986, 1992). In North America, these processes occurred multiple times in at least two different genera (e.g., *Nannipus*, *Pseudhipparion*) (Gould and MacFadden, 2004). Likewise, Old World hipparionins followed comparable shrinking tendencies that led to the appearance of small-sized taxa in Eurasia and Africa (Forsten, 1978a; Eisenmann, 1980; Alberdi, 1989; Bernor and Tobien, 1989; Bernor et al., 1996). As in the case of the first Eurasian *Equus*, the first hipparionins that reached the Old World were probably large-sized forms, which subsequently differentiated in size (Alberdi et al., 1995; Cantalapiedra et al., 2017). To date, the smaller-sized hipparionins from the Old World have usually been assigned to the genus *Cremohipparion*, which according to Bernor et al. (1996) includes a lineage that underwent a size decrease trend and another group composed of larger and more robust forms. The ubiquity of small hipparionins in different regions of the Old World during the late Miocene (Eisenmann, 1980; Bernor and Tobien, 1989; Pesquero, 2003; Koufos, 2016) and the early Pliocene (Alberdi, 1986), would indicate the existence of more than one clade of small-sized hipparionins (Bernor et al., 2016) and the occurrence of independent size decrease trends (Woodburne and MacFadden, 1982). These size decrease trends have been interpreted as the outcome of different scenarios: (i) an adaptation to energy economization (Forsten, 1968, 1978a), (ii) a response to habitat changes toward more open biomes (Bernor et al., 1996; Saarinen, 2009), or (iii) toward warmer and more forested habitats (Ortiz-Jaureguizar and Alberdi, 2003).

1.1.2. The Old World Hipparionins

This thesis focuses specifically on Old World hipparionins, which have been studied for more than 175 years. These equids have traditionally been included within the genus *Hipparion*, which was erected by Christol (1832) and generally comprises those horses that have tridactyl limbs and isolated protocones in their upper cheek teeth (Alberdi, 1989). The arrival of hipparionins in Eurasia, the so called as "*Hipparion* Datum", is dated at around 11 Ma (Bernor et al., 1988, 2017; Garcés et al., 1996, 1997; Woodburne, 2009) and marks the start of the Vallesian European Land Mammal Age (Fahlbusch, 1976). These earliest Eurasian hipparionins probably originated from members of the North American *Cormohipparion* genus, as evidenced by the similarities between both groups (Bernor et al., 1988; Woodburne, 2007, 2009). Commonly, Old World Vallesian hipparionins have been associated with a single large-sized robust form (Forsten, 1968, 1978b); however, various morphotypes can be distinguished already on early Vallesian assemblages (Eisenmann, 1995). Indeed, soon after the hipparionin dispersal, some vicariant processes took place and Eurasian hipparionins began to differentiate in form (Bernor et al., 1988, 1990b, 1996, 2003). This radiation originated distinct forms that are usually grouped around the "*Hippotherium primigenium* Complex" proposed by Bernor et al. (1996). The magnitude of this diversification, however, differs between regions (Bernor et al., 1988, 1990a, 2003). Central European hipparionins were little diverse and showed a conservative body plan during most part of the Vallesian (Bernor et al., 1988, 1996), while multiple and differentiated taxa were present in western (Bernor et al., 1996; Forsten, 1997) and eastern Mediterranean areas (Bernor et al., 1990a, 1996, 2003; Koufos, 2016). It was during the end of the Vallesian period, and particularly during the Turolian period, that hipparionin diversity substantially increased and sympatric taxa occurred in many localities (Forsten, 1989). The rapid diversification of hipparionins is thought to have been related to increased seasonality regimes and their impact on vegetation communities (Bernor et al., 1990a).

The systematics and phylogeny of Old World hipparionins have proven to be difficult because of (i) the diversity of forms found in many of the hipparionin associations, (ii) the poor stratigraphic control of some fossil assemblages, (iii) the large intraspecific variability, (iv) the existence of homoplasic characters, and (v) the ontogenetic variation in diagnostic traits (Alberdi, 1989; Bernor et al., 1990b). Following previous work on New World equids (Skinner and MacFadden, 1977), some authors based systematic and phylogenetic relationships of the Old World hipparionin on skull characters, with special emphasis on the morphology and position of the preorbital fossa (Woodburne and Bernor, 1980; Bernor et al., 1990b, 1996). These studies suggest that Old World hipparionins are represented by different evolutionary lineages of supraspecific rank (Woodburne and Bernor, 1980; Bernor et al., 1990b). Under this scope, hipparionin systematics rely strongly on the availability of complete cranial material (Bernor et al., 1996), which is scarce or virtually non-existent for many taxa. Different authors (Forsten, 1983; Eisenmann et al., 1987; Alberdi, 1989), moreover, have questioned the validity of the preorbital fossa as being the sole character for generic-differentiation. Alternatively, the *Hipparion* s.l. genus has been divided within different morphotypes by means of cranial and postcranial characters (Alberdi, 1989; Vlachou, 2013).

Currently, the supraspecific groupings proposed by Bernor et al. (1996) are the most widely used. Following their division, the earliest Old World hipparionins are mainly included in the "*Hippotherium primigenium* Complex" (Bernor et al., 1996). This group represents a paraphyletic lineage (Bernor et al., 1988) that was specially prolific during the Vallesian but that also persisted afterwards during the Turolian (Woodburne and Bernor, 1980; Bernor et al., 1996). These large hipparionins are characterized by exhibiting primitive traits such as robust metapodials, marked preorbital fossa, long preorbital bar, and complex enamel folding in the cheek teeth (Woodburne, 1989; Bernor et al., 1990b, 1996). This group can be broadly related to morphotype 1 of Alberdi (1989) and the morphotype *primigenium* of Vlachou (2013). The other clade is represented by the genus *Hipparion* sensu stricto as defined by Bernor et al. (1996). These hipparionins might have originated from some representatives of the former group (Bernor et al., 1990b, 1996) or from an independent migratory wave of North American hipparionins (Woodburne and MacFadden, 1982; Woodburne, 1989). The *Hipparion* s.s. genus is composed of medium-sized forms that have a preorbital fossa situated in a high position, a short preorbital bar, slender metapodials, and simplified enamel ornamentation (Woodburne and Bernor, 1980; Bernor et al., 1990b, 1996). Vlachou (2013) includes these forms in the *dietrichi* morphotype. The "*Cremohipparion* group" represents the other hipparionin supraspecific clade proposed by Bernor et al. (1996). The members of this group are differentiated by their short preorbital bar and elongated metapodials (Bernor et al., 1990b, 1996).

These hipparionins were particularly prolific during the Eurasian Turolian period, although they are also found in Vallesian fossil assemblages (Bernor et al., 1996, 2016; Koufos, 2016) and in North African localities (Bernor et al., 1996). Two distinct evolutionary pathways are comprised within this group: a lineage characterized by the reduction of facial fossae and dwarfism, and another group of large-sized hipparionins that show multiplication and sharpening of the facial fossae (Bernor et al., 1996). These two lineages, respectively, correspond to the *macedonicum* and *proboscideum* morphotypes suggested by Vlachou (2013). The small-sized hipparionins from western Eurasia have been commonly assigned to the *Cremohipparion* group and, particularly, referred to the species *Cremohipparion matthewi* (= *Hipparion matthewi*) (Pesquero et al., 2007; Bernor et al., 2016; Koufos, 2016), although in some cases without solid evidence (Koufos, 2016). Finally, a late diversification of Old World hipparionins took place from the latest Miocene to the Pliocene and Pleistocene (Bernor et al., 1990b). This radiation was undergone by the members of the "*Sivalhippus* Complex" of Bernor et al. (1990b), which are characterized by having reduced or absent preorbital fossa, very hypsodont teeth, and very large body sizes (Bernor et al., 1996).

1.1.2.1. *Eastern Mediterranean (Balkans and Western Anatolia)*

Western Eurasian hipparionins had a marked provincial distribution during the late Neogene (Bernor et al., 1996). In the eastern Mediterranean, these horses exhibited a high taxonomic diversity (Koufos, 1987; Bernor et al., 2003; Vlachou, 2013), which contrasted with that of the western Mediterranean province but particularly with Central Europe (Forsten, 1978b; Bernor et al., 1990a, 1996, 2003; Fortelius et al., 1996). Compared to this latter area, the richer hipparionin assemblages of circum-Mediterranean domains have been associated with the presence of more open habitats due to increased seasonality regimes (Bernor et al., 1990a). Accordingly, different studies have indicated that the eastern Mediterranean paleoenvironments were dry and open during the late Miocene (Bonis et al., 1992a; Merceron et al., 2005; Koufos, 2006; Strömberg et al., 2007; Ioakim and Koufos, 2009; Merceron et al., 2016a), while in other regions of Europe—particularly in Central Europe—there were more humid and wooded biomes (Bernor et al., 1988; Bonis et al., 1992b).

After their dispersal through the eastern Mediterranean, hipparionins experienced a short period of relative stasis, followed by a radiation at the end of the early Vallesian (MN9) (Bernor et al., 2003). During the early Vallesian in the southern Balkans (Koufos, 2013), the small-sized *Hipparion macedonicum* (~ 100 kg) was already co-existing with larger and more primitive forms of the *primigenium* morphotype (~ 150–200 kg) (Vlachou, 2013; Koufos, 2016). Evidence of the coexistence of members from the *primigenium* and the *macedonicum* morphotypes is commonly found in Vallesian localities from this area (Koufos, 1986; Vlachou, 2013; Koufos et al., 2016).

For most of the Turolian period, the faunal assemblages differed between the southern Balkans and the western Anatolian sectors of the eastern Mediterranean (Kostopoulos, 2009; Koufos and Vlachou, 2016), probably because of a biogeographical barrier (Kostopoulos, 2009). As a consequence, the existing hipparionin lineages evolved separately and gave rise to different taxa (Vlachou, 2013; Koufos and Vlachou, 2016). For instance, while the small-sized *macedonicum* morphotype was mainly represented by the species *H. matthewi* in western Anatolia, this group was characterized by *H. macedonicum* in the southern Balkans (Vlachou, 2013; Koufos, 2016). Interestingly, the members of this morphotype decreased further in body size during their evolutionary history (Vlachou, 2013; Koufos, 2016). From the early Turolian onwards, the different hipparionin lineages continued to diversify (Bernor et al., 1996), and the fossil associations commonly included three or more species (Koufos, 1987; Koufos and Vlachou, 2016). The taxa comprised within the *dietrichi* and the *proboscideum* morphotypes became an important element of the eastern Mediterranean hipparionin associations (Vlachou, 2013; Koufos and Vlachou, 2016), also co-existing with representatives of the former *primigenium* and *macedonicum* groups (Hristova, 2009; Vlachou and Koufos, 2009; Vlachou, 2013; Koufos and Vlachou, 2016). The *dietrichi* morphotype of Vlachou (2013) includes the gracile medium to large-sized hipparionins referred to as *Hipparion* s.s. by Bernor et al. (1996), such as *Hipparion dietrichi* or *Hipparion philippus*. On the other hand, the *proboscideum* morphotype comprises the large-sized hipparionins that pertain to one of the two lineages of the "*Cremohipparion* group" defined by Bernor et al. (1996). *Hipparion proboscideum* or the well represented *Hipparion mediterraneum* from Pikermi are included within this latter morphotype (Vlachou, 2013). After this period of huge taxonomic and morphologic diversity, there was a marked decline in the number of hipparionin taxa during the earliest Pliocene (MN14) (Eisenmann and Sondaar, 1989, 1998; Bernor et al., 1996). The lasts hipparionins inhabiting the eastern Mediterranean were larger species that migrated from Asia (Eisenmann and Sondaar, 1998; Bernor and Sen, 2017).

1.1.2.2. Western Mediterranean (Iberian Peninsula)

Hipparionin diversity in the western Mediterranean was lower than in the eastern counterpart (Bernor et al., 1996; Fortelius et al., 1996), but not as low as in Central Europe (Bernor et al., 1990a). Similar to the eastern Mediterranean region, the diversification of hipparionin forms have been related to the presence of open habitats in this area (Bernor et al., 1990a; Forsten, 1997). Nevertheless, the western Mediterranean biomes during the late Miocene were roughly characterized by woodland landscapes (Hernández Fernández et al., 2006; Domingo et al., 2013), which were generally more closed and humid than the eastern ones (Bonis et al., 1992b; Fortelius et al., 2006). Indeed, some humid forested environments have been clearly identified in the Iberian Peninsula during the early Vallesian (Marmi et al., 2012), although other sectors were dominated by drier, more open habitats (Van Dam, 2006; Jiménez-Moreno et al., 2010; Pound et al., 2011). The more humid and dense forests shifted later to more open woodlands (Agustí et al., 2003; Van Dam, 2006; Domingo et al., 2013) probably due to a stronger seasonality from the late Vallesian onwards (Agustí et al., 2003).

The earliest hipparionins that inhabited the Iberian Peninsula have commonly been included within the species *Hipparion primigenium* (Forsten, 1968, 1978b; Alberdi, 1972). These large-sized forms [~ 180 kg (Ortiz-Jaureguizar and Alberdi, 2003)] already showed some differences between them and the more primitive members of the *H. primigenium* s.s. taxon as defined by Bernor et al. (1996). Because of this, they have been differentiated at subspecific level by different authors (Sondaar, 1961; Alberdi, 1974; Tomàs et al., 2010). As soon as during the early Vallesian (Casanovas-Vilar et al., 2011), hipparionins of small to medium stature co-existed in some localities from the eastern Iberian Peninsula with larger and more primitive forms (Forsten, 1997). In other Iberian basins, a slender, medium-sized hipparionin, clearly differentiated from the *primigenium* group, has also appeared in early Vallesian sites (Bernor et al., 1996; Pesquero and Alberdi, 2012).

Hence, throughout this region, hipparionins underwent an early radiation similar to what occurred in the eastern Mediterranean (Forsten, 1997). However, the main divergence between hipparionin lineages took place during the late Vallesian (Bernor et al., 1996). By this time, the Iberian Peninsula basins also registered the appearance of very large gracile species (Pesquero et al., 2006) and small-sized hipparionins that had previously been unreported (Romano et al., 2017). These different hipparionin forms, however, did not tend to live sympatrically until the early Turolian (Alberdi and Alcalá, 1989-1990; Pesquero et al., 2011).

Hipparionins of medium stature such as *Hipparion concudense*, dominated the middle Turolian faunas from Iberia (Alberdi, 1974, 1978; Bernor et al., 1996). Posteriorly, the late Turolian (MN13) was characterized by a higher diversity of hipparionins, since three sympatric forms can be commonly recognized within some localities (Alberdi, 1974; Alberdi and Alcalá, 1989; Ortiz-Jaureguizar and Alberdi, 2003; Pesquero, 2003; Pesquero et al., 2007). The largest hipparionins from these assemblages have been related to the *H. primigenium* lineage (Pesquero, 2003; Pesquero et al., 2007), while the other two forms are usually represented by the dwarf taxa *Hipparion gromovae* (59 kg) and *Hipparion periafricanum* (23 kg) (Fig. 1.1) (Alberdi, 1974, 1978; Ortiz-Jaureguizar and Alberdi, 2003; Pesquero, 2003). These two forms are thought to be the result of a progressive size decrease trend (Forsten, 1968; Alberdi, 1989; Pesquero, 2003; Pesquero et al., 2011) that culminated in the appearance of the smallest of the Old World hipparionins, *H. periafricanum* (Bernor et al., 1996). The presence and diversity of hipparionins decreased considerably from the beginning of the Pliocene onwards (Alberdi, 1986), mirroring what occurred in the eastern Mediterranean (Eisenmann and Sondaar, 1989; Bernor et al., 1996).

Figure 1.1.
First phalanges and distal portions of the central metatarsals of the three sympatric hipparionin species from the El Arquillo fossil site (Teruel Basin, central eastern Iberian Peninsula). From left to right, *Hipparion primigenium truyolsi*, *Hipparion gromovae*, and *Hipparion periafricanum*. Measurements on these elements of the autopodium have shown to be highly related to the equid body mass (Alberdi et al., 1995; Eisenmann and Sondaar, 1998). Each division of the scale corresponds to 1 cm.

1.2. Life History Theory

The life history (LH) of an organism comprises all of its ontogenetic stages and scheduled events that are related to growth, survival, and reproduction (Stearns, 1992; Roff, 2002; Flatt and Heyland, 2011). It is clear that the reproductive performance of an organism (i.e., the individual fitness) is linked to the timing and magnitude of LH characteristics such as the growth rate, age at maturity, number of offspring, or lifespan (Stearns, 1992). Indeed, some of these so-called LH traits are important demographic elements that directly affect population growth (Stearns, 1992, 2000). Because of their importance as fitness components (Braendle et al., 2011), hence, LH traits represent adaptive features sensitive to natural selection (Stearns, 1992; Roff, 2002). Based on this scheme, life history theory (LHT) aims to explain (i) the diversity of LH strategies found in nature and (ii) the way that ecological factors—or selective pressures—shape LH traits (Roff, 1992, 2002; Stearns, 1992, 2000).

To address the evolution of LHs, evolutionary biologists have traditionally used optimization models (Stearns, 2000). Ideally, a hypothetical organism could maximize fitness by infinitely extending its reproductive life, while also increasing the number of offspring produced, which would lead to the known as a "Darwinian demon" (Law, 1979). However, as happens with the rest of organismal characteristics, the evolution of LH traits is determined by important intrinsic constraints that prevent this from happening (Roff, 1992; Stearns, 1992). These constraints limit the increase of one particular fitness component through the co-varying changes in other fitness traits (trade-offs) (Stearns, 1992; Flatt and Heyland, 2011). From a physiological point of view, the compromise resides in the fact that the available resources are limited; if resources are devoted to one function they cannot be invested in another (Cody, 1966; de Jong, 2006; Ricklefs, 2008). In this regard, the most relevant and generic compromise involves the assigning of resources between current and future reproduction (Stearns, 1992). During the juvenile stage, the dichotomy is whether to keep growing or start reproducing (age at maturity), while in adults it is between reproducing, or postponing reproduction in favor of maintenance and repair (Stearns, 1992). In LHT, the identification of these trade-offs has been of central importance for a correct understanding of the limits of LH evolution (Roff, 1992, 2002; Stearns, 1992). As well as these important intrinsic constraints, LHs are also shaped by extrinsic elements that affect the organism's survival and reproductive chances (Stearns, 2000). Considering the effect of intrinsic and extrinsic factors, organisms channel the available energy to different fitness components following a specific schedule of LH traits (i.e., the LH strategy) to maximize their fitness under given ecological conditions (Roff, 1992; Stearns, 1992).

The r-K- selection of MacArthur and Wilson (1967) expanded by Pianka (1970), was the first proposed framework that addressed the differences in LH between species and populations (Reznick et al., 2002). This r-K selection scheme focuses on density-dependent mortality regimes, and considers resource availability as the major driver of LH variations (Pianka, 1970). Under this scope, selection promotes traits that maximize the intrinsic population growth (*r*, Malthusian parameter) in populations facing unpredictable environments and density-independent extrinsic mortalities (e.g., catastrophic mortality or higher predation pressures). On the other hand, those traits linked to soma maintenance are selected in populations that occur in stable, resource-poor environments that are near carrying capacity (*K*) (Pianka, 1970). From the r-K selection point of view, the populations occupying these latter settings are exposed to density-dependent mortality and thus selection favors LH strategies that confer higher competitive capacity (K-strategist) (e.g., long lifespan, late reproduction). In contrast, those organisms adapted to unpredictable high-resource environments invest most of the energy in reproduction earlier in life (r-strategist) (Pianka, 1974).

The over-simplistic r-K selection was posteriorly relegated by studies under the focus of LHT (Law, 1979; Roff, 1992; Stearns, 1992; Charlesworth, 1994), which included demographic models and highlighted the importance of age and size-specific mortality and fertility rates (Reznick et al., 2002). Concretely, the LHT approach focuses on extrinsic mortality as the major selective pressure driving LH evolution (Law, 1979; Promislow and Harvey, 1990; Roff, 1992; Stearns, 1992). Later LH models, however, also incorporated resource availability as a selective agent affecting LH (Reznick et al., 2002). Under the LHT framework, therefore, the LH of an organism is shaped by extrinsic factors that influence age/size-specific survival and reproduction rates, which at the same time are determined by the intrinsic constraints to LH trait variation—i.e., trade-offs (Stearns, 1992). In this regard, one LH strategy will only evolve if its benefits for fitness counterbalance the associated costs in a specific ecological setting (Stearns, 2000; Koons et al., 2008). For instance, when populations are subject to high extrinsic mortality (predation), selection favors an advance in maturity attainment and a higher reproductive effort (Gadgil and Bossert, 1970; Stearns, 1992; Reznick et al., 1996; Ricklefs, 2008). The advantages of this earlier maturation are a shorter generation time and the increased possibility of successfully reproducing before falling prey to a predator (Stearns, 2000). On the other hand, a later age at maturity is selected for in environments with low extrinsic mortality, as a later maturity allows to grow larger and to increase fecundity (Stearns, 1992). A similar delay in maturation can also be adaptive under high levels of juvenile mortality (Stearns and Koella, 1986; Promislow and Harvey, 1990) because larger and more experienced progenitors, and the production of better-quality offspring, might compensate for the high mortality among juveniles (Stearns and Koella, 1986; Stearns, 2000).

Much of the variation in LHs has been explained in the context of covariance between LH traits and body size, where size is usually considered to be the direct target of selection (Lindstedt and Calder, 1981; Peters, 1983; Calder, 1984). Although the evidence of this strong tie, studies based on LHT highlight the influence of ecological conditions on LH traits—as we have already seen. Therefore, there is, in fact, an adaptive size-independent source of variation in LH strategies (Stearns, 1983; Read and Harvey, 1989; Promislow and Harvey, 1990; Sibly and Brown, 2007), which is mainly triggered by differences in extrinsic mortality (Read and Harvey, 1989; Promislow and Harvey, 1990) and resource availability (Sibly and Brown, 2007). In this regard, comparative analyses of mammalian LHs have led to the proposal of a fast—slow continuum along which the organisms' LH strategies are arranged, and in which body size still has an important influence (Stearns, 1983; Read and Harvey, 1989; Promislow and Harvey, 1990). However, organisms can even be characterized by following slower or faster LHs once the effect of size is removed (Read and Harvey, 1989). In general terms, therefore, taxa situated at the fast end of the LHs continuum are smaller, develop fast, reproduce early, have high fecundity, and are short-lived. Conversely, at the slow end of the continuum, we find larger organisms that develop slowly, mature later, and have long lifespans (Read and Harvey, 1989; Gaillard et al., 2006).

1.2.1. Body Size Shifts and Life History Theory

Because of the central role that size plays in the biology of an organism (Peters, 1983; Calder, 1984; Eisenberg, 1990; McNab, 1990), the evolution of body size and its drivers are of particular relevance in evolutionary ecology. In insular organisms, shifts in body size toward dwarfism or gigantism [Island Rule (Foster, 1964; Van Valen, 1973)] are commonly considered to be a direct outcome of selection for size through reduced competition, absence of predation, and resource scarcity (Foster, 1964; Sondaar, 1977; Case, 1978; Lomolino, 1985). Because of the aforementioned coupling between LH and body size, however, others have argued that selection on fitness components might have indirectly triggered the shifts in body size (Brown et al., 1993; Palkovacs, 2003; Raia et al., 2003; Brown and Sibly, 2006; Raia and Meiri, 2006). In this way, trends in decreasing size, undergone by insular organisms, have been associated with selection toward increased productivity rates and thus more energy allocation to reproduction at the expense of growth and maintenance (faster LH, r-selection) (Bromage et al., 2002; Raia et al., 2003; Raia and Meiri, 2006; Palombo, 2007).

In contrast with these explanations, Palkovacs (2003) proposed a model explicitly based on LHT (Stearns, 1992), which explains size shifts of insular organisms (both decreasing and increasing) as the indirect result of variations in LH traits. In his model, variations on LH traits to which body size is sensitive (i.e., growth rate and age at maturity) are caused by changes in mortality regimes and resource availability from mainland to insular environments (Palkovacs, 2003). The relative influence of these two changes will therefore determine the direction of the size shift (Palkovacs, 2003). In small organisms for which decreased extrinsic mortality plays a more important role than resource limitation, selection will favor a delay in age at maturity that results in a size increase [e.g., the giant glirids of the Balearic islands (Orlandi-Oliveras et al., 2016)]. In larger organisms, for which a decrease in resource levels has more relevance than release from predation pressure, a significant decrease in growth rate leads to a shift toward a smaller size (Palkovacs, 2003; Köhler and Moyà-Solà, 2009; Köhler, 2010). In both cases, organisms channel energy from reproduction to maintenance following slower life histories, as evidenced by their delayed development and extended lifespan (Adler and Levins, 1994; Köhler and Moyà-Solà, 2009; Köhler, 2010; Jordana et al., 2012; Orlandi-Oliveras et al., 2016). Although hitherto only applied to insular settings, Palkovacs' predictive model could be perfectly applicable to mainland ecosystems because of the universality of the underlying LHT mechanisms driving size modifications. In this sense, this thesis mainly focuses on the dwarfed hipparionin forms and their growth patterns, which can help to unravel the evolutionary processes driving shifts in body size on the continent.

1.3. Life History and Ecology of the Equidae

1.3.1. Extant *Equus*

Most living equid species are classified by the IUCN Red list at different levels of extinction risk (Moehlman, 2002). Since the LH of an organism influences its vulnerability to extinction (Reynolds, 2003), the study of equids' LHs is of key importance in addressing their conservation plans. The body mass of living wild equids, a good general predictor of LH (Calder, 1984), ranges from 200 kg to 450 kg (Nowak, 1999). *E. grevyi* has the highest average weight (384 kg) while *E. hemionus* is the lightest extant equid (230 kg) (Ernest, 2003). Generally, females (mares) are physiologically sexually mature after their second year of life, while males (stallions) reach maturity later, around the age of three (Smuts, 1976ab; Monfort et al., 1994; Nowak, 1999; Tacutu et al., 2018). However, mares and stallions do not start to reproduce until one or even two years after they have attained sexual maturity (Grubb, 1981; Churcher, 1993; Monfort et al., 1994; Nowak, 1999). There are interspecific differences on the timing of some LH traits: for instance, *E. grevyi* tend to mature and reproduce later than the other equid species (Churcher, 1993), which is to be expected due to their larger body size (Calder, 1984). The age at which the animal reaches adult size (i.e., skeletal maturity) is difficult to determine, and is usually not reported in wild equids. Smuts (1975), however, indicated that *E. quagga* individuals may reach adult height after the first year of growth, and reach their adult body weight at the age of three. The reported life expectancies among extant equids are variable depending upon the wild or captive status of the specimen. In general, equids living in the wild have an average lifespan of 20 years (Smuts, 1974; MacFadden, 1992; Churcher, 1993) and live 30 years in captivity (Ernest, 2003; Tacutu et al., 2018). Some domesticated *E. ferus* and *E. africanus* have been shown to live more than 45 years in captivity (Tacutu et al., 2018).

Equids are hindgut fermenters that can process large quantities of low-quality fibrous foods (Janis, 1976). Most extant species are classified as strict grazers since their diet is almost only composed of grasses (Nowak, 1999). In accordance with these dietary preferences, they inhabit open landscapes such as savanna woodlands, grasslands, shrublands, and semi-deserts (Nowak, 1999; Moehlman, 2002). Although they are mainly grazers, some species broaden their diet when monocots become scarce during drought periods (Grubb, 1981; Moehlman, 2002). Consequently, the taxa that dwell in more arid environments (i.e., *E. hemionus* and *E. africanus*) include higher proportion of browse than other species (Schulz and Kaiser, 2013).

1.3.2. Extinct Equids

Understanding the LH adaptations and ecology of past organisms are key aspects of paleobiological studies. To date, the LH of extinct equids has been addressed from three different approaches: population dynamics (cohort analyses) (for a review see MacFadden, 1992), dental eruption patterns (Domingo et al., 2018), and paleohistological analyses (Martinez-Maza et al., 2014; Nacarino-Meneses et al., 2017; Nacarino-Meneses and Orlandi-Oliveras, 2019). Extinct equids' ecological preferences have also focused on ecomorphology, dental wear, and isotopic analysis (see section 1.3.2.4).

1.3.2.1. Population Dynamics

Studies on the population dynamics of fossil equids are based on the determination of dental wear stages to classify individuals in discrete age classes (Woodburne and MacFadden, 1982). Therefore, in order to obtain characteristic demographic traits, these studies rely strongly on tooth height and on different assumptions regarding (i) the wear and eruption patterns, (ii) the nature of the fossil assemblage, and (iii) the existence of a stable age distribution, and seasonal breeding/mortality events (Kurtén, 1953; Voorhies, 1969; Hulbert, 1982, 1984). Although the aforementioned points are difficult to address, these studies have generally proposed an earlier attainment of maturity and a shorter potential lifespan for Miocene horses compared to extant forms (Woodburne and MacFadden, 1982). For instance, the potential lifespan—measured as the age of death due to completely worn teeth—has been suggested to be 9 to 15 years in different middle and late Miocene taxa (Van Valen, 1964; Voorhies, 1969; Hulbert, 1982, 1984), and their age at maturity is thought to have been at 1 to 2.8 years old (Van Valen, 1964; Voorhies, 1969).

Based on these latter studies, as well as on the allometric scaling between lifespan and body size (Calder, 1984), MacFadden (1992) suggested a fivefold increase in potential longevity from the first small-sized "hyracotheres" (3–4 years) to the much larger extant equids (20–25 years). As in the case of the general size increase trend (see section 1.1.1), the inferred increase in longevity should not has been progressive (MacFadden, 1992). Indeed, MacFadden (1992) indicated that the major increase in potential lifespan might have occurred from 15 Ma onwards, coinciding with the diversification in equid body sizes (MacFadden, 1986, 1992). MacFadden (1992) also raised questions regarding the LHs of North American dwarfing lineages in relation to their increased hypsodonty indices and decreased body sizes (e.g., *Pseudhipparion simpsoni*). In contrast with the general scaling rule, he proposed that the small hipparionin *P. simpsoni* probably had a long lifespan, perhaps comparable to *Equus*, by means of its almost hypselodont cheek teeth (MacFadden, 1992). In a similar way, it has been suggested that high-crowned *Nannippu*s taxa or the larger *Dinohippus* had longer lifespans (Woodbourne and MacFadden, 1982; Hulbert, 1982) and presumably more delayed maturities (Woodbourne and MacFadden, 1982).

Since these first demographic surveys, the study of the LHs of extinct equids has long been set aside. Currently, however, new studies based on different approaches are shedding new light on this issue (Martinez-Maza et al., 2014; Domingo et al., 2018; Nacarino-Meneses and Orlandi-Oliveras, 2019).

1.3.2.2. Dental Eruption Pattern

Smith (2000) introduced the concept of Schultz's Rule, which states that the tooth eruption sequence is a trait that reflects the pace of LH. Although the observations were first made in primates (Schultz, 1935), Smith (2000) confirmed the trend and extended its validity to ungulates. In this context, long-lived mammals with slow growth rates tend to have a relatively late molar eruption compared with the premolar replacement. Conversely, an earlier eruption of molars relative to the permanent premolars is associated with faster growing taxa (Smith, 2000). The study of dental replacement, therefore, has the potential to provide insights into the LHs of extinct mammals (Harvati and Frost, 2007; Jordana et al., 2013; Gomes Rodrigues et al., 2017).

The relative emergence of the permanent dentition is quite similar within the equid family (Domingo et al, 2018). However, hipparionins erupt the lower third molar after the fourth premolar (Domingo et al, 2018), while in *Equus* the fourth premolar tends to be the last cheek tooth to erupt, although there is some variability (Smuts, 1974; Grubb, 1981; Hoppe et al., 2004). Domingo et al. (2018) related this late m3 eruption—coupled with an earlier p4 emergence—to a shorter durability of the decidual dentition (dp4) or, according to Schultz's Rule, to a slower LH in hipparionin horses. Because some authors have questioned the predictive value of Schultz's Rule, highlighting the effect of phylogeny on the tooth eruptive pattern (Veitschegger and Sánchez-Villagra, 2016; Monson and Hlusko, 2018), further studies are necessary to confirm the interpretation of a slower pace of growth in hipparionins from dental eruption.

1.3.2.3. Paleohistological Approach

The analysis of fossilized tissues (i.e., paleohistology) represents the most promising method for inferring the LH of extinct taxa (see section 1.4). Until recently, however, very few paleohistological studies reconstructed the LH of fossil equids (Martinez-Maza et al., 2014; Nacarino-Meneses and Orlandi-Oliveras, 2019), as previous descriptive work did not aim to infer aspects of LHs (Enlow and Brown, 1958; Sander and Andrássy, 2006).

Martinez-Maza et al. (2014) identified a similar but somewhat accelerated LH of *Hipparion concudense* compared to that of extant equids. They determined that individuals of this species might have reached skeletal maturity, and arguably sexual maturity, during their third year of life, by means of the observation of two cyclical growth marks before the deposition of slow-growing tissue in the bone periosteum. Moreover, they indicated that the older hipparionin individuals died at the age of ten, based on the counting of the total number of growth marks (Martinez-Maza et al., 2014). In this context, they suggested that larger *Equus* species tend to have longer lifespans and reach maturity later than *H. concudense* due to the scaling of LH traits with body size (Calder, 1984). More recently, Nacarino-Meneses (2018) provided a broad comparative sample for a proper inference of LH traits from equid bone and dental histology. While comparing metapodial histology of large-sized Middle Pleistocene *Equus* species with that of extant smaller representatives, Nacarino-Meneses and Orlandi-Oliveras (2019) found similar skeletal maturity times but increased growth rates in the metapodials of the larger taxa. In this study, the increased growth rate was suggested to be related to greater resource availability.

1.3.2.4. Ecological Preferences of Hipparionins

Because of their hypsodont teeth, hipparionins have traditionally been interpreted as open-habitat grazers comparable to extant equids (Stirton, 1947; MacFadden and Hulbert, 1988). More recently, however, hypsodonty has also been related to extended lifespans apart from a dietary adaptation (Veiberg et al., 2007b; Jordana et al., 2012; Witzel et al., 2018). Moreover, recent studies have indicated a broader spectrum of dietary and habitat preferences within this group (Hayek et al., 1992; Eisenmann, 1995; Fortelius and Solounias, 2000; Kaiser, 2003; Tütken et al., 2013; Semprebon et al., 2016). In this sense, the ecological diversity among hipparionins tends to resemble to which is exhibited nowadays by bovids (Gagnon and Chew, 2000), and contrasts with the more specialized strategies of living equids (Nowak, 1999).

Hipparionins that show morphological traits such as elongated metapodials, relatively high-crowned teeth, simple enamel plication, and reduced preorbital fossae—that are arguably related to the presence of an upper lip for selective feeding (Bernor et al., 1996)—have commonly been considered as being adapted to grazing in open and dry environments (Forsten, 1968, 1978b; Eisenmann, 1995; Bernor et al., 1996). Conversely, hipparionins with the opposite set of characters are usually associated with more forested landscapes and browse-dominated diets, as in the case of the primitive Vallesian *H. primigenium* populations of Central Europe (Forsten, 1968, 1978b; Bernor et al., 1988). Nonetheless, other Vallesian hipparionin forms were arguably more adapted to more open environments (Eisenmann, 1995; Bernor et al., 2003; Scott and Maga, 2005; Scott et al., 2013). However, recent isotopic and dental wear studies have shown that central European hipparionins followed rather opportunistic diets, feeding on browse and grass depending on availability (Kaiser, 2003; Wolf et al., 2012; Tütken et al., 2013; Johnson and Geary, 2016). As a result, these horses were able to dwell on a broad range of habitats (Kaiser, 2003; Tütken et al., 2013; Johnson and Geary, 2016).

In general, most western Eurasian Turolian hipparionins show characters such as gracile metapodials associated with open, dry environments (Forsten, 1968; Eisenmann, 1995). Analysis of micro and mesowear patterns suggest that these hipparionins were mainly grazers, but also to mixed feeders in some cases (Koufos et al., 2006, 2009; Solounias et al., 2010; Clavel et al., 2012; Merceron et al., 2016a) and even browsers (Kaiser et al., 2003). Notably, all isotopic studies point to the lack of C_4 grasses in the diet of the western Eurasian hipparionins during the late Miocene (Cerling et al., 1997; Van Dam and Reichart, 2009; Domingo et al., 2013; Rey et al., 2013; Tütken et al., 2013).

In this thesis, I aim to shed new light on the LHs and the ecology of the diverse hipparionin forms that inhabited the circum-Mediterranean area (see "Aims and Objectives"). My underlying purpose, moreover, is to integrate the concepts of LHT into a concrete case (hipparionin dwarfing) in order to determine the mechanisms and causes that drove the evolution of body size. In this thesis, I specifically focus my approach on the predictive model of Palkovacs (2003), which explains how changes on the environment trigger LH shifts, indirectly influencing adult body size (see section 1.2.1). To this end, paleohistological techniques were used to reconstruct the LHs of different-sized hipparionins, while microwear analyses have been performed to infer their probable ecology.

In Chapter 4 of this thesis, I study the metapodial histology of dwarfed hipparionins from the Balkan and the Iberian peninsulas and compare them with that of larger forms. By this, I reconstruct their growth patterns and explore, through the prism of the LHT framework, the body shifts that occurred. To gain further insights on the growth patterns and LHs followed by hipparionin horses, and especially by those that experienced size decrease trends, I subsequently analyze the dental histology of different-sized hipparionins from the Teruel Basin and compare it with a extant equid (Chapter 5). Next, I investigate the relationship between body size and the paleoecology of different hipparionins from various late Miocene localities (Chapter 6). This, moreover, helps me to evaluate the interpretations that have been made in the previous Chapters, and to further understand the ecological preferences that this group exhibited across the circum-Mediterranean area.

1.4. Paleohistology as a Method for Life History Inferences

Vertebrate hard tissues are formed in an accretional way, in most cases preserving a permanent growth record within their microstructure (Klevezal, 1996; Dean, 2000; Hogg, 2018). Dental formation can therefore be quantified through the analysis of the periodical increments present in enamel and dentine (Dean, 2000; Smith, 2006, 2008). Similarly, bone growth can be reconstructed through the identification of the embedded growth marks (Castanet et al., 2004; Woodward et al., 2013), and the information drawn from bone tissue typology and its vascular arrangement (de Margerie et al., 2004; Montes et al., 2010; Huttenlocker et al., 2013). Bone histology studies, however, should take into account the bone remodeling process (Enlow, 1962) and thus the probable lost record (Woodward et al., 2013). As the rates and timing of both dental and bone formation are strongly linked to the development of the organism, the analysis of fossilized tissues represents a powerful tool for reconstructing the growth strategies and LHs of extinct taxa (Chinsamy-Turan, 2005; Dean, 2006; Padian and Lamm, 2013; Hogg, 2018). Likewise, because of the environmental influences on LHs (selective pressures acting on LH traits, see section 1.2), paleohistology allows us to gain further insights into past ecological conditions (Castanet, 2006; Hogg, 2018).

1.4.1. Bone Paleohistology

Most of the studies that used bone histology to reconstruct the biology of extinct taxa have usually been centered on archosaurs (Chinsamy et al., 1995; Curry, 1999; Horner et al., 1999, 2000; Padian et al., 2001; Erickson et al., 2001, 2004; Horner and Padian, 2004; Chinsamy-Turan, 2005; Bybee et al., 2006; Sander et al., 2006; Lee and O'Connor, 2013; Woodward et al., 2015). The reason for this is that mammals were traditionally supposed to grow rapidly and continuously, leaving no marks on their bone cortex (Klevezal, 1996; Chinsamy-Turan, 2005). Because of the refutation of this belief (Castanet, 2006; Sander and Andrássy, 2006; Köhler et al., 2012) and the studies relating bone histology and LH in extant mammals (García-Martínez et al., 2011; Marín-Moratalla et al., 2013; Nacarino-Meneses et al., 2016ab; Calderón et al., 2019), there has been a recent increase in studies addressing mammalian paleohistology (Köhler and Moyà-Solà, 2009; Martinez-Maza et al., 2014; Amson et al., 2015; Kolb et al., 2015a; Moncunill-Solé et al., 2016; Orlandi-Oliveras et al., 2016; Nacarino-Meneses and Orlandi-Oliveras, 2019). Therefore, studies applying bone histology to fossil forms will enrich this field of research. For detailed information on the analysis of bone histology and the LH data obtained from it, refer to Methods (section 3.2.1.2).

1.4.2. Dental Paleohistology

As in the case of bone histology, the study of ungulates' dental tissues and its use for LH reconstruction have largely been unexplored. Indeed, almost all the studies that inferred the ontogenetic development and LH of extinct taxa from dental histology have focused on hominoids and other primates (e.g., lemurs) (Beynon et al., 1998; Dean, 2006; Dean et al., 2001; Ramirez-Rozzi, 1993; Schwartz et al., 2007, 2002; reviewed in Smith, 2008). Recently, however, this methodology has yielded interesting results for fossil species of other mammalian groups such as ungulates and proboscideans (Bromage et al., 2002; Dirks et al., 2009, 2012; Jordana and Köhler, 2011; Nacarino-Meneses et al., 2017). Moreover, current advances in our understanding of the formation of the higher-crowned teeth of ungulates (Iinuma et al., 2004; Kierdorf et al., 2013; Nacarino-Meneses et al., 2017; Witzel et al., 2018) provide a more solid framework for studying LH of extinct taxa through their dental histology.

The study of the dental histology of hipparionins may not only yield information on their LH but may also improve our understanding of the way in which their teeth grow. Because hipparionin dental tissues are frequently used for isotopic analyses, the characterization of their accretional growth will provide a better basis for future sampling protocols. For more information on the analysis of dental histology and the LH data that can be obtained from it, see Methods (section 3.2.1.3).

1.5. Microwear as a Method for Reconstructing Dietary and Habitat Preferences

The diet of an animal represents one of its most important direct links to the environment, and thus a central aspect of its ecology. In extinct mammals, tooth morphology provides a first broad idea of the tooth function and its possible diet (Lucas, 2004). Finer dietary reconstructions, however, are obtained through form-independent proxies such as analyses of stable isotopes (reviewed in Clementz, 2012) and dental wear. In this regard, isotopic studies of ungulates' enamel allows us to separate C_3 and C_4 plant consumers (Cerling and Harris, 1999). Since most plants following the C_4 photosynthesis pathway are grasses (Ehleringer et al., 1997; Tipple and Pagani, 2007), the isotopic signal on mammals' enamel related to C_4 plant consumption indicates a feeding preference for grazing (Cerling and Harris, 1999). However, isotopic analysis may not discriminate between grazing or browsing species if the plants consumed follow the same photosynthetic pathway (i.e., C_3 grasses). Dental wear studies, alternatively, can discern between feeding strategies by means of the macroscopic (Fortelius and Solounias, 2000) and microscopic (Walker et al., 1978; Solounias and Semprebon, 2002) wear signatures produced during food processing. Moreover, because of the association between dietary behavior and the availability of the consumed items (McNaughton and Georgiadis, 1986), dental wear studies have the potential to reconstruct past habitats through the exploration of the diets of herbivores (e.g., Ungar et al., 2007). Concretely, dental microwear analysis has proven to be a reliable method for inferring the diet of extant and extinct mammals (Walker et al., 1978; Solounias et al., 1988; Ungar, 1996; Solounias and Semprebon, 2002; Merceron et al., 2004; Scott, 2012; Scott et al., 2012). For detailed information on the microwear methodology used here, see Methods (section 3.2.2).

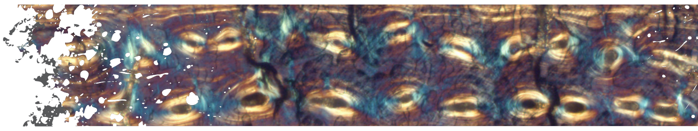

Chapter 2

Aims and Objectives

Chapter 2

Aims and Objectives

Hipparionin horses had an important ecological role in the late Neogene ecosystems of Eurasia as some of the more abundant and diverse primary consumers (Bernor and Lipscomb, 1995). Traditionally, most studies concerning Old World hipparionins have centered on their systematics, phylogeny, and biochronology (Forsten, 1968; Koufos 1987; Alberdi, 1989; Bernor et al., 1996; among others). More recently, however, an increasing number of studies have been devoted to reconstructing the hipparionin foraging ecology using micro- and mesowear analysis, as well as isotopes (e.g., Kaiser, 2003; Solounias et al., 2010; Tütken et al., 2013). The study of hipparionin LHs, on the other hand, has received little interest, even though it has a great potential to shed light on the ecological pressures that acted on these animals. In this sense, only a few studies have begun to explore this issue (Martinez-Maza et al., 2014; Domingo et al., 2018), but the obtained LH data have not yet been used to infer their ecological setting. Life histories are nevertheless a potential source of information on the ecological pressures when analyzed within the framework of LHT. Here I focus on this approach, while exploring the conspicuous body size decrease trends followed by some circum-Mediterranean hipparionins, which have long been overlooked from an ecological perspective.

This thesis aims, therefore, to fill the gap in the study of the LHs of this ecologically important group of ungulates. In particular, it addresses the differences in LH strategies and foraging ecologies associated with the hipparionin body size decrease trends. To this end, I reconstruct the LHs of different-sized hipparionins (especially of dwarfed forms) from the histological study of their bone and dental microstructure. The results will then be analyzed in the framework of LH theory. Therefore, I will apply the predictive model of Palkovacs (2003), which relates changes in LH with body size shifts, in order to infer the ecological pressures behind dwarfing in hipparionins. Following this model, a trend in body size decrease accompanied by a slow LH is predicted under low resource availability, while dwarfing associated with a fast LH is predicted to evolve under increased predation pressures (see section 1.2.1). Finally, I will test these predictions considering the inferred environments and the reconstructed resource preferences through the study of DMT (see Methods). In order to obtain data on hipparionin LH from paleohistological analyses, this thesis further relies on the inclusion of extant equids material in the sample studied, and on previous studies on extant mammalian bone and dental tissues (see sections 3.2.1.2 and 3.2.1.3), with special stresses on those performed on equids (Nacarino-Meneses, 2018).

This thesis seeks, therefore, to achieve the following specific objectives:

(I) Reconstruction of the growth pattern of bone/dental tissues in hipparionin horses, with a comparison between different-sized hipparionins and between hipparionins and extant equid species.

(II) Inferences on the LH strategies of the analyzed hipparionins, with particular emphasis on the dwarfed taxa, within the framework of Palkovacs' predictive LH model.

(III) Reconstruction of the foraging ecology of the hipparionin groups of different body sizes to test the interpretations obtained from the predictive model.

(IV) Relate the body size differences with differences in the LH strategies and/or the dietary preferences.

These goals are addressed in the following chapters:

Thesis Chapter	Objective Addressed
Chapter 4. Bone Histology Provides Insights into the Life History Mechanisms Underlying Dwarfing in Hipparionins	I, II, IV
Chapter 5. Dental Histology of Late Miocene Hipparionins Compared with Extant Equus, and its Implications for Equidae Life History	I, II
Chapter 6. Feeding Strategies of Circum-Mediterranean Hipparionins during the Late Miocene: Exploring Dietary Preferences Related to Size through Dental Microwear Texture Analysis	III, IV

Chapter 3

Materials and Methods

Chapter 3

Materials and Methods

3.1. Materials

I analyzed material from six hipparionin forms from western Mediterranean basins with body masses ranging from less than 40 kg to more than 150 kg (Ortiz-Jaureguizar and Alberdi, 2003). From the eastern Mediterranean basins, the hipparionins analyzed corresponded to four differentiated morphotypes (Vlachou, 2013), one of which typically weighed approximately 80 kg, while others and others easily surpassed 150 kg (Vlachou, 2013). The extant equid comparative material included specimens from different-sized horse varieties and three wild species that, on average, weigh 230 kg the smallest (*E. hemionus*) and 384 kg the largest (*E. grevyi*) (Ernest, 2003) (Table 3.1). Detailed information on the sample can be found in the following subsections.

In total, the entire sample analyzed in this thesis included 435 samples that correspond to 63 thin sections used for the analysis of the bone and dental microstructure, and 372 silicon molds used for the analysis of DMT. The sectioning and molding of the specimens were realized after obtaining the required permission.

3.1.1. Histological Analyses

Most of the thin histological sections came from fossil material (48 specimens, see Table 3.2). Additionally, 15 histological slides of extant equid elements were analyzed for comparative purposes (Table 3.2). Information on these specimens can be found in the following subsections, in Chapter 4 for the postcranial material, and in Chapter 5 for the dental samples.

Table 3.1.
Summary of the equid groups analyzed in this thesis and the total number of samples included, both histological sections and dental microwear molds. The mean body masses shown have been taken from Chapter 6 (a) and from Ernest (2003) (b). (*) The horse sample analyzed here comprises different varieties/breeds that actually differ on body mass.

WEST. MEDITERRANEAN HIPPARIONINS

AGE	GROUP	MEAN BODY MASS[a]	TOTAL NUMBER OF SAMPLES
Vallesian	?*primigenium* small	154 kg	13
	primigenium	200 kg	58
Turolian	*periafricanum*	31 kg	22
	gromovae	84 kg	48
	cf. *matthewi*	124 kg	20
	concudense	178 kg	30
	primigenium	192 kg	6

EAST. MEDITERRANEAN HIPPARIONINS (BALKANS + ANATOLIA)

AGE	GROUP	MEAN BODY MASS[a]	TOTAL NUMBER OF SAMPLES
Vallesian	*macedonicum*	92 kg	8
	primigenium	191 kg	19
Turolian	*macedonicum*	81 kg	79
	dietrichi	155 kg	52
	proboscideum	202 kg	48
	primigenium	256 kg	17

EXTANT EQUIDS

AGE	GROUP	MEAN BODY MASS[b]	TOTAL NUMBER OF SAMPLES
Extant	*E. ferus caballus*	300 kg*	4
	E. hemionus	230 kg	2
	E. grevyi	384 kg	2
	E. quagga	280 kg	7

Table 3.2.
Summary of the bone and dental thin sections analyzed in this thesis.

FOSSIL HIPPARIONINS

	CHAPTER 4	CHAPTER 5
WESTERN MEDITERRANEAN SPECIES	Nº OF METAPODIAL SLIDES	Nº OF LOWER MOLAR SLIDES
H. periafricanum	-	5
H. gromovae	8	6
H. concudense	-	6
H. primigenium truyolsi	1	-

EASTERN MEDITERRANEAN GROUPS	Nº OF METAPODIAL SLIDES
macedonicum morphotype	9
dietrichi morphotype	8
primigenium morphotype	5

EXTANT *EQUUS*

EXTANT SPECIES	Nº OF FEMUR SLIDES	Nº OF LOWER MOLAR SLIDES
E. ferus caballus	4	-
E. hemionus	2	-
E. grevyi	2	-
E. quagga	-	7

3.1.1.1. Fossil Hipparionins

All the fossils histologically studied herein correspond to isolated skeletal and dental elements. The sample does not include the bones of newborns or highly worn teeth. The isolated nature of the teeth favors their histological sampling, but precludes an unambiguous differentiation between some tooth types (Eisenmann et al., 1988). Therefore, the selected molars (see Chapter 5 for further information on the selection process) were divided into two categories: first/second lower molars in one category, and third lower molars on the other. The postcranial sample was composed of central metapodials, as these are far more common in fossil assemblages than other long bones (e.g., femurs), and are therefore more available for paleohistological analysis. Moreover, previous studies addressing bone histology on equids have endorsed the value of this element for LH reconstruction (Martinez-Maza et al., 2014; Nacarino-Meneses et al., 2016b) as it registers a similar number of cyclical bone growth marks (CGM) than the femur and presents less loss of register than other bones due to remodeling and resorption processes (Nacarino-Meneses et al., 2016b). In this thesis, metapodial histology has been explored in hipparionins from eastern and western Mediterranean basins, whereas dental histology has been studied in western Mediterranean taxa (Table 3.2). Information on the hipparionin diversity in these regions can be found in sections 1.1.2.1 and 1.1.2.2. Because this dissertation focuses on the body size differences within this group, dental and postcranial material has been always sampled in different-sized hipparionin forms (ordered from small to large in Table 3.2).

The metapodials of eastern Mediterranean hipparionins were accessed from the collections of the Laboratory of Geology and Paleontology of the Aristotle University of Thessaloniki (Greece). This material came from various late Miocene localities from the southern Balkans (see Chapter 4 for further information on the sample, and Appendix 1 in Chapter 6 for details of the fossil sites). Dental and postcranial elements of western Mediterranean hipparionins belong to the collections of the Institut Català de Paleontologia Miquel Crusafont (ICP, Barcelona). The analyzed teeth were found at the Concud and El Arquillo fossil sites, both situated in central-eastern Iberian Peninsula and dated on the middle and the late Turolian, respectively (van Dam et al. 2001) (see Chapter 5 for more information on the sample, and Appendix 1 in Chapter 6 for further details of the fossil sites). The sectioned metapodials mainly pertain to the smaller-sized *H. gromovae* from El Arquillo (Table 3.2), as previous studies have already explored the bone histology and LH of a larger Iberian hipparionin (i.e., *H. concudense*) (Martinez-Maza et al., 2014). These results on the bone histology of *H. concudense* will be compared and discussed in the light of the data obtained here.

3.1.1.2. *Extant* Equus

The extant *Equus* specimens used for comparison belong to four taxa: plains zebra (*E. quagga*), Grevy's zebra (*E. grevyi*), Asiatic wild ass (*E. hemionus*), and horse (*E. ferus caballus*). Within the horse sample, four domestic breeds of different body sizes are represented (Iceland, Welsh, Hackney, and Shetland). The postcranial material consists of femurs from these four domestic varieties, and from two wild species: the larger *E. grevyi* and the smaller *E. hemionus* (Table 3.2). These specimens were chosen to illustrate most of the diversity in body size shown by extant equids. Femurs have been considered in this case because, when available for sectioning, their use is preferred for growth reconstructions (Nacarino-Meneses et al., 2016b).

Dental histology has been analyzed in lower molars from *E. quagga* (Table 3.2). This species was selected in order to typify a standard extant equid that does not show any extreme LH adaptation within the group (Ernest, 2003), nor has it experienced artificial selection. Following the methods of Nacarino-Meneses et al. (2017), *E. quagga* teeth in different stages of wear were studied in order to reconstruct the entire dental growth (see Chapter 5 for more information).

The specimens came from various museum collections and pertained to wild, semi-captive, and captive equids. The femurs of domestic horses came from the Zoologisches Institut und Museum of Universität Kiel (Germany). The *E. hemionus* individuals lived in the Gobi Desert (Mongolia) and their remains belong to the Museum für Haustierkunde at the Universität Halle-Wittenberg (Germany). Most of the molars of *E. quagga* and one of the femurs of *E. grevyi* are part of the collection of the Zoologisches Museum of the Universität Hamburg (Germany) and pertained to animals from the Hagenbeck Zoo (Hamburg). The *E. quagga* molar MZB-94-1229 was taken from an individual that lived at Barcelona Zoo whose skeleton is now at the Museu de Ciències Naturals de Barcelona. The rest of the material came from semi-captive *E. grevyi* and *E. quagga* specimens from the Réserve Africaine de Sigean (France), whose remains are stored at the collections of the Institut Català de Paleontologia (ICP).

3.1.2. Microwear Texture Analyses

The study of the microwear signature has been addressed through 3D dental microwear texture analysis (DMTA) (see section 3.2.2 for detailed information on this method). The enamel texture has been quantified from molds of the enamel facets of hipparionin cheek teeth. The molding was conducted on isolated specimens and on teeth present in the maxillae and mandibles. For preference, second upper and lower molars were selected, although other cheek teeth have also been sampled as dental microwear texture (DMT) does not vary significantly along the tooth row

(Ramdarshan et al., 2017). Deciduous, unworn, and very worn teeth were dismissed. In all cases, only one facet per specimen was considered. In total, the sample comprised 372 scanned molds after discarding those showing post-mortem alterations (see section 3.2.2.1).

As in the histological analyses, the microwear sampling was performed on different-sized hipparionins from the circum-Mediterranean basins. The specimens came from Vallesian and Turolian localities from both sides of the Mediterranean, particularly from sites that yielded rich and diverse hipparionin assemblages (Table 3.3). In comparison with the sample analyzed histologically, material was also included from the western Anatolian Turolian. The eastern Mediterranean specimens were then divided into those from the Balkans and from Anatolia considering the faunistic differences found in these areas for most of the late Miocene (Kostopoulos, 2009).

Table 3.3.
Summary of the dental molds analyzed in this thesis.

CHAPTER 6

VALLESIAN HIPPARIONIN GROUPS

WEST. MEDITERRANEAN	Nº OF MOLDS	LOCALITIES SURVEYED
?*primigenium* small	13	Santiga
primigenium	58	Can Llobateres, Can Poncic

EAST. MEDIT. (BALKANS)	Nº OF MOLDS	LOCALITIES SURVEYED
macedonicum	6	Pentalophos, Ravin de la Pluie, Nikiti-1
primigenium	14	Pentalophos, Ravin de la Pluie, Nikiti-1

TUROLIAN HIPPARIONIN GROUPS

WEST. MEDITERRANEAN	Nº OF MOLDS	LOCALITIES SURVEYED
periafricanum	17	El Arquillo
gromovae	34	El Arquillo
cf. *matthewi*	20	Venta del Moro
concudense	24	Concud
primigenium	5	El Arquillo

EAST. MEDIT. (BALKANS)	Nº OF MOLDS	LOCALITIES SURVEYED
macedonicum	45	Nikiti-2, Ravin des Zouaves-5, Perivolaki, Dytiko
dietrichi	31	Nikiti-2, Perivolaki, Dytiko
proboscideum	20	Ravin des Zouaves-5, Hadjidimovo, Perivolaki
primigenium	17	Hadjidimovo

EAST. MEDIT. (W. ANATOLIA)	Nº OF MOLDS	LOCALITIES SURVEYED
macedonicum	27	Gülpınar, Şerefköy-2, Samos new Collections
dietrichi	13	Gülpınar, Samos new Collections
proboscideum	28	Şerefköy-2, Samos new Collections

The hipparionins were organized into groups following Vlachou (2013) morphotypes for the eastern Mediterranean forms, and following specific and body size differences in the western ones (Table 3.1 and 3.3). Detailed information on all the analyzed hipparionins and the fossil localities can be found in Appendix 1 and 2 in Chapter 6.

The western Mediterranean sample were accessed from the collections of the Institut Català de Paleontologia and the Museo Nacional de Ciencias Naturales (Madrid). The Balkan material belongs to the collection at the Laboratory of Geology and Paleontology of the Aristotle University of Thessaloniki, except for the specimens from Hadjidimovo, which are part of the Asenovgrad Paleontological Museum (pertaining to the National Museum of Natural History of Sofia, Bulgaria). The Samos sample came from the Paleontological Museum of Mytilinii (Greece) and the sample from Anatolia came from the Natural History Museum of Ege University of Izmir (Turkey).

3.2. Methods

3.2.1. Histological Analyses

3.2.1.1. Histological Sections of Bones and Teeth

Because most histological procedures either partially or completely destroy the specimen, all of its details were recorded in order to avoid the loss of valuable information (Lamm, 2013). This meant that the entire sample—both extant and fossil material—was photographed and measured before the histological sectioning. In addition, casts of the complete specimens, or of their extracted portions, were taken in many cases. To the fullest possible, fragmentary fossils of undoubted assignment and preserving the surface of interest were selected to prevent the destruction of complete specimens. All the associated information, measurements, photographs, and casts of the fossil and extant material were stored and are available in the database of the Evolutionary Paleobiology department of the ICP.

The first step in obtaining of the histological thin sections was to embed the specimens, or part of them, in epoxy resin (Araldite 2020). Teeth of extant equids were previously removed from the mandibles where they were inserted, following a dehydration treatment with different alcohol solutions (24 hours curing at concentrations of 70%, 96% and 100%). Next, these teeth were completely encased in resin, like in the case of the isolated fossil teeth (Fig. 3.1A). On the other hand, only mid-shaft chunks of long bones were embedded (Fig. 3.1A). These long bone sections of approximately 3 cm were extracted using a hand-held rotary tool (Navfram N120). The surfaces of interest of all the specimens were then exposed using an Isomet low-speed saw (Buehler)

(Fig. 3.1B). Bone blocks were transversely cut through the mid-shaft (Fig. 3.1C), while teeth were cut longitudinally in the bucco-lingual plane through the protoconid cusp (Fig. 3.1D). Some highly curved molars were first sectioned transversally to allow two longitudinal cuts covering the entire tooth height (Fig. 3.1D). The exposed surfaces were then polished with carborundum powder of decreasing particle size (350, 800, and 1,000 grit) or with a grinder-polisher (Buehler, MetaServ 250) (Fig. 3.1E). Afterwards, the polished blocks were glued to a frosted glass slide using either epoxy resin or ultraviolet curing glue (Loctite 352). Finally, the thin sections were obtained after cutting the mounted samples down to a thickness of ~ 300 µm with a PetroThin diamond saw (Buehler) (Fig. 3.1F) before grinding them to ~ 150 µm using the PetroThin's polisher disc. Thin sections were posteriorly polished again, using the carborundum powder or the grinder-polisher, down to a thickness of ~ 100 µm for bones and to 70-120 µm in the case of teeth. This allowed their histological features to be observed under the microscope. Before covering the slides, water was removed using alcohol baths of increasing concentrations and with a clearing agent (Histo-Clear II). Finally, the thin sections were covered with the same epoxy resin or with a DPX medium (Scharlau) in order to enhance their preservation and visualization. These procedures were carried out at the thin section laboratory of the ICP.

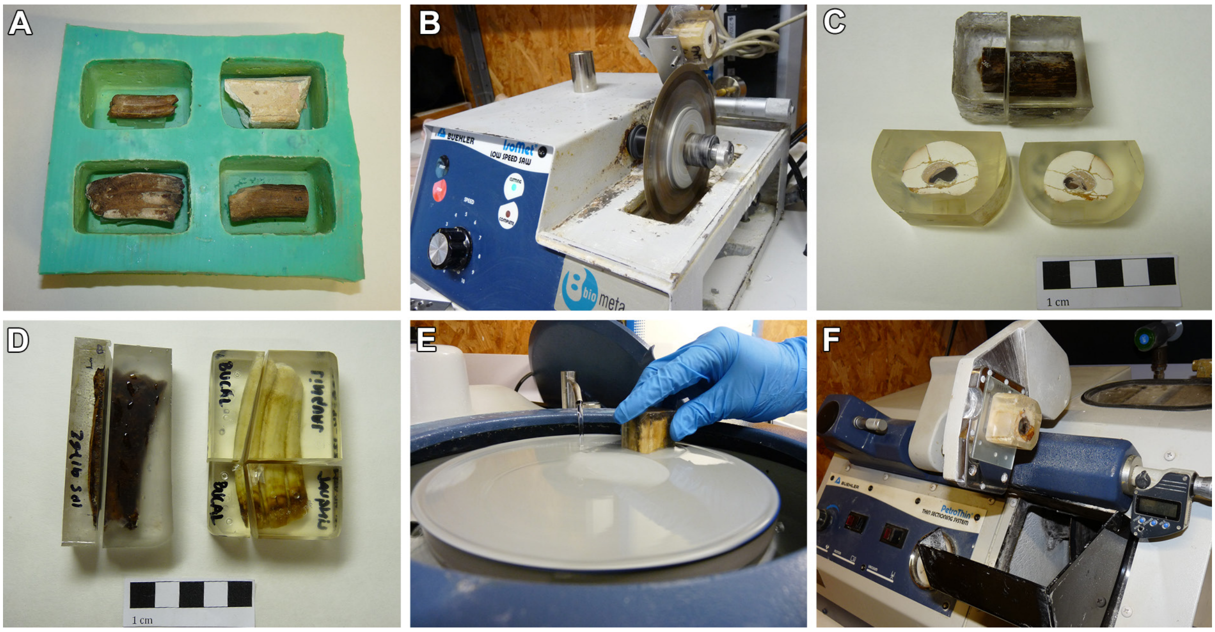

Figure 3.1.
Paths followed for the obtainment of the histological thin sections. **A)** Specimens are embedded in epoxy resin. **B)** The resin blocks containing the specimens are cut using a low-speed diamond saw. **C)** The mid-shaft region is exposed from the bone blocks. **D)** Teeth are sectioned longitudinally through the protoconid, but with a previous transverse cut in those curved specimens. **E)** Grinder-polisher machine used for polishing the resin blocks before gluing them to the glass slides. **F)** The thin sections are performed and ground by a PetroThin saw. All photographs were taken at the ICP thin section laboratory.

The histological slides obtained were observed using circularly polarized light in a Zeiss Scope A1 microscope. This type of microscopy uses emitted light beams which are modulated by two filters: the polarizer, which is situated between the light and the thin section, and the analyzer, situated between the thin section and the observer or camera. When there is no sample, or the specimen is formed by an isotropic material, the light emitted by the polarizer is blocked by the 90º vibration direction of the analyzer. In contrast, if the material is birefringent, such as the bone collagen and the crystallites of the enamel, the vibrational direction of the light is modified by the sample, and the light crosses the analyzer forming an image (Bromage and Werning, 2013). Therefore, this specific filter alignment increases the contrast, and allows us to obtain further insights into the arrangement of the tissues observed (Bromage et al., 2003; Bromage and Werning, 2013). Moreover, bone tissues were analyzed using the retardation lambda filters (λ and ¼λ), which delay the received wavelength and add color allowing for better discernment of the histological features (Turner-Walker and Mays, 2008). The images of bone and dental tissues were acquired with a digital camera (AxioCam ICc5) attached to the microscope and processed with ZEN 2011® software (Carl Zeiss). The compound images were adjusted and merged using Adobe Photoshop®.

3.2.1.2. Bone Histology Analysis

Bone is a dynamic tissue that experiences changes during the lifetime of the animal. Its histomorphology is influenced by factors related to ontogeny, mechanics, phylogeny, and the environment (Padian, 2013).Variations in the organisms' physiology are reflected in the bone microstructure by the deposition of growth marks and by changes in the growing matrix and its vascularization (Castanet, 2006; Huttenlocker et al., 2013). Taking all this into account, researchers can get information from extinct taxa that could not be approached in any other way (Padian, 2013). Regarding our interest in LH reconstruction, bone histology analyses have provided insights on key LH traits such as the age at maturity, the age at death, and the growth rate (Castanet, 2006; Marín-Moratalla et al., 2011; Cubo et al., 2012; Marín-Moratalla et al., 2013; Lee et al., 2013; Nacarino-Meneses et al., 2016ab; Calderón et al., 2019).

Bone Tissues

In this thesis, I follow the classification and nomenclature on bone histology detailed in Francillon-Vieillot et al. (1990) and Ricqlès et al. (1991). During the ossification process, the first bonel tissue deposited constitutes the primary bone (Currey, 2002). Three main types of primary bone matrices can be differentiated: the woven-fibered, the parallel-fibered, and the lamellar-fibered.

Woven bone represents a highly vascularized tissue composed of randomly and loosely arranged collagen fibers (Fig. 3.2A), while lamellar bone is a highly organized tissue with little or no vascularization, which is formed by thin layers of closely packed collagen fibers (i.e., lamellae) deposited in alternating directions (Fig. 3.2A). When the collagen fibers are oriented in the same direction, the tissue is referred as parallel-fibered bone (PFB) (Francillon-Vieillot et al., 1990; Weiner and Wagner, 1998; Huttenlocker et al., 2013). The aggregate of woven and lamellar matrices constitutes a complex known as fibrolamellar bone (Fig. 3.2A, B, and C) (de Ricqlès et al., 1991), which composes most of the long bone cortex in large mammals (Marín-Moratalla et al., 2013; Kolb et al., 2015b). The fibrolamellar-complex (FLC) can then be classified into different categories taking into account the orientation of the vascular canals filled with lamellar bone (i.e., primary osteons) (Francillon-Vieillot et al., 1990).

From the study of the bone matrix typology and vascularization patterns, we can extract information regarding the bone growth rate (Francillon-Vieillot et al., 1990; de Ricqlès et al., 1991; de Margerie et al., 2002; Huttenlocker et al., 2013). The relationship between these histological traits and the velocity of bone deposition is commonly referred as “Amprino’s rule”, since it was first identified by Rodolfo Amprino (1947). Thereafter, a series of quantitative studies demonstrated the validity of this pattern (Castanet et al., 2000; de Margerie et al., 2002, 2004; Montes et al., 2010). In this sense, the matrix with the fastest depositional rate is the woven-fibered bone, while at the other extreme there is the slow-growing lamellar bone (Francillon-Vieillot et al., 1990; Weiner and Wagner, 1998; Castanet et al., 2000; de Margerie et al., 2002; Huttenlocker et al., 2013). Other tissue types present intermediate growth rates: parallel-fibered tissue is also laid down somewhat slowly, while the FLC shows particularly high depositional rates (Huttenlocker et al., 2013). The orientation of the vascular canals also provides information on the relative rate at which the bone was deposited, although the link is not as significant as when considering the different matrix typologies and their vascularization content (de Margerie et al., 2004; Lee et al., 2013). For instance, FLC with numerous radial canals, known as radial FLC (Fig. 3.2B), is generally associated with faster rates of growth compared to that with longitudinal canals or with more circular ones (Fig. 3.2C), which is known as laminar FLC (de Margerie et al., 2004).

The primary tissue can be posteriorly resorbed due to modeling and remodeling processes, which lead in most cases to the deposition of secondary bone (Currey, 2002). Bone remodeling results in the formation of secondary osteons or Haversian Systems (HS) (Currey, 2003), while bone modeling generally entails the resorption of the medullary cavity and the posterior deposition of endosteal bone (EB) (Chinsamy-Turan, 2005) (Fig. 3.2D). Because of these processes, the growth record registered in the primary bone is sometimes partially or completely erased.

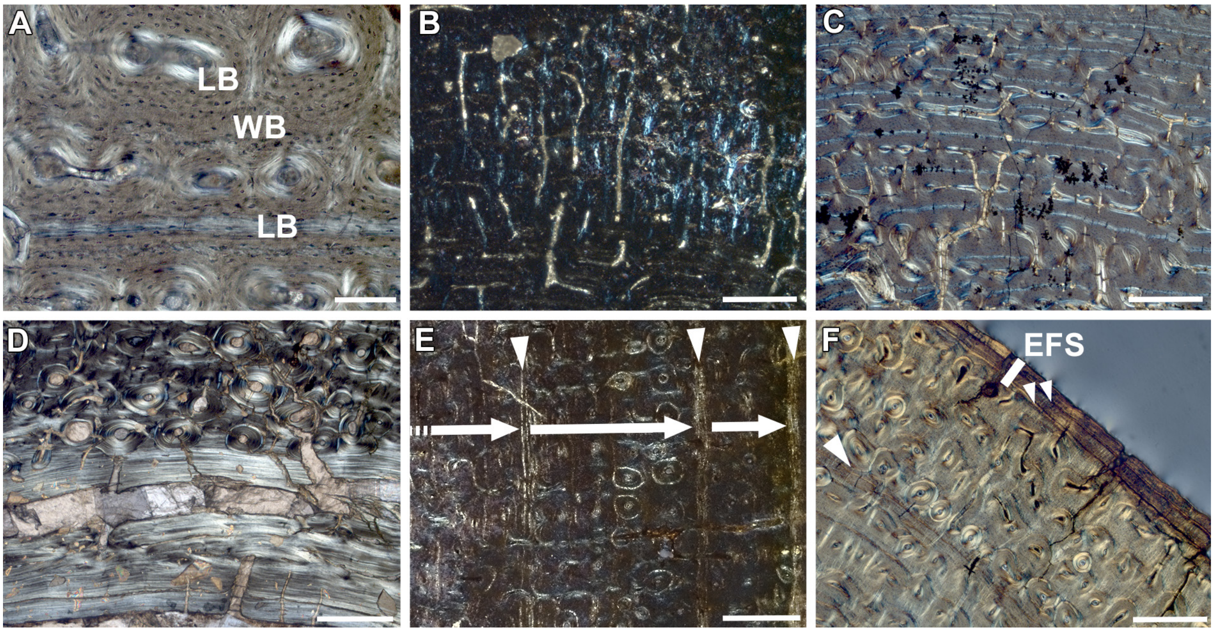

Figure 3.2.
Micrographs showing bone histology features. All micrographs were done under polarized light and with a ¼λ filter. The scales shown represent 500 µm unless indicated. **A)** Woven bone (WB) and lamellar bone (LB) conforming a fibrolamellar tissue on the bone cortex of a *Hipparion gromovae* metacarpal (IPS-96275). Lamellar bone shows an alternating dark and bright pattern because of the characteristic disposition of the collagen fibers. Scale bar = 100 µm. **B)** Fibrolamellar bone complex with radial vascular canals on the cortex of a *Hipparion philippus* metatarsal (PER-1211). **C)** Fibrolamellar bone complex predominantly showing circularly arranged vascular canals, *Hipparion gromovae* metacarpal (IPS-96274). **D)** Secondary bone tissues near the medullary cavity of a *Hipparion primigenium truyolsi* metatarsal (IPS-28842). At the top, secondary lamellar tissue is infilling the Haversian Systems or secondary osteons, and at the bottom it conforms the endosteal bone (EB) deposited in the inner cavity. **E)** Growth zones (long arrows) separated by growth marks (signaled by arrow heads) in the cortex of a metatarsal of *Hipparion* aff. *platygenys* (DTK-106). **F)** External fundamental system (EFS) found in the periosteal surface of the metatarsal IPS-28842. Arrowheads signal the growth marks.

Growth Marks

The "time factor"—crucial for the inference of the LH traits—is revealed by skeletochronology, the study of CGMs (Castanet, 2006; Woodward et al., 2013). These histological features illustrate periods of reduction or cessation of bone growth (annuli and lines of arrested growth, respectively) occurring cyclically (Klevezal, 1996; Chinsamy-Turan, 2005; Woodward et al., 2013). Non-cyclical growth marks, on the other hand, record exceptional periods of physiological stress such as birth or weaning (Castanet et al., 2004; Nacarino-Meneses and Köhler, 2018). It is well-established that the CGMs denote an annual rhythm of bone deposition influenced by the photoperiod (Peabody, 1961; Castanet et al., 1993, 2004). These physiological cycles are conspicuous in different taxonomic groups of vertebrates, and are synchronized with seasonal variations of environmental resource availability (Köhler et al., 2012). The identification, counting, and quantification of all the bone growth marks allow the reconstruction of the growth trajectory of a vertebrate when the entire bone growth record is considered. From this, we can infer how fast the organism was growing, when it reached maturity, and how many years it lived (Castanet et al., 2004; Lee et al., 2013; Marín-Moratalla et al., 2013; Woodward et al., 2013, 2015).

Growth Reconstruction

The growth variations that occur during ontogeny are recorded on the bone tissues as growth marks and as changes in the histological organization (Huttenlocker et al., 2013; Jordana et al., 2016). During embryonic development, the bones of mammals are entirely composed of fast-growing woven tissue (Klevezal, 1996). After birth, a growth line signaling this event is recorded (Nacarino-Meneses and Köhler, 2018) and the vascular canals of the woven matrix start to be filled by lamellar bone, thus becoming a fibrolamellar tissue (Francillon-Vieillot et al., 1990; de Ricqlès et al., 1991). Posteriorly, juveniles of large mammals (that grow over several years) tend to deposit thick zones of FLC—separated by CGMs (Fig. 3.2E)—reducing the zone thickness as the growth rate begins to decrease (Marín-Moratalla et al., 2013). Finally, a layer of slow-growing lamellar bone is laid down in the periosteum when maturity is reached, forming the external fundamental system (EFS) (Fig. 3.2F) (Cormack, 1987; Huttenlocker et al., 2013).

Taking this into account, the age at maturity can be determined by counting the CGMs present before the deposition of the lamellar EFS (Woodward et al., 2013). Some researchers have further attributed this tissue transition to the attainment of physiological and reproductive maturity (Köhler and Moyà-Solà, 2009; Marín-Moratalla et al., 2011, 2013; Jordana et al., 2016), as EFS formation may indicate the channeling of energy from growth to reproduction (Stearns, 1992). Indeed, the formation of this structure in the femur of extant equids, but not in other bones, has been correlated with the age of first reproduction (Nacarino-Meneses et al., 2016b). Alternatively, the decrease in periosteal growth signals epiphyseal closure and the finalization of the longitudinal growth in most other bones such as metapodials (Nacarino-Meneses et al., 2016b). The age at death is another trait that can be determined, in this case through the count of all the CGMs present in the bone (Woodward et al., 2013). Insights into the growth rate, on the other hand, can either be obtained from the observation of the bone tissues (qualitative) or through quantification of surface areas, perimeters, or distances between CGMs (Lee et al., 2013).

There are, however, limitations associated with all these skeletochronological analyses, which are chiefly linked to the bone resorption and remodeling processes that erase the growth record later on in the ontogeny (Woodward et al., 2013). It is therefore essential to dispose of juvenile specimens in order to know the modifications experienced and to reconstruct the growth marks that may have been lost. In this regard, the obscured growth marks are usually retrocalculated by superimposing the register of juvenile individuals with that of adult ones (Woodward et al., 2013; Nacarino-Meneses et al., 2016a). The low accuracy of the age determination in older individuals represents another problem (Klevezal, 1996; Castanet et al., 2004; Castanet, 2006), partly because of the difficult recognition and doubtful significance of growth marks within the EFS—as the cyclical nature of the growth marks deposited there has not yet been proven (Horner et al., 1999).

The bone histology analyses performed in this thesis have been focused on the quantification of the bone growth marks and the qualitative analysis of bone tissues in hipparionin metapodials. From the measure of the growth mark perimeters, it has been modeled the metapodial growth trajectory using non-linear growth curves (Ricklefs, 1967; Zullinger et al., 1984) (see Chapter 4 for further details). The identification and measure of the neonatal line in these metapodials (Nacarino-Meneses and Köhler, 2018) allowed a timezero point for the curves. From these growth reconstructions, a relative age at skeletal maturity was obtained and different growth parameters were calculated. Moreover, the growth rate in relation to body size in extant equids has been determined for comparison. A general measure of the growth rate was calculated through the quantification of the growth between the first and second CGM. All the measurements were taken with Image J 1,48v software (Schneider et al., 2012). The growth curves of the fossil metapodials were fitted with the non-linear least squares fitting of the PAST software (Hammer et al., 2001), and all the analyses and graphs were performed using PAST and Microsoft Office Excel® (the graphs were posteriorly redrawn using Adobe Illustrator®).

3.2.1.3. Dental Histology Analysis

Analyzing the dental microstructure provides another source of information on the growth patterns and LH of extinct vertebrates (Dean, 2006; Smith, 2008; Hogg, 2018). Teeth are composed of enamel, dentine, and cement (Fig. 3.3A) (Hillson, 2005; Nanci, 2008), three tissues that preserve in their structure a growth record in the form of incremental features (Klevezal, 1996; Risnes, 1998; Dean, 2000; Smith, 2008). The quantification of these increments allows the calibration of the growth of the tissue and, by extension, that of the tooth and the whole organism (Hillson, 2005; Hogg, 2018). Cement is a slow-growing mineralized tissue that has a similar composition to bone (Hillson, 2005); accordingly, it registers annual marks comparable to the CGMs of bone tissues (Klevezal, 1996). On the other hand, enamel and dentine are secreted at a faster rate and contain different types of increments of shorter periodicity, predominantly of circadian and supra-daily rhythmicity (Fitzgerald, 1998; Dean, 2000; Smith, 2006). These similarly recurring marks in enamel and dentine are considered to be the result of the same underlying rhythms of the tissues' secretory activity (Fitzgerald and Rose, 2008). Because of the simpler pattern of enamel, and its resistance to alterations due to a higher mineral content (Dauphin and Williams, 2004), most studies that addressed the reconstruction of dental development have focused on this tissue (Hillson, 2005; Fitzgerald and Rose, 2008).

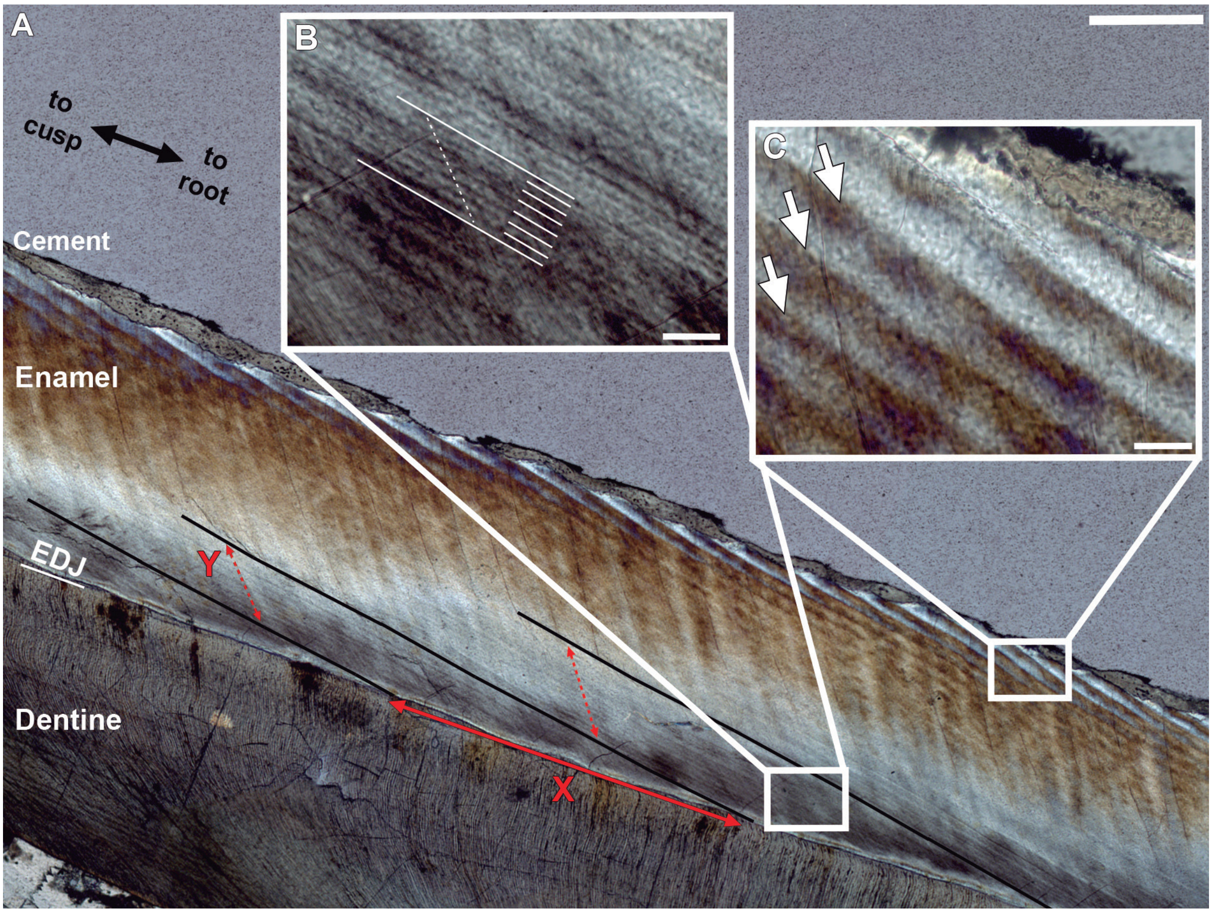

Figure 3.3.
Dental histological features and methodology used to assess the enamel formation parameters. Micrographs were taken on the buccal enamel band of a *Hipparion periafricanum* first/second molar (IPS-91734) using polarized light microscopy. **A)** General view showing the dental tissues that compound an equid tooth. Three enamel incremental marks are outlined (black lines) to show the method used to quantify the crown extension rate: the distance through the enamel dentine junction (EDJ) that separates two incremental marks (X) is divided by the time that it required for being formed, in turn calculated by measuring the amount of enamel that separates these lines through the prism course (Y) divided by the daily secretion rate. Scale = 0.5 mm. **B)** Close-up showing enamel prisms (dashed line shows the prim's direction) and laminations (continuous white lines). The daily secretion rate is estimated by dividing the distance that separate a set of daily increments, following the prism course, by the total number of laminations. Scale = 50 μm. **C)** Close-up showing long-term Striae of Retzius (signaled by white arrows) clearly identifiable at the outer enamel surface. Scale = 50 μm.

Enamel formation starts with the differentiation of ameloblasts on the dentine horns, which will constitute the future tooth cusps. Once differentiated, ameloblasts begin to secrete an organic matrix and the precursors of the enamel crystallites on top of the dentine (Nanci, 2008). This deposition makes the ameloblasts move away from the enamel dentine junction (EDJ) toward the future enamel outer surface, thickening the enamel layer (appositional growth). Simultaneously, adjacent ameloblasts begin to differentiate and extend from the cusp toward the cervical portion of the tooth (Thesleff, 1995), thus making the crown increase in height (extension growth) (Smith, 2008; Hogg, 2018). After the first phase of matrix secretion, it follows the maturation stage of amelogenesis. At this moment, the proteins and water of the enamel matrix are removed, and the enamel crystallites expand significantly (Lacruz et al., 2017). The resulting organized bundles of crystallites form the basic unit of dental enamel, the prism (Hillson, 2005; Smith, 2006). It is within the prism's structure that we find some of the incremental markings derived from the rhythmical fluctuations of amelogenesis (Hillson, 2005; Smith, 2006; Lacruz et al., 2012).

Three different types of marks have been differentiated depending on their cyclicity: sub-daily, daily, and supra-daily lines (Dean, 2000; Smith, 2006; Kierdorf et al., 2014). The best-known features of daily periodicity are cross striations, which appear as bright and dark bands crossing the enamel prism perpendicularly (Bromage, 1991; Dean, 2000; Smith, 2006; Hogg, 2018). While these marks are the most conspicuous daily increments present in primate enamel, in ungulates the main short-period lines are laminations (Tafforeau et al., 2007; Jordana and Köhler, 2011; Kierdorf et al., 2013, 2014). Unlike cross-striations, laminations appear as closely spaced bands that follow the course of the enamel formation front obliquely to the EDJ (Fig. 3.3) (Tafforeau et al., 2007; Kierdorf et al., 2013). Via fluorescent labeling experiments, both types of daily increments have been shown to contain sub-daily marks between them (Smith, 2006; Kierdorf et al., 2014). Finally, the Striae of Retzius are the increments caused by supra-daily growth discontinuities. These incremental marks signal successive positions of the enamel formation front as the growth discontinuities affect all the active ameloblasts simultaneously (Risnes, 1998; Smith, 2006). Because of their long-term periodicity, it is possible to identify laminations running parallel between successive Retzius lines. The secretion fluctuations underlying this supra-daily pattern have been hypothesized to result either from the interaction between two short-period rhythms (Newman and Poole, 1993; Smith, 2006) or from the expression of an independent rhythm generated by the internal clock that modulates bone and dental formation (Bromage et al., 2009, 2016).

Enamel Formation Parameters

By using the incremental markings of known periodicity, we can reconstruct the entire enamel development and calculate the parameters that characterize the rate and timing of tooth formation (Smith, 2008; Hogg, 2018). To do this, we should consider the way in which enamel is formed and then determine (i) its appositional rate, daily secretion rate (DSR), (ii) and the rate of increase in crown height—the enamel extension rate (EER) (Smith, 2008). Moreover, we can quantify the total time that it takes the enamel band to be formed, which is known as the total crown formation time (CFT). In all cases, these parameters have been assessed here in the buccal enamel band of the protoconid to standardize and allow comparisons (Nacarino-Meneses et al., 2017) since the enamel formation parameters may differ between cusps and enamel bands (Kierdorf et al., 2013).

The DSR defines the amount of enamel secreted per ameloblast every day (Smith, 2008), and its calculation relies on assuming the circadian nature of enamel laminations, as has been demonstrated (Smith, 2006; Kierdorf et al., 2013). This parameter is therefore calculated by measuring the distance that separates various laminations through the prism length, and then dividing it by the number of days that it took for these marks to be formed (Fig. 3.3B). Many random measures within the total tooth length and at different enamel zones have been performed, since the DSR have been shown to vary between different enamel portions (Smith, 2008; Metcalfe and Longstaffe, 2012; Kierdorf et al., 2013). Thus, it has been obtained a representative mean that includes all the variation.

The EER represents the daily rate of crown height increase, which is determined by the length of the cohort of the differentiated ameloblasts secreting enamel (Shellis, 1984; Smith, 2008). This parameter has been measured here by dividing the EDJ length between two accentuated incremental marks (X, Fig. 3.3A) by the days required to form that distance (Smith, 2008; Jordana and Köhler, 2011). This formation time is in turn calculated by dividing the space that separates these two lines through the prism's course (Y, Fig. 3.3A) by the previously measured DSR. By repeating this process along the entire EDJ, the EER of different tooth portions is obtained. By this method, the CFT can be determined by adding up all the days that it takes to form the entire tooth crown. Finally, based on the equid dental formation model of Nacarino-Meneses et al. (2017), the eruption time has been inferred through the reconstruction of the dental growth. Concretely, the eruption can be recognized by identifying the significant decrease in the EER (Nacarino-Meneses et al., 2017) (see detailed information in Chapter 5).

Because of the well-known relationship between dental development and life history (Dean, 2006; Dirks and Bowman, 2007; Hogg and Walker, 2011), all these data on dental formation provide insights into certain aspects of the LH strategy of extinct taxa (Dean, 2006; Dirks et al., 2009; Jordana and Köhler, 2011). For instance, values that characterize faster forming teeth (high EERs) are exhibited by extant species that wean early (Hogg and Walker, 2011), have an advanced foraging independence (Godfrey et al., 2001), or an early age at first reproduction (Jordana et al., 2014)—all aspects of faster LHs. The eruption timing also represents a good proxy for the determination of the pace of LH (Smith, 1991a, 2000; Dean, 2006), as in some tooth types it matches key LH events such as weaning (Smith, 1991b; Dirks and Bowman, 2007) and the attainment of maturity (Engström et al., 1983; Dean, 2006).

The measurements used to calculate the DSR were here taken using ZEN 2011® software (Carl Zeiss), while those to assess the EER and the CFT were performed with Image J 1,48v (Schneider et al., 2012). DSR differences were tested by non-parametric Kruskall-Wallis tests using

PAST software (Hammer et al., 2001) as data did not always meet normality thresholds. Because of the EER diminution from cusp to cervix (Jordana and Köhler, 2011; Nacarino-Meneses et al., 2017), the EER differences between hipparionin species were explored via ANCOVA analyses after testing for the model's assumptions (see Chapter 5 for further details). The statistical tests and the graphs were done using IBM SPPS Statistics 20® and, in the case of the graphs, posteriorly redrawn using Adobe Illustrator®. The significance level of all tests was set to $\alpha = 0.05$.

3.2.2. Dental Microwear Texture Analysis (DMTA)

Dental microwear analysis has proven to be a reliable technique to infer the diet of extant and extinct mammals (Walker et al., 1978; Solounias et al., 1988; Ungar, 1996; Solounias and Semprebon, 2002; Scott, 2012). It is based on the principle that food items produce characteristic microscopic scars on the wear facets during mastication. These microwear features reflect the physical and mechanical properties of the food (hardness, toughness, and abrasiveness) (Schulz et al., 2013; Merceron et al., 2016b; Ramdarshan et al., 2016). For instance, the processing of tougher materials (e.g., grasses) tends to yield more scratches in the wear surface, while the major presence of pits indicates the consumption of harder or more brittle items (e.g., woody browse) (Solounias and Semprebon, 2002). Because of the turnover of the enamel surface, this signal generally reflects the properties of the items ingested during the last days or weeks of the animals' life (Teaford and Oyen, 1989; Teaford et al., 2017).

Microwear studies have usually involved the observation of the wear surfaces in 2D using scanning electronic microscopy or light microscopy, so the microwear features were characterized and quantified semi-automatically (Walker et al., 1978; Solounias and Semprebon, 2002; Merceron et al., 2004; DeSantis et al., 2013). In a pioneering paper, Ungar et al. (2003) described a new approach in which the whole 3D microwear texture is scanned using confocal microscopy and then automatically quantified through Scale-sensitive fractal analysis (SSFA). This method, known as dental microwear texture analysis (DMTA), was later developed by Scott et al. (2005, 2006) and has proven to generate more objective, robust, comparable, and repeatable results than previous 2D approaches (DeSantis et al., 2013). To date, DMTA has been extensively applied to many extant and extinct taxa pertaining to a broad range different groups (see reviews on DMTA studies in Calandra and Merceron, 2016 and DeSantis, 2016).

3.2.2.1. *Specimens Molding and Scanning*

The microwear texture is analyzed from molds rather than directly from the enamel facets. As stated in section 3.1.2, the molds were preferably taken from second upper and lower molars, but in some cases other cheek teeth were selected (after discarding those specimens showing taphonomical alterations). Before the molding, the dental occlusal surfaces were cleaned with acetone-soaked cotton swabs to remove dust and glue. Thereafter, molds of the dental facets were made with a silicone material (polyvinyl siloxane, President Regular Body, Coltène-Whaledent).

The obtained vinyl impressions (Fig. 3.4A) were then examined with a white-light confocal profilometer Leica DCM8 equipped with a x100 lens (numerical aperture = 0.90; working distance = 0.9 mm) (Fig. 3.4B, "TRIDENT" at PALEVOPRIM lab CNRS, Université de Poitiers). The lingual facet of the paracone and the buccal facet of the protoconid have been preferentially scanned, although the metacone and hypoconid were considered if the former were not properly preserved. Finally, the scanning produced a digital elevation model of the enamel surface (Fig. 3.4C) with a vertical spacing of less than 0.002 µm and a lateral resolution (x,y) of 0.129 µm.

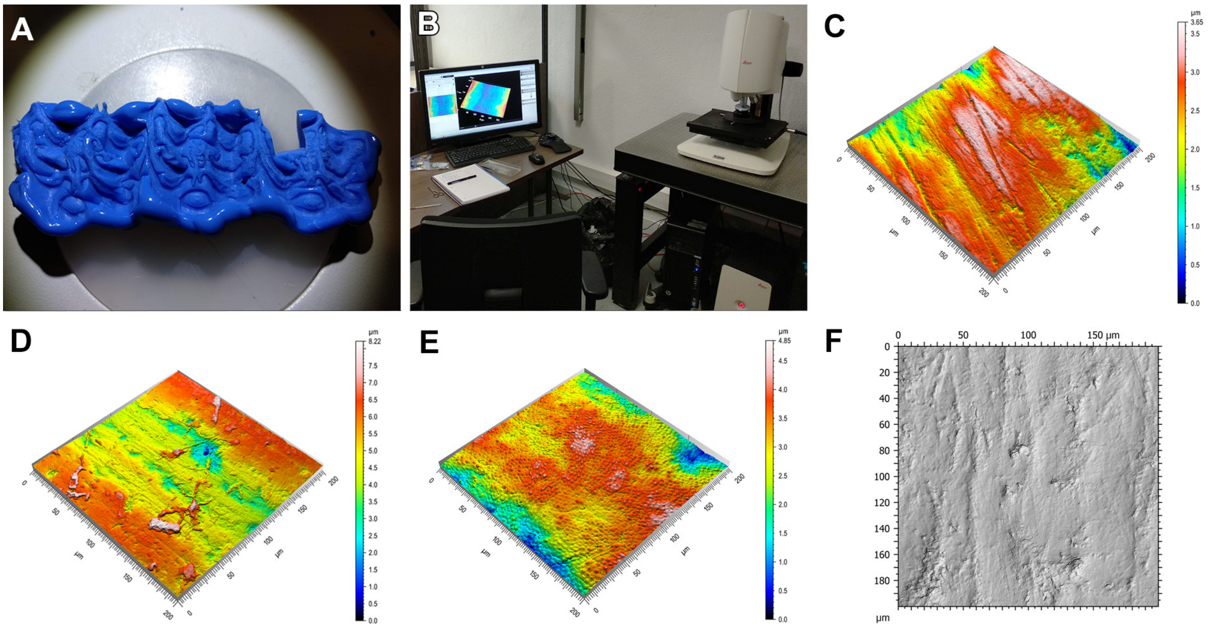

Figure 3.4.
Analysis of the dental microwear texture. **A)** Occlusal mold of three hipparionin upper molars (P4-M2) from where the paracone of the M2 has been extracted for its analysis. **B)** Profilometer Leica DCM8 used for the scanning of the microwear surface (photo at PALEVOPRIM lab). **C)** Portion (200 µm x 200 µm) of the obtained 3D surface simulation of a *Hipparion concudense* molar. **D)** Enamel surface clearly showing post-mortem alteration. **E)** Enamel prisms showing up at the enamel surface because of chemical attacking. **F)** Photosimulation of the enamel surface of an *Hipparion periafricanum* molar.

The analyzed surfaces should only be the result of food-related wear (Teaford, 1988), thus the scans showing post-mortem transformations were discarded. These alterations can be easily identified (Teaford, 1988; Calandra and Merceron, 2016) and can, for instance, include the deposition of sediment/particles, glue on the enamel surface (Fig. 3.4D), or the attack of the microwear surface due to mechanical or chemical preparation procedures (Fig. 3.4E). The selected scans were finally saved as .plµ files by LeicaScan® software (Leica Microsystems) and imported to LeicaMap® for processing. This processing involved the correction of missing points (which always represent < 2%) and aberrant peaks using automatic operators that replaced them with a smooth shape calculated from adjacent points. The same filling was used when deleting larger artifacts with a 3 µm diameter eraser or a user-defined contour eraser. As a final step, the surfaces were leveled and a 200 µm x 200 µm area was extracted and saved as a .sur file. Photosimulations (Fig. 3.4F) of all the analyzed specimens were then saved (Appendix 3 of the Chapter 6).

3.2.2.2. Textural Parameters and Statistical Analyses

The surfaces (.sur files) were analyzed using Toothfrax and Sfrax software (Surfract, http://www.surfract.com) applying SSFA, as detailed in Scott et al. (2006). Through this method, the microwear texture is automatically quantified by a set of textural attributes (Ungar et al., 2003; Scott et al., 2005, 2006). Four of these DMT parameters have shown to be more related to the properties of the diet (Scott et al., 2005, 2006):

Complexity (Area-scale of fractal complexity, *Asfc*) is a measure of the changes on the surface relief across different scales of observation. Enamel surfaces with high complexity exhibit numerous pits of different sizes and/or many microwear features superposed to each other (Fig. 3.5A).

Anisotropy (exact proportion of length scale anisotropy of relief, *epLsar*) calculates the orientation concentration of surface roughness at a given scale. Surfaces with high anisotropy show parallel oriented scratches (Fig. 3.5B).

Heterogeneity of complexity (heterogeneity of the area-scale of fractal complexity, *HAsfc*) quantifies the variation of complexity across the surface. To calculate *HAsfc*, the whole scanned area is subdivided and the *Asfc* differences between subregions are measured (Fig. 3.5C). In this thesis, this variable has been calculated in an 8 x 8 mesh (64 cells, see Chapter 6 for more information).

Textural fill volume (*Tfv*) indicates the volume of cuboids of 2 µm per side that can fill the surface, characterizing the total volume occupied by the microwear features (Fig. 3.5D). For further details on the DMT parameters, see Scott et al. (2006).

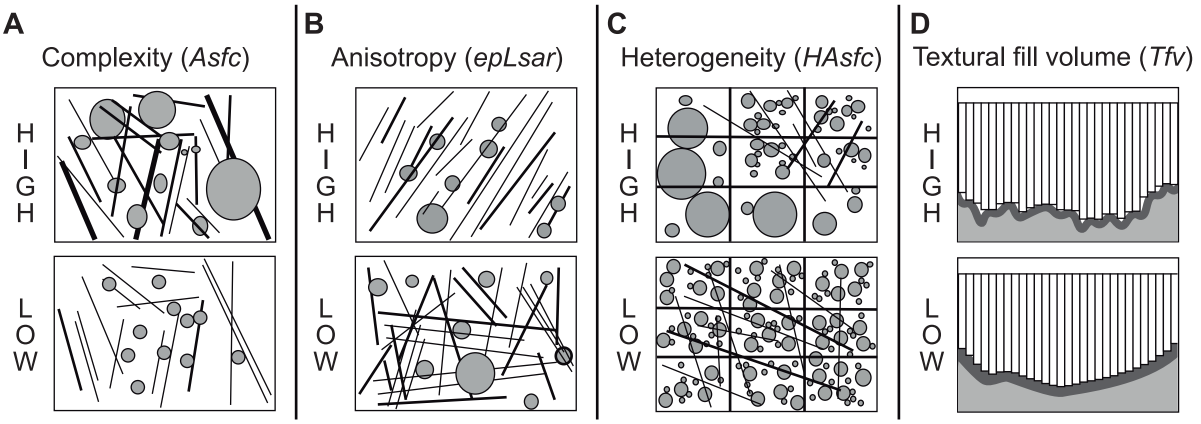

Figure 3.5.
Schematic representations of surfaces with high and low values of each dental microwear parameter considered. **A)** Complexity. **B)** Anisotropy. **C)** Heterogeneity of complexity calculated in a nine-cell mesh. **D)** Textural fill volume.

Based on these variables, it is possible to determine the nature of the items consumed. Concretely, anisotropy and complexity have shown to be the most useful DMT parameters for locating a herbivore on the grazer-browser continuum (Ungar et al., 2007; Scott, 2012). Anisotropy is positively correlated with the consumption of abrasive and tough items, such as grasses. On the other hand, brittle and hard browse produces textures of low anisotropy and with a wide range of complexities (Scott, 2012). In this thesis, moreover, a linear combination of the four DMT parameters has been performed using Principal Component Analysis (detailed information can be found in Chapter 6). By this, a new variable (PC1) has been obtained, which gathers most of the sample DMT variance and characterizes the surface.

To test the link between the size of the hipparionins and their diet and habitat, the DMT parameters and the calculated PC1 were regressed using the linear least-squares method with hipparionin body mass estimations (see next section). Subsequent analyses of variance exploring the DMT differences between hipparionins involved rank-transformed data, since the DMT variables tend to not conform to assumptions of parametric tests (Conover and Iman, 1981). The differences were tested with a set of three-way crossed and nested ANOVAs. Details on the ANOVA models performed can be found in Chapter 6. Moreover, pairwise comparisons with Tukey's Honest Significant Differences (HSD) and Fisher's Least Significant Differences (LSD) were used to determine the source of variation. The significance level was set at $\alpha = 0.05$ for all these tests, which were performed using RStudio software (Rstudio Team, 2016).

3.2.3. Body Mass Estimations

Body size plays a central role in an organism's biology as it is related to ecological and LH traits (Case, 1979; Peters, 1983; Calder, 1984), some of which are inferred herein from histology and DMTA (e.g., age at maturity or dietary preferences). Considering that this thesis aims to explore the size decrease processes from an LHT framework (Chapter 2), this parameter becomes a key point of relevance. As in most studies, body size has been represented by its proxy: body mass (MacFadden, 1986; Damuth and MacFadden, 1990). The obtaining of this variable for extinct taxa relies on the allometric scaling of the organism's mass with its body dimensions (Damuth and MacFadden, 1990). Skeletal and dental measures of living forms are then related to their body mass to compute regression lines, which later allow us to predict the weight of fossil species from linear measurements (Janis, 1990; Scott, 1990; Alberdi et al., 1995).

In this thesis, all the body mass data of extinct forms is based on measures of weightbearing elements (Scott, 1990), as these yield more reliable predictions than cranial and dental measurements (Alberdi et al., 1995). Some estimations were compiled from the literature (Ortiz-Jaureguizar and Alberdi, 2003; Pesquero and Alberdi, 2012; Vlachou, 2013) while the rest were performed herein. In the case of the hipparionins from the southern Balkans, their predicted weights come from the calculations that Vlachou (2013) made using metapodial measures. The body mass estimations performed in this thesis are accordingly based on the same measures: the distal maximal supra-articular breath of metacarpals and metatarsals (Mc10 and Mt10 of Eisenmann et al., 1988) and the distal minimal depth of the lateral condyles of metacarpals and metatarsals (Mc13 and Mt13 of Eisenmann et al., 1988). These measures were taken from museum collection specimens using a digital electronic precision caliper (0.05 mm error), and were also compiled from the literature (Forsten and Kaya, 1995; Clavel et al., 2012). Afterwards, the metric data was applied to the equations provided by Eisenmann and Sondaar (1998) and Scott (1990) to obtain the body mass estimations. The inferred body masses provided here correspond to the arithmetic mean of those estimates.

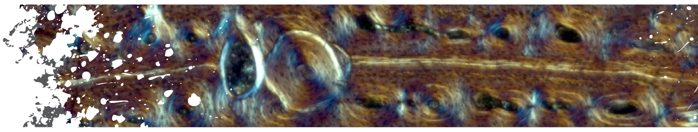

Chapter 4

Bone Histology Provides Insights into the Life History Mechanisms Underlying Dwarfing in Hipparionins

Reproduced from ***Scientific Reports***
DOI:10.1038/s41598-018-35347-x

www.nature.com/scientificreports

SCIENTIFIC REPORTS

Corrected: Publisher Correction

Bone histology provides insights into the life history mechanisms underlying dwarfing in hipparionins

Received: 1 May 2018
Accepted: 1 November 2018
Published online: 21 November 2018

Guillem Orlandi-Oliveras[1], Carmen Nacarino-Meneses[1], George D. Koufos[2] & Meike Köhler[1,3]

Size shifts may be a by-product of alterations in life history traits driven by natural selection. Although this approach has been proposed for islands, it has not yet been explored in continental faunas. The trends towards size decrease experienced by some hipparionins constitute a good case study for the application of a life history framework to understand the size shifts on the continent. Here, we analysed bone microstructure to reconstruct the growth of some different-sized hipparionins from Greece and Spain. The two dwarfed lineages studied show different growth strategies. The Greek hipparions ceased growth early at a small size thus advancing maturity, whilst the slower-growing Spanish hipparion matured later at a small size. Based on predictive life history models, we suggest that high adult mortality was the likely selective force behind early maturity and associated size decrease in the Greek lineage. Conversely, we infer that resource limitation accompanied by high juvenile mortality triggered decrease in growth rate and a relative late maturity in the Spanish lineage. Our results provide evidence that different selective pressures can precipitate different changes in life history that lead to similar size shifts.

Body size is a key aspect of organisms' biology as it is tightly correlated with many aspects of their physiology, ecology and life history[1–3]; body size, hence, is a fitness component[4]. Based on the coupling between life history traits and body mass, some authors[5–8] have addressed size shifts in insular environments within the framework of life history theory.

Life history theory is built around the idea that selection acts on the life history characteristics of an organism to maximise its reproductive success or fitness[9,10]. To explain the range of life history strategies observed in nature, evolutionary biologists have traditionally used the approach of life history optimization[11]. Different optimality studies have provided a broad range of predictive models for the evolution of life cycle traits under different ecological constraints[9,12,13]. These models provide an explanatory framework for understanding how selective pressures can shape the life history of an organism.

Based on this scheme, Palkovacs[7] proposed that body size shifts on islands can indirectly result from variation in life history traits instead of direct selection acting on size, as previously suggested by other authors[14–16]. He pointed out that two factors, extrinsic mortality and resource availability, influence life history traits to which adult size is sensitive, especially individual growth rate and age at maturity[7]. Although this approach has been theoretically proposed[7] and tested[17–20] in insular environments, it has not yet been explored in continental settings, where predictive life history models should also be applicable to explain body size evolution.

On continents, trends in size reduction have been identified in various taxonomic groups from different stratigraphic ages[21–23]. For instance, contrary to the notion of size increase over geological time within the horse lineage (Copes' Rule)[24], some equid clades experienced dwarfing[21,25,26]. This is the case of the *Arenahippus* lineage during the Paleocene-Eocene Thermal Maximum[27], of some hipparionins during the European late Miocene[28–30], and of the *Equus* lineage during the Pleistocene[25,31,32].

The first hipparionins that dispersed throughout the Old World in the Vallesian were large sized hipparions[33] that likely evolved from a large ancestor[34]. Late Miocene hipparionins from the Eastern and Western Mediterranean basins exemplify an interesting case of continental trends in size decrease. The Western Mediterranean late Turolian (MN13) dwarf hipparions from the Teruel Basin (Spain) have been interpreted to

[1]Institut Català de Paleontologia Miquel Crusafont (ICP), Campus de la Universitat Autònoma de Barcelona, 08193, Bellaterra, Barcelona, Spain. [2]Department of Geology, Laboratory of Geology and Palaeontology, Aristotle University of Thessaloniki, 54124, Thessaloniki, Greece. [3]ICREA, Pg. Lluís Companys 23, 08010, Barcelona, Spain. Correspondence and requests for materials should be addressed to G.O.-O. (email: guillem.orlandi@icp.cat)

represent an evolutionary gradation towards reduced body size, simplified enamel abrasive figures, increasing hypsodonty and gracility[29,30]. This size reduction led to some of the smallest *Hipparion sensu lato* forms of the Old World, *Hipparion gromovae* and *Hipparion periafricanum*, with estimated mean body masses of 59 kg and 23 kg respectively[29]. These two taxa coexisted sympatrically with the larger 138 kg *Hipparion truyolsi*[29]. In the Eastern Mediterranean basins, the existence of the small *macedonicum* morphotype is already reported in the early Vallesian (MN9), and its temporal range extends up to the middle Turolian (MN12), and possibly to the late Turolian (MN13)[28,35]. Similar to the Spanish small hipparionins, the Greek *Hipparion macedonicum* underwent a body mass decrease coupled with a simplification of the enamel plication and an increased gracility of the metapodials[28]. The body mass estimations for this taxon range from 72.3–121 kg during the Vallesian (MN9-MN10) to 49.5–94.7 kg during the early-middle Turolian (MN11-12)[28]. This small morphotype coexisted with larger species that pertain to the *primigenium*, the *dietrichi* and the *proboscideum* morphotypes, which almost double the body mass of the small forms[35].

The occurrence of these dwarfed hipparionins in the European late Miocene represents a good opportunity to test for the coupling of life history changes and size shifts. In the present study, we aim to unravel the possible mechanisms and causes underlying trends in size reduction of these hipparions from a life history approach. For this purpose, we reconstruct the bone growth pattern of different-sized hipparionins through bone histology. Due to the fact that tissue type and bone growth marks reflect tempo and rate of bone growth[36,37], bone histology is a valuable tool for reconstructions of life histories[38,39] and growth patterns[40–42].

Results

Bone histology. Bone microstructure is generally better preserved in the Spanish specimens (Supplementary Fig. S1a), while some Greek metapodials have suffered different taphonomical alterations. In most cases this does not erase histological details such as vascularization or bone growth marks (Supplementary Fig. S1b). The sample from the Nikiti-2 (NIK) fossil site, however, is especially damaged diagenetically or through microbiological attack (Supplementary Fig. S1c), and it has therefore not been used for our growth curves reconstruction.

Both metacarpals and metatarsals of all the groups studied present a similar tissue and vascular arrangement. Their primary bone consists of a fibrolamellar complex (FLC) with longitudinal primary osteons oriented in circular rows (Fig. 1a). A similar histological pattern has been observed in previous studies in the metapodials of extant[43] and fossil equids[44,45]. The amount of parallel fibered bone (PFB) within the FLC[46] is higher in the innermost cortex of the metapodials than in the outer cortical area, coinciding with a smaller diameter of the primary osteons in the inner cortex (Fig. 1a). This observation is in agreement with the tissue pattern observed in extant equid bones[43,47].

We also have identified the following primary tissues and vascular orientations within the histological samples: Laminar bone is present in the posterior inner cortical zone (Fig. 1b) in some metapodials. Half of the Spanish *H. gromovae* specimens exhibit this tissue in the innermost cortex, while it is present in only some metapodials from Greek Vallesian sites. Radial canals are also identified within the first growth cycle of metatarsals of the large *dietrichi* morphotype (Fig. 1c) and one *primigenium* metatarsal (PNT-4). Radial canals are also sparsely situated in some regions of one *dietrichi* metacarpal (DTK-58) and in metapodials of the *macedonicum* morphotype (PER-23 and PER-425). The different vascular arrangements exhibit modest differences in growth rate compared to the bone matrix typology[48]. Nevertheless, tissues with radial osteons present higher growth rates compared to those with predominant circular osteons, as laminar tissues, when observed within the same bone[49,50]. Accordingly, the radial canals mainly observed in some *dietrichi* and *primigenium* metatarsals can be related to higher growth rates, while the laminar bone tissue present in four of the eight *H. gromovae* specimens can be an indicator of slower growth rates. These extrapolations from bone vascularization patterns must be done carefully in fossil taxa because of the high range of variability[48,49].

We identified large resorption cavities (RC) distributed near the medullary cavity within the posterior area of almost all metapodials. These RC appear early in ontogeny and, in some cases, lamellar bone is deposited at their margins, resulting in a high concentration of secondary tissue in the inner posterior zone of the metapodials (Fig. 1d). Besides, dense Haversian tissue is identified in our samples (Fig. 1d). The Haversian tissue is mainly concentrated within the lateral posterior and medial posterior areas, where the lateral metapodials (II and IV) contact the central one. The major secondary remodelling of these areas is related to higher biomechanical loadings[43,44]. Two metapodials show an extensive distribution of Haversian systems (PER-X and IPS-28842), though the growth marks are still identifiable (Supplementary Fig. S2). Superimposition of different ontogenetic stages shows that neither medullary expansion nor Haversian canals completely eroded the cyclical growth marks (CGMs). Lamellar bone is present in the outermost cortex of some metapodials, forming the external fundamental system (EFS, see Material and Methods) in adult individuals that have attained their final size (Figs 2 and 3).

Skeletocronology. We have used the specimens that approached their final size for skeletocronological analysis and growth reconstruction. In most cases, the three Greek morphotypes present two CGMs embedded in the FLC matrix, both in the metacarpals (Fig. 2a,b) and the metatarsals (Fig. 3a,b,e). However, one of the three metatarsals of the *dietrichi* morphotype (DTK-106) exhibits three CGMs in the FLC prior to deposition of the EFS in the lateral and medial areas, while two of the five specimens of the *macedonicum* morphotype (PER-23 and VAT-112) have only one CGM each. This can suggest an advanced maturity in the small Greek representatives though there appears to be some variability. The main difference between the Greek forms, however, lies in the spacing between the last growth mark of the FLC and the EFS. Generally, when analogous regions are compared, the large *primigenium* and *dietrichi* metacarpals (Fig. 2a,b) continue to grow after the second CGM compared to the *macedonicum* morphotype (Fig. 2c). Similarly, a higher amount of tissue is deposited during the third growth cycle of the larger metatarsals of *primigenium* and *dietrichi* morphs (Fig. 3a–c), while the small *macedonicum* metatarsals deposits fewer tissue in this zone (Fig. 3e). This early narrowing of the growth zones[51] lends support to the idea of

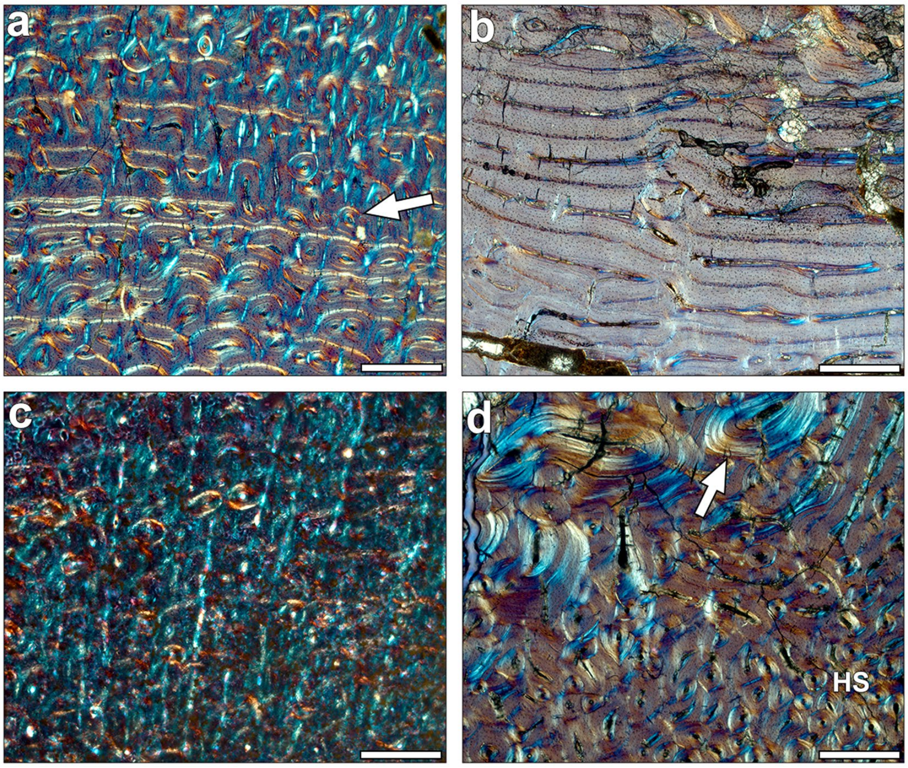

Figure 1. Hipparionin metapodial histology observed under polarised light using a 1/4λ filter. Scale: 0.5 mm. (**a**) Primary bone tissue formed by fibrolamellar complex (FLC) in the innermost cortex of the *Hipparion truyolsi* metatarsal IPS-28842. The arrow points out the transition between a FLC with higher parallel fibered bone component (PFB) to a FLC with higher fibrous component and larger osteons. (**b**) Laminar bone tissue in the inner cortex of the *Hipparion* cf. *sebastopolitanum* (*primigenium* morphotype) PNT-22. (**c**) Radial vascular canals present in the first growth cycle of the *Hipparion philippus* (*dietrichi* morphotype) metatarsal PER-342. (**d**) Secondary bone tissue in the lateral posterior area of the *Hipparion gromovae* metacarpal IPS-101807. Dense Haversian systems (HS) are concentrated in the contact zone with the lateral metapodials, and lamellar tissue is filling the resorption cavities near the medullary area (arrow indicating resorption line).

an earlier attainment of maturity in the smaller Greek form compared to the larger ones. Within the Spanish hipparionins, the *H. gromovae* metapodials show three CGMs in the bone cortex prior to the EFS (Figs 2d and 3d), while the larger *H. truyolsi* metatarsal has only two CGMs embedded in the FLC (Fig. 3f). Although it has not reached maturity, the *H. gromovae* metacarpal IPS-96275 (Supplementary Fig. S1a) also points towards extended growth period as it exhibits open vascular canals in the periosteum after the deposition of the second CGM. Consequently, the metapodials of the small *H. gromovae* present three or more cycles of active growth, contrary to the small Greek morphotype and the larger Spanish taxon. These differences in growth cessation can also be identified by the overall growth trajectory reconstruction.

Growth Curves Reconstruction. The curve fitting allowed us to obtain characteristic growth parameters and to estimate growth variables (Table 1, see Material and Methods). At birth, metapodial size shows an almost isometric relationship (0.834-slope) with the asymptotic maximum size obtained for each specimen (parameter *A*) ($R^2 = 0.908$; p-value (Pearson) < 0.001) (Fig. 4a). Therefore, metapodial postnatal growth starts at analogous sizes in each hipparionin group, depending on their adult final circumference. If we consider bone perimeter as a proxy of body mass[50,52], these values correspond to those predicted from isometric scaling of eutherian neonatal mass with adult body mass[1]. This contrasts with insular dwarf lineages where neonate size is smaller than predicted from allometry[18]. After birth, the growth rate during the first growth cycle (age = 0.5 years, Table 1) also scales positively with adult bone size (Fig. 4b, $R^2 = 0.543$; p-value (Pearson) < 0.001). However, when the same relationship is established but considering the relative growth rate at that point (size factor extracted), the correlation is not significant ($R^2 = 0.160$; p-value (Pearson) > 0.05). During the first stages of growth, hence, metapodials grow at analogous velocities relative to their size, and the allometrical relationship with a 1.46 slope results in slightly higher growth rates in the metapodials of large forms compared to the small ones. For comparison, we have also related the growth rate and the femoral lateromedial diameter, a good proxy of body size in

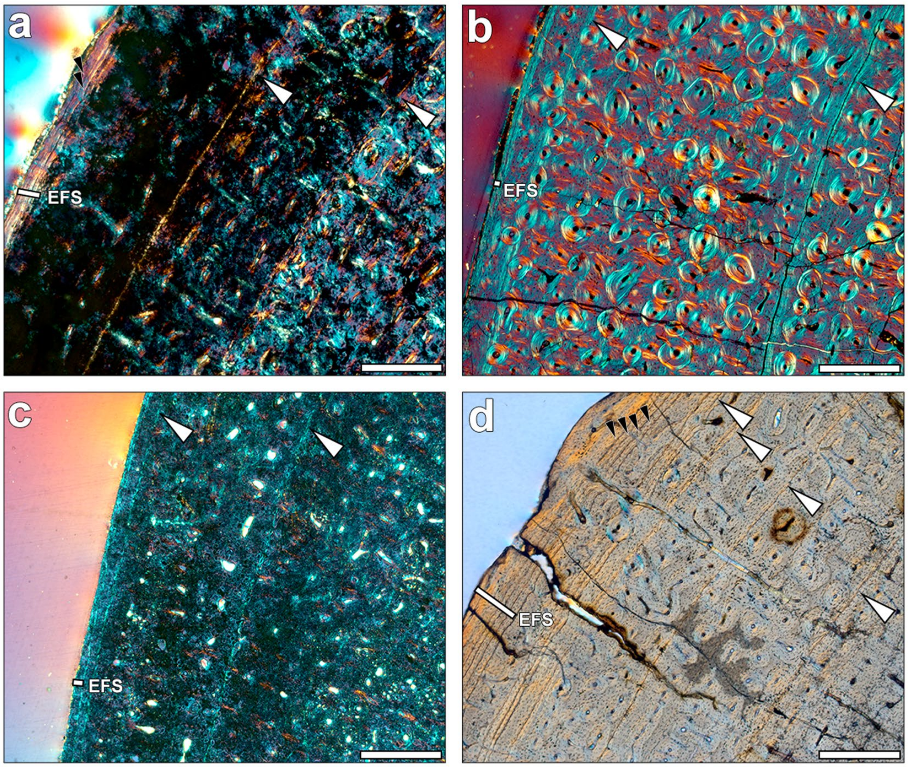

Figure 2. Bone growth marks in the periosteum of adult metacarpals. Growth marks are indicated by white arrows, small black arrows mark the growth lines present within the EFS, which is identified by a white line. The images were obtained under polarised light using a 1/4λ filter. Scale: 0.5 mm. (**a**) *Hipparion* aff. *giganteum* (*primigenium* morphotype) metacarpal NKT-22. (**b**) *H. philippus* (*dietrichi* morphotype) metacarpal PER-X. (**c**) *Hipparion macedonicum* (*macedonicum* morphotype) metacarpal PER-23. (**d**) *H. gromovae* metacarpal IPS-96274.

equids[53], on a sample of different-sized extant equid femurs (see Material and Methods). Although the points of the obtained regression are scattered ($R^2 = 0.387$) (Supplementary Fig. S3) and the correlation is not statistically significant (p-value (Pearson) = 0.099), we can identify a trend indicating higher growth rates in larger taxa and lower growth rates in the smaller species or breeds. Similar to what we observe in hipparionins, hence, extant smaller equid species and horse breeds, such as *Equus hemionus* and the Shetland pony, tend to grow at absolute slower rates than larger representatives of the genus *Equus*.

The overall growth patterns in hipparionins are graphically visualised in the curves from discrete measurements of the CGMs (Fig. 5, dashed lines). From the obtained logistic parameters (Table 1), we reconstructed the mean growth trajectory for each group (Table 1 and Fig. 5, solid lines). In the mean and individual growth curves, we identified the point where the growth rate is reduced as the change in the slope of the trajectory[43] (Fig. 5, arrow), which coincides with the lower bone deposition observed histologically. This signal has been related to epiphyseal fusion and reflects the end of longitudinal bone growth[43]. The growth rate of the larger Greek metapodials substantially declines by around ~2.5 years after birth, and generally at sizes above 75 mm of perimeter (Fig. 5). Growth deceleration starts earlier in the small Greek *macedonicum* morphotype, about the first year in the metatarsals and within the second year in the metacarpals, both at perimeter sizes around ~65 mm. The Spanish dwarf form, on the contrary, grows at sustained rates over a longer period until the age of approximately ~2.5 years (Fig. 5), comparable to the large Greek morphs. Indeed, the growth in *H. gromovae* metapodials and the larger Greek morphs declines later compared to the small Greek morphotype and to the larger Spanish *H. truyolsi* (Fig. 5), in which the absolute (GR) and relative (RGR) growth rates are considerably low at the second and third year of growth (Table 1 and Supplementary Fig. S4).

The logistic growth parameters (Table 1) also show the aforementioned growth differences. Accordingly, the growth parameter *k*, that represents the relative growth velocity (see Material and Methods), tends to be higher in the metapodials of the *macedonicum* morphotype ($k_{MCmc} = 1$ in metacarpals and $k_{MTmc} = 1.6$ in metatarsals, Table 1) than in the specimens of the other groups (e.g. *dietrichi* morphotype metacarpals $k_{MCdt} = 0.84$ and metatarsals $k_{MTdt} = 1$, Table 1), when metacarpals and metatarsals are compared separately. This indicates an initially

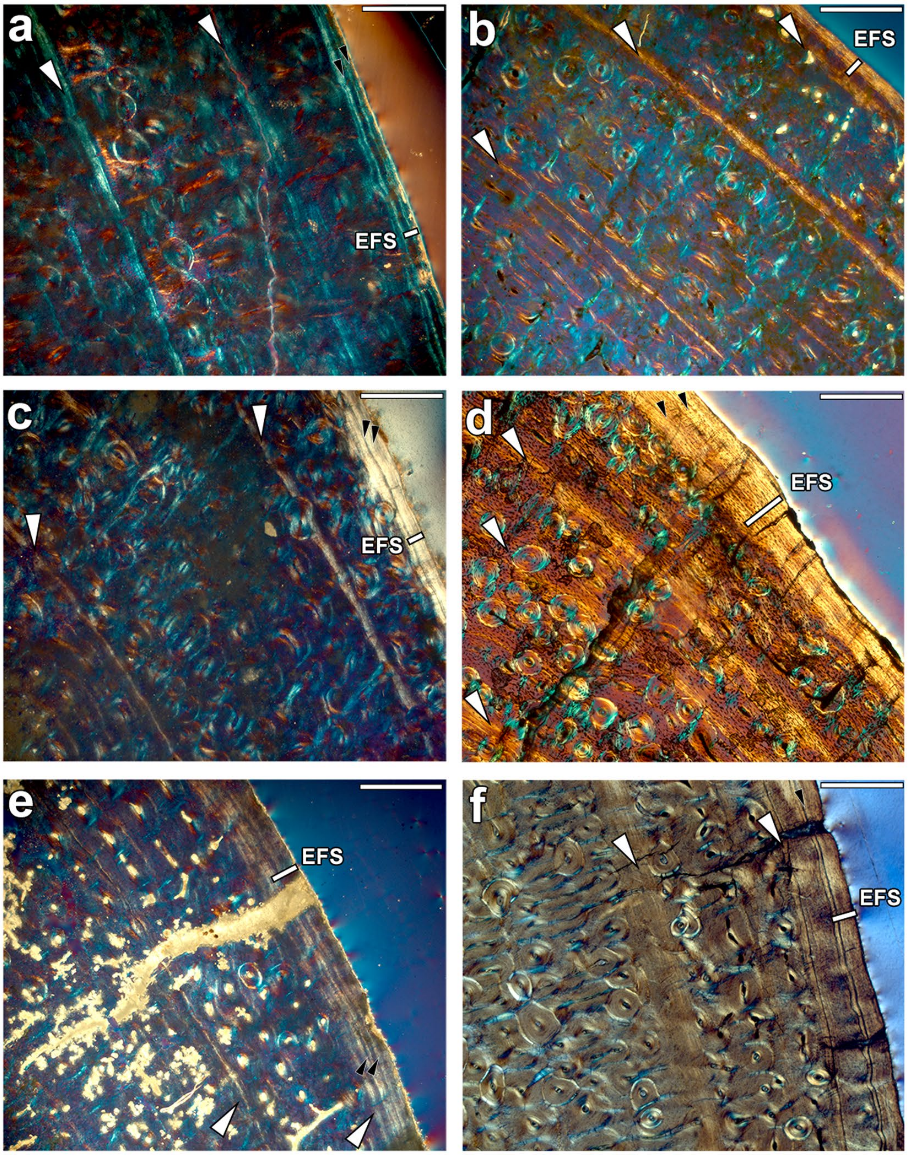

Figure 3. Bone growth marks in the periosteum of adult metatarsals. Growth marks are indicated by white arrows, small black arrows mark the growth lines present within the EFS, and EFS is identified by a white line. The images were obtained under polarised light using a 1/4λ filter. Scale: 0.5 mm. (**a**) *H*. cf. *sebastopolitanum* (*primigenium* morphotype) metatarsal PNT-4. (**b**) *Hipparion* aff. *platygenys* (*dietrichi* morphotype) metatarsal DTK-106. (**c**) *H. philippus* (*dietrich*i morphotype) metatarsal PER-1211. (**d**) *H. gromovae* metatarsal IPS-101809. (**e**) *H. macedonicum* (*macedonicum* morphotype) metatarsal PER-485. (**f**) *H. truyolsi* metatarsal IPS-28842.

faster growth relative to size, and an earlier attainment of maturity in this Greek dwarf form. In contrast, the small metapodials from *H. gromovae* and the larger from the large Greek morphotypes (*primigenium* and *dietrichi*) exhibit lower *k* values (e.g. $k_{MCgr} = 0.78$ and $k_{MTgr} = 0.98$, Table 1), which indicates a longer growth period and a later onset of maturity. Conversely, the large Spanish *H. truyolsi* has one of the highest *k* value ($k_{MTty} = 1.3$, Table 1) as it grows fast and decreases the deposition rate before the second year of life (Fig. 5). The growth period, or the time required to attain the 95% of its final size (*t95A*), illustrates the same fast development in the *macedonicum* morphotype compared to the Spanish small species and the larger Greek morphs (Table 1). For instance, while the metatarsals of the *macedonicum* morphotype complete the 95% of growth by the age of 1 year ($t95A_{MTmc} = 1.01$,

GROUP	BONE	CODE	A (mm)	k (year^{-1})	t95A (year)	GR (t = 0.5) (mm/year)	RGR (t = 0.5) (year^{-1})	GR (t = 1) (mm/year)	RGR (t = 1) (year^{-1})	GR (t = 2) (mm/year)	RGR (t = 2) (year^{-1})	GR (t = 3) (mm/year)	RGR (t = 3) (year^{-1})
primigenium morphotype	MC	NKT-22	81.54	0.66	2.46	7.35	0.108	5.79	0.081	3.36	0.044	1.85	0.023
	MC	RPL-nn	83.74	1.02	1.81	11.89	0.170	8.20	0.110	3.41	0.043	1.30	0.016
	MT	PNT-4	86.53	0.99	2.00	13.07	0.186	9.29	0.123	4.07	0.049	1.61	0.019
	Mean	***pgMC***	**82.64**	**0.84**	**2.07**	**9.60**	**0.139**	**7.08**	**0.097**	**3.49**	**0.045**	**1.60**	**0.020**
		pgMT	**86.53**	**0.99**	**2.00**	**13.07**	**0.186**	**9.29**	**0.123**	**4.07**	**0.049**	**1.61**	**0.019**
macedonicum morphotype	MC	RPL-44	69.06	0.86	1.94	7.75	0.133	5.63	0.091	2.69	0.041	1.20	0.018
	MC	PER-23	65.57	1.27	1.42	10.31	0.184	6.30	0.105	2.00	0.031	0.59	0.009
	MC	PER-425	64.47	0.88	1.83	6.99	0.127	5.01	0.086	2.35	0.038	1.03	0.016
	MT	VAT-112	64.60	1.88	0.90	10.91	0.188	4.83	0.078	0.79	0.012	0.12	0.002
	MT	PER-485	70.71	1.32	1.16	9.32	0.149	5.38	0.081	1.57	0.023	0.43	0.006
	Mean	***mcMC***	**66.37**	**1.00**	**1.69**	**8.40**	**0.149**	**5.74**	**0.096**	**2.39**	**0.037**	**0.92**	**0.014**
		mcMT	**67.66**	**1.60**	**1.01**	**10.28**	**0.170**	**5.21**	**0.081**	**1.14**	**0.017**	**0.23**	**0.003**
dietrichi morphotype	MC	PER-X	78.02	0.65	3.05	8.59	0.141	7.03	0.108	4.33	0.061	2.48	0.034
	MC	DTK-58	76.29	0.85	2.14	9.34	0.148	6.92	0.103	3.42	0.048	1.56	0.021
	MT	PER-1211	82.96	0.94	2.16	12.46	0.188	9.11	0.127	4.23	0.054	1.77	0.022
	MT	PER-342	86.29	1.04	2.02	14.63	0.213	10.32	0.138	4.35	0.053	1.64	0.019
	MT	DTK-106	87.97	1.02	1.97	13.80	0.194	9.71	0.126	4.13	0.049	1.59	0.018
	Mean	***dtMC***	**77.15**	**0.75**	**2.54**	**9.08**	**0.146**	**7.08**	**0.107**	**3.92**	**0.055**	**2.00**	**0.027**
		dtMT	**85.74**	**1.00**	**2.04**	**13.63**	**0.198**	**9.72**	**0.130**	**4.24**	**0.052**	**1.67**	**0.020**
H. gromovae	MC	IPS-101807	65.53	0.79	2.25	7.42	0.137	5.62	0.098	2.93	0.048	1.42	0.022
	MC	IPS-96274	63.83	0.77	2.29	6.93	0.131	5.29	0.095	2.82	0.047	1.40	0.023
	MT	IPS-101809	81.00	0.95	2.15	12.34	0.191	9.00	0.129	4.15	0.054	1.73	0.022
	MT	IPS-96276	66.09	1.01	1.92	9.94	0.184	6.96	0.119	2.96	0.047	1.14	0.018
	Mean	***grMC***	**64.68**	**0.78**	**2.27**	**7.17**	**0.134**	**5.45**	**0.096**	**2.88**	**0.047**	**1.41**	**0.023**
		grMT	**73.55**	**0.98**	**2.04**	**11.15**	**0.188**	**7.97**	**0.124**	**3.53**	**0.051**	**1.42**	**0.020**
H. truyolsi	MT	IPS-28842	97.00	1.30	1.39	15.41	0.185	9.27	0.104	2.85	0.030	0.80	0.008
	Mean	***tyMT***	**97.00**	**1.30**	**1.39**	**15.41**	**0.185**	**9.27**	**0.104**	**2.85**	**0.030**	**0.80**	**0.008**

Table 1. Logistic growth curve parameters and growth estimates for each adult metapodial. Mean growth curve parameters and estimates for the metacarpals (MC) and metatarsals (MT) of each group are also provided. *A:* asymptotic circumferential metapodial size; *k*: mean relative velocity; *t95A*: time required to attain the 95% of the final size. Growth rates (GR) and relative growth rates (RGR) at different points of the metapodial growth are also shown.

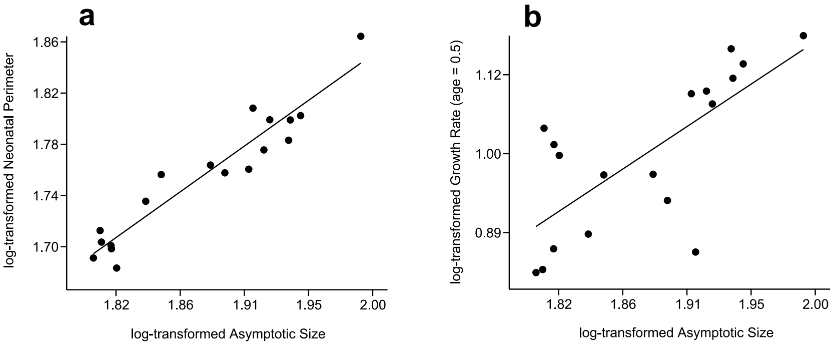

Figure 4. (**a**) Linear regression between the neonatal metapodial size and the adult final size (*A*) of mature metapodials. (**b**) Allometric regression relating the growth rate during the first growth cycle (t = 0.5 years) and the adult final body size (*A*) of mature metapodials. All variables were log-transformed to linearise the relationship. See main text for statistics information.

Table 1), the small metatarsals of *H. gromovae* and the larger ones from *dietrichi* and *primigenium* morphotypes double this time ($\text{t95A}_{\text{MT}gr} = 2.04$, $\text{t95A}_{\text{MT}dt} = 2.04$, $\text{t95A}_{\text{MT}pg} = 2$, Table 1). The single metatarsal of the larger *H. truyolsi* ($\text{t95A}_{\text{MT}ty} = 1.39$, Table 1) ceases growth earlier than the metatarsals of the other taxa except for the

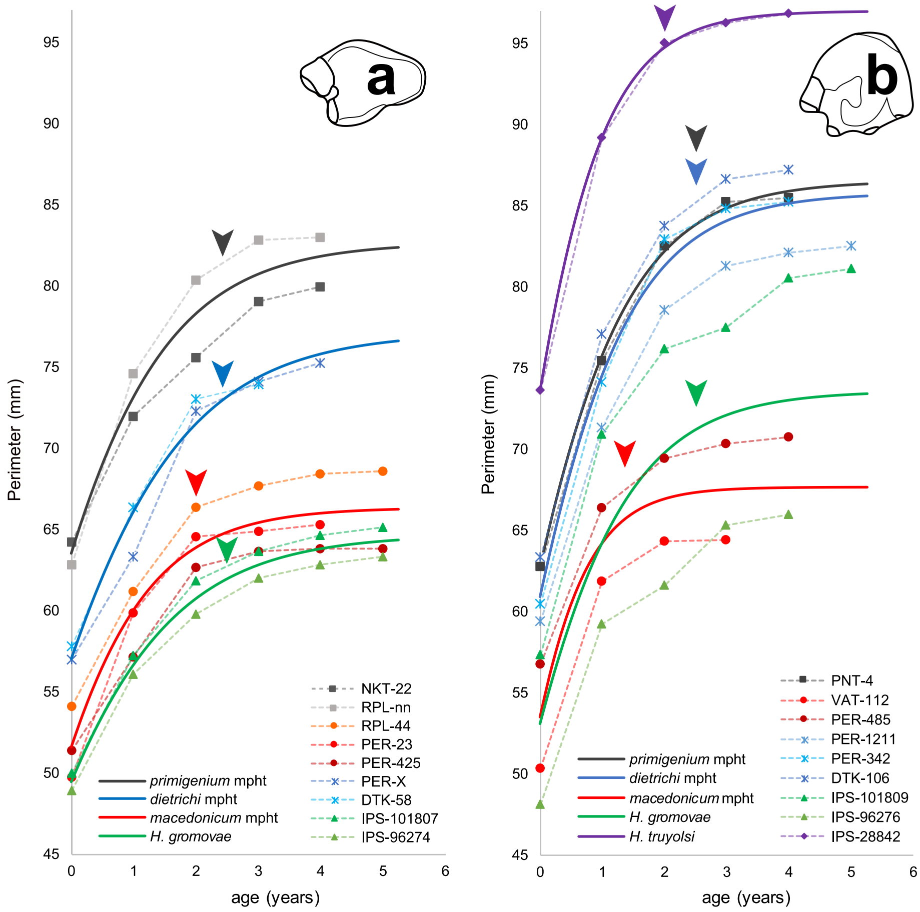

Figure 5. Growth curves of mature metapodials. Dashed lines represent each metapodial growth trajectory while solid lines indicate the mean fitted logistic growth curves for the different groups. Arrows pointed out the change of slope of the growth curves that characterises metapodial maturity[43]. (**a**) Metacarpal growth curves. (**b**) Metatarsal growth curves. The unusual size of the *H. gromovae* metatarsal IPS-101809 is due to a more proximal cut of the specimen, however, the growth trajectory is still identifiable.

macedonicum morphotype. This earlier maturity in *H. truyolsi*, however, should be taken with caution since there is only one remodelled metatarsal available and there is no other metatarsal of this species to compare with. In all groups analysed, the metacarpals attain their final size later than metatarsals, as shown both by the parameter *k* and by the time required to complete growth (Table 1). This finding can be related to the variability reported between other limb bones of equids[43] and the ontogenetic differences between bones[54]. Distinct loading charges and biomechanics between hipparion metapodials may be the reason underlying this difference[55].

Discussion

Body size variations in continental settings, and concretely in equid lineages, have been hypothesised to represent direct adaptations to habitat change[25,29], resources shifts[27,30,31,34] or to climate change[25,27]. These hypotheses are closely linked because of the strong relationship between climate, habitat and resources. Alternatively, life history theory provides a theoretical background to explain size shifts as a by-product of life history adaptations to environmental conditions. This approach has been proposed for islands[7]; however, it has not been explored in mainland size trends. Our analysis of the growth strategies of different-sized hipparionins provides a first attempt to understanding the possible causes behind continental trends in size decrease within a life history framework.

In the present study, we inferred the growth trajectories of small and large hipparionin groups from two continental bioprovinces using metapodial bone histology. Although the bone microstructure of metapodials does not provide the absolute age of physiological maturity[43], it informs about the relative maturity that, within the context of body mass, indicates whether these size reductions were coupled with shifts towards either slower or faster life histories. Future histological analysis on adult femurs could provide an absolute estimation of the age at sexual maturity and, thus, help to support our inferences.

We found that the metapodials of the larger hipparionins grow at higher rates than the metapodials of the smaller forms during the first growth stages (Fig. 4b and Table 1). We can infer, hence, lower growth rates for the small taxa and higher rates for the larger forms as predicted from allometry[1] and observed in dinosaurs[36,56] and in extant and fossil artiodactyls[6,18,39,57]. Moreover, we identified a similar trend in extant equids, since femora of larger wild equids and of larger domestic breeds tend to grow at higher rates than the smaller-sized species or breeds (Supplementary Fig. S3). In hipparionins, although the differences in development have principally been identified from growth curve reconstructions, bone tissue microstructure also indicates distinct growth velocities. Thus, we principally found radial vascularity in the large *dietrichi* and *primigenium* metatarsals, and laminar bone in the small *H. gromovae*. In fact, growth rate is particularly low in *H. gromovae*, where besides the growth rate scaling (Fig. 4b), the relative growth rate expressed by the logistic growth parameter k is also lower (Table 1). On the other hand, the small *macedonicum* morphotype metapodials exhibit in some cases disperse radial canals, indicating a probable higher growth rate for its size, which is supported by the greater k values. Regarding the attainment of relative maturity, the small *macedonicum* morphotype and the large *H. truyolsi* considerably decrease their growth rate between the first and the second year, while the two large Greek morphotypes and the small Spanish *H. gromovae* decrease growth rate after the second year. The large Greek forms, hence, grew at high rates and attained their maturity later than the small Greek *macedonicum* morphotype that advance the growth rate decline. The small Greek *macedonicum* morphotype, thus, shifted towards a faster life history. The small Spanish *H. gromovae*, on the contrary, matured relatively late, similar to the large Greek representatives. However, it does it at much lower growth rates. *H. truyolsi*, on the other hand, grew at high rates and decreased growth early (based on a single specimen). Martinez-Maza *et al.*[44] observed two CGMs within the cortex of the metapodials of the larger (160–186 kg[58]) *Hipparion concudense* from a Vallesian and a middle Turolian Spanish locality. These growth marks are situated close to the periosteal surface[44], suggesting an early decrease in growth rate. Moreover, in half of the metapodials of their middle Turolian sample, only one CGM is situated within the bone cortex[44]. From allometric scaling[1], the smaller *H. gromovae* should be expected to show less CGMs within the cortex than *H. truyolsi* or *H. concudense*; however, it exhibits more growth marks indicating a delayed maturity in relation to these larger Spanish species. Besides, our results have also shown that in some cases metacarpals tend to decrease their growth later than metatarsals. This difference is beyond the scope of the present study, but may indicate different timings in the growth cessation between these bones.

In summary, we did not only find differences in the growth patterns between the small and the large Greek morphotypes as predicted from scaling, but also between the small Greek *macedonicum* morphotype and the small Spanish *H. gromovae*, since the Spanish species matured later than expected from size. The two dwarf lineages, hence, followed different growth strategies that led to a similar reduction in adult size. Our results, thus, are congruent with two different evolutionary scenarios where dwarfing is caused by distinct selective pressures. Following life history theory, attainment of sexual maturity and growth rate are the two main characteristics that determine the final size of an organism[7,9]. These factors, in turn, are modulated by environmental changes in mortality regimes and resource availability respectively[7,9,12,59–61]. Palkovacs[7], in his life history based model for size evolution on islands, considered the changes in resource levels and mortality rates (caused by low predation) between mainland and islands as the principal selective pressures involved in size shifts. However, variations in ecological factors over time and space can be far more complex on the continent where, for example, predation pressure can either increase or decrease, and can affect specific ontogenetic stages differently. As age-specific survival and fecundity indexes are the basis of life history and demographic studies[9,10,60], it is important to determine which is the life cycle stage affected by a shift in the selective agent. Organisms that suffer from high extrinsic mortality regimes acting on *adult* stages will maximise their fitness following a different life history strategy compared to those exposed to high *juvenile* mortality[61,62]. Concretely, when the *adult* stage is affected by high predation pressure, animals maximise their fitness by reproducing earlier[62]. By this, organisms are able to increase their reproductive output before they fall prey to carnivores, hence accelerating their life history. Both theoretical[60,62] and comparative surveys[59,61,63] provide evidence for advancement of reproductive maturity in populations facing high adult mortality regimes. This suggests that increased predation pressure upon adult individuals selected for advanced maturity through earlier growth cessation, leading to dwarfing in the *macedonicum* lineage. On the other hand, under high *juvenile* mortality, organisms maximise fitness by reproducing later in time[12,13,60,61]. A delay in maturity is predicted if the benefits outweigh the disadvantages of a late reproduction[12,64]. These advantages are based on two key assumptions; fecundity increases with size, and juvenile mortality decreases with increasing age and size at maturity of the progenitor[12]. Because equids are monotocous[65], a significant increase in fecundity related to larger size is not expected; however, a delay in maturity can compensate high juvenile mortality by increasing juvenile survival rates due to more experienced progenitors[59]. Age-specific juvenile mortality increases during periods of low resource availability[59,66–70], which are common in arid and semi-arid environments[71]. Seasonal or unpredictable fluctuations in food quantity and quality have a high influence on juvenile mortality[72], since at this ontogenetic stage young mammals are more sensitive to environmental stresses due to their smaller size, lower fat reserves, immature immunological system and inexperience[61]. Furthermore, resource availability affects individual growth, with low resource levels constraining growth rates[7,9]. Under this scenario, individuals are forced to grow over an extended period to attain a size large enough for successful reproduction[12,13], which leads to a delay in maturity[7]. This suggests that low resource availability played an important role in the dwarfing process of *H. gromovae*, triggering a decrease in growth rate and an associated delay in maturity. Hence, we interpret the small size of the later maturing *H. gromovae* as a consequence of low growth rates and a high juvenile mortality regime due to low resource availability. The analysis of the growth strategies indicates that dwarfing in the two small hipparionins resulted from different adaptive shifts in their life histories under distinct selective pressures.

Extant equids are less diverse in size, form and ecology than they used to be in the past[73]. Nowadays, only domestic horse breeds show a large size range, while size differences in wild taxa are much less pronounced (e.g. *Equus hemionus* weighting 230 kg[74] and *Equus grevyi* 384 kg[74]). Despite the size disparity, different-sized horse breeds have comparable growth patterns[75]. Gestation lengths also show little variation between breeds[76], and the time of growth plates closure is similar between small and large horses[77]. Considering this, the size difference in domestic horses is not caused by variations in the duration of growth, but by the higher or lower prenatal[76] and postnatal[77] growth rates. Accordingly, we identified a trend indicating higher growth rates in femora of larger extant equids compared to smaller representatives of *Equus*. Hence, differences in growth rates lead to size diversity in extant equids. Similar to the case of *H. gromovae*, epiphyseal closure in the small Iceland horse is delayed, and even later compared to that in Thoroughbreds[77,78]. The lower growth rates and delayed growth plate closure in the small Iceland horse have been related to the original harsher living conditions in which this breed evolved[78]. Likewise, one of the smallest extant wild equid, *Equus hemionus*, dwells in resource-poor environments as the arid and semi-arid steppes and deserts from Asia[79]. In this case, resource limitation led to reduced growth rates and, thus, to a smaller size at maturity. The body size differences between extant taxa, hence, are likely the result of differences in somatic growth rates triggered by differential selective pressures (e.g. resource availability).

Our different life history deductions for the small hipparionins are supported by the different ecological settings inferred for the two bioprovinces. Small ungulates suffer stronger predation pressure than larger ones[80]. They therefore prefer habitats with dense canopy cover (forested areas) that provide shelter and that are more secure than open areas[80–84], albeit the poor forage supply[80–83]. From Vallesian through Turolian, the Eastern Mediterranean bioprovince was characterised by open dry bushlands and grasslands with low tree cover[85–87], a risky habitat for small ungulates[80]. The presence of diverse carnivore associations dominated by hyaenids and felids[85], provides support to our inference from life history models that early maturity and a corollary size decrease in the *macedonicum* morphotype was triggered by high predation pressure. In contrast, the Western Mediterranean biomes during the late Turolian were composed of deciduous forests and xeric woodlands with shrublands and grasslands[88–90]. At the *H. gromovae* site – Rambla de Valdecebro II (=El Arquillo) –, the climate was characterised by a high aridity regime[91]. There was a high carnivore diversity in this area at that time[92,93], but within a patchy landscape there were forest and xeric woodland areas available for cover. These more forested areas could have provided site humidity and increased protection against predation[82,83], habitat parameters preferred by extant small ungulates[80]. This suggests that *H. gromovae*, and possibly also the sympatric smaller *Hipparion periafricanum*, likely dwelled in such forested and more secure habitats. Although conferring the advantage of protection, closed areas support fewer grasses and forbs compared to open habitats because of the shading effect of the canopy[83]. The quantity of available forage, hence, is lower under denser tree cover[82,83,94]. Additionally, these small hipparions must have faced longer periods of resource stress because of the high aridity of El Arquillo site[91], which most likely affected the quality and quantity of available resources[71]. Such adverse climatic conditions must have been an additional problem for equids because their digestive strategy of hindgut fermentation makes them dependent on continuous resource supply[95]. The environmental scenario of low and fluctuating resource levels provides support to our inference from life history models that *H. gromovae* grew at low rates and delayed maturity, which led to a reduction of adult body size. It is conceivable that these resource conditions might have also affected juvenile mortality as observed in extant ungulate populations[59,66–70].

The causes and mechanisms behind size decrease trends on continents are not completely understood. In this survey focused on the bone histology of different-sized hipparionins, we tested if changes in life history traits are related to size decrease in continental settings. We recognised opposed growth strategies in the two dwarfed lineages, a faster life history characterised by an early maturity in the Greek small hipparion vs. a slower strategy with slow growth and later maturity in the Spanish one; otherwise leading to parallel size shrinking under different ecological scenarios. Based on Palkovacs[7] life history model, we consider the size decrease as a by-product of life adaptations to differential ecological constraints. Specifically, we interpret the shift of the Spanish small *H. gromovae* towards a slow life history as a response to limited and unpredictable resource supply and an associated increase in juvenile mortality, and the shift of the Greek small *macedonicum* morphotype towards a fast life history as an adaptation to cope with increased adult mortality regimes. Our results show that there is more than one possible life history strategy behind evolutionary dwarfing, and that bone histology is a powerful tool to unravel the mechanisms involved.

Material and Methods

Previous studies of the characterization and variability of equid bone tissue[43,44] have provided evidences of the usefulness of metapodial bone microstructure for life history reconstruction in this group. Moreover, we used metapodials due to their higher abundance in fossil assemblages and the possibility to assign them to a specific morphotype. We sectioned 31 hipparionin metapodials from the late Miocene of Greece and Spain for histological analysis. The Greek sample comprises metacarpals and metatarsals of one small (*macedonicum* morphotype) and two large (*primigenium* and *dietrichi* morphotypes *sensu* Vlachou[35]) hipparionin morphotypes from seven fossil sites ranging from early Vallesian to late Turolian (Table 2). Large-sized hipparions are used for comparative purposes. The Spanish sample includes metapodials from one small species (*Hipparion gromovae*) and one specimen of the large *H. truyolsi*, both from a late Turolian fossil site of the Teruel Basin (Table 2). Metapodial histology of other large-to-medium sized hipparionins from early Vallesian and middle Turolian of Spain have already been studied in an exhaustive survey by Martinez-Maza *et al.*[44].

To support our interpretations of the growth rates in hipparionins, we also analysed bone appositional rates in extant equids of different body sizes. Because the femur develops over a longer time period[96], its use in *Equus* bone histology is preferred if possible[43]. Hence, we calculated the appositional growth in femora to estimate the growth rates of different-sized extant equids. The entire extant sample was composed by eight femora of wild and

	Group	Body Mass estimation (kg)	Fossil Site and Age (MN)	Element	Specimen	Collection	LM mid-shaft Diameter (mm)
Eastern Mediterranean	*primigenium* morphotype	**188.92** (±43.35 SD, N = 99)	Pentalophos (MN9)	Metacarpal	PNT-22	LGPUT	26.17
			Pentalophos (MN9)	Metatarsal	PNT-4	LGPUT	25.81
			Ravin de la Pluie (MN10)	Metacarpal	RPL-nn	LGPUT	28.53
			Ravin de la Pluie (MN10)	Metatarsal	RPL-3	LGPUT	27.05
			Nikiti-1 (MN10)	Metacarpal	NKT-22	LGPUT	27.75
	dietrichi morphotype	**143.16** (±28.69 SD, N = 279)	Nikiti-2 (MN11)	Metacarpal	NIK-1736	LGPUT	21.92
			Perivolaki (MN12)	Metacarpal	PER-X	LGPUT	21.99
			Perivolaki (MN12)	Metatarsal	PER-1211	LGPUT	22.76
			Perivolaki (MN12)	Metatarsal	PER-342	LGPUT	25.21
			Dytiko-1 (MN13)	Metacarpal	DTK-58	LGPUT	24.42
			Dytiko-1 (MN13)	Metatarsal	DTK-149	LGPUT	24.92
			Dytiko-1 (MN13)	Metatarsal	DTK-106	LGPUT	27.01
			Dytiko-1 (MN13)	Metatarsal	DTK-104	LGPUT	26.34
	macedonicum morphotype	**76.09** (±15.04 SD, N = 258)	Ravin de la Pluie (MN10)	Metacarpal	RPL-44	LGPUT	21.51
			Nikiti-1 (MN10)	Metatarsal	NKT-nn	LGPUT	20.33
			Nikiti-2 (MN11)	Metacarpal	NIK-1698	LGPUT	19.85
			Nikiti-2 (MN11)	Metacarpal	NIK-nn	LGPUT	18.65
			Vathylakos-2 (MN11)	Metatarsal	VAT-112	LGPUT	19.71
			Perivolaki (MN12)	Metacarpal	PER-23	LGPUT	20.43
			Perivolaki (MN12)	Metacarpal	PER-425	LGPUT	20.49
			Perivolaki (MN12)	Metatarsal	PER-380	LGPUT	20.50
			Perivolaki (MN12)	Metatarsal	PER-485	LGPUT	20.29
Western Mediterranean	*Hipparion gromovae*	**84.33** (±12.86 SD, N = 80)	Rambla de Valdecebro II (MN13)	Metacarpal	IPS-96274	ICP	21.91
			Rambla de Valdecebro II (MN13)	Metacarpal	IPS-96275	ICP	19.02
			Rambla de Valdecebro II (MN13)	Metacarpal	IPS-101807	ICP	21.12
			Rambla de Valdecebro II (MN13)	Metacarpal	IPS-101810	ICP	20.43
			Rambla de Valdecebro II (MN13)	Metatarsal	IPS-96276	ICP	20.92
			Rambla de Valdecebro II (MN13)	Metatarsal	IPS-96277	ICP	21.51
			Rambla de Valdecebro II (MN13)	Metatarsal	IPS-101808	ICP	22.22
			Rambla de Valdecebro II (MN13)	Metatarsal	IPS-01809	ICP	22.81
	H. truyolsi	**192.46** (±17.37 SD, N = 8)	Rambla de Valdecebro II (MN13)	Metatarsal	IPS-28842	ICP	28.73

Table 2. Sample analysed and results of body mass estimations. Lateromedial diameter (LM) at mid-shaft is provided as a metapodial size proxy. LGPUT: Material sampled from the collections of the Laboratory of Geology and Paleontology at the University of Thessaloniki; ICP: Material sampled from the collections of the Institut Català de Paleontologia Miquel Crusafont.

domestic equids; two belonging to *Equus grevyi*, two to *Equus hemionus*, and four to different-sized horse breeds (Iceland, Welsh, Hackney and Shetland) (Supplementary Table S1).

Adult body mass estimations of the fossil Greek morphotypes were calculated from the material published in Vlachou[35] and were kindly provided by the author. Body mass estimations of the Spanish sample were calculated (Supplementary Table S2) following the same measurements and regressions used for the Greek metapodials (Table 2). These estimations were obtained for each morphotype from measurements on metapodials (Mc10, Mt10, Mc13, Mt13, following Eisenmann *et al.*[97]) and using the equations provided by Eisenmann and Sondaar[98] and Scott[53].

Preparation of histological slides. Histological slides were produced following the standard protocol of our laboratory[43,99]. Mid-shaft blocks of each metapodial were embedded in epoxy resin (Araldite 2020) and sectioned using an IsoMet low-speed saw (Buehler). The exposed surfaces were polished using a grinder polisher (Buehler, MetaServ 250) and glued to a glass slide using the same epoxy resin. The mounted samples were cut using a diamond saw (Buehler, Petrothin) up to a thickness of 300 µm and grounded to 150–100 µm, using the grinder polisher. Finally, the slides were dehydrated in alcohol gradients and immersed in a histological clearing agent (Histo-Clear II) prior to cover them with a DPX medium.

The histological samples were studied under polarised light using a Zeiss Scope.A1 microscope with an attached digital camera (AxioCam ICc5). The slides were examined using a retardation filter of ¼ λ to improve the observation of the bone tissues and growth marks[100]. The micrographs of the cortex were merged using Adobe Photoshop® and analysed with Image J software.

Bone histology. We analysed bone tissues and bone growth marks to reconstruct metapodial growth. Description of bone tissues types follows the classification of Francillon-Viellot *et al.*[101] and de Margerie *et al.*[48].

The analysis of cyclical growth marks (CGM) of annual periodicity[99] provide the temporal basis for the reconstruction of metapodial growth and the assessment of certain life history traits[6,37,38]. Where the growth marks were faint due to poor tissue preservation or partially eroded by secondary osteons, we retrocalculated their track by superimposition[102]. The identification of a non-cyclical growth mark, the neonatal line[47], in the innermost cortical area of almost all metapodials allowed the estimation of bone size at birth.

The significant decrease in bone growth rate marks the attainment of bone maturity. This event is identified by the periosteal deposition of slow-growing lamellar bone after fast-growing fibrous tissue[37] and by the narrowing of consecutive growth zones[51]. By counting the CGM that precede the deposition of the avascular lamellar bone found in the outermost cortex of bone (external fundamental system (EFS) *sensu* Woodward *et al.*[102]), some authors have inferred the organism's age at sexual maturity[38,103] or skeletal maturity[44,57] from mainly tibia and femora tissues. Nacarino-Meneses *et al.*[43], however, provided evidence that the decrease in periosteal growth rate in equids metapodials – represented by the inflection point of the growth curves – is an indicator of their epiphyseal fusion and the end of longitudinal growth. As metapodials fuse their epiphyses earlier than other long bones[96], the identification of the moment of metapodial growth decrease only provides a relative age at skeletal maturity. Thus, we obtain a proxy of maturity attainment, instead of an absolute age at which the animal should end its growth. We used this '*relative maturity*' to compare between taxa and to identify which species tends to delay or to advance it.

In the extant femur sample used for comparative purpose, we estimated the growth rate between the first and the second year of growth. We identified these two CGM and measured their perimeter. The estimation of the growth rate was calculated as the perimeter difference between the second and the first CGM.

Growth curves. Growth data in metapodials were obtained by counting the bone growth marks and by calculating their perimeters. Contrary to studies on dinosaurs[41,104] that use body mass estimations for each growth cycle, our growth curves are based on direct measures. We did not estimate body mass at each growth cycle because the correlation between equid metapodial mid-shaft dimensions and body mass is not significant[25], and the regressions are based adult individuals. Instead, we took the direct skeletal measurement of the mid-shaft circumference as a proxy of body size, a more conservative alternative to an estimate of body mass[52]. In those cases where exact mid-shaft cuts were not possible due to the fragmentary nature of the specimen (IPS-101809, *H. gromovae* metatarsal), the bone circumference is slightly overestimated. This is particularly true in metatarsals which are anteroposteriorly wider in more proximal planes; however, the growth trajectory can be equally reconstructed. From the available sample, we used only those specimens for the growth curve reconstructions where the radial growth was finished (18 metapodials). The other specimens have been analysed for bone tissue characterization, growth mark superimposition, and the study of the ontogenetic development.

Similar to other biological processes, growth is generally modelled using nonlinear sigmoidal equations[105,106]. Among several models, and considering the nature of our data, we used the logistic equation (1) [1,107] to describe the pattern of metapodial radial growth because it presents good fitting values (Akaike Information Criterion) (Supplementary Table S3) and provides the most realistic asymptotic size values. A similar logistic model has been used to describe the circumferential growth of dinosaurian femora and tibiae[40,108], as well as dinosaur body mass growth[104]. We used the nonlinear least squares fitting of the PAST software to fit the curves equations to our data[109].

$$y(t) = \frac{A}{(1 + be^{-kt})} \tag{1}$$

In sigmoidal equations, the parameter A represents the final asymptotic value to which the response variable approaches in an exponentially decreasing rate after reaching the growth inflection point[50]. In our case, the A parameter shows the final adult metapodial circumferential size. The mean relative growth rate, or the relative velocity at which the response variable is approaching to this final size, is characterised by the exponent k[108], while the parameter b represents the quotient between the initial and final size[110]. Hence, the parameter k expresses the ratio of the maximum growth rate in relation to the adult size, indicating delayed maturity when k is low and advanced maturity when k is high[111]. These growth curve parameters were calculated for each specimen and the results were also averaged to obtain a mean growth curve for the metacarpals and metatarsals of each group[42]. The rate at which bone grows was calculated from the derivative (2) of this logistic equation (1), representing the instantaneous growth rate at a concrete time. It should be considered that the calculated growth rate values expressed as mm/year do not represent a real approximation of the rate at which those bones were growing, because bone growth rate varies with the season of the year[99]. However, these values represent useful estimates for comparison[42]. In order to compare the growth rates between species, we estimated the relative growth rate (RGR) extracting the effect of size (3), because growth rates tightly scale with size[1]. The relative growth rate is defined as the increase per unit of time relative to the size at a concrete point[112].

$$GR(t) = \frac{\partial y}{\partial t} = \frac{A\,b\,k\,e^{kt}}{(b + e^{kt})^2} \tag{2}$$

$$RGR(t) = \frac{1}{y(t)}\frac{\partial y}{\partial t} = \frac{A\,b\,k\,e^{kt}}{y(t)(b + e^{kt})^2} \tag{3}$$

Additionally, we calculated the time required to attain the 95% of the final size (4) as an indicator of the growth duration time[108].

$$t_{95A} = -\frac{1}{k}\ln\left(\frac{0.05A}{0.95A\,b}\right) \tag{4}$$

Statistics. Statistical analyses and graphs were performed using Past 3.14[109] and Microsoft Office Excel. Pearson's correlation was used for the linear correlation analysis. A significance level of 0.05 was used for all tests.

Data Availability

The data sets generated and/or analysed during the current study are included on this published article. Raw data not included is available from the corresponding author on reasonable request.

References

1. Calder, W. A. *Size, Function, and Life History*. (Harvard University Press, 1984).
2. Peters, R. H. *The Ecological Implications of Body Size. Cambridge Studies inEcology*, https://doi.org/10.1017/CBO9780511608551 (Cambridge University Press, 1983).
3. Damuth, J. D. & MacFadden, B. J. *Body Size in Mammalian Paleobiology: Estimation and Biological Implications*. (Cambridge University Press, 1990).
4. Barbault, R. In *Evolutionary Biology* 261–286, https://doi.org/10.1007/978-1-4613-0931-4_6 (Springer US, 1988).
5. Raia, P. & Meiri, S. The island rule in large mammals: paleontology meets ecology. *Evolution* **60**, 1731–1742 (2006).
6. Köhler, M. & Moyà-Solà, S. Physiological and life history strategies of a fossil large mammal in a resource-limited environment. *Proc. Natl. Acad. Sci. USA* **106**, 20354–8 (2009).
7. Palkovacs, E. P. Explaining adaptive shifts in body size on islands: a life history approach. *Oikos* **103**, 37–44 (2003).
8. Bromage, T. G. *et al*. A life history and climate change solution to the evolution and extinction of insular dwarfs: a Cypriot experience. In Waldren, W. H., Ensenyat, J. A. *(Eds) World Islands in Prehistory. International Insular Investigations, V Deià Conference of Prehistory*. 420–427 (Archaeopress, 2002).
9. Stearns, S. C. *The Evolution of Life Histories*. (Oxford University Press, 1992).
10. Roff, D. A. *The Evolution of Life Histories: Theory and Analysis*. (Chapman & Hall, 1992).
11. Stearns, S. C. Life history evolution: Successes, limitations, and prospects. *Naturwissenschaften* **87**, 476–486 (2000).
12. Stearns, S. C. & Koella, J. C. The evolution of phenotypic plasticity in life-History traits: predictions of reaction norms for age and size at maturity. *Evolution (N. Y)*. **40**, 893 (1986).
13. Berrigan, D. & Koella, J. C. The evolution of reaction norms: simple models for age and size at maturity. *J. Evol. Biol.* **7**, 549–566 (1994).
14. Lomolino, M. V. Body size of mammals on islands: the Island Rule reexamined. *Am. Nat.* **125**, 310–316 (1985).
15. Case, T. J. A general explanation for insular body size trends in terrestrial vertebrates. *Ecology* **59**, 1–18 (1978).
16. Foster, J. B. Evolution of mammals on islands. *Nature* **202**, 234–235 (1964).
17. Jordana, X. & Köhler, M. Enamel microstructure in the fossil bovid Myotragus balearicus (Majorca, Spain): Implications for life-history evolution of dwarf mammals in insular ecosystems. *Palaeogeogr. Palaeoclimatol. Palaeoecol.* **300**, 59–66 (2011).
18. Köhler, M. Fast or slow? The evolution of life history traits associated with insular dwarfing. In Pérez-Mellado, V. & Ramon, Ma. M. (Eds), *Islands and Evolution* **19**, 261–280 (Institut Menorquí d'Estudis, Recerca, 2010).
19. Orlandi-Oliveras, G., Jordana, X., Moncunill-Solé, B. & Köhler, M. Bone histology of the giant fossil dormouse *Hypnomys onicensis* (Gliridae, Rodentia) from Balearic Islands. *Comptes Rendus - Palevol* **15**, 247–253 (2016).
20. Moncunill-Solé, B., Orlandi-Oliveras, G., Jordana, X., Rook, L. & Köhler, M. First approach of the life history of *Prolagus apricenicus* (Ochotonidae, Lagomorpha) from Terre Rosse sites (Gargano, Italy) using body mass estimation and paleohistological analysis. *Comptes Rendus - Palevol* **15**, 235–245 (2016).
21. Gould, G. C. & MacFadden, B. J. Gigantism, dwarfism, and Cope's Rule: "nothing in evolution makes sense without a phylogeny". *Bull. Am. Museum Nat. Hist.* **285**, 219–237 (2004).
22. Kurtén, B. *Pleistocene Mammals of Europe*. (Aldine Transaction, 2009).
23. Prothero, D. R. & Sereno, P. C. Allometry and paleoecology of medial Miocene dwarf rhinoceroses from the Texas Gulf Coastal Plain. *Paleobiology* **8**, 16–30 (1982).
24. Stanley, S. An explanation for Cope's Rule. *Evolution (N. Y)*. **27**, 1–26 (1973).
25. Alberdi, M. T., Prado, J. L. & Ortiz-Jaureguizar, E. Patterns of body size changes in fossil and living Equini (Perissodactyla). *Biol. J. Linn. Soc.* **54**, 349–370 (1995).
26. MacFadden, B. J. Evolution. Fossil horses–evidence for evolution. *Science* **307**, 1728–1730 (2005).
27. D'Ambrosia, A. R. D., Clyde, W. C., Fricke, H. C., Gingerich, P. D. & Abels, H. A. Repetitive mammalian dwarfing during ancient greenhouse warming events. *Sci. Adv*. 1–19 (2017).
28. Koufos, G. D. Hipparion macedonicum revisited: New data on evolution of hipparionine horses from the Late Miocene of Greece. *Acta Palaeontol. Pol.* **61**, 519–536 (2016).
29. Ortiz-Jaureguizar, E. & Alberdi, M. T. El patrón de cambios en la masa corporal de los Hipparionini (Perissodactyla, Equidae) de la península ibérica durante el Mioceno Superior-Plioceno Superior. *Coloquios Paleontol.* **1**, 499–509 (2003).
30. Pesquero, M. D. Hipparion del Turoliense superior de Las Casiones (Fosa de Teruel). *Coloquios Paleontol*. Volumen Ex, 511–548 (2003).
31. Guthrie, R. D. Rapid body size decline in Alaskan Pleistocene horses before extinction. *Nature* **426**, 169–171 (2003).
32. Forstén, A. Size decrease in pleistocene-holocene true or caballoid horses of europe. *Mammalia* **55**, 407–420 (1991).
33. Bernor, R. L. *et al*. Systematic, stratigraphic, and paleoenvironmental contexts of first-appearing *Hipparion* in the Vienna Basin, Austria. *J. Vertebr. Paleontol.* **8**, 427–452 (1988).
34. Cantalapiedra, J. L., Prado, J. L., Hernández Fernández, M. & Alberdi, M. T. Decoupled ecomorphological evolution and diversification in Neogene-Quaternary horses. *Science (80-.)*. **355**, 627–630 (2017).
35. Vlachou, T. D. *Palaeontological, Biostratigraphical and Palaeoecological Study of the Greek Hipparions*. (Aristotle University of Thessaloniki, 2013).
36. Chinsamy-Turan, A. *The Microstructure of Dinosaur Bone*. (The Johns Hopkins University Press, 2005).
37. Padian, K. & Lamm, E.-T. *Bone Histology of Fossil Tetrapods: Advancing Methods, Analysis, and Interpretation*. (University of California Press, 2013).
38. Marín-Moratalla, N., Jordana, X. & Köhler, M. Bone histology as an approach to providing data on certain key life history traits in mammals: Implications for conservation biology. *Mamm. Biol.* **78**, 422–429 (2013).
39. Amson, E., Kolb, C., Scheyer, T. M. & Sánchez-Villagra, M. R. Growth and life history of Middle Miocene deer (Mammalia, Cervidae) based on bone histology. *Comptes Rendus - Palevol* **14**, 637–645 (2015).
40. Bybee, P. J., Lee, A. H. & Lamm, E.-T. Sizing the Jurassic Theropod Dinosaur *Allosaurus*: Assessing Growth Strategy and Evolution of Ontogenetic Scaling of Limbs. *J. Morphol.* **267**, 347–359 (2006).

41. Lehman, T. M. & Woodward, H. N. Modeling growth rates for sauropod dinosaurs. *Paleobiology* **34**, 264–281 (2008).
42. Woodward, H. N., Freedman Fowler, E. A., Farlow, J. O. & Horner, J. R. *Maiasaura*, a model organism for extinct vertebrate population biology: a large sample statistical assessment of growth dynamics and survivorship. *Paleobiology* **41**, 1–25 (2015).
43. Nacarino-Meneses, C., Jordana, X. & Köhler, M. Histological variability in the limb bones of the Asiatic wild ass and its significance for life history inferences. *PeerJ* **4**, e2580 (2016).
44. Martinez-Maza, C., Alberdi, M. T., Nieto-Diaz, M. & Prado, J. L. Life-history traits of the miocene *Hipparion concudense* (Spain) inferred from bone histological structure. *PLoS One* **9**, e103708 (2014).
45. Sander, P. M. & Andrássy, P. Lines of arrested growth and long bone histology in Pleistocene large mammals from Germany: what do they tell us about dinosaur physiology? *Palaeontogr. A* **277**, 143–159 (2006).
46. Prondvai, E., Stein, K. H. W., de Ricqlès, A. J. & Cubo, J. Development-based revision of bone tissue classification: the importance of semantics for science. *Biol. J. Linn. Soc.* **112**, 799–816 (2014).
47. Nacarino-Meneses, C. & Köhler, M. Limb bone histology records birth in mammals. *PLoS One* **13**, e0198511 (2018).
48. de Margerie, E., Cubo, J. & Castanet, J. Bone typology and growth rate: Testing and quantifying 'Amprino's rule' in the mallard (*Anas platyrhynchos*). *Comptes Rendus - Biol.* **325**, 221–230 (2002).
49. de Margerie, E. *et al.* Assessing a relationship between bone microstructure and growth rate: a fluorescent labelling study in the king penguin chick (*Aptenodytes patagonicus*). *J. Exp. Biol.* **207**, 869–79 (2004).
50. Lee, A. H., Huttenlocker, A. K., Padian, K. & Woodward, H. N. In *Bone Histology of Fossil Tetrapods - Advancing Methods, Analysis, and Interpretation* **086**, 217–251 (2013).
51. Chinsamy, A. & Valenzuela, N. Skeletochronology of the endangered Side-Neck Turtles Podocnemis expansa. *S. Afr. J. Sci.* **104**, 311–314 (2008).
52. Campione, N. E. & Evans, D. C. A universal scaling relationship between body mass and proximal limb bone dimensions in quadrupedal terrestrial tetrapods. *BMC Biol.* **10**, 60 (2012).
53. Scott, K. M. In *Body Size in Mammalian Paleobiology: Estimation and Biological Implications* (eds Damuth, J. & Macfadden, B. J.) 301–335 (Cambridge University Press, 1990).
54. Horner, J. R., Ricqlès, Ade & Padian, K. Variation in Dinosaur Skeletochronology Indicators: Implications for Age Assessment and Physiology. *Paleobiology* **25**, 295–304 (1999).
55. Castanet, J., Rogers, K. C., Cubo, J. & Boisard, J.-J. Periosteal bone growth rates in extant ratites (ostriche and emu). Implications for assessing growth in dinosaurs. *C. R. Acad. Sci. III.* **323**, 543–550 (2000).
56. Martin Sander, P., Mateus, O., Laven, T. & Knötschke, N. Bone histology indicates insular dwarfism in a new Late Jurassic sauropod dinosaur. *Nature* **441**, 739–741 (2006).
57. Kolb, C. *et al.* Growth in fossil and extant deer and implications for body size and life history evolution. *BMC Evol. Biol.* **15**, 19 (2015).
58. Pesquero, M. D. & Alberdi, M. T. New evidence of conspecificity between *Hipparion primigenium melendezi* Alberdi, 1974 from Los Valles de Fuentidueña (Segovia) and *Hipparion concudense concudense* Pirlot, 1956 from Concud (Teruel) Spain. *Estud. Geológicos* **68**, 247–260 (2012).
59. Gaillard, J.-M., Festa-Bianchet, M., Yoccoz, N. G., Loison, A. & Toïgo, C. Temporal Variation in Fitness Components and Population Dynamics of Large Herbivores. *Annu. Rev. Ecol. Syst.* **31**, 367–393 (2000).
60. Law, R. Optimal life histories under age-specific predation. *Am. Nat.* **114**, 399–417 (1979).
61. Promislow, D. E. L. & Harvey, P. H. Living fast and dying young: A comparative analysis of life-history variation among mammals. *J. Zool.* **220**, 417–437 (1990).
62. Gadgil, M. & Bossert, W. H. Life historical consequences of natural selection. *American Naturalist* **104**, 1–24 (1970).
63. Skogland, T. Natural selection of wild reindeer life history traits by food limitation and predation. *Oikos* **55**, 101 (1989).
64. Koons, D. N., Metcalf, C. J. E. & Tuljapurkar, S. Evolution of delayed reproduction in uncertain environments: a life-history perspective. *Am. Nat.* **172**, 797–805 (2008).
65. Moehlman, P. D. *Equids: Zebras, Asses, and Horses: Status Survey and Conservation Action Plan*. (IUCN/SSC Equid Specialist Group, 2002).
66. Georgiadis, N., Hack, M. & Turpin, K. The influence of rainfall on zebra population dynamics: Implications for management. *J. Appl. Ecol.* **40**, 125–136 (2003).
67. Bartmann, R. M., White, G. C. & Carpenter, L. H. Compensatory Mortality in a Colorado Mule Deer Population. *Wildl. Monogr.* **121**, 1–39 (1992).
68. Grange, S. *et al.* What limits the Serengeti zebra population? *Oecologia* **140**, 523–532 (2004).
69. Choquenot, D. Density-dependent growth, body condition, and demography in feral donkeys: testing the food hypothesis. *Ecology* **72**, 805–813 (1991).
70. Sand, H. Life history patterns in female moose (*Alces alces*): the relationship between age, body size, fecundity and environmental conditions. *Oecologia* **106**, 212–220 (1996).
71. Illius, A. W. & O'Connor, T. G. Resource heterogeneity and ungulate population dynamics. *Oikos* **89**, 283–294 (2000).
72. Rubenstein, D. I. Life history and social organization in arid adaptated ungulates. *J. Arid Environ.* **17**, 145–156 (1989).
73. MacFadden, B. J. Fossil Horses–Evidence for Evolution. *Science (80-.).* **307**, 1728–730 (2005).
74. Tacutu, R. *et al.* Human Ageing Genomic Resources: Integrated databases and tools for the biology and genetics of ageing. *Nucleic Acids Res.* **41**, D1027–D1033 (2013).
75. Green, D. A. A review of studies on the growth rate of the horse. *Br. Vet. J.* **117**, 181–191 (1961).
76. Heck, L., Clauss, M. & Sánchez-Villagra, M. R. Gestation length variation in domesticated horses and its relation to breed and body size diversity. *Mamm. Biol.* **84**, 44–51 (2017).
77. Strand, E., Braathen, L. C., Hellsten, M. C., Huse-Olsen, L. & Bjornsdottir, S. Radiographic closure time of appendicular growth plates in the Icelandic horse. *Acta Vet. Scand.* **49**, 19 (2007).
78. Łuszczyński, J., Pieszka, M. & Kosiniak-Kamysz, K. Effect of horse breed and sex on growth rate and radiographic closure time of distal radial metaphyseal growth plate. *Livest. Sci.* **141**, 252–258 (2011).
79. Kaczensky, P., Lkhagvasuren, B., Pereladova, O., Hemami, M. & Bouskila, A. Equus hemionus. *IUCN Red List Threat. Species* **2015** (2015).
80. Djagoun, C. A. M. S. *et al.* Hunting affects dry season habitat selection by several bovid species in northern Benin. *Wildlife Biol.* **20**, 83–90 (2014).
81. Fischhoff, I. R., Sundaresan, S. R., Cordingley, J. & Rubenstein, D. I. Habitat use and movements of plains zebra (*Equus burchelli*) in response to predation danger from lions. *Behav. Ecol.* **18**, 725–729 (2007).
82. Godvik, I. M. R. *et al.* Temporal scales, trade-offs, and functional responses in red deer habitat selection. *Ecology* **90**, 699–710 (2009).
83. Mysterud, A. & Ostbye, E. Cover as a habitat element for temperate ungulates: effects on habitat selection and demography. *Wildl. Soc. Bull.* **27**, 385–394 (1999).
84. Wiens, J. A. In *The Ecology of Natural Disturbance and Patch Dynamics* (eds Pickett, S. & White, P.) 169–193, https://doi.org/10.1016/B978-0-08-050495-7.50015-6 (Academic Press, 1985).
85. Koufos, G. D. & Konidaris, G. E. Late Miocene carnivores of the Greco-Iranian Province: Composition, guild structure and palaeoecology. *Palaeogeogr. Palaeoclimatol. Palaeoecol.* **305**, 215–226 (2011).

86. Merceron, G. *et al.* Stable isotope ecology of Miocene bovids from Northern Greece and the ape/monkey turnover in the Balkans. *J. Hum. Evol.* **65**, 185–198 (2013).
87. Merceron, G., Blondel, C., Viriot, L., Koufos, G. D. & De Bonis, L. Dental microwear analysis of bovids from the Vallesian (late Miocene) of Axios Valley in Greece: Reconstruction of the habitat of Ouranopithecus macedoniensis (Primates, Hominoidea). *Geodiversitas* **29**, 421–433 (2007).
88. García-Alix, A. A multiproxy approach for the reconstruction of ancient continental environments. The case of the Mio-Pliocene deposits of the Granada Basin (southern Iberian Peninsula). *Glob. Planet. Change* **131**, 1–10 (2015).
89. Domingo, L. *et al.* Late Neogene and Early Quaternary paleoenvironmental and paleoclimatic conditions in southwestern Europe: isotopic analyses on mammalian taxa. *PLoS One* **8**, e63739 (2013).
90. Hernández Fernández, M. *et al.* Identification problems of arid environments in the Neogene-Quaternary mammal record of Spain. *J. Arid Environ.* **66**, 585–608 (2006).
91. Matson, S. D. & Fox, D. L. Stable isotopic evidence for terrestrial latitudinal climate gradients in the Late Miocene of the Iberian Peninsula. *Palaeogeogr. Palaeoclimatol. Palaeoecol.* **287**, 28–44 (2010).
92. Salesa, M. J. *et al.* A rich community of Felidae (Mammalia, Carnivora) from the late Miocene (Turolian, MN 13) site of Las Casiones (Villalba Baja, Teruel, Spain). *J. Vertebr. Paleontol.* **32**, 658–676 (2012).
93. Alcalá, L. *Macromamiferos Neogenos de la Fosa de Alfambra-Teruel*. (Instituto de Estudios Turolenses, 1994).
94. Mysterud, A. & Ims, R. Functional Responses in Habitat Use: Availability Influences Relative Use in Trade-Off Situations. *Ecology* **79**, 1435–1441 (1998).
95. Janis, C. M. The evolutionary strategy of the equidae and the origins of rumen and cecal digestion. *Evolution (N. Y).* **30**, 757 (1976).
96. Silver, I. A. In *Science* in *Archaeology* (eds Brothweel, D. & Higgs, E.) 250–268 (1969).
97. Eisenmann, V., Alberdi, M. T., De Giuli, C. & Staesche, U. Studying fossil horses. *Collected papers after the "New York International Hipparion Conference, 1981"* **1**, 1–72 (1988).
98. Eisenmann, V. & Sondaar, P. Y. Pliocene vertebrate locality of Çalta, Ankara, Turkey. 7. *Hipparion. Geodiversitas* **20**, 409–439 (1998).
99. Köhler, M., Marín-Moratalla, N., Jordana, X. & Aanes, R. Seasonal bone growth and physiology in endotherms shed light on dinosaur physiology. *Nature* **487**, 358–361 (2012).
100. Turner-Walker, G. & Mays, S. In *Advances in Human Palaeopathology* 121–146, https://doi.org/10.1002/9780470724187.ch7 (John Wiley & Sons, Ltd, 2008).
101. Francillon-Vieillot, H. *et al.* In *Skeletal Biomineralization: Patterns, Processes and Evolutionary* Trends (ed. Carter, J. C.) l, 471–530 (Van Nostrand Reinhold, 1990).
102. Woodward, H. N., Padian, K. & Lee, A. H. In *Bone Histology of Fossil Tetrapods - Advancing Methods, Analysis, and Interpretation* (eds Padian, K. & Lamm, E.-T.) 195–216 (2013).
103. Jordana, X., Marín-Moratalla, N., Moncunill-Solé, B., Nacarino-Meneses, C. & Köhler, M. Ontogenetic changes in the histological features of zonal bone tissue of ruminants: A quantitative approach. *Comptes Rendus - Palevol* **15**, 265–276 (2016).
104. Erickson, G. M., Curry, K. A. & Yerby, S. A. Dinosaurian growth patterns and rapid avian growth rates. *Nature* **412**, 429–433 (2001).
105. Ricklefs, R. E. *The Economy of Nature*. (Macmillan, 2008).
106. Zullinger, E. M., Ricklefs, R. E., Redford, K. H. & Mace, G. M. Fitting sigmoidal equations to mammalian growth curves. *J. Mammal.* **65**, 607–636 (1984).
107. Ricklefs, R. E. Adaptation, constraint, and compromise in avian postnatal development. *Biol. Rev.* **54**, 269–290 (1979).
108. Lee, A. H. & O'connor, P. M. Bone histology confirms determinate growth and small body size in the noasaurid theropod *Masiakasaurus knopfleri*. *J. Vertebr. Paleontol.* **33**, 865–876 (2013).
109. Hammer, Ø., Harper, D. A. Ta. T. & Ryan, P. D. PAST: Paleontological Statistics Software Package for Education and Data Analysis. *Palaeontol. Electron.* **4**(1), 1–9 (2001).
110. Brody, S. *Bioenergetics and Growth*. (Reinhold Publishing Corporation: New York, 1945).
111. Lupi, T. M., Nogales, S., Leon, J. M., Barba, C. & Delgado, J. V. Characterization of commercial and biological growth curves in the Segurena sheep breed. *Animal* **9**, 1341–1348 (2015).
112. von Bertalanffy, L. A quantitative theory of organic growth (inquiries on growth laws. *II). Hum. Biol.* **10**, 181–213 (1938).

Acknowledgements

We would like to thank M. Soteras for access to the museum collections at the Institut Català de Paleontologia Miquel Crusafont (ICP). G.O.-O. would also like to thank D. Kostopoulos (Aristotle University of Thessaloniki, AUT) for the help during his visit to the Laboratory of Geology and Palaeontology at the University of Thessaloniki collections, and to T. Vlachou (AUT) for the help on the taxonomic identification and the body mass estimations of the Greek material. We are grateful to M. Fernández, G. Prats-Muñoz and L. Gordón for preparation of the thin slices, and to the ICP preparators for moulding the specimens. B. Lamglait (currently at Université de Montréal) together with the Réserve Africaine de Sigean are acknowledged for the donation extant equid specimens to the ICP collections. Thanks go further to T. Kaiser and R. Schafberg for loans and permission to cut bones of extant *Equus* from the collections of the Zoologisches Museum of Universität Hamburg, and the Museum für Haustierkunde of the Martin-Luther-Universität Halle-Wittenberg, respectively, and also to the Zoologisches Institut und Museum, Christian-Albrechts-Universität Kiel. A. García-Alix (Universidad de Granada) is acknowledged for valuable discussion and two anonymous referees for their helpful comments on the manuscript. Finally, G.O.-O. thanks the assistance of A. Capalvo in the growth curves modelling. Funding for this study was provided by the Spanish Ministry of Economy and Competitiveness (MINECO) (PI: M.K., CGL2015-63777) and the CERCA Programme (Generalitat de Catalunya). The research group formed by M.K., C.N.-M. and G.O.-O. is recognised without funding by AGAUR (Generalitat de Catalunya) (2017 SGR 960). G.O.-O. is supported by a FI-DGR 2016 grant (2016FI_B00202) awarded by AGAUR (Generalitat de Catalunya) and C.N.-M. held FPI grant 2013 from the MINECO (BES-2013-066335).

Author Contributions

G.O.-O. and M.K. conceived and designed the experiments. C.N.-M. provided helpful advice during interpretation of the histological part and contributed with the analysis of the extant equids' material. G.O.-O. wrote the manuscript and prepared the figures and tables. M.K. supervised the histological study, the interpretation and discussion of the results, and the preparation of the manuscript. G.D.K. provided the Greek material for analysis. All authors reviewed the manuscript.

Additional Information

Supplementary information accompanies this paper at https://doi.org/10.1038/s41598-018-35347-x.

Competing Interests: The authors declare no competing interests.

Publisher's note: Springer Nature remains neutral with regard to jurisdictional claims in published maps and institutional affiliations.

Supplementary Material for:

Bone histology provides insights into the life history mechanisms underlying dwarfing in hipparionins.

Guillem Orlandi-Oliveras, Carmen Nacarino-Meneses, George D. Koufos & Meike Köhler

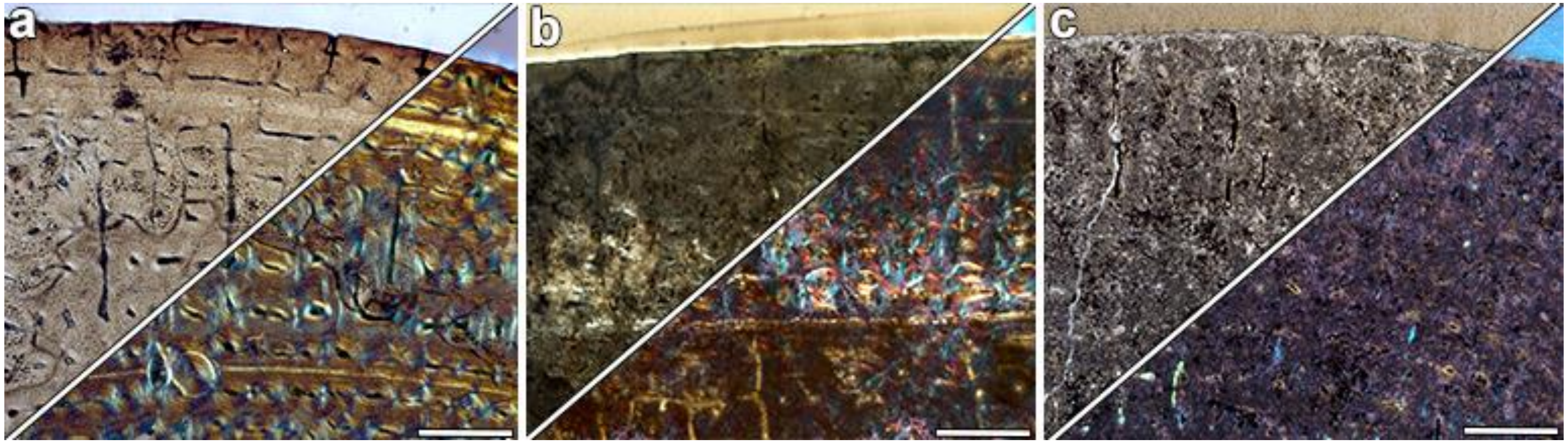

Supplementary Figure S1. Histological preservation of the sample. Top half part of the microphotographs shows bone cross-sections observed under polarised light, lower half images show bone cross-sections observed under polarised light using a 1/4λ filter. Scale: 0.5 mm. **(a)** Well preserved bone tissue in the metapodials from the Teruel basin (Spain). *H. gromovae* metacarpal IPS-96275. **(b)** Poorly preserved bone tissue where histological structures are still distinguishable in almost all the Greek specimens. *H.* aff. *platygenys* (*dietrichi* morphotype) metatarsal DTK-104. **(c)** Severely damaged microstructure in the samples from Nikiti-2 (NIK) fossil site (Greece). *H. philippus* (*dietrich*i morphotype) metacarpal NIK-nn.

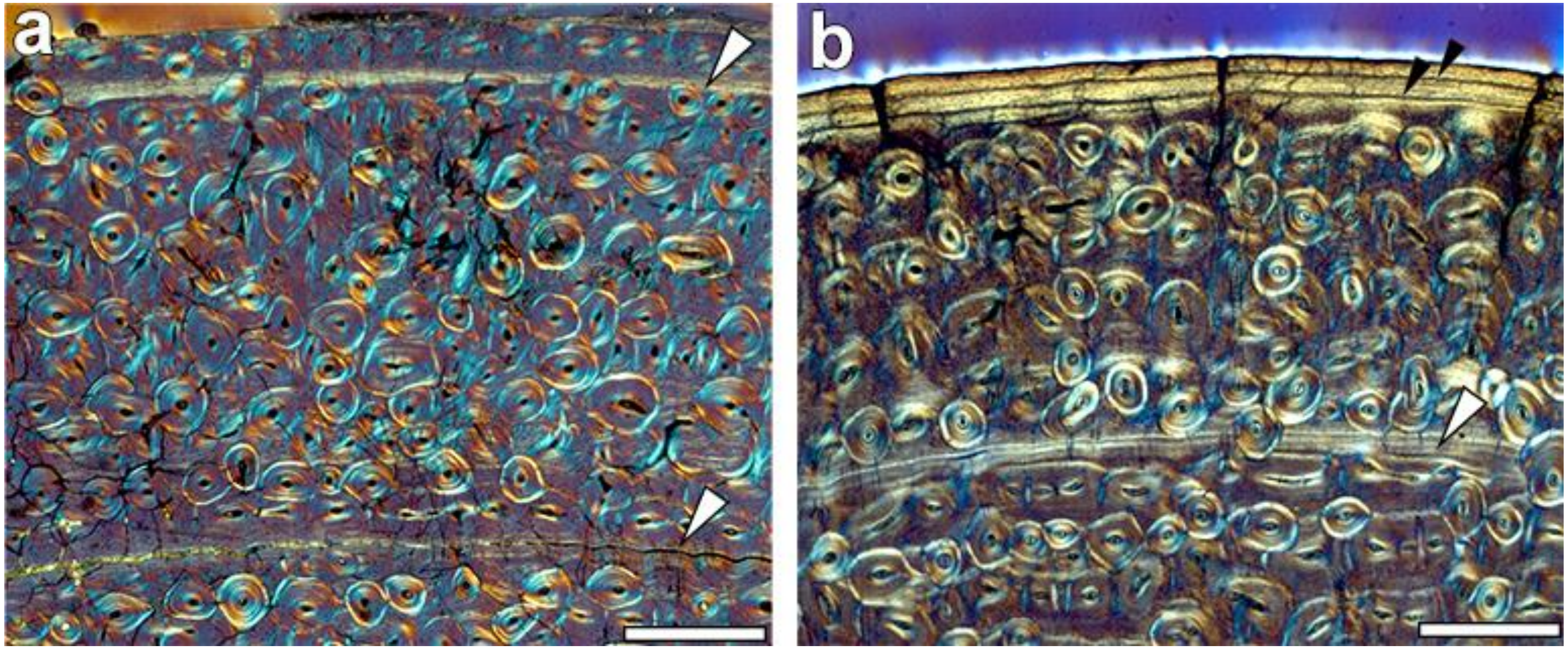

Supplementary Figure S2. Bone cortex with a high density of Haversian Systems, albeit conserving bone growth marks. Images were obtained under polarised light using a 1/4λ filter. Scale: 0.5 mm. **(a)** *H. philippus* (*dietrich*i morphotype) metacarpal PER-X. **(b)** *H. truyolsi* metatarsal IPS-28842.

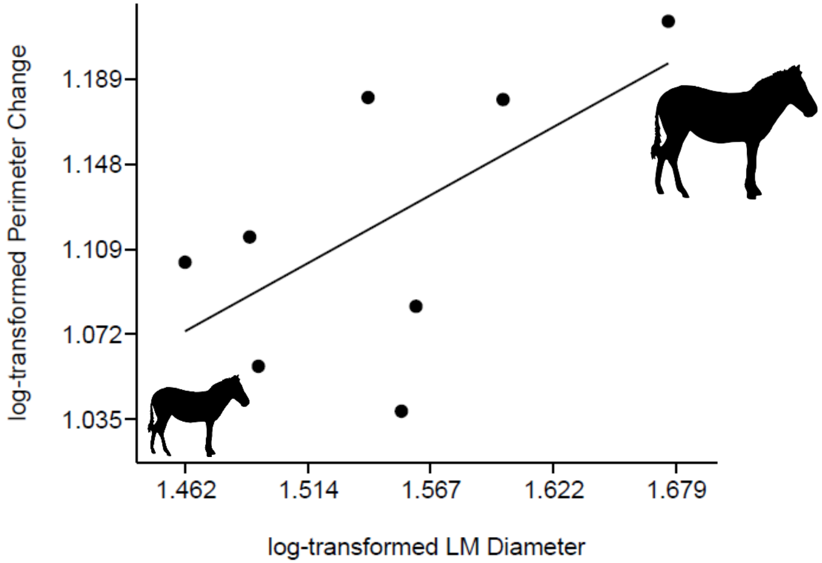

Supplementary Figure S3. Linear regression relating the increase in perimeter between the first and the second cyclical growth mark and the lateromedial (LM) diameter of extant equid femurs. Both variables were log-transformed to linearise the relationship. See main text for statistics information.

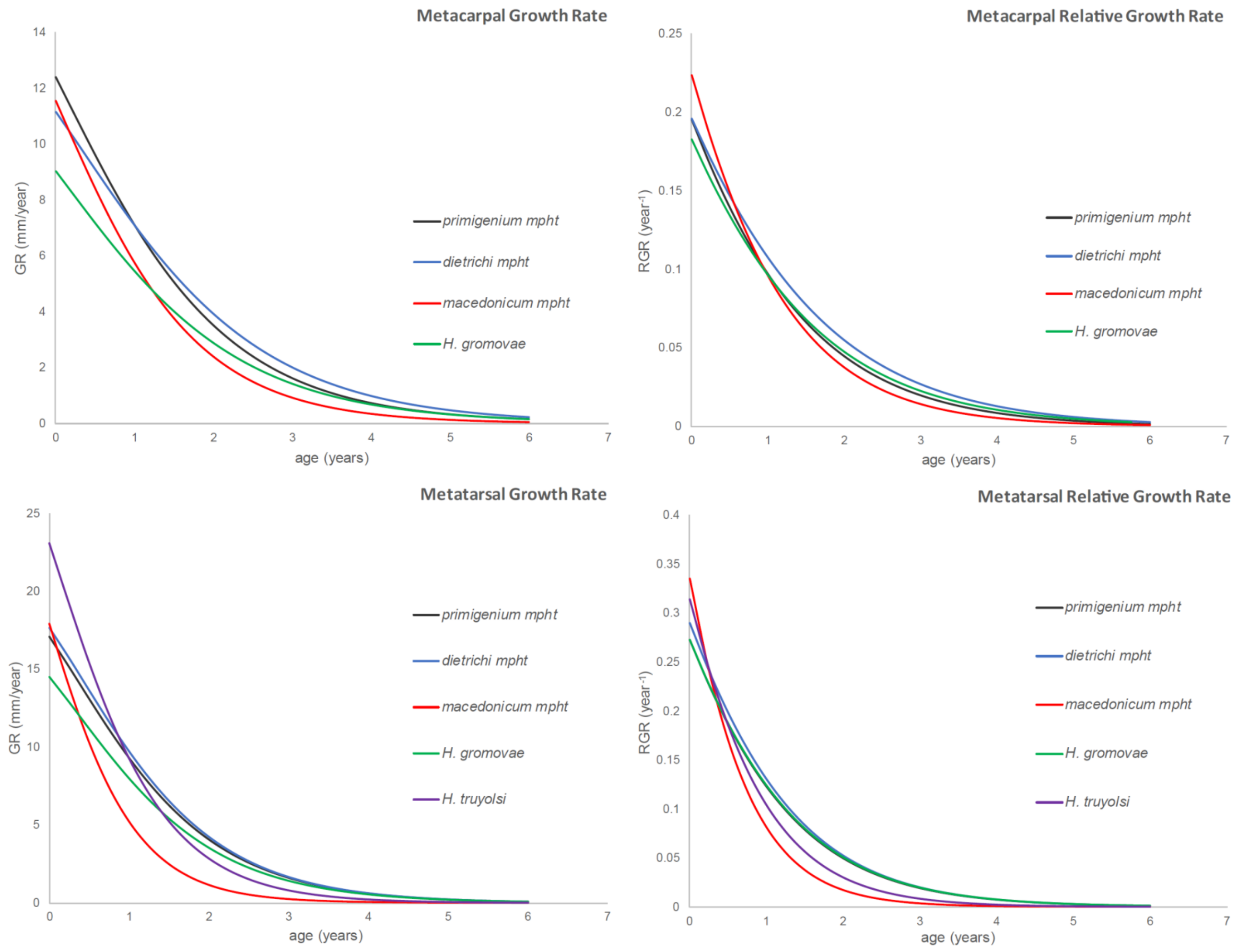

Supplementary Figure S4. Mean growth rate and mean relative growth rate curves for the metacarpals and metatarsals of the hipparionins studied.

Code	Species and Breed	Collection	LM mid-shaft Diameter (mm)	First CGM Perimeter (mm)	Second CGM Perimeter (mm)
IPS-84964	*Equus grevyi*	Zoological Institute of Hamburg University (Hamburg, Germany)	34.63	98.73	113.85
IPS-101804	*Equus grevyi*	Catalan Institute of Paleontology (Barcelona, Spain)	47.35	140.26	156.73
IPS-83876	*Equus hemionus*	Museum of Domesticated Animals (Halle, Germany)	30.83	87.78	100.80
IPS-83877	*Equus hemionus*	Museum of Domesticated Animals (Halle, Germany)	31.09	86.93	98.35
IPS-64287	*Equus caballus* (Iceland)	Zoological Institute and Museum of Kiel University (Kiel, Germany)	39.73	108.76	123.84
IPS-64288	*Equus caballus* (Welsh)	Zoological Institute and Museum of Kiel University (Kiel, Germany)	36.34	105.71	117.81
IPS-64290	*Equus caballus* (Hackney)	Zoological Institute and Museum of Kiel University (Kiel, Germany)	35.81	113.16	124.09
IPS-64291	*Equus caballus* (Shetland)	Zoological Institute and Museum of Kiel University (Kiel, Germany)	28.98	85.78	98.47

Supplementary Table S1. Femurs of the extant equids analysed. Lateromedial diameter (LM) at mid-shaft is provided as a proxy of size. The estimation of the growth rate has been calculated as the difference between the second and the first cyclical growth mark (CGM).

					Scott (1990) Mc10		Eisenmann & Sondaar (1998) Mc10/Mt10		Eisenmann & Sondaar (1998) Mc13/Mt13		Eisenmann & Sondaar (1998) Mc/t10*Mc/t13	
IPS Code	Bone	Species	Mc10 (mm)	Mc13 (mm)	logBM	BM (kg)	lnBM	BM (kg)	lnBM	BM (kg)	lnBM	BM (kg)
28808-1	Metacarpal	*H. gromovae*	27.24	17.50	1.88	76.45	4.18	65.52	4.48	87.86	4.32	75.06
28808-2	Metacarpal	*H. gromovae*	29.20	19.64	1.97	92.29	4.39	80.77	4.78	119.49	4.58	97.85
28808-6	Metacarpal	*H. gromovae*	28.20	18.67	1.92	83.97	4.29	72.73	4.65	104.40	4.46	86.56
28808-8	Metacarpal	*H. gromovae*	27.31	18.44	1.89	76.91	4.19	65.96	4.62	101.01	4.40	81.17
28808-9	Metacarpal	*H. gromovae*	27.01	16.4	1.87	74.64	4.16	63.80	4.30	73.90	4.21	67.53
28808-10	Metacarpal	*H. gromovae*	27.88	18.55	1.91	81.42	4.25	70.27	4.63	102.62	4.44	84.37
29015-7	Metacarpal	*H. gromovae*	27.65	18.35	1.90	79.61	4.23	68.54	4.60	99.70	4.41	82.09
29015-2	Metacarpal	*H. gromovae*	26.10	17.05	1.83	68.10	4.05	57.61	4.41	81.97	4.22	68.01
29015-3	Metacarpal	*H. gromovae*	27.95	-	1.91	81.97	4.26	70.80	-	-	-	-
29015-4	Metacarpal	*H. gromovae*	28.68	19.90	1.94	87.90	4.34	76.52	4.82	123.75	4.50	90.38
29015-5	Metacarpal	*H. gromovae*	-	18.92	-	-	-	-	4.68	108.17	-	-
IPS Code	Bone	Species	Mt10 (mm)	Mt13 (mm)	logBM	BM (kg)	lnBM	BM (kg)	lnBM	BM (kg)	lnBM	BM (kg)
29015-IV	Metatarsal	*H. gromovae*	25.95	17.30	1.89	78.57	4.22	67.68	4.29	72.62	4.23	68.53
29015-V	Metatarsal	*H. gromovae*	27.07	18.80	1.94	87.05	4.33	75.65	4.54	93.97	4.41	82.12
29015-VI	Metatarsal	*H. gromovae*	27.50	17.82	1.96	90.44	4.37	78.85	4.38	79.60	4.35	77.76
29015-VII	Metatarsal	*H. gromovae*	28.94	18.80	2.01	102.35	4.50	90.20	4.54	93.97	4.51	90.43
29015-VIII	Metatarsal	*H. gromovae*	28.63	-	1.99	99.71	4.47	87.68	-	-	-	-
29015-IX	Metatarsal	*H. gromovae*	-	17.33	-	-	-	-	4.29	73.01	-	-
38842-7	Metatarsal	*H. gromovae*	27.38	18.51	1.95	89.48	4.36	77.95	4.49	89.40	4.40	81.57
38842-9	Metatarsal	*H. gromovae*	27.65	19.20	1.96	91.64	4.38	79.99	4.61	100.31	4.47	87.28
28802-2	Metatarsal	*H. gromovae*	28.88	19.11	2.01	101.84	4.50	89.71	4.59	98.70	4.52	92.24
28002-4	Metatarsal	*H. gromovae*	27.50	19.05	1.96	90.44	4.37	78.85	4.58	97.90	4.45	85.63
28002-5	Metatarsal	*H. gromovae*	29.05	18.75	2.01	103.30	4.51	91.10	4.54	93.20	4.51	90.58
28002-12	Metatarsal	*H. gromovae*	25.88	17.09	1.89	78.06	4.21	67.20	4.25	69.92	4.21	67.07
28837	Metatarsal	*H. truyolsi*	37.90	24.21	2.29	196.85	5.21	183.55	5.33	205.55	5.26	192.12
28842	Metatarsal	*H. truyolsi*	36.55	24.90	2.26	180.27	5.12	166.82	5.41	224.55	5.25	189.99

Supplementary Table S2. Measurements of metacarpals and metatarsals of *Hipparion gromovae* and *Hipparion truyolsi* from Rambla de Valdecebro II (= El Arquillo) fossil site used for the body mass estimations. See Methods for information about the body mass estimations.

	Measure: Diaphyseal Perimeter		
Model **Specimen**	**von Bertalanffy AIC**	**Logistic AIC**	**Gompertz AIC**
NKT-22	30.502	30.540	30.520
RPL-nn	30.439	30.228	30.321
RPL-44	19.040	18.700	18.887
PER-23	30.070	30.470	30.560
PER-425	20.920	20.468	20.690
PER-X	37.012	36.097	36.547
DTK-58	NA	NA	NA
101807	18.227	18.110	18.160
96274_2	14.073	14.124	14.088
PNT-4	31.010	30.523	30.747
VAT-112	NA	NA	NA
PER-485	30.004	30.015	30.008
PER-1211	19.092	18.451	18.730
PER-342	33.156	32.046	32.574
28842	30.218	30.090	30.143
96276	32.524	33.085	32.791
DTK-106	30.317	30.104	30.187
101809	30.148	30.048	30.068

Supplementary Table S3. Akaike Information Criterion (AIC) for the curve fitting of three different equation growth models (von Bertalanffy. Logistic. Gompertz) in 18 adult hipparionine metapodials. The model exhibiting lower AIC values has been shadowed.

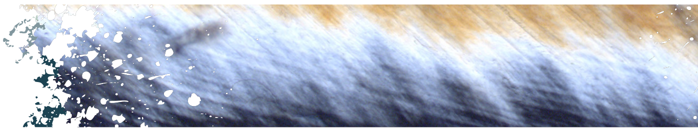

Chapter 5

Dental Histology of Late Miocene Hipparionins Compared with Extant *Equus*, and its Implications for Equidae Life History

Reproduced from ***Palaeogeography, Palaeoclimatology, Palaeoecology***
DOI:10.1016/j.palaeo.2019.04.016

Palaeogeography, Palaeoclimatology, Palaeoecology 528 (2019) 133–146

Contents lists available at ScienceDirect

Palaeogeography, Palaeoclimatology, Palaeoecology

journal homepage: www.elsevier.com/locate/palaeo

Dental histology of late Miocene hipparionins compared with extant *Equus*, and its implications for Equidae life history

Guillem Orlandi-Oliveras[a,*], Carmen Nacarino-Meneses[a,b], Meike Köhler[a,c]

[a] Institut Català de Paleontologia Miquel Crusafont (ICP), Carrer de les Columnes s/n, Campus de la Universitat Autònoma de Barcelona, 08193 Bellaterra, Barcelona, Spain
[b] University of Cape Town, Department of Biological Sciences, Private Bag X3, Rhodes Gift, 7700, South Africa
[c] Institut Català de Recerca i Estudis Avançats (ICREA), Pg. Lluís Companys 23, 08010 Barcelona, Spain

ARTICLE INFO

Keywords:
Paleohistology
Enamel
Growth rate
Body size
Hipparion
Tooth growth

ABSTRACT

Hipparionins were a dominant element of the late Miocene faunas of Europe; however, their biology and ecology remain incompletely understood. In this paper, we explore the pace of life history of different-sized hipparionin horses, using dental histology, and compare it with extant equids. In doing so we consider (i) the size diversity of hipparionins, (ii) their generally smaller size compared to extant equids, and (iii) the allometric coupling between size and life history. In particular, we reconstruct the dental growth in lower first/second molars and in later-formed lower third molars for three hipparionin taxa: two dwarf species (*Hipparion periafricanum* and *H. gromovae*), and a larger species (*H. concudense*). We also analyze dental growth in an extant zebra (*Equus quagga*) for comparative purposes. Our results reveal that, within each species, there are differences in enamel growth parameters between the first/second molars and third molars. These results illustrate the differences in the developmental timing of these teeth and the existence of a relationship between dental growth parameters with somatic growth. We also find that hipparionin teeth grow at slower rates and tend to erupt later in time than in extant *Equus*. Dwarf hipparionins, moreover, exhibit lower enamel extension rates than the larger species, but similar formation and eruption times. Considering the link between dental development and life history, these results suggest a slower pace of growth of selected hipparionins compared to extant equids, and a further slower life history than expected for their size in the two dwarf forms.

1. Introduction

The first hipparionins arrived in the Old World around 11 Ma, marking the start of the Vallesian European Land Mammal Age, and signaling one of the most important biochronological events of the Neogene in Europe (Bernor et al., 1996; Garcés et al., 1997, 2003). After their dispersal, hipparionins became dominant in European mammal associations and rapidly diversified into different forms in circum-Mediterranean areas, while they retained a more conservative body plan in central Europe (Alberdi, 1989; Bernor et al., 1990, 1996; Eisenmann, 1995; Woodburne, 1989). Besides their morphological diversity, hipparionin horses were highly diverse in size (Eisenmann, 1995; Ortiz-Jaureguizar and Alberdi, 2003), especially during the Turolian European Land Mammal Age (late Miocene) (Bernor et al., 1990, 1996). In the western Mediterranean late Turolian (MN13), for example, there were at least three sympatric hipparionins present (Alberdi, 1974; Alberdi and Alcalá, 1989; Ortiz-Jaureguizar and Alberdi, 2003; Pesquero, 2003): the scarce and large *Hipparion primigenium truyolsi* (138 kg), the small *H. gromovae* (59 kg), and the dwarf *H. periafricanum* (23 kg) (Ortiz-Jaureguizar and Alberdi, 2003). Different scenarios have been proposed to explain these size differences. On the one hand, based on the evolutionary size response model in Equini (Alberdi et al., 1995), the two small taxa have been hypothesized as representing species adapted to closed and forested areas (Ortiz-Jaureguizar and Alberdi, 2003). On the other hand, some authors have argued that these gracile and small-sized taxa were adapted to open habitats (Eisenmann, 1995; Pesquero, 2003), and that the small size represents an adaptation to energy economization due to the less nutritive xerophyte plants that typify open habitats (Forsten, 1968, 1978). Recently, however, hipparionin size shifts have been considered as a probable outcome of the evolution of life history strategies that indirectly affect body size (Orlandi-Oliveras et al., 2018) as has been previously proposed for island ecosystems (Köhler, 2010; Palkovacs, 2003).

---

[*] Corresponding author.
E-mail address: guillem.orlandi@icp.cat (G. Orlandi-Oliveras).

https://doi.org/10.1016/j.palaeo.2019.04.016
Received 8 November 2018; Received in revised form 8 April 2019; Accepted 15 April 2019

Hipparionins have long been suggested to follow faster life histories than *Equus* based on population dynamics studies (Hulbert, 1982; Kurtén, 1953; Van Valen, 1964). Through the study of age classes defined by dental wear stages (Hulbert, 1982; Kurtén, 1953; Van Valen, 1964; Woodburne and MacFadden, 1982), and considering their smaller size (Van Valen, 1964), some authors proposed shorter lifespans and earlier maturity ages in hipparionins compared to extant equids. Body mass frequently correlates with life history (Calder, 1984). However, this is not always the case since there are other factors on which life history traits depend and that are associated with an organism's ecology (Sibly and Brown, 2007; Stearns, 1992). Indeed, the pace of growth of hipparionins has recently been questioned based on the study of their molar eruption sequence interpreted within the context of Schultz's Rule (Domingo et al., 2018). Grounded on the idea that the tooth replacement pattern is a valuable proxy of an animal's life history, Schultz's Rule states that the later eruption of the permanent molars compared to that of the replacement teeth (e.g. permanent premolars) is typically found in slow-growing taxa (Smith, 2000). Domingo et al. (2018), therefore, suggested that hipparionins might have followed a slow pace of growth due to their late third molar eruption, which occurs prior to the appearance of the fourth premolar in some extant equids (Easley et al., 2005; Hoppe et al., 2004; Joubert, 1972; Lkhagvasuren et al., 2013; Smuts, 1974).

Recent studies, however, claim that the eruption sequence is more influenced by phylogeny than by life history in primates (Monson and Hlusko, 2018a) and artiodactyls (Monson and Hlusko, 2018b; Veitschegger and Sánchez-Villagra, 2016), challenging the predictive value of the Schultz's Rule. Within equids, the timing of third molar and fourth premolar eruption generally differs between extant and extinct representatives of the family, with basal equines, Miocene anchitheriines, and hipparionins showing a later m3 eruption (Domingo et al., 2018). However, in some taxa of the *Equus* genus the fourth premolar is the last to erupt (Easley et al., 2005; Hoppe et al., 2004; Joubert, 1972; Lkhagvasuren et al., 2013; Smuts, 1974) while in others it is the third molar (Grubb, 1981; McDonald, 1996; Penzhorn, 1982). This intrageneric variability suggests an adaptive component in the eruption pattern and takes issue with the idea of a phylogenetic meaning of this trait. The differences in the eruption sequence (Domingo et al., 2018), in dietary preferences (Semprebon et al., 2016), and in dental wear rates (Famoso and Davis, 2016; Hulbert, 1984) between extant equids and hipparionins make us reconsider the previous life history interpretations founded on population dynamics from the study of the dentition ontogeny (Hulbert, 1982; Kurtén, 1953; Van Valen, 1964). The deviations from the allometric coupling between life history and size (Sibly and Brown, 2007) also challenge the idea that faster life histories are necessarily associated with smaller sizes. Moreover, bearing in mind the hipparionin ecological and size diversity (Hayek et al., 1992; MacFadden et al., 1999; Ortiz-Jaureguizar and Alberdi, 2003; Tütken et al., 2013), we could further expect diverse life history adaptations within the group.

Dental histology has proved to be a valuable tool for inferring life histories of extinct species since tooth formation times and growth rates are closely related to the animal's pace of life history (Dean, 2006; Jordana et al., 2014; Schwartz et al., 2002). Additionally, the emergence sequence of the permanent dentition has shown to generally correlate with the organism's postnatal growth (Smith, 2000), and the eruption time of certain teeth is linked to key life history traits such as weaning and attainment of maturity (Dean, 2006; Dirks and Bowman, 2007; Engström et al., 1983; Hillson, 2005; Smith, 1991, 2000). In this way, the study of dental growth has allowed the reconstruction of the life strategy of many extinct mammals (Dirks et al., 2009, 2012; Jordana and Köhler, 2011; Schwartz et al., 2002; Smith, 2016). Current advances in dental histology of extant equids, moreover, have characterized the growth of hypsodont teeth of the genus *Equus* (Nacarino-Meneses et al., 2017), providing a solid framework for studying and inferring the life history of fossil equid taxa.

Here we aim to explore the life history strategies of hipparionin horses and compare them to those of extant equids, focusing on the differences linked to body size variations within the clade. The high diversity and abundance of Turolian hipparionins in the western Mediterranean provides an excellent opportunity to study their pace of life history in relation to their size. Therefore, we analyze for the first time the dental development in different-sized hipparionins to shed light on their life history strategies. Specifically, we reconstructed the tooth growth patterns of lower first/second molars and lower third molars of three hipparionin taxa (*Hipparion periafricanum*, *Hipparion gromovae*, and the larger *Hipparion concudense*) together with the first and third molar growth of an extant equid. Among wild extant equids, we have chosen *Equus quagga* as a model because unlike the larger *Equus grevyi* or the longer-lived *Equus hemionus*, it does not show any extreme life history trait (Ernest, 2003; Grubb, 1981; Lkhagvasuren et al., 2013; Smuts, 1974). We have analyzed first and third lower molars as these are formed and erupt during different moments of ontogeny that are characterized by two major life history events, weaning and attainment of maturity, respectively. Furthermore, the eruption of the first molar has been shown to correlate with different life history traits, and thus it can be used as a predictor of the organisms' pace of life history (Dirks and Bowman, 2007; Smith, 2000; Veitschegger and Sánchez-Villagra, 2016). The dental mineralization sequence – intimately related to the enamel matrix formation – is the same between hipparionin horses and extant horses (Domingo et al., 2018; Hoppe et al., 2004): the first lower molar (m1) begins to mineralize before birth, followed by the m2, and later by the p2 and the p3. Although the p4 eruption occurs earlier in hipparionins, the p4 starts to mineralize before the m3 as it happens in extant *Equus* (Domingo et al., 2018; Hoppe et al., 2004). This similar onset of the tooth formation, and the same degree of overlap between extant equids and hipparionins (e.g. the third molar is still being formed when the m1 and the m2 are fully in wear), endorse our interpretations obtained from individual tooth growth reconstructions. Due to their diversity and abundance, hipparionins constitute a key mammalian group widely used in paleoecological studies, especially in those involving isotopes (Domingo et al., 2009; Matson and Fox, 2010; Nelson, 2005; Rey et al., 2013; van Dam and Reichart, 2009). Besides the importance of dental growth pattern as a life history proxy, the understanding of hipparionin molar growth patterns provides an important basis for future paleoecological inferences from hipparionin dental analyses.

2. Material and methods

The extremely high-crowned molars of *Equus* are produced by delaying the root formation (Hoppe et al., 2004; Nacarino-Meneses et al., 2017), which leads to extended dental growth periods. Eruption of the crown occurs gradually, and tooth wear starts before the roots are formed (Kirkland et al., 1996). For this reason, the entire tooth development in *Equus* must be reconstructed from compositions of molars with different wear degrees (Nacarino-Meneses et al., 2017). Based on differences in the pattern of growth during the crown formation of unworn and worn extant equid molars, Nacarino-Meneses et al. (2017) defined three crown developmental stages (CDS) that differed in growth rate. The first stage is characterized by a fast and linear growth (CDS I), followed by a significant decrease in growth rate (CDS II) and the attainment of an almost residual enamel extension rate in the last formed part of the cervix (CDS III). These CDS described in *Equus*, further agree with the morphological appearance of the molar. The transition from stage I to stage II matches the tooth eruption time, and that of CDS II to CDS III represents the macroscopic root appearance (Nacarino-Meneses et al., 2017). The hypsodont teeth of hipparionins, however, tend to finish the crown formation shortly after the tooth eruption, allowing the observation of little worn rooted teeth (Supplementary material Fig. S1). The histological analysis of unworn or slightly worn hipparionin teeth, thus, allows the reconstruction of the complete tooth growth.

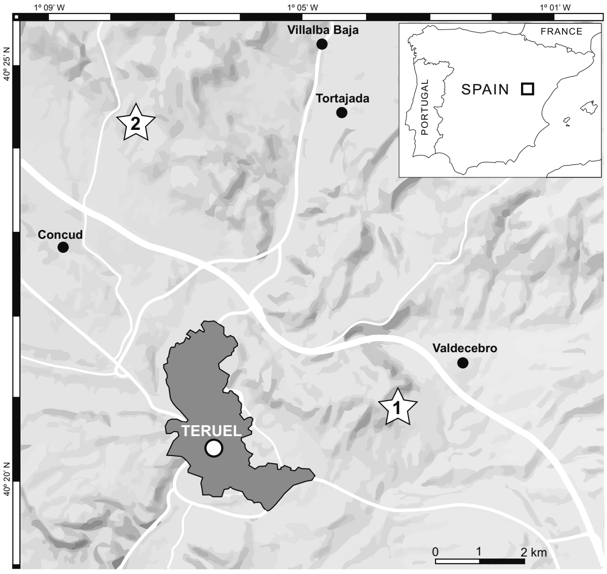

Fig. 1. Map of the area around the city of Teruel (Aragon, Spain). The fossil sites of El Arquillo (1) and Concud (2) are indicated with a star.

2.1. Fossil material

In this study, we studied isolated lower molars from three different hipparionin species of the Spanish Turolian. The teeth of the dwarf hipparionins *H. periafricanum* and *H. gromovae* come from the El Arquillo fossil site (Teruel Basin, Spain), also known as Rambla de Valdecebro II. This fossil site is dated to the late Turolian (MN13) and establishes the reference fauna for the MN13 with an estimated age of 6.2 Ma (de Bruijn et al., 1992; van Dam et al., 2001). The *H. concudense* molars were from Concud, a classical and rich fossil site from the same Teruel Basin. This locality is < 10 km away from El Arquillo and is dated around 7 Ma on the middle Turolian (MN12) (Pesquero et al., 2010) (Fig. 1). All fossil samples are accessioned in the Institut Català de Paleontologia (Barcelona, Spain) collections (IPS-91731, IPS-91732, IPS-91733, IPS-91734, IPS-91762, IPS-91763, IPS-40644, IPS-40665, IPS-40668, IPS-85504, IPS-85506, IPS-85508, IPS-86850, IPS-86851, IPS-87855, IPS-87856, IPS-87857, Table 1).

Based on sectioned material, we analyzed two lower first/second molars (m1/m2) and three lower third molars (m3) for the smallest Old World hipparionin *Hipparion periafricanum*, four lower m3 molars and two lower m1/m2 molars from the small-sized *Hipparion gromovae*, and four lower m3 molars and two lower m1/m2 molars from the large *Hipparion concudense* (Table 1). To the greatest extent possible, the less worn teeth were selected in order to retain the maximal growth record and make analogous comparisons. Following Sondaar (1961) and Pesquero (2003), we used tooth width and length measurements at 1 cm above the base of the tooth as a biometric criterion for interspecific differentiation between the two contemporaneous small species *H. gromovae* and *H. periafricanum* (Supplementary material Fig. S2 and S3). Body mass estimations based on first phalanx measurements (Alberdi et al., 1995) were obtained from the literature (Ortiz-Jaureguizar and Alberdi, 2003; Pesquero and Alberdi, 2012). Hypsodonty indices calculated from measurements of m1/m2 molars were also compiled from literature (Cantalapiedra et al., 2017; Pesquero, 2003). Using the same procedure described in Cantalapiedra et al. (2017), we calculated the hypsodonty indices for m3 molars (Table 1).

2.2. Extant Equus material

Our sample also includes four first molars of extant *Equus quagga* from the Hagenbeck Zoo (Hamburg, Germany). These teeth represent different eruption and wear stages (Table 1), thus comprising the entire tooth development of *Equus* molars (Nacarino-Meneses et al., 2017). We also sectioned three third molars from *E. quagga* depicting different eruption and wear stages (Table 1). These third molars came from the Réserve Africaine de Sigean (Sigean, France), the Barcelona Zoo (Barcelona, Spain) and the Hagenbeck Zoo (Hamburg, Germany). The extant samples from the Hagenbeck Zoo are accessioned in the Centrum für Naturkunde of the Universität Hamburg (Hamburg, Germany), the Barcelona Zoo specimen is accessioned in the Museu de Ciències Naturals de Barcelona (Barcelona, Spain), and the specimen from Sigean is housed at the Institut Català de Paleontologia Miquel Crusafont (Barcelona, Spain).

2.3. Thin section preparation and study

The dental histological sections were prepared following the standard procedures of our laboratory (Jordana et al., 2014; Nacarino-Meneses et al., 2017). Each molar was embedded in epoxy resin (Araldite 2020) and sectioned buccolingually through the higher mesial cusps (protoconid and metaconid) using an IsoMet low-speed saw (Buehler). In some cases, highly curved third molars were previously cut in a transversal plane. At this stage, the exposed buccolingual surfaces were polished using a grinder polisher (Buehler, MetaServ 250) and glued to a glass slide using ultraviolet curing glue (Loctite 352). Thereafter, the glass-mounted samples were cut using a diamond saw (Buehler, Petrothin) up to a thickness of 300 μm and grounded to around 120–70 μm using the grinder polisher. Finally, each sample was dehydrated in alcohol gradients and immersed in a histological clearing agent (Histo-Clear II) prior to covering them with a DPX medium.

The resulting thin sections were studied under polarized light using a Zeiss Scope A1 microscope with an attached digital camera (AxioCam ICc5). To estimate the tooth growth parameters, the acquired images of the overall enamel band (Fig. 2A) were merged using Adobe Photoshop® and analyzed with ZEN 2011® (Carl Zeiss) and Image J software.

2.4. Histological analysis techniques and dental growth parameters

We used measurements and counts of enamel incremental markings to assess the tooth growth patterns of the species. As the dental growth parameters depend on the cusp and enamel side studied (Jordana and Köhler, 2011; Kierdorf et al., 2013), we decided to standardize and analyze the buccal enamel band of the protoconid in agreement with previous work on equid teeth (Nacarino-Meneses et al., 2017). This allows future comparisons between extinct and extant equids. We did not analyze the lingual enamel band of the metaconid due to the presence of more marked Hunter-Schreger bands that hindered the correct observation of incremental markings. Enamel band thickness of each tooth was measured perpendicular to the enamel-dentine junction at a homologous zone situated 1 cm above the root. In order to reconstruct the entire tooth growth curve, the length of the cuspal enamel lost in worn molars was estimated by considering both the profile of unworn teeth (Tafforeau et al., 2007) and the hypoconulid wear degree (Stirton, 1941). We used the mean enamel extension rate of the nearest area to extrapolate the time that the worn portion required to be formed.

In ungulates, the main short-period enamel incremental features are laminations, which have a circadian periodicity and run oblique from the enamel-dentine junction (EDJ) (Jordana and Köhler, 2011; Kierdorf et al., 2013; Smith, 2006; Tafforeau et al., 2007). The other common incremental features are the Retzius lines or striae of Retzius, which correspond to the successive positions of the ameloblast secretory front (Dean, 2000). These long-period marks represent variations in the secretory activity, hypothesized to be ruled by two independent intern

Table 1
Teeth analyzed in the present study. Mean body mass (BM) is provided per each species and hypsodonty indices (HI) per each species' tooth type.

	Species	Tooth	BM (kg)	HI	Code	Locality	Age	Wear
m1/m2	*H. concudense*	m1/m2	160[a]	2.8[d]	IPS-91762	Concud	middle Turolian (MN12)	Slight
	H. concudense	m1/m2			IPS-91763	Concud	middle Turolian (MN12)	Slight -
	H. gromovae	m1/m2	59[b]	2.9[d]	IPS-91731	El Arquillo	late Turolian (MN13)	Slight
	H. gromovae	m1/m2			IPS-91732	El Arquillo	late Turolian (MN13)	Slight
	H. periafricanum	m1/m2	29[b]	3.2[d]	IPS-91733	El Arquillo	late Turolian (MN13)	Slight
	H. periafricanum	m1/m2			IPS-91734	El Arquillo	late Turolian (MN13)	Slight +
	Equus quagga	m1	250[c]	4.4[c]	IPS-92341	Hagenbeck Zoo	Extant	Slight +
	Equus quagga	m1			IPS-92342	Hagenbeck Zoo	Extant	Null
	Equus quagga	m1			IPS-92345	Hagenbeck Zoo	Extant	Crypt
	Equus quagga	m1			IPS-92346c	Hagenbeck Zoo	Extant	Moderate
m3	*H. concudense*	m3	160[a]	2.0[e]	IPS-40644	Concud	middle Turolian (MN12)	Null
	H. concudense	m3			IPS-40665	Concud	middle Turolian (MN12)	Slight
	H. concudense	m3			IPS-40668	Concud	middle Turolian (MN12)	Slight
	H. concudense	m3			IPS-87855	Concud	middle Turolian (MN12)	Null
	H. gromovae	m3	59[b]	1.9[e]	IPS-85506	El Arquillo	late Turolian (MN13)	Slight -
	H. gromovae	m3			IPS-85508	El Arquillo	late Turolian (MN13)	Slight
	H. gromovae	m3			IPS-86851	El Arquillo	late Turolian (MN13)	Slight +
	H. gromovae	m3			IPS-87856	El Arquillo	late Turolian (MN13)	Slight +
	H. periafricanum	m3	29[b]	2.1[e]	IPS-85504	El Arquillo	late Turolian (MN13)	Slight -
	H. periafricanum	m3			IPS-86850	El Arquillo	late Turolian (MN13)	Slight +
	H. periafricanum	m3			IPS-87857	El Arquillo	late Turolian (MN13)	Moderate
	Equus quagga	m3	250[c]	2.5[e]	IPS-104358	Réserve Africaine Sigean	Extant	Crypt
	Equus quagga	m3			MZB-94-1229	Barcelona Zoo	Extant	Slight +
	Equus quagga	m3			IPS-92346e	Hagenbeck Zoo	Extant	Moderate

Body mass data from [a]Pesquero and Alberdi (2012), [b]Ortiz-Jaureguizar and Alberdi (2003), and [c]Cantalapiedra et al. (2017). Hypsodonty indices calculated for first/second molars are taken from [d]Pesquero (2003) and
[c]Cantalapiedra et al. (2017).
[e]Hypsodonty indices for third molars were calculated from our sample using the less worn specimens.

cycles (Smith, 2006) or by a general chronobiological rhythm (Bromage et al., 2016). Due to their known cyclical and regular nature, both laminations and Retzius lines permit the calculation of the following tooth growth parameters: the enamel daily secretion rate (DSR), or the amount of enamel secreted by an ameloblast per day; the enamel extension rate (EER), or the enamel growth rate along the EDJ; and the total crown formation time (CFT). Firstly, and following prior studies on ungulate teeth (Jordana et al., 2014; Jordana and Köhler, 2011), we calculated the DSR quantifying the distance between laminations through the course of the enamel prisms (Fig. 2B). The DSR values have been seen to increase from inner to outer enamel regions (Kierdorf et al., 2014; Metcalfe and Longstaffe, 2012; Smith, 2008), although in some cases no significant differences between enamel areas have been identified (Nacarino-Meneses et al., 2017). We made many random counts in different enamel zones within all the tooth length to gather all the variation and obtain a representative mean. Because we were not

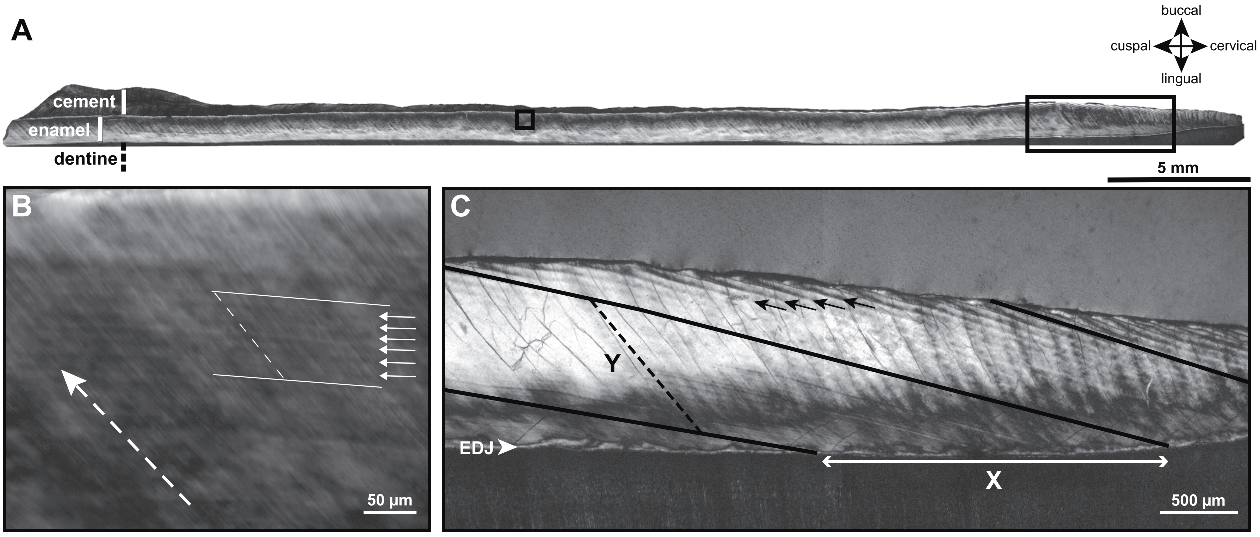

Fig. 2. A: Protoconid buccal enamel band of a *Hipparion periafricanum* first/second molar (IPS-91733) sectioned longitudinally and observed under polarized light. B: Detail of the enamel band depicted in (A) illustrating the method used to calculate the daily secretion rate (DSR). The distance between laminations through the prism path (dashed line) is divided by the number of laminations (arrows). Dashed arrow represents the prisms' direction. C: Detail of the cervical zone in (A), showing the methodology used for the enamel extension rate (EER) determination. "X" represents the increase in crown height between two incremental features (black lines) and "Y" indicates the distance following the enamel prism between those two enamel marks. Black arrows point to Retzius lines that outcrop the outer enamel, and "EDJ" depicts the enamel dentine junction.

able to perform the same amount of DSR measures in all the crown regions and enamel zones due to fossil preservation, direct comparison between the mean obtained DSRs should be taken with caution. We calculated EER following the methodology described in Jordana and Köhler (2011): the time that takes to form the distance that separate two incremental lines through the EDJ (X, Fig. 2C) is determined by dividing the prism length that separates those two incremental features (Y, Fig. 2C) by the rate of daily enamel deposition (DSR). This calculation is based on the ideas that the enamel prisms mark the enamel growth path and that accentuated lines indicate the position of the developing enamel front at a determinate moment (Dean, 2000). Applying this methodology through the entire enamel band, we obtained EER values in different tooth portions. The EERs were calculated at the intersection of clearly visible accentuated Retzius or stress lines, rather than at regularly spaced points (Dirks et al., 2012). In order to permit analogous comparisons, we divided the enamel band of each tooth into three thirds (cuspal, middle and cervical). Finally, the CFT was estimated calculating the overall time required to form the enamel band.

Differences between groups within each dental growth parameter were tested with a degree of significance of $\alpha = 0.05$. Non-parametric Kruskall-Wallis tests were used to test for differences in the DSR values between species since normality was not always met. Differences in EER values between fossil species were compared using an ANCOVA model, as this considers the decrease in EER along the crown height. Prior to the ANCOVA analysis, we tested for the significance of the interaction between the categoric predictive variable (species) and the continuous covariate (crown height) in the two different subsets analyzed (first/second molars and third molars). Moreover, we tested for the homogeneity variances (Levene test). In both cases, when the extant *Equus* data was excluded, we did not find significant violations of the assumptions of the ANCOVA model (Supplementary material Tables S1-S8). The statistical tests and graphs were performed using IBM SPPS Statistics 20 ® and PAST v. 3.18 (Hammer et al., 2001).

3. Results

Laminations represent the main incremental features observed in our sample. These are more appreciable on the central and inner enamel zones, although also identifiable between some striae of Retzius that outcrop at the outer enamel surface. In the inner enamel zone, laminations are less regularly spaced and more difficult to distinguish as some sub-daily incremental lines appear. Retzius lines are clearer in the outer enamel (Fig. 2C). These Retzius lines are also more discernible in the cervical region (Fig. 2C), where the angles between those and the EDJ are more obtuse (~ 10°) than in the middle or cuspal region (< 5°). These observations agree with previous findings on equid enamel histology (Hoppe et al., 2004; Nacarino-Meneses et al., 2017).

3.1. Enamel daily secretion rates

In our sample, the mean daily secretion rates vary from ~14 to ~17 μm/day (Table 2). Contrary to hipparionins, *Equus quagga* shows different DSRs within the three different tooth zones (cuspal, middle, cervical) considered from the reconstructed third molar ($p < 0.001$). These differences are only observed in the m3, since the m1 does not show significant variations on the DSR through the tooth length ($p = 0.08$). The first formed region of the third molar presents higher DSRs, while it decreases in the middle zone and reaches its minimum at the final formed root zone (Table 2). Considering this, the calculation of the other parameters in third molars of *Equus* has been done using the mean DSR of each stage, not the general mean of the taxon. When compared within hipparionin species, the DSRs of the first/second molars are significantly higher than those reported in third molars ($p < 0.001$) (Table 2). We do not find these significant differences between the DSR of m1 and m3 in extant *Equus* ($p = 0.34$), when we use the medial region DSR of the m3 as a general mean for the third molar.

The DSR is significantly different between species, both in the case of the analyzed m1/m2 ($p < 0.001$) and the m3 ($p < 0.001$). Among the first/second molars, the *H. concudense* m1/m2 exhibit the lowest DSR values with a mean value of 15.76 μm/day, which is significantly different from the higher secretion rates of *H. gromovae* ($p = 0.009$) and *Equus* ($p < 0.001$) (Table 2). The first/second molars of *H. periafricanum* have a mean DSR of 16 μm/day, which is significantly different ($p = 0.009$) to the higher rates of *Equus quagga* (~17 μm/day). The DSR of the third molars differ significantly between most species ($p < 0{,}001$), except for *H. concudense* and *H. periafricanum*, which present similar low DSRs (Table 2). In general, therefore, *H. gromovae* exhibit greater mean DSR values than the other two hipparionin species, both in the third and in the first/second molars, and this is only surpassed by the always higher DSRs of *Equus quagga*. This pattern is followed both in the m3 and the m1/m2, with lower values of DSR in the later formed third molars (Table 2). It should be noted that the same number of DSR measures within the crown regions and the enamel zones was not possible in our sample. We should, hence, be prudent when interpreting the differences in DSRs found between species and tooth types. However, since the DSRs in the equids' first molars tend to do not vary significantly between regions (Nacarino-Meneses et al., 2017), we assume that our results are more reliable than if the same measures were performed on taxa that reported high variations on the DSRs, like pigs (Kierdorf et al., 2014, 2019).

3.2. Enamel extension rates

The first/second molars' ameloblasts differentiated along the EDJ at higher rates than in the third molars in all the studied taxa, particularly in the cuspal and medium zones (Table 2). Due to these differences, and in order to make interspecific comparisons, we separated the higher EER values of the m1/m2 from the lower EERs of the m3. We always observed higher EERs in the first formed enamel area, while the rates were lower towards the cervical region (Table 2, Fig. 3 and Supplementary material Fig. S4). For example, the first third of the crown of the m1/m2 of *H. periafricanum* grow at a mean rate of 166.62 μm/day, while at the end of the enamel band the mean EER is 37.27 μm/day. This diminution is present in all taxa and in both tooth types, thus representing a general decrease in the tooth growth rate through the development of the tooth (Table 2, Fig. 3 and Supplementary material Fig. S4). Taking into account this growth rate decrease, the intraspecific variation in EER within the crown height is high, thus hindering the growth rate comparisons between species. To evaluate the EER differences between species, therefore, we considered the crown height as a covariate affecting the EER. By doing this, interspecific differences between EER in fossil first/second molars and third molars are significant ($p < 0.001$). These differences are found between all groups of hipparionin teeth ($p \leq 0.001$), except for the m1/m2 of *H. gromovae* and *H. periafricanum*, which grow at similar rates ($p = 0.075$). In all cases, *H. concudense* teeth grow at higher rates, while the teeth of the dwarf species grow at a slower pace. Although not directly tested by the ANCOVA model (see Section 2.4), *Equus quagga* teeth develop at higher rates compared to the three hipparionin species (Table 2 and Fig. 3). The higher EER of extant *Equus* molars compared to hipparionins molars is comparably more pronounced in m1/m2 than in m3 (Table 2 and Fig. 3).

3.3. Growth reconstruction and crown formation times

To reflect the whole tooth growth pattern, we plotted the crown height against the crown formation time (CFT) for each species tooth type (Fig. 4). Extant *Equus* tooth development has been plotted considering the entire tooth growth reconstruction using differently worn teeth (Nacarino-Meneses et al., 2017) (see Section 2). All the reconstructed tooth growth curves fit well with von Bertalanffy growth models (Fig. 4 and Supplementary material Fig. S5). Compared to

Table 2

Dental growth parameters – daily secretion rate (DSR) and enamel extension rate (EER) – estimated through dental histology analyses. Mean, standard deviation, and number of observations are provided. DSR values of *Equus* m3 are shown separately due to the significant differences in the DSR values within the different areas of *Equus* third molar. The division of *E. quagga* molars for the EER considers the complete tooth development and corresponds to the different CDS defined by Nacarino-Meneses et al. (2017).

	Species	Overall DSR (μm/day)	Cuspal EER (μm/day)	Middle EER (μm/day)	Cervical EER (μm/day)
m1/m2	*H. concudense*	15.76 ± 0.96 (*N* = 90)	211.50 ± 27.25 (*N* = 6)	177.08 ± 24.71 (N = 6)	82.52 ± 38.96 (N = 9)
	H. gromovae	16.27 ± 1.15 (*N* = 104)	144.73 ± 28.05 (N = 7)	131.32 ± 29.63 (N = 6)	55.75 ± 35.85 (*N* = 16)
	H. periafricanum	15.96 ± 1.37 (*N* = 85)	166.62 ± 33.08 (N = 7)	121.14 ± 8.11 (*N* = 5)	37.27 ± 19.84 (*N* = 15)
	Equus quagga	16.98 ± 1.63 (N = 45)	441.69 ± 152.37 (*N* = 10)	316.18 ± 146.18 (*N* = 13)	78.37 ± 73.25 (*N* = 30)
m3	*H. concudense*	14.08 ± 1.73 (*N* = 78)	150.39 ± 45.50 (N = 9)	95.54 ± 18.87 (N = 12)	41.30 ± 22.43 (N = 15)
	H. gromovae	15.37 ± 1.78 (*N* = 93)	119.09 ± 10.51 (*N* = 7)	95.36 ± 14.25 (N = 11)	43.06 ± 20.59 (N = 15)
	H. periafricanum	13.72 ± 1.70 (*N* = 36)	116.35 ± 18.17 (N = 6)	75.14 ± 9.74 (*N* = 8)	43.19 ± 20.36 (*N* = 12)
	Equus quagga	Cuspal: 18.11 ± 1.02 (*N* = 25) Middle: 17.23 ± 1.05 (*N* = 40) Cervical: 15.92 ± 1.78 (*N* = 73)	199.42 ± 66.11 (N = 8)	112.44 ± 23.99 (*N* = 13)	25.00 ± 18.99 (*N* = 44)

recently erupted *Equus* teeth (Nacarino-Meneses et al., 2017), we confirm that unworn or slightly worn hipparionin teeth register most of the tooth development, since asymptotic size is being reached (Fig. 4). Some residual cervical enamel, however, could be further deposited although without increasing the tooth height substantially. Steeper slopes than those for the *H. gromovae* and *H. periafricanum* teeth indicate the higher growth rates of the *Equus* and *H. concudense* molars (Fig. 4). We also identify the higher EER in m1/m2 compared to m3 in the steeper slopes of the first molars within each species (Supplementary material Fig. S5). These intraspecific EER differences between m3 and m1/m2 are more pronounced in the *Equus quagga* molars than in hipparionin horses, as first molars show comparably much higher crown extension rates (Fig. 3 and Supplementary material Fig. S5).

The complete growth period or CFT is explored in the teeth that have not lost cuspal growth register and that have started forming roots (Table 3). Despite having the higher crowns, the m1/m2 of *H. concudense* take 500 days to be formed, a similar time to that of the smaller species' teeth (Table 3 and Fig. 4). When we compare the third molars total CFT, these generally take more time to form than first/second molars. Within species, the m3 of *H. gromovae* and *H. periafricanum* require similar time to form (around 600 days), whereas the *H. concudense* m3 spans 100 days more to finish formation (Table 3). The total crown formation time of the composite *Equus* tooth is much higher, taking 785 days in the case of the first molar and 1750 days in the third. However, these *Equus* CFTs are the product of differently worn teeth compositions, as they keep growing after eruption and delay their root closure, depositing residual enamel (Nacarino-Meneses et al., 2017). Analogous comparisons of the formation time in *Equus* and *Hipparion*

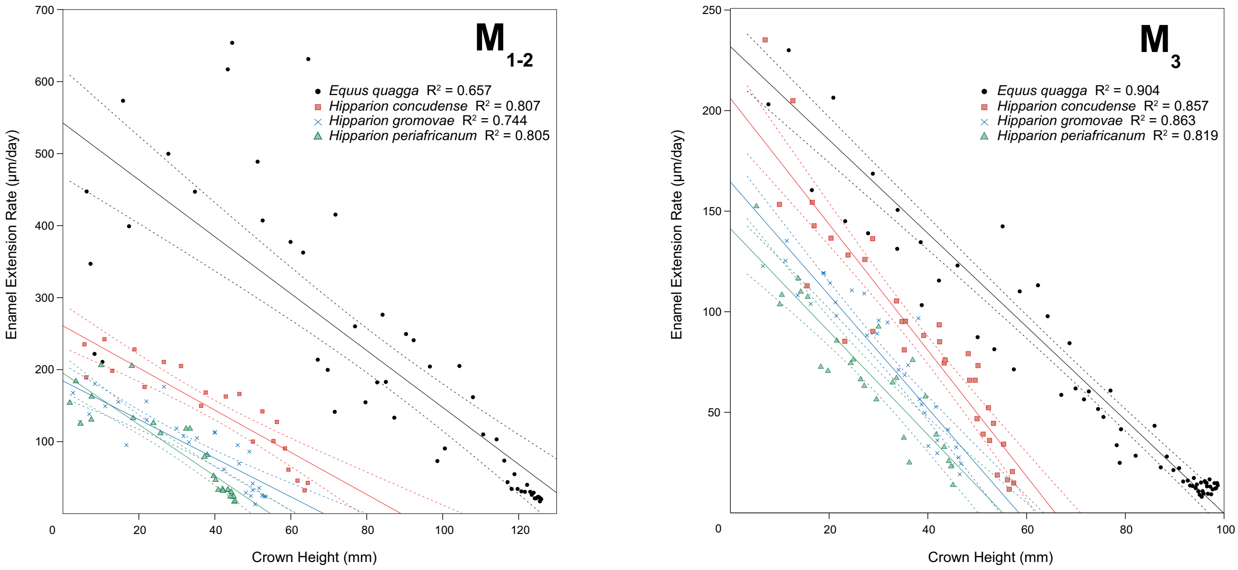

Fig. 3. Enamel extension rate values (EER) plotted against the crown height from the first formed zone (cuspal, left side) to the last formed region (cervical, right side). Left chart shows EERs for first/second molars and right chart for third molars. Note the different scales between the two charts.

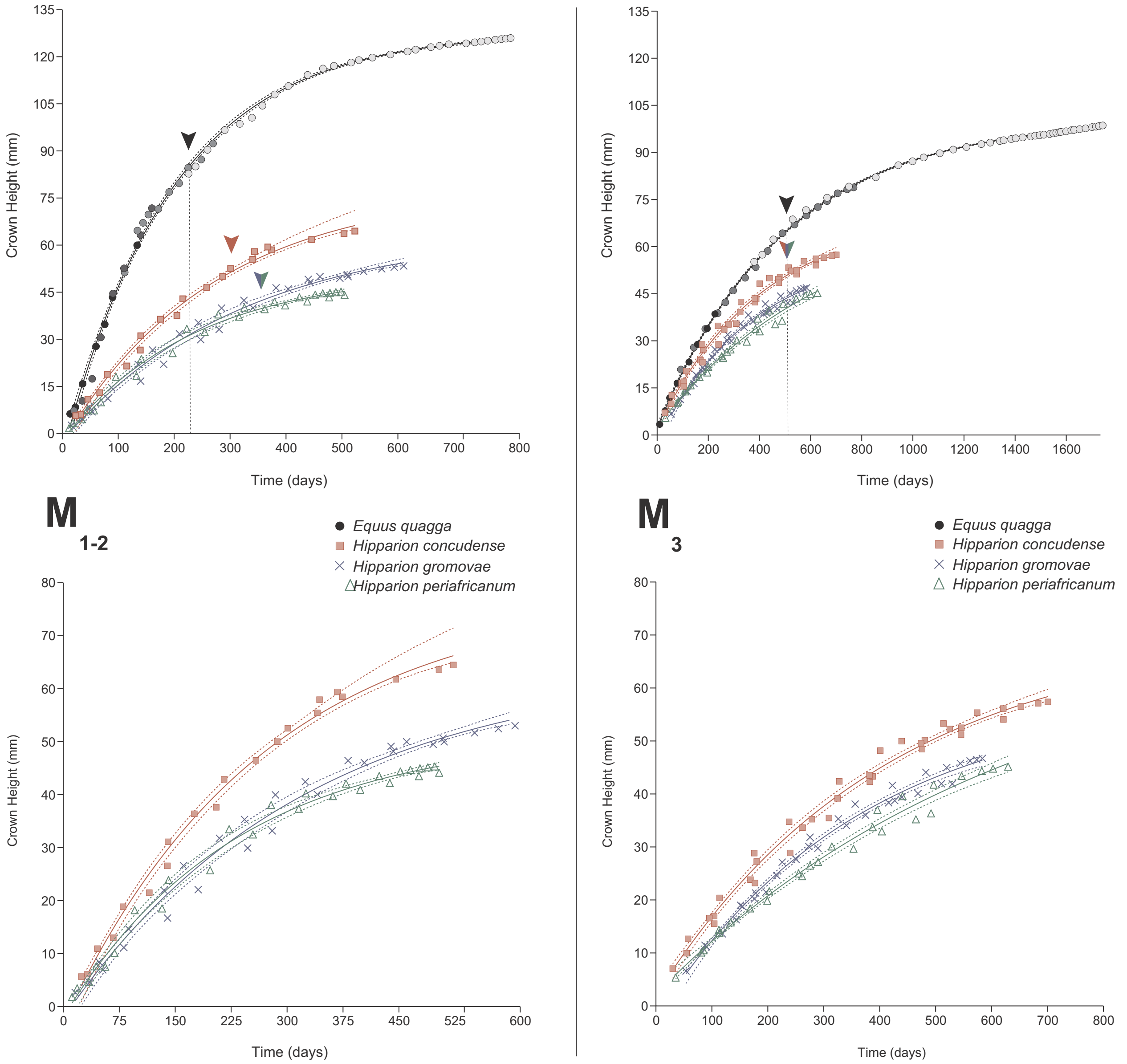

Fig. 4. Molar growth curves obtained from plotting the crown height through the enamel band (mm, y axis) against the crown formation time (days, x axis), from the cusp to the root area. Left plots show mean curves for first/second molars while right plots the third molar mean curves. Upper graphs represent the growth curves of all the species analyzed, while lower graphs only show hipparionin teeth. *Equus* growth curves obtained from the composition of differently worn teeth, which are represented by different grey scale dots. Note that the plot axes are not equally scaled. Dashed lines represent the 95% confidence intervals and the arrows the inferred eruption times.

teeth that present a similar ontogenetic stage (recently erupted and little worn, Table 1: *Equus quagga* IPS-92342 and *Hipparion concudense* IPS-91763) show that, although the *H. concudense* tooth (IPS-91763) lost the final part of enamel due to preservation, it took more time (367 days) to be formed than the extant *Equus* tooth (160 days) (Fig. 5). Growth rate differences between these two teeth are also evident (Fig. 5).

Aside from the total growth span, eruption times can be inferred considering that the different crown developmental stages are identifiable in the reconstructed growth curve (Nacarino-Meneses et al., 2017). Hence, here we estimated tooth eruption from the transition from the first CDS to the second CDS (arrowheads, Fig. 4), following Nacarino-Meneses et al. (2017). That is, from the change of an almost linear growth (CDS I) over a reduced growth rate (CDS II) that represents intermediate rates of growth (Nacarino-Meneses et al., 2017). Based on the *Equus quagga* m1 growth curve, we can identify this point at around 230 days, thus indicating the eruption of the first molar. For the *Equus quagga* m3, on the other hand, we estimate a time of eruption of around 500 days after the start of the formation (Fig. 4). As the first molars of extant zebras erupt around 9 months after birth (270 days) (Smuts, 1974), our estimation for the m1 seems reliable. In zebras, the third molar erupts at the age of 3 years and 3 months (Smuts, 1974) (39 months). Assuming that zebras' m3 starts to develop at a similar age as when the third molar of *Equus caballus* starts to mineralize

Table 3
Crown heights through the enamel band and crown formation times of the most complete teeth. *Equus quagga* calculations (*) relative to the total reconstructed molar growth.

	Species	Tooth	Code	Crown height (mm)	CFT (days)
m1/m2	*H. concudense*	m1/m2	IPS-91762	64.47	523
	H. gromovae	m1/m2	IPS-91731	53.39	610
	H. gromovae	m1/m2	IPS-91732	49.97	511
	H. periafricanum	m1/m2	IPS-91733	44.10	504
	H. periafricanum	m1/m2	IPS-91734	45.29	498
	Equus quagga	m1	Composition	125.94*	785*
m3	*H. concudense*	m3	IPS-87855	57.38	701
	H. gromovae	m3	IPS-85506	46.71	584
	H. periafricanum	m3	IPS-85504	41.51	591
	Equus quagga	m3	Composition	98.71*	1750*

[21 months of age (Hoppe et al., 2004)], the estimated eruption time of 500 days (~16.5 months) (Fig. 4) also agrees quite well. The decrease in growth rate is more progressive in hipparionin teeth than in *Equus* (Fig. 4), thus, the transitions between the CDSs in the hipparionin growth curves are less clear. Nevertheless, a change in the slope of the curves is identifiable (arrowheads, Fig. 4) and might match the eruption time as in the extant equid model. Applying this methodology, we infer a later eruption time in hipparionins' first/second molars compared to extant *Equus* [300 days to 350 days of formation (Fig. 4)]. The hipparionin third molars, on the other hand, likely erupted around 500 days after the beginning of their formation, similar to extant *E. quagga* third molars. Besides using the equid tooth growth model by Nacarino-Meneses et al. (2017), we can further endorse the inferences of the eruption times based on radiographic evidence of hipparionin eruptive sequences (Domingo et al., 2018). Judging from the radiographs provided in Domingo et al. (2018), the enamel band of the mesial lobe of an hipparionin m1 close to eruption measures ~53 mm, and that of a fully erupted one ~60 mm. Considering the tooth growth curve of the larger hipparionin species (Fig. 4), these teeth may have taken ~300 to ~350 days to be formed, respectively. In the third molars, an unerupted – still in crypt – hipparionin m3 measures ~45 mm and a totally erupted m3 measures ~55 mm, which represent ~350 and ~600 days of formation respectively. Thereafter, our inferred eruption times in hipparionin lower first/second molars and third molars are in agreement with the estimated CFTs of the teeth that have erupted or are close to eruption.

4. Discussion

Our study represents the first comprehensive analysis of hipparionin tooth growth through dental histology. The addition of extant *Equus quagga* teeth, moreover, allows us to compare the growth patterns and to identify differences in the tooth formation between extant and extinct representatives of the Equinae subfamily. Dental growth variations between different sets of permanent teeth have hitherto not been explored in ungulate mammals. Here, we analyze and compare, for the first time in ungulates, two different sets of permanent teeth, thus characterizing the growth of dental tissues during two distinct ontogenetic stages. A few other studies have addressed the differences in growth parameters between tooth loci, but these have been focused on hominoids (Guatelli-Steinberg et al., 2012; Shellis, 1984; Smith, 2016; Smith et al., 2007). Besides the growth characterization of the hipparionin teeth, widely used in many paleoecological studies (Domingo et al., 2009; Matson and Fox, 2010; Nelson, 2005; Rey et al., 2013; van Dam and Reichart, 2009), our approach also allows us to make further inferences of the life history of the studied taxa. The assessment of the dental growth patterns, thus, led us to infer differences in the lifestyles of the different-sized hipparionin taxa. Moreover, the comparison between hipparionin and *Equus* molars has highlighted significant tooth growth differences that can be both involved in life history differences and in the formation of the higher crowned teeth of *Equus*.

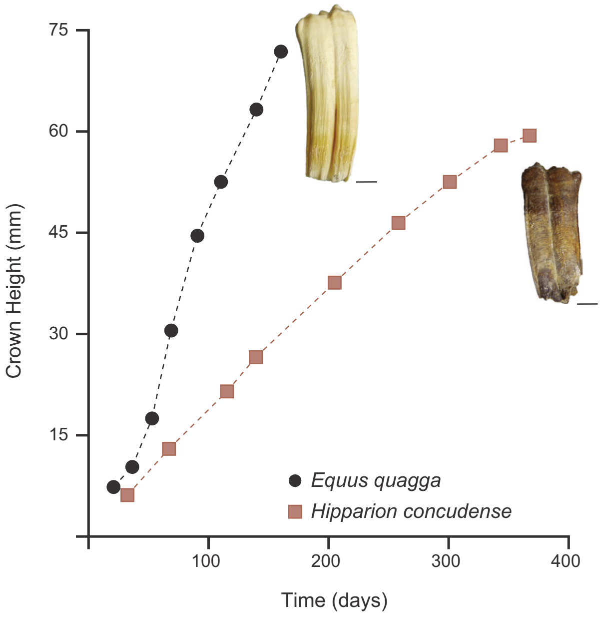

Fig. 5. Growth curves of two molars of comparable developmental stage (*Equus quagga* IPS-92342 and *Hipparion concudense* IPS-91763). The curve represents the growth from the cusp to the root. Scale shown in the teeth images correspond to 1 cm.

4.1. Dental growth parameters: daily secretion rate

We identified that the dominant incremental markings in hipparionin enamel are laminations, which is in agreement with previous findings on ungulate teeth (Jordana and Köhler, 2011; Kierdorf et al., 2013, 2014; Nacarino-Meneses et al., 2017; Tafforeau et al., 2007). The daily secretion rates obtained through quantification of the lamination spacing (Table 2) are congruent with those determined in the aforementioned studies focused on ungulate species. Nevertheless, our estimated DSR values ranging from 14 to 17 μm/day do not correspond to previous values of 5 μm/day calculated in domestic horses (Hoppe et al., 2004). As formerly pointed out by other authors (Kierdorf et al., 2013, 2014), and already addressed in previous studies with equid teeth (Nacarino-Meneses et al., 2017), we consider those undervalued preliminary measures a result of the misinterpretation of laminations and sub-daily incremental marks.

In our sample, we identified higher DSRs in the hipparionin first/second molars compared to third molars (Table 2). Although the mean DSRs can be skewed to some extent by the unbalanced counts between the different enamel and crown portions, the higher DSR values in m1/m2 compared to those of the m3 are commonly found within all zones. The few previous studies that compared daily enamel secretion rate between hominoid tooth types did not detect variations between the molars' DSRs (Smith, 2016; Smith et al., 2007). In a similar way, we do not identify DSR differences between the *Equus quagga* tooth types. In our case, we interpret the lack of differences in *Equus* tooth types as being a result of the lumped measures, the lower number of observations done in the *Equus* first molars ($n = 45$) compared to the third molars ($n = 138$), and to the significant DSR decrease observed in the consecutive developmental stages of the *Equus* third molars. Similarly, a decrease in the enamel secretion rate at the end of the third molar formation has been observed in human teeth (Guatelli-Steinberg et al., 2012). We suggest that these lowered secretion rates on the *Equus* third molars might be related to a general depletion of tissue depositional rates after the eruption of the third molar (transition from CDS I to CDS II sensu Nacarino-Meneses et al. (2017), as this event is broadly correlated with the attainment of skeletal maturity (Dean, 2006). Thus, the lower DSRs of hipparionin third molars compared to the first/second molars can also be linked to the differences in the formation timing.

In ungulates, however, the DSR parameter has shown to be more correlated with the tooth morphology (i.e. hypsodonty degree) than to the pace of life history or somatic growth (Jordana et al., 2014). This would agree with the differences observed in the DSRs between the hipparionin tooth types, since third molars are lower crowned and less hypsodont than first/second molars (Tables 1 and 3). The DSR, moreover, can also be related to the enamel band thickness, since the amount of enamel secreted per day (i.e. DSR) and the ameloblast secretory lifespan determine the final width of the enamel (Kierdorf et al., 2014). Accordingly, we measured the linear enamel thickness in our sample (Supplementary material Fig. S6). Despite their lower DSRs, the third molars tend to have somewhat thicker enamel bands than the first/second molars. This result suggests that enamel thickness differences between tooth types are more influenced by the secretory lifespan of the ameloblasts (Kierdorf et al., 2014) or the total CFT (Kierdorf et al., 2019) than by the DSR. Regarding intergeneric comparisons, the higher DSR values of extant *Equus*' molars compared to those of hipparionins are expected considering the proposed relationship between hypsodonty and DSR (Jordana et al., 2014) but also considering the *Equus*' thicker enamel bands (Supplementary material Fig. S6). However, interspecific differences in the hipparionin DSR do not seem to be directly linked to differences in hypsodonty (Table 1), nor to differences in enamel thickness (Supplementary material Fig. S6). For example, the smallest and most hypsodont *H. periafricanum* presents low DSRs comparable to those of the less hypsodont *H. concudense*, which has considerably thicker enamel bands. Therefore, the ameloblast secretory lifespan and the CFTs may have more important roles than DSR in the formation of thicker enamel bands (Kierdorf et al., 2019) and more hypsodont teeth (Nacarino-Meneses et al., 2017; Witzel et al., 2018). Hence, the small differences in the hypsodonty between these high-crowned hipparionins might be of little importance in terms of DSR changes. We suggest that the relationship between hypsodonty and DSR (Jordana et al., 2014) could be more easily observed in large-scale comparisons between more brachydont to more hypsodont species. Alternatively, the differences identified here could represent interspecific variations in the quotient between enamel and dentine, a characteristic that together with hypsodonty determine tooth durability (Famoso et al., 2013; Jordana et al., 2012; Winkler and Kaiser, 2015). Thus, we interpret that DSR is probably influenced by many other factors besides hypsodonty, such as tooth morphology, phylogeny (Dirks et al., 2012), enamel thickness (Kierdorf et al., 2014), tooth formation timing or even general somatic growth. The interplay of many of these factors might determine the overall DSR of the tooth. Further studies addressing the relationship between this parameter and the disposal and proportion of enamel could shed light on this topic.

4.2. *Dental growth parameters: extension rate*

Various isotopic studies have already inferred hipparionin tooth growth in height thanks to the identification of cyclic variations in δ13C and δ18O signal (Matson and Fox, 2010; Nelson, 2005; van Dam and Reichart, 2009). These estimations represent mineralization rates rather than matrix secretion rates. However, since the enamel starts to mineralize soon after matrix deposition, the extension rates estimated from isotopic studies tend to resemble those calculated using histology (Metcalfe and Longstaffe, 2012). Accordingly, the tooth growth rates calculated from the isotopic cyclicity in hipparionin teeth agree well with the enamel extension rates calculated here from incremental growth marks. For example, van Dam and Reichart (2009) estimated a growth rate of 40 mm/year (= 109.60 μm/day) for the upper third molar of *H. concudense* from Concud. In our study, we obtained a similar mean EER of 95.54 μm/day in the middle region of the lower third molar from the same species population, supporting the link between formation and mineralization rates, which has also been corroborated in extant equids' molars (Nacarino-Meneses et al., 2017).

In general, the proper estimation of a representative EER mean in high-crowned teeth is difficult since there is a general decrease of this parameter through the course of tooth formation (Fig. 3). This declining in the tooth growth pace from the cusp to the cervix is a reflection of a non-linear dental growth pattern (Bendrey et al., 2015), and has already been described in other mammalian groups (Guatelli-Steinberg et al., 2012; Jordana and Köhler, 2011; Kierdorf et al., 2013; Shellis, 1984) and in extant equids (Nacarino-Meneses et al., 2017). Due to the larger crowns' heights, the variation in the EER values through the enamel band is especially high in hypsodont ungulate teeth and should be considered when making comparisons. Moreover, apart from the within-tooth variation, the extension rates of the first/second molars and the third molars differed in our sample, being always higher in the first/second molars of all taxa. Similarly, Shellis (1984) found that in humans the first formed deciduous teeth grow eight times faster than third molars do, and higher crown extension rates have been calculated in first molars compared to third molars in other hominoids (Smith, 2016; Smith et al., 2007, 2010). Higher EERs might be influenced by the need to form the tooth within a shorter CFT (Kierdorf et al., 2014), as tooth crowns in m1/m2 tend to take less time to be formed than those of m3 (Table 3 and Supplementary material Fig. S5). Moreover, we interpret the higher EER values of the m1/m2 compared to those of the m3 as a reflection of the higher growth rates of the organism. Mammalian first molars are formed and erupt earlier in the ontogeny, while third molars finish their formation when skeletal maturity is being reached (Dean, 2006; Hillson, 2005; Hoppe et al., 2004). For this reason, we can expect greater EERs in m1/m2 since there are more activated ameloblasts due to the higher general somatic growth than posteriorly in ontogeny, when m3 are being formed. The fact that the deposition of bone lamella is coupled with the Retzius line formation (Bromage et al., 2009), and that there is an endogenous rhythm controlling both functions (Bromage et al., 2016), endorses the relationship between enamel growth rates with bone growth and, then, the general somatic growth. The same idea has recently been suggested due to the discovery of lower EER in mammaliamorphs that experienced an earlier reduction of the overall skeletal growth rates (O'Meara et al., 2018). The influence of growth hormones (GH and IGF-1) and their receptors in the differentiation and proliferation of the odontogenic cells involved in the formation of teeth (Symons and Seymour, 2000; Young, 1995; Zhang et al., 1992) further supports this link.

Besides the variations in intraspecific somatic growth rates during ontogeny, the differences EERs between taxa might also be indicative of differences in the organism's pace of growth (Jordana et al., 2014). The estimation of this parameter, therefore, might allow further interpretations to be made on the biology of animals, although caution should be taken due to the variation of these parameters between and within tooth types. Considering the differences between the third and first/second molars, and the decreasing of EER through the enamel band, we could identify higher EER in *E. quagga* compared to all hipparionin horses, and higher EER in the larger hipparionin species compared to the dwarfed taxa. Within a sample of 21 ruminant species and taking into account their phylogenetic relationships, Jordana et al. (2014) found a significant correlation between the residuals of the age at first reproduction – a proxy of the pace of life history corrected by body size – and the tooth enamel extension rate. Hence, lower EER values have shown to be indicative of a slower pace of growth than those expected from body size scaling (Jordana et al., 2014). Additionally, slower extension rates have also been associated to a later attainment of foraging independence in cebids (Hogg and Walker, 2011) and to the prolonged growth periods of modern humans compared to *Homo erectus* and earlier hominins (Dean et al., 2001). The influence of the EER in the formation of a tooth at the required time for its eruption, might be the reason underlying the EER relationship with the timing of life history events, since the tooth development is strongly tied to the mammals' life cycle (Smith, 1991, 2000). In terms of EER, therefore, we can infer a slower pace of growth in the analyzed hipparionin species in comparison to extant equids. Moreover, the extension rates of the dwarf late Turolian Spanish forms further suggest a slower pace of growth compared to *H. concudense*.

Some authors have considered the existence of an allometric coupling of the EER with total crown height (Dirks et al., 2012) or body mass (O'Meara et al., 2018). Taking this into account, the lower EERs of the hipparionins compared to extant equids, and the lower EER of dwarf hipparionins compared to larger representatives, could represent the consequence of the allometric scaling of this parameter. The same relationship between tooth size and EER was also identified in humans by Guatelli-Steinberg et al. (2012), estimating higher EERs in those teeth with larger enamel dentine junction lengths. On the other hand, however, the formation of larger canines in male gorillas has been related to longer formation times rather than to higher growth rates (Schwartz and Dean, 2001). Smith (2016) also found that taller fossil teeth from larger extinct pongines had lower EERs compared to those of extant orangutans. Similarly, Jordana and Köhler (2011) identified lower EERs in the higher crowned insular *Myotragus balearicus*, which was a slow-growing mammal with a delayed life history schedule compared to extant caprines (Jordana et al., 2012; Köhler, 2010; Köhler and Moyà-Solà, 2009). In our case, *H. periafricanum* and *H. gromovae* were relatively higher crowned – more hypsodont – than the larger hipparionin species from the late Miocene (Pesquero, 2003). Thus, to form those more hypsodont teeth, we should expect higher EERs compared to less hypsodont species (*H. concudense*), especially if we consider that they would have advanced the general life history schedule due to their reduced size and the theoretical size coupling with life history traits (Calder, 1984; Stearns, 1992). Our results suggest the opposite scenario, namely more hypsodont dwarf hipparionin species exhibiting lower EER, which we further relate to a slower life history than the expected from their size.

4.3. Formation and eruption times

The previous life history interpretations are not only supported by the EER values, but also by the estimated formation and eruption times, two parameters that are strongly correlated with the life history of an organism (Dean, 2006; Macho and Williamson, 2002; Smith, 1991, 2000).

Regarding the formation times, we generally identified higher CFTs in third molars compared to those of first molars. Similarly, CFTs in human third molars are much higher than in the case of other teeth (Shellis, 1984), as has also been observed in other hominoids where the first molars form faster and in less time than third molars (Smith et al., 2007, 2010). The longer formation times in the third molars might be related to their lower EER. When comparing between taxa, the overall crown formation times in *Equus* are much higher than in hipparionins, since *Equus* CFTs are the result of a composite growth reconstruction as they extend the molar formation. When we compare growth curves and, thus, observe the total crown formation times of individual teeth of similar developmental stages, we observe higher CFTs in hipparionin teeth compared to *Equus* (Fig. 5), and in some cases higher CFTs in the small hipparionins compared to the larger species (Fig. 4). Macho and Williamson (2002) found a significant correlation between the crown formation times corrected by body mass and the relative gestation length in African bovids. Although they arguably overestimated the CFTs due to the misinterpretation of sub-daily striations with daily increments (Kierdorf et al., 2013, 2014), the similar repeat intervals that they reported relating these features across the studied taxa (Macho and Williamson, 2002) might maintain the proportionality of the correction and thus the significance of the correlation. Hence, taking in mind the high relative CFTs obtained in hipparionins, and especially the two dwarf taxa, we might infer higher relative gestation lengths, a characteristic of a slower pace of life history compared to *Equus* and to larger hipparionins.

Table 4
Eruption dates of first and third molars contrasted with life history information in two extant equid species.

Species	Event	Age (months)	Reference
Equus caballus	First molar eruption	8–12	(Hoppe et al., 2004)
	Weaning age (feral)	8–9	(Waran et al., 2008)
	Third molar eruption	42–48	(Hoppe et al., 2004)
	Femoral epiphysis fusion	36–42	(Silver, 1969)
	Breeding (Przewalski's horse)	36–48	(Monfort et al., 1994)
Equus quagga	First molar eruption	9–12	(Smuts, 1974)
	Weaning age	8–12	(Pluháček et al., 2007)
	Third molar eruption	39	(Smuts, 1974)
	Adult body mass attainment	36	(Smuts, 1975)
	Sexual physiological maturity	42	(Smuts, 1976a)

However, a more direct life history proxy not related to the continuous growth of extant equid teeth is the timing of dental eruption (Smith, 2000). On the one hand, the first molar eruption is considered as an indicator of the weaning event (Dirks and Bowman, 2007; Smith, 1991, 2000), and the age of eruption is an informative estimate of postnatal growth rate, with faster-growing animals erupting their first molars earlier in life (Smith, 2000). The age of first molar eruption, moreover, has been shown to positively correlate with important life history traits such as longevity or female sexual maturity (Veitschegger and Sánchez-Villagra, 2016). On the other hand, the onset of the third molar eruption has been shown to be correlated with skeletal maturity (Dean, 2006; Engström et al., 1983). Data relative to the weaning and maturity attainment of extant equids coincide with those of the first and third molar eruption times (Table 4). This endorses our interpretations based on the hipparionin eruption times. In extant foals, the first molar starts to be formed close to the birth event, and begins mineralization two weeks after (Hoppe et al., 2004). Taking into account the growth curve reconstruction, we identified the emergence time of extant *Equus* molars (Nacarino-Meneses et al., 2017) at ~230 days (Fig. 4), which agrees quite well with that reported in the literature (Smuts, 1974). Assuming a similar age of the first molar formation onset in hipparionins, we can infer later eruption times compared to extant equids. By this, we roughly estimate the weaning age of the hipparionins analyzed in a span from 300 to 350 days of age (10–12 months).

The absolute eruption age of the third molar is difficult to establish because we do not know at which age hipparionins started to form the third molar. However, the hipparionin tooth mineralization pattern has shown to be analogous to that of extant *Equus* (Domingo et al., 2018). From the growth curves, we estimated a similar third molar eruption time of ~500 days after the onset of the formation in all analyzed taxa. If we conservatively assume that hipparionin third molars begin to form as in *Equus*, where third molar mineralization starts at the age of 21 months (Hoppe et al., 2004), the hipparionin third molars should have erupted around the age of ~37.5 months. Considering the allometric coupling between size and life history, we would expect that the smaller species followed faster life history strategies and, thus, they would have matured earlier (Calder, 1984). However, we observe how hipparionins, and especially the dwarf Spanish species, had a similar maturity age to extant equids. In this sense, we could infer a slower lifestyle in hipparionin horses bearing in mind the similar timing despite the smaller size (Sibly and Brown, 2007). Our results on weaning and maturity schedules, together with the hipparionin smaller size compared to extant equids, further support our previous interpretation of slower life histories. Conforming to the Schultz's Rule (Smith, 2000), moreover, the hipparionin eruption sequence have already indicated a slow-growing strategy (Domingo et al., 2018). Besides the slower pace of life history compared to *Equus*, our results also suggest that the dwarf taxa from the Spanish late Turolian followed slower lifestyles than the larger middle Turolian species; because although they were smaller, which predicts faster life history from body mass scaling (Calder, 1984), they followed similar life history schedules.

4.4. *Hypsodonty and life history interpretations*

The more hypsodont *Equus* molars erupt earlier compared to those of hipparionins, probably related to a faster ontogenetic development. In a similar way, the South American notoungulates with ever-growing teeth exhibited an earlier eruption of permanent molars compared to premolars, which has also been linked to an accelerated life history (Gomes Rodrigues et al., 2017). The higher wear exposure due to earlier eruption of the permanent molars would have been compensated by the observed extended dental growth span and a late root formation. After the earlier *Equus* molar eruption, therefore, the subsequent slower growth and extended formation time helps to counterbalance the height loss due to wear (Nacarino-Meneses et al., 2017). Moreover, the higher EERs related to earlier formation, and the extended crown formation times in *Equus*, may be involved in the higher hypsodonty indices exhibited within the genus. As a result, extant equids could have increased the endurance of their masticatory apparatus and, thus, incremented their potential lifespan (Damuth and Janis, 2011; Jordana et al., 2012; Veiberg et al., 2007). Hipparionins, on the other hand, would have erupted their permanent molars later than extant equids, thus having a prolonged potential tooth lifespan as teeth began to wear later. Moreover, instead of increased crown heights, hipparionin horses relied on occlusal enamel-band complexity as a way to expand their tooth durability (Famoso et al., 2016; Famoso and Davis, 2016).

Previous inferences on the life history of the Hipparionini tribe suggested an earlier maturity attainment and shorter lifespan compared to modern equids (Hulbert, 1982; Kurtén, 1953; Van Valen, 1964). These first surveys were based on age-structure and population dynamics studied from attritional equid fossil populations by means of their dentition ontogeny (Woodburne and MacFadden, 1982). Therefore, to define and characterize discrete age stages for the reconstruction of the demographic profile, these studies depended on models of age determination for extant species and their eruption patterns (Kurtén, 1953; Spinage, 1972). For this reason, the inferences of accelerated life history in hipparionins, and especially the interpretations of shorter potential lifespan, strongly relied on the lower crown height of these taxa compared to present-day equids (Hulbert, 1982) and on the smaller size of some species (Van Valen, 1964). However, as we have seen, hipparionins do not follow the same formation, nor eruption pattern as extant equids (Domingo et al., 2018), and probably they also had different wear rates (Hulbert, 1984) due to their different dietary niches (Semprebon et al., 2016). Hence, there are arguments in support of the thesis that hipparionins were slow-growing mammals, as has also been recently proposed from their molar eruption pattern based on the Schultz's Rule (Domingo et al., 2018).

More recent approaches using bone paleohistological analyses have provided a new framework to test for the life history adaptations of this diverse and successful group (Martinez-Maza et al., 2014; Orlandi-Oliveras et al., 2018). Thus, the study of the bone histology of *Hipparion concudense* has provided evidence of the attainment of skeletal maturity during the third year of life (Martinez-Maza et al., 2014), coinciding with our inferred age of third molar eruption. Although Martinez-Maza et al. (2014) pointed out similar life history patterns between *H. concudense* and extant equids, they suggested that *H. concudense* developed over a shorter time span. Their interpretation was based on an estimated age of sexual maturity at three years old in *H. concudense*, while most extant equids reach reproductive maturity during or after the fourth year of life (Martinez-Maza et al., 2014). However, the identification of absolute sexual maturity attainment from bone histology analysis is an issue still under debate (Marín-Moratalla et al., 2013; Nacarino-Meneses et al., 2016), as Martinez-Maza et al. (2014) already indicated, and the results should be considered carefully. Furthermore, wild equid populations can exhibit a wide range of variability in sexual maturity attainment since there are many possible factors influencing it (Choquenot, 1991; Penzhorn and van der Merwe, 1988; Smuts, 1976a, 1976b; Westlin-van Aarde et al., 1988). The dental histology parameters and eruption times calculated here, however, point towards a slower life strategy in hipparionins compared to extant equids. Considering their size, the Spanish dwarf taxa would have followed an even relative slower lifestyle than the larger hipparionins, as was also proposed by Orlandi-Oliveras et al. (2018) from the study of *H. gromovae* bone histology. This slower pace of growth can be related to a different ecology of the smaller species compared to the larger hipparionin forms (Orlandi-Oliveras et al., 2018). In African bovids, Macho and Williamson (2002) also found that the small-sized taxa tend to follow slower life history strategies due to their relatively longer gestation lengths. In this case, small ruminants showed different habitat preferences than the larger ones, browsing in more wooded habitats. Future paleodietary reconstructions using micro or mesowear techniques (Calandra and Merceron, 2016; Kaiser and Solounias, 2003) on the teeth of these dwarf hipparionins could shed light on their diet and habitat preferences.

5. Conclusions

Our analyses of the dental histology of hipparionin teeth allow the characterization of their growth and comparisons both between different-sized taxa and with an extant equid model. In all cases, hipparionin teeth grow and develop differently from those of the genus *Equus*. Variations are also found between hipparionin species and between the two tooth types analyzed within each taxon. We have associated the higher enamel secretion and extension rates of the first/second molars compared to the third molars with differences in the formation timing, although the variation in the secretion rates could also be influenced by the crown height or other characteristics related to tooth morphology. The higher enamel extension rates of the first/second molars are a reflection of the fast somatic growth of early ontogenetic stages, while the third molars are formed close to maturity attainment. Moreover, third molars generally take more time to be formed and to erupt than first/second molars, which is probably linked to their lower extension rates. Regarding the differences between groups, we found lower daily secretion rates in hipparionin teeth in comparison to *E. quagga*. We hypothesize that these distinct secretion rates, together with the disparity between hipparionin species, are the consequence of the interplay of numerous factors, such as hypsodonty, enamel thickness, secretory ameloblast lifespan, and overall tooth morphology.

Due to the link between pace of life history and dental growth development, we could also draw inferences on the life history of the studied taxa. The parameters that are more related to the pace of growth are the enamel extension rate and the formation time. The formation and eruption of first and third molars are further linked to key life history events such as weaning and maturity attainment, respectively. As a result, we were able to compare the hipparionin life history strategies with an extant equid model, and also to make comparisons between the two dwarf forms and the larger one. Hipparionin teeth grow more slowly and erupt relatively later than those of extant equids, suggesting a slower pace of growth. In addition, the dwarf hipparionins exhibit lower extension rates but similar formation and eruption schedules than the larger species, which considering their smaller size indicates that they had slower life histories than expected. These results point towards a slow-growing strategy in hipparionin horses, as has recently been suggested from dental eruption patterns

(Domingo et al., 2018), and debunk previous hypotheses of general shorter lifespans and earlier maturity. Dwarfed hipparionin species from the late Turolian of Spain, moreover, do not follow the size scaling of the life history schedule but show a similar life history strategy as larger hipparionins, which is slower than predicted from the body mass.

Acknowledgments

We would like to thank T. Kaiser (Centrum für Naturkunde, Universität Hamburg) and J. Quesada (Museu de Ciències Naturals de Barcelona) for their permission to analyze extant *Equus* material from their respective institutions. B. Lamglait (currently at Université de Montréal) together with the Réserve Africaine de Sigean are acknowledged for the donation of extant equid specimens. We also acknowledge M. Soteras March for the access to the museum collection of the Institut Català de Paleontologia Miquel Crusafont (ICP), M. Fernández (ICP) for the slide preparation, the ICP's preparation team for the molding of the specimens, R. Molonwy (Centre de Recerca Ecològica i Aplicacions Forestals) for the statistical advice received, and X. Jordana (Universitat Autònoma de Barcelona) for the help during the choice of the material and the discussion of the first analyses. We further thank the reviewers and editors for their helpful comments. Funding for this study was provided by the Ministerio de Economía, Industria y Competitividad (MINECO), Gobierno de España (PI: M.K., CGL2015-63777), and the CERCA Programme, Generalitat de Catalunya. The Paleobiology research group (ICP) is recognized without funding by AGAUR (2017 SGR 960). G.O.-O. was supported by a FI-DGR 2016 grant (2016FI_B00202) awarded by AGAUR (Generalitat de Catalunya). The support of the DST-NFR Centre of Excellence in Palaeosciences (CoE-Pal) towards this research for C.N.-M. (COE2019-PD03) is hereby acknowledged. Opinions expressed and conclusions arrived at, are those of the author and are not necessarily to be attributed to the CoE-Pal.

Data availability

Relevant data is shown within the paper and in Supplementary material. Raw data related to this article can be found at http://dx.doi.org/10.17632/h2ywzbcs59.1, an open-source online data repository hosted at Mendeley Data.

Appendix A. Supplementary data

Supplementary data to this article can be found online at https://doi.org/10.1016/j.palaeo.2019.04.016.

References

Alberdi, M.T., 1974. Las “faunas de *Hipparion*” de los yacimientos españoles. Estud. Geol. 30, 189–212.

Alberdi, M.T., 1989. A review of old world hipparionine horses. In: Prothero, D.R., Schoch, R.M. (Eds.), The Evolution of Perissodactyls. Oxford University Press, New York, pp. 234–261.

Alberdi, M.T., Alcalá, L., 1989. El género *Hipparion* en la fosa de Alfambra-Teruel. Paleontol. i Evol. 105–109.

Alberdi, M.T., Prado, J.L., Ortiz-Jaureguizar, E., 1995. Patterns of body size changes in fossil and living Equini (Perissodactyla). Biol. J. Linn. Soc. 54, 349–370. https://doi.org/10.1111/j.1095-8312.1995.tb01042.x.

Bendrey, R., Vella, D., Zazzo, A., Balasse, M., Lepetz, S., 2015. Exponentially decreasing tooth growth rate in horse teeth: Implications for isotopic analyses. Archaeometry 57, 1104–1124. https://doi.org/10.1111/arcm.12151.

Bernor, R.L., Tobien, H., Woodburne, M.O., 1990. Patterns of Old World hipparionine evolutionary diversification and biogeographic extension. In: Lindsay, E.H., Fahlbusch, V., Mein, P. (Eds.), European Neogene Mammal Chronology. Plenum Press, New York, pp. 263–319. https://doi.org/10.1007/978-1-4899-2513-8_18.

Bernor, R.L., Koufos, G.D., Woodburne, M.O., Fortelius, M., 1996. The evolutionary history and biochronology of European and Southwest Asian Late Miocene and Pliocene hipparionine horses. In: Bernor, R.L., Fahlbusch, V., Mittmann, H.-W. (Eds.), The Evolution of Western Eurasian Neogene Mammal Faunas. Columbia University Press, New York, pp. 307–338.

Bromage, T.G., Lacruz, R.S., Hogg, R.T., Goldman, H.M., McFarlin, S.C., Warshaw, J., Dirks, W., Perez-Ochoa, A., Smolyar, I., Enlow, D.H., Boyde, A., 2009. Lamellar bone is an incremental tissue reconciling enamel rhythms, body size, and organismal life history. Calcif. Tissue Int. 84, 388–404. https://doi.org/10.1007/s00223-009-9221-2.

Bromage, T.G., Idaghdour, Y., Lacruz, R.S., Crenshaw, T.D., Ovsiy, O., Rotter, B., Hoffmeier, K., Schrenk, F., 2016. The swine plasma metabolome chronicles “many days” biological timing and functions linked to growth. PLoS One 11, 1–19. https://doi.org/10.1371/journal.pone.0145919.

de Bruijn, H., Daams, R., Daxner-Höck, G., Fahlbusch, V., Ginsburg, L., Mein, P., Morales, J., Heinzmann, E., Mayhew, D.F., van der Meulen, a J., Schmidt Kittler, N., Telles Antunes, M., 1992. Report of the RCMNS working group on fossil mammals, Reisensburg 1990. Newsl. Stratigr. 26, 65–118. https://doi.org/10.1127/nos/26/1992/65.

Calandra, I., Merceron, G., 2016. Dental microwear texture analysis in mammalian ecology. Mammal Rev. 46, 215–218. https://doi.org/10.1111/mam.12063.

Calder, W.A., 1984. Size, Function, and Life History. Harvard University Press, Cambridge. https://doi.org/10.2307/4086807.

Cantalapiedra, J.L., Prado, J.L., Hernández Fernández, M., Alberdi, M.T., 2017. Decoupled ecomorphological evolution and diversification in Neogene-Quaternary horses. Science 355, 627–630. https://doi.org/10.1126/science.aag1772.

Choquenot, D., 1991. Density-dependent growth, body condition, and demography in feral donkeys: testing the food hypothesis. Ecology 72, 805–813. https://doi.org/10.2307/1940583.

Damuth, J.D., Janis, C.M., 2011. On the relationship between hypsodonty and feeding ecology in ungulate mammals, and its utility in palaeoecology. Biol. Rev. 86, 733–758. https://doi.org/10.1111/j.1469-185X.2011.00176.x.

Dean, M.C., 2000. Incremental markings in enamel and dentine: what they can tell us about the way teeth grow. In: Teaford, M.F., Meredith Smith, M., Ferguson, M.W.J. (Eds.), Development, Function and Evolution of Teeth. Cambridge University Press, Cambridge, pp. 119–130. https://doi.org/10.1017/CBO9780511542626.009.

Dean, M.C., 2006. Tooth microstructure tracks the pace of human life-history evolution. Proc. Biol. Sci. 273, 2799–2808. https://doi.org/10.1098/rspb.2006.3583.

Dean, M.C., Leakey, M.G., Reid, D.J., Schrenk, F., Schwartz, G.T., Stringer, C., Walker, A., 2001. Growth processes in teeth distinguish modern humans from *Homo erectus* and earlier hominins. Nature 414, 628–631. https://doi.org/10.1038/414628a.

Dirks, W., Bowman, J.E., 2007. Life history theory and dental development in four species of catarrhine primates. J. Hum. Evol. 53, 309–320. https://doi.org/10.1016/j.jhevol.2007.04.007.

Dirks, W., Anemone, R.L., Holroyd, P.A., Reid, D.J., Walton, P., 2009. Phylogeny, life history and the timing of molar crown formation in two archaic ungulates, *Meniscotherium* and *Phenacodus* (Mammalia, ’Condylarthra’). Front. Oral Biol. 13, 3–8. https://doi.org/10.1159/000242381.

Dirks, W., Bromage, T.G., Agenbroad, L.D., 2012. The duration and rate of molar plate formation in *Palaeoloxodon cypriotes* and *Mammuthus columbi* from dental histology. Quat. Int. 255, 79–85. https://doi.org/10.1016/j.quaint.2011.11.002.

Domingo, L., Grimes, S.T., Domingo, M.S., Alberdi, M.T., 2009. Paleoenvironmental conditions in the Spanish Miocene-Pliocene boundary: isotopic analyses of *Hipparion* dental enamel. Naturwissenschaften 96, 503–511. https://doi.org/10.1007/s00114-008-0500-y.

Domingo, M.S., Cantero, E., García-Real, I., Chamorro Sancho, M.J., Martín Perea, D.M., Alberdi, M.T., Morales, J., 2018. First radiological study of a complete dental ontogeny sequence of an extant equid: implications for equidae life history and taphonomy. Sci. Rep. 8, 8507. https://doi.org/10.1038/s41598-018-26817-3.

Easley, J., Dixon, P.M., Schumacher, J., 2005. Equine Dentistry, third ed. Elsevierhttps://doi.org/10.1016/B0-7020-2724-3/X5001-4.

Eisenmann, V., 1995. What metapodial morphometry has to say about some Miocene hipparions. In: Vrba, E.S., Denton, G.H., Partridge, T., Burckle, L.H. (Eds.), Paleoclimate and Evolution, With Emphasis on Human Origins. New Haven and London, pp. 149–164.

Engström, C., Engström, H., Sagne, S., 1983. Lower third molar development in relation to skeletal maturity and chronological age. Angle Orthod. 53, 97–106. https://doi.org/10.1043/0003-3219(1983)053<0097:LTMDIR>2.0.CO;2.

Ernest, S.K.M., 2003. Life history characteristics of placental nonvolant mammals. Ecology 84https://doi.org/10.1890/02-9002. (3402–3402).

Famoso, N.A., Davis, E.B., 2016. On the relationship between enamel band complexity and occlusal surface area in Equids (Mammalia, Perissodactyla). PeerJ 4, e2181. https://doi.org/10.7717/peerj.2181.

Famoso, N.A., Feranec, R.S., Davis, E.B., 2013. Occlusal enamel complexity and its implications for lophodonty, hypsodony, body mass, and diet in extinct and extant ungulates. Palaeogeogr. Palaeoclimatol. Palaeoecol. 387, 211–216. https://doi.org/10.1016/j.palaeo.2013.07.006.

Famoso, N.A., Davis, E.B., Feranec, R.S., Hopkins, S.S.B., Price, S.A., 2016. Are hypsodonty and occlusal enamel complexity evolutionarily correlated in ungulates? J. Mamm. Evol. 23, 43–47. https://doi.org/10.1007/s10914-015-9296-7.

Forsten, A., 1968. Revision of the palearctic *Hipparion*. Acta Zool. Fenn. 119, 1–134.

Forsten, A., 1978. *Hipparion* and possible Iberian-North African Neogene connections. Ann. Zool. Fenn. 15, 294–297.

Garcés, M., Cabrera, L., Agustí, J., Maria Parés, J., 1997. Old World first appearance datum of “*Hipparion*” horses: Late Miocene large-mammal dispersal and global events. Geology 25, 19. https://doi.org/10.1130/0091-7613(1997)025<0019:OWFADO>2.3.CO;2.

Garcés, M., Krijgsman, W., Peláez-Campomanes, P., Álva, M.A., Daams, R., 2003. *Hipparion* dispersal in Europe: magnetostratigraphic constraints from the Daroca area (Spain). Coloquios Paleontol. 1, 171–178.

Gomes Rodrigues, H., Herrel, A., Billet, G., 2017. Ontogenetic and life history trait changes associated with convergent ecological specializations in extinct ungulate mammals. Proc. Natl. Acad. Sci. 114, 1069–1074. https://doi.org/10.1073/pnas.

1614029114.

Grubb, P., 1981. Equus burchelli. Mamm. Species 157, 1. https://doi.org/10.2307/3503962.

Guatelli-Steinberg, D., Floyd, B.A., Dean, M.C., Reid, D.J., 2012. Enamel extension rate patterns in modern human teeth: two approaches designed to establish an integrated comparative context for fossil primates. J. Hum. Evol. 63, 475–486. https://doi.org/10.1016/j.jhevol.2012.05.006.

Hammer, Ø., Harper, D.A.T.a.T., Ryan, P.D., 2001. PAST: paleontological statistics software package for education and data analysis. Palaeontol. Electron. 4 (1), 1–9. https://doi.org/10.1016/j.bcp.2008.05.025.

Hayek, L.-A.C., Bernor, R.L., Solounias, N., Steigerwald, P., 1992. Preliminary studies of hipparionine horse diet as measured by tooth microwear. Ann. Zool. Fenn. 28, 187–200.

Hillson, S., 2005. Teeth. Cambridge University Press.

Hogg, R.T., Walker, R.S., 2011. Life-history correlates of enamel microstructure in cebidae (platyrrhini, primates). Anat. Rec. 294, 2193–2206. https://doi.org/10.1002/ar.21503.

Hoppe, K.A., Stover, S.M., Pascoe, J.R., Amundson, R., 2004. Tooth enamel biomineralization in extant horses: implications for isotopic microsampling. Palaeogeogr. Palaeoclimatol. Palaeoecol. 206, 355–365. https://doi.org/10.1016/j.palaeo.2004.01.012.

Hulbert, R.C., 1982. Population dynamics of the three-toed horse *Neohipparion* from the late Miocene of Florida. Paleobiology 8, 159–167. https://doi.org/10.2307/2400452.

Hulbert, R.C., 1984. Paleoecology and population dynamics of the early Miocene (Hemingfordian) horse *Parahippus leonensis* from the Thomas Farm site, Florida. J. Vertebr. Paleontol. 4, 547–558. https://doi.org/10.1080/02724634.1984.10012030.

Jordana, X., Köhler, M., 2011. Enamel microstructure in the fossil bovid *Myotragus balearicus* (Majorca, Spain): implications for life-history evolution of dwarf mammals in insular ecosystems. Palaeogeogr. Palaeoclimatol. Palaeoecol. 300, 59–66. https://doi.org/10.1016/j.palaeo.2010.12.008.

Jordana, X., Marín-Moratalla, N., DeMiguel, D., Kaiser, T.M., Köhler, M., 2012. Evidence of correlated evolution of hypsodonty and exceptional longevity in endemic insular mammals. Proc. R. Soc. B Biol. Sci. 279, 3339–3346. https://doi.org/10.1098/rspb.2012.0689.

Jordana, X., Marín-Moratalla, N., Moncunill-Solé, B., Köhler, M., 2014. Ecological and life-history correlates of enamel growth in ruminants (Artiodactyla). Biol. J. Linn. Soc. 112, 657–667. https://doi.org/10.1111/bij.12264.

Joubert, E., 1972. Tooth development and age determination in the Hartmann zebra *Equus zebra hartmannae*. Madoqua 5–16.

Kaiser, T.M., Solounias, N., 2003. Extending the tooth mesowear method to extinct and extant equids. Geodiversitas 25, 321–345.

Kierdorf, H., Kierdorf, U., Frölich, K., Witzel, C., 2013. Lines of evidence-incremental markings in molar enamel of soay sheep as revealed by a fluorochrome labeling and backscattered electron imaging study. PLoS One 8, e74597. https://doi.org/10.1371/journal.pone.0074597.

Kierdorf, H., Breuer, F., Richards, A., Kierdorf, U., 2014. Characterization of enamel incremental markings and crown growth parameters in minipig molars. Anat. Rec. 297, 1935–1949. https://doi.org/10.1002/ar.22951.

Kierdorf, H., Breuer, F., Witzel, C., Kierdorf, U., 2019. Pig enamel revisited – incremental markings in enamel of wild boars and domestic pigs. J. Struct. Biol. 205, 48–59. https://doi.org/10.1016/J.JSB.2018.11.009.

Kirkland, K.D., Baker, G.J., Marretta, S.M., Eurell, J.A.C., Losonsky, J.M., 1996. Effects of aging on the endodontic system, reserve crown, and roots of equine mandibular cheek teeth. Am. J. Vet. Res. 57, 31–38.

Köhler, M., Ramon, M^{a}.M., 2010. Fast or slow? The evolution of life history traits associated with insular dwarfing. In: Pérez-Mellado, V. (Ed.), Islands and Evolution. Institut Menorquí d'Estudis, Recerca, pp. 261–280.

Köhler, M., Moyà-Solà, S., 2009. Physiological and life history strategies of a fossil large mammal in a resource-limited environment. Proc. Natl. Acad. Sci. U. S. A. 106, 20354–20358. https://doi.org/10.1073/pnas.0813385106.

Kurtén, B., 1953. On the variation and population dynamics of fossil and recent mammal populations. Acta Zool. Fenn. 76, 1–122.

Lkhagvasuren, D., Ansorge, H., Samiya, R., Schafberg, R., Stubbe, A., Stubbe, M., 2013. Age determination of the Mongolian wild ass (*Equus hemionus* Pallas, 1775) by the dentition patterns and annual lines in the tooth cementum. J. Species Res. 2, 85–90. https://doi.org/10.12651/JSR.2013.2.1.085.

MacFadden, B.J., Solounias, N., Cerling, T.E., 1999. Ancient diets, ecology, and extinction of 5-million-year-old horses from Florida. Science 283, 824–827. https://doi.org/10.1126/science.283.5403.824.

Macho, G.A., Williamson, D.K., 2002. The effects of ecology on life history strategies and metabolic disturbances during development: an example from the African bovids. Biol. J. Linn. Soc. 75, 271–279. https://doi.org/10.1046/j.1095-8312.2002.00013.x.

Marín-Moratalla, N., Jordana, X., Köhler, M., 2013. Bone histology as an approach to providing data on certain key life history traits in mammals: implications for conservation biology. Mamm. Biol. 78, 422–429. https://doi.org/10.1016/j.mambio.2013.07.079.

Martinez-Maza, C., Alberdi, M.T., Nieto-Diaz, M., Prado, J.L., 2014. Life-history traits of the Miocene *Hipparion concudense* (Spain) inferred from bone histological structure. PLoS One 9, e103708. https://doi.org/10.1371/journal.pone.0103708.

Matson, S.D., Fox, D.L., 2010. Stable isotopic evidence for terrestrial latitudinal climate gradients in the Late Miocene of the Iberian Peninsula. Palaeogeogr. Palaeoclimatol. Palaeoecol. 287, 28–44. https://doi.org/10.1016/j.palaeo.2009.12.010.

McDonald, H.G., 1996. Population structure of the late Pliocene (Blancan) zebra *Equus simplicidens* (Perissodactyla: Equidae) from the Hagerman Horse Quarry, Idaho. In: Stewart, K., Seymour, K.L. (Eds.), Paleoecology and Paleoenvironments of Late Cenozoic Mammals. University of Toronto Press, Toronto, pp. 134–155.

Metcalfe, J.Z., Longstaffe, F.J., 2012. Mammoth tooth enamel growth rates inferred from stable isotope analysis and histology. Quat. Res. 77, 424–432. https://doi.org/10.1016/j.yqres.2012.02.002.

Monfort, S.L., Arthur, N.P., Wildt, D.E., 1994. Reproduction in the Przewalski's horse. In: Boyd, L., Houpt, K.A. (Eds.), Przewalski's Horse: The History and Biology of an Endangered Species. State University of New York Press, Albany, pp. 173–194.

Monson, T.A., Hlusko, L.J., 2018a. Breaking the rules: phylogeny, not life history, explains dental eruption sequence in primates. Am. J. Phys. Anthropol. 167, 217–233. https://doi.org/10.1002/ajpa.23618.

Monson, T.A., Hlusko, L.J., 2018b. The evolution of dental eruption sequence in artiodactyls. J. Mamm. Evol. 25, 15–26. https://doi.org/10.1007/s10914-016-9362-9.

Nacarino-Meneses, C., Jordana, X., Köhler, M., 2016. Histological variability in the limb bones of the Asiatic wild ass and its significance for life history inferences. PeerJ 4, e2580. https://doi.org/10.7717/peerj.2580.

Nacarino-Meneses, C., Jordana, X., Orlandi-Oliveras, G., Köhler, M., 2017. Reconstructing molar growth from enamel histology in extant and extinct *Equus*. Sci. Rep. 7, 15965. https://doi.org/10.1038/s41598-017-16227-2.

Nelson, S.V., 2005. Paleoseasonality inferred from equid teeth and intra-tooth isotopic variability. Palaeogeogr. Palaeoclimatol. Palaeoecol. 222, 122–144. https://doi.org/10.1016/j.palaeo.2005.03.012.

O'Meara, R.N., Dirks, W., Martinelli, A.G., 2018. Enamel formation and growth in non-mammalian cynodonts. R. Soc. Open Sci. 5, 172293. https://doi.org/10.1098/rsos.172293.

Orlandi-Oliveras, G., Nacarino-Meneses, C., Koufos, G.D., Köhler, M., 2018. Bone histology provides insights into the life history mechanisms underlying dwarfing in hipparionins. Sci. Rep. 8, 17203. https://doi.org/10.1038/s41598-018-35347-x.

Ortiz-Jaureguizar, E., Alberdi, M.T., 2003. El patrón de cambios en la masa corporal de los Hipparionini (Perissodactyla, Equidae) de la Península Ibérica durante el Mioceno superior-Plioceno superior. Coloquios Paleontol. 1, 499–509.

Palkovacs, E.P., 2003. Explaining adaptive shifts in body size on islands: a life history approach. Oikos 103, 37–44. https://doi.org/10.1034/j.1600-0706.2003.12502.x.

Penzhorn, B.L., 1982. Home range sizes of Cape mountain zebras *Equus zebra zebra* in the Mountain Zebra National Park. Koedoe 25, 103–108. https://doi.org/10.4102/koedoe.v25i1.607.

Penzhorn, B.L., van der Merwe, 1988. Testis size and onset of spermatogenesis in Cape mountain zebra (*Equus zebra zebra*). J. Reprod. Fertil. 83, 371–375. https://doi.org/10.1530/jrf.0.0830371.

Pesquero, M.D., 2003. *Hipparion* del Turoliense superior de Las Casiones (Fosa de Teruel). Coloquios Paleontol. Volumen Ex 511–548.

Pesquero, M.D., Alberdi, M.T., 2012. New evidence of conspecificity between *Hipparion primigenium melendezi* Alberdi, 1974 from Los Valles de Fuentidueña (Segovia) and *Hipparion concudense concudense* Pirlot, 1956 from Concud (Teruel) Spain. Estud. Geol. 68, 247–260. https://doi.org/10.3989/egeol.40499.152.

Pesquero, M.D., Ascaso, C., Alcalá, L., Fernández-Jalvo, Y., 2010. A new taphonomic bioerosion in a Miocene lakeshore environment. Palaeogeogr. Palaeoclimatol. Palaeoecol. 295, 192–198. https://doi.org/10.1016/j.palaeo.2010.05.037.

Pluháček, J., Bartoš, L., Doležalová, M., Bartošová-Víchová, J., 2007. Sex of the foetus determines the time of weaning of the previous offspring of captive plains zebra (*Equus burchelli*). Appl. Anim. Behav. Sci. 105, 192–204. https://doi.org/10.1016/j.applanim.2006.05.019.

Rey, K., Amiot, R., Lécuyer, C., Koufos, G.D., Martineau, F., Fourel, F., Kostopoulos, D.S., Merceron, G., 2013. Late Miocene climatic and environmental variations in northern Greece inferred from stable isotope compositions (δ18O, δ13C) of equid teeth apatite. Palaeogeogr. Palaeoclimatol. Palaeoecol. 388, 48–57. https://doi.org/10.1016/j.palaeo.2013.07.021.

Schwartz, G.T., Dean, M.C., 2001. Ontogeny of canine dimorphism in extant hominoids. Am. J. Phys. Anthropol. 115, 269–283. https://doi.org/10.1002/ajpa.1081.

Schwartz, G.T., Samonds, K.E., Godfrey, L.R., Jungers, W.L., Simons, E.L., 2002. Dental microstructure and life history in subfossil Malagasy lemurs. Proc. Natl. Acad. Sci. U. S. A. 99, 6124–6129. https://doi.org/10.1073/pnas.092685099.

Semprebon, G.M., Rivals, F., Solounias, N., Hulbert, R.C., 2016. Paleodietary reconstruction of fossil horses from the Eocene through Pleistocene of North America. Palaeogeogr. Palaeoclimatol. Palaeoecol. 442, 110–127. https://doi.org/10.1016/j.palaeo.2015.11.004.

Shellis, R.P., 1984. Variations in growth of the enamel crown in human teeth and a possible relationship between growth and enamel structure. Arch. Oral Biol. 29, 697–705. https://doi.org/10.1016/0003-9969(84)90175-4.

Sibly, R.M., Brown, J.H., 2007. Effects of body size and lifestyle on evolution of mammal life histories. Proc. Natl. Acad. Sci. 104, 17707–17712. https://doi.org/10.1073/pnas.0707725104.

Silver, I.A., 1969. In: Brothweel, D., Higgs, E. (Eds.), The ageing of domestic animals. Science in Archaeology, New York, pp. 250–268.

Smith, B.H., 1991. Dental development and the evolution of life history in Hominidae. Am. J. Phys. Anthropol. 86, 157–174. https://doi.org/10.1002/ajpa.1330860206.

Smith, B.H., 2000. 'Schultz's Rule' and the evolution of tooth emergence and replacement patterns in primates and ungulates. In: Teaford, M.F., Meredith Smith, M., Ferguson, M.W.J. (Eds.), Development, Function and Evolution of Teeth. Cambridge University Press, Cambridge, pp. 212–228. https://doi.org/10.1017/CBO9780511542626.015.

Smith, T.M., 2006. Experimental determination of the periodicity of incremental features in enamel. J. Anat. 208, 99–113. https://doi.org/10.1111/j.1469-7580.2006.00499.x.

Smith, T.M., 2008. Incremental dental development: methods and applications in hominoid evolutionary studies. J. Hum. Evol. 54, 205–224. https://doi.org/10.1016/j.jhevol.2007.09.020.

Smith, T.M., 2016. Dental development in living and fossil orangutans. J. Hum. Evol. 94, 92–105. https://doi.org/10.1016/j.jhevol.2016.02.008.

Smith, T.M., Reid, D.J., Dean, M.C., Olejniczak, A.J., Martin, L.B., 2007. Molar development in common chimpanzees (*Pan troglodytes*). J. Hum. Evol. 52, 201–216. https://doi.org/10.1016/j.jhevol.2006.09.004.

Smith, T.M., Tafforeau, P., Reid, D.J., Pouech, J., Lazzari, V., Zermeno, J.P., Guatelli-Steinberg, D., Olejniczak, A.J., Hoffman, A., Radovcic, J., Makaremi, M., Toussaint, M., Stringer, C., Hublin, J.-J., 2010. Dental evidence for ontogenetic differences between modern humans and Neanderthals. Proc. Natl. Acad. Sci. 107, 20923–20928. https://doi.org/10.1073/pnas.1010906107.

Smuts, G.L., 1974. Age determination in Burchell's zebra (*Equus burchelli antiquorum*) from the Kruger National Park. S. Afr. J. Wildl. Res. 4, 103–115.

Smuts, G.L., 1975. Pre-and postnatal growth phenomena of Burchell's Zebra *Equus burchelli antiquorum*. Koedoe 18, 69–102. https://doi.org/10.4102/koedoe.v18i1.915.

Smuts, G.L., 1976a. Reproduction in the zebra mare *Equus burchelli antiquorum* from the Kruger National Park. Koedoe 19, 89–132. https://doi.org/10.4102/koedoe.v19i1.1186.

Smuts, G.L., 1976b. Reproduction in the zebra stallion *Equus burchelli antiquorum* from the Kruger National Park South Africa. Zool. Afr. 11, 207–220. https://doi.org/10.1080/00445096.1976.11447525.

Sondaar, P.Y., 1961. Les *Hipparion* de l'Aragon meridional. Estud. Geol. 17, 209–305.

Spinage, C.A., 1972. Age estimation of zebra. Afr. J. Ecol. 10, 273–277. https://doi.org/10.1111/j.1365-2028.1972.tb00871.x.

Stearns, S.C., 1992. The Evolution of Life Histories. Oxford University Press, New York.

Stirton, R.A., 1941. Development of characters in horse teeth and the dental nomenclature. J. Mammal. 22, 434–446. https://doi.org/10.2307/1374940.

Symons, A.L., Seymour, G.J., 2000. A histological study of the effect of growth hormone on odontogenesis in the Lewis dwarf rat. Arch. Oral Biol. 45, 123–131. https://doi.org/10.1016/S0003-9969(99)00123-5.

Tafforeau, P., Bentaleb, I., Jaeger, J.-J., Martin, C., 2007. Nature of laminations and mineralization in rhinoceros enamel using histology and X-ray synchrotron microtomography: potential implications for palaeoenvironmental isotopic studies. Palaeogeogr. Palaeoclimatol. Palaeoecol. 246, 206–227. https://doi.org/10.1016/j.palaeo.2006.10.001.

Tütken, T., Kaiser, T.M., Vennemann, T., Merceron, G., 2013. Opportunistic feeding strategy for the earliest old world hypsodont equids: evidence from stable isotope and dental wear proxies. PLoS One 8, e74463. https://doi.org/10.1371/journal.pone.0074463.

van Dam, J., Reichart, G.J., 2009. Oxygen and carbon isotope signatures in late Neogene horse teeth from Spain and application as temperature and seasonality proxies. Palaeogeogr. Palaeoclimatol. Palaeoecol. 274, 64–81. https://doi.org/10.1016/j.palaeo.2008.12.022.

van Dam, J., Alcalá, L., Zarza, A.A., Calvo, J.P., Garcés, M., Krijgsman, W., 2001. The upper Miocene mammal record from the Teruel-Alfambra region (Spain). The MN system and continental stage/age concepts discussed. J. Vertebr. Paleontol. 21, 367–385. https://doi.org/10.1671/0272-410.1671/0272-4634(2001)021[0367:TUMMRF]2.0.CO;2.

Van Valen, L., 1964. Age in two fossil horse populations. Acta Zool. 45, 93–106. https://doi.org/10.1111/j.1463-6395.1964.tb00712.x.

Veiberg, V., Mysterud, A., Gaillard, J.M., Delorme, D., Van Laere, G., Klein, F., 2007. Bigger teeth for longer life? Longevity and molar height in two roe deer populations. Biol. Lett. 3, 268–270. https://doi.org/10.1098/rsbl.2006.0610.

Veitschegger, K., Sánchez-Villagra, M.R., 2016. Tooth eruption sequences in cervids and the effect of morphology, life history, and phylogeny. J. Mamm. Evol. 23, 251–263. https://doi.org/10.1007/s10914-015-9315-8.

Waran, N.K., Clarke, N., Farnworth, M., 2008. The effects of weaning on the domestic horse (*Equus caballus*). Appl. Anim. Behav. Sci. 110, 42–57. https://doi.org/10.1016/j.applanim.2007.03.024.

Westlin-van Aarde, L.M., van Aarde, R.J., Skinner, J.D., 1988. Reproduction in female Hartmann's zebra, *Equus zebra hartmannae*. J. Reprod. Fertil. 84, 505–511. https://doi.org/10.1530/jrf.0.0840505.

Winkler, D.E., Kaiser, T.M., 2015. Uneven distribution of enamel in the tooth crown of a Plains Zebra (*Equus quagga*). PeerJ 3, e1002,. https://doi.org/10.7717/peerj.1002.

Witzel, C., Kierdorf, U., Frölich, K., Kierdorf, H., 2018. The pay-off of hypsodonty - timing and dynamics of crown growth and wear in molars of Soay sheep. BMC Evol. Biol. 18, 207. https://doi.org/10.1186/s12862-018-1332-9.

Woodburne, M.O., 1989. *Hipparion* horses: a pattern of endemic evolution and intercontinental dispersal. In: Prothero, D.R., Schoch, R.M. (Eds.), The Evolution of Perissodactyls. Oxford University Press, New York, pp. 197–233.

Woodburne, M.O., MacFadden, B.J., 1982. A reappraisal of the systematics, biogeography, and evolution of fossil horses. Paleobiology 8, 315–327. https://doi.org/10.1017/S0094837300007077.

Young, W.G., 1995. Growth hormone and insulin-like growth factor-I in odontogenesis. Int. J. Dev. Biol. 39, 263–272. https://doi.org/10.1387/IJDB.7626416.

Zhang, C.Z., Young, W.G., Li, H., Rolinson, S., Waters, M.J., 1992. Growth hormone regulates nucleolar organizer regions during odontogenesis in the rat. J. Oral Pathol. Med. 21, 395–400. https://doi.org/10.1111/j.1600-0714.1992.tb01026.x.

Supplementary Material for:

Dental histology of late Miocene hipparionins compared with extant *Equus*, and its implications for Equidae life history

Guillem Orlandi-Oliveras [a*], Carmen Nacarino-Meneses[a,b], Meike Köhler[a,c].

[a] *Institut Català de Paleontologia Miquel Crusafont (ICP), Carrer de les Columnes s/n, Campus de la Universitat Autònoma de Barcelona, 08193 Bellaterra, Barcelona, Spain*

[b] *University of Cape Town, Department of Biological Sciences, Private Bag X3, Rhodes Gift, 7700 South Africa*

[c] *Institut Català de Recerca i Estudis Avançats (ICREA), Pg. Lluís Companys 23, 08010, Barcelona, Spain*

*Corresponding author e-mail: guillem.orlandi@icp.cat

1. Comparison between *Equus quagga* and *Hipparion concudense* molars

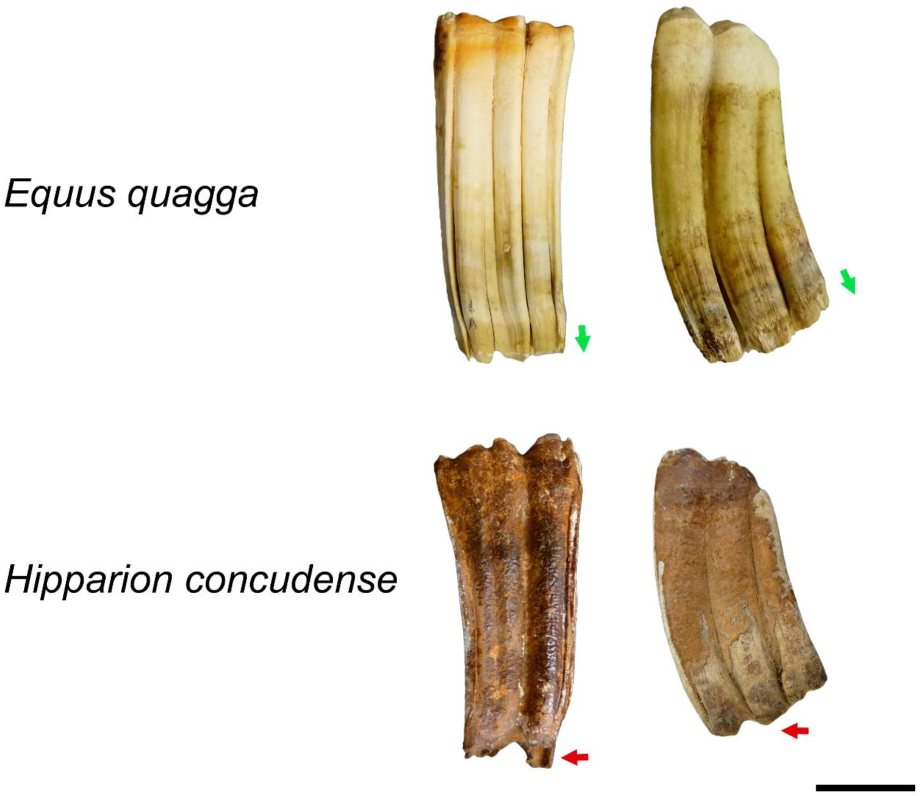

Figure S1. Molars of *Equus quagga* clearly showing occlusal wear and open roots. Enamel is still being deposited in these teeth (green arrows). Unworn or little worn molars of *Hipparion concudense* with identifiable closed roots (red arrows). First/second molars shown in lingual view (*Equus quagga* IPS-92341 and *Hipparion concudense* IPS-91762). Third molars shown in buccal view (*E. quagga* MZB-94-1229 and *H. concudense* IPS-87855). Scale 2 cm.

2. Scatterplots of molar measurements

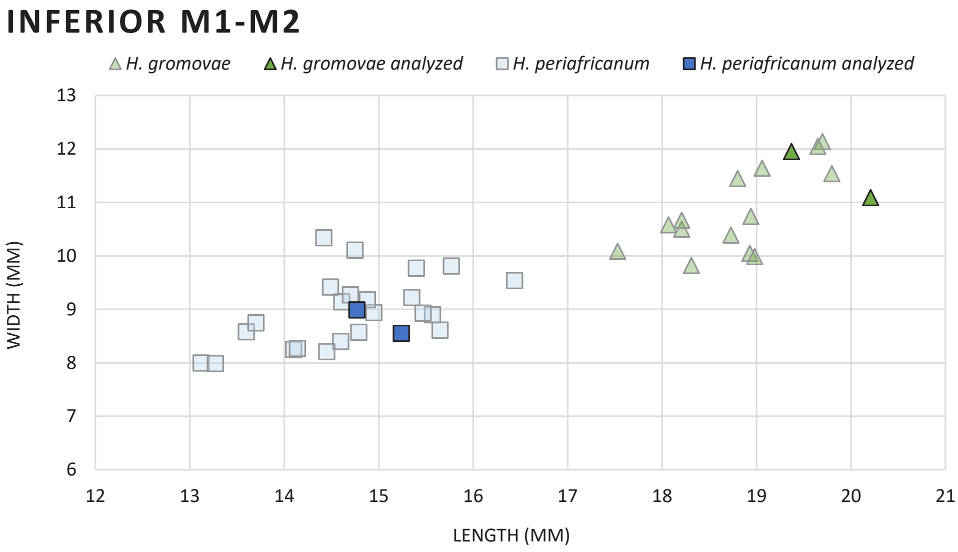

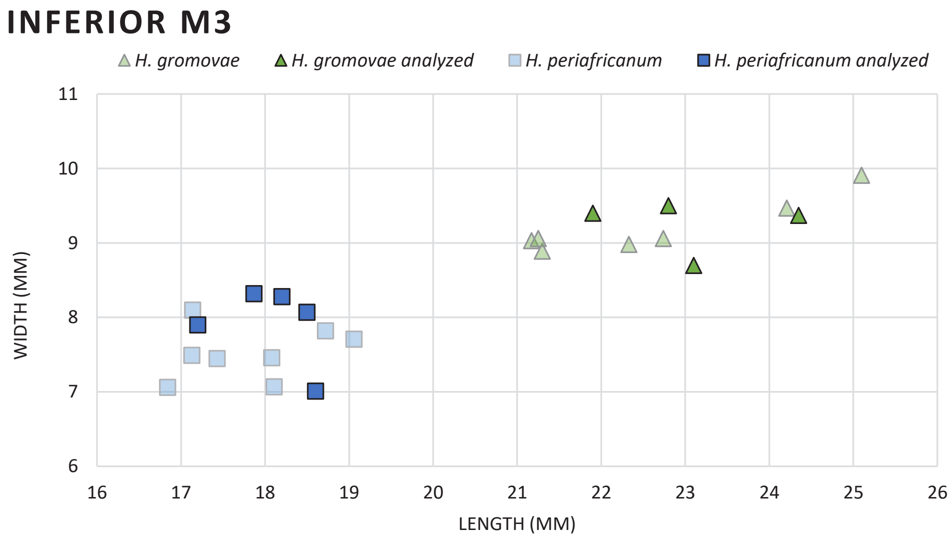

Figure S2 and Figure S3. Scatterplots of the width and length measurements at 1 cm above the crown base in hipparionin molars from El Arquillo fossil site. The specimens selected for histological study are represented in darker color.

3. Tests for ANCOVA assumptions:

3.1 With *Equus quagga* data:

3.1.1 All first/second molars

- **Table S1.** Test for equality of variances (Levene's Test) in all first/second molars.

F	df1	df2	Sig.
5.965	3	93	**0.001**

- **Table S2.** ANOVA table for the EER of all first/second molars. Checking for the significance of the interaction between the predictive variable (Species) and the continuous covariate (Crown Height) of the ANCOVA model.

  Model: EER ~ Intercept + Species + Crown Height + (Species : Crown Height)

	SS	df	Mean squares	F	p-value
Intercept	27051.17	1	27051.17	41.38	0.000
Species	19190.67	3	6396.89	9.79	0.000
CrownHeight	44868.68	1	44868.68	68.63	0.000
Species:CrownHeight	3957.502	3	1319.17	2.02	0.117
Error	58182.76	89	653.74		
Total	1198735.19	97			

There is no significant interaction between the predictive variable and the covariate (p = 0.117). However, Levene's test rejects the hypothesis of equality of variances between groups (p = 0.001). The slopes of the regressions between the enamel extension rate and the crown height of the four groups are similar (Fig. 3, main text).

3.1.2 All third molars

- **Table S3.** Test for equality of variances (Levene's Test) in all third molars.

F	df1	df2	Sig.
0.605	3	156	0.615

- **Table S4.** ANOVA table for the EER of all third molars. Checking for the significance of the interaction between the predictive variable (Species) and the continuous covariate (Crown Height) of the ANCOVA model.

  Model: EER ~ Intercept + Species + Crown Height + (Species : Crown Height)

	SS	df	Mean squares	F	p-value
Intercept	673670.37	1	673670.37	1925.10	0.000
Species	26905.87	3	8968.62	25.63	0.000
CrownHeight	183825.53	1	1 83825.53	525.30	0.000
Species:CrownHeight	5364.69	3	1788.23	5.11	**0.002**
Error	53191.06	152	349.94		
Total	1320630.94	160			

There is a significant interaction between the predictive variable and the covariate (p = 0.02). However, Levene's test fails to reject the hypothesis of equality of variances between groups (p = 0.615). The slopes of the regressions between the enamel extension rate and the crown height of the four groups are similar (Fig. 3, main text).

3.2 Without *Equus quagga* data:

3.2.1 Hipparionin first/second molars

- **Table S5.** Test for equality of variances (Levene's Test) in hipparionin first/second molars.

F	df1	df2	Sig.
0.527	2	74	0.593

- **Table S6.** ANOVA table for the EER of hipparionin first/second molars. Checking for the significance of the interaction between the predictive variable (Species) and the continuous covariate (Crown Height) of the ANCOVA model.

  Model: EER ~ Intercept + Species + Crown Height + (Species : Crown Height)

	SS	df	Mean squares	F	p-value
Intercept	686008.31	1	686008.31	867.67	0.000
Species	15909.98	2	7954.99	10.06	0.000
CrownHeight	208030.85	1	208030.85	263.12	0.000
Species:CrownHeight	2901.08	2	1450.54	1.83	0.167
Error	56134.75	71	790.63		
Total	1165851.56	77			

There is no significant interaction between the predictive variable and the covariate (p = 0.167). Moreover, Levene's test fails to reject the hypothesis of equality of variances between groups (p = 0.593). The regression slopes between the three groups are similar (Fig. 3, main text).

3.2.2 Hipparionin third molars

- **Table S7.** Test for equality of variances (Levene's Test) in hipparionin third molars.

F	df1	df2	Sig.
1.390	2	92	0.254

- **Table S8.** ANOVA table for the EER of hipparionin third molars. Checking for the significance of the interaction between the predictive variable (Species) and the continuous covariate (Crown Height) of the ANCOVA model.

  Model: EER ~ Intercept + Species + Crown Height + (Species : Crown Height)

	SS	df	Mean squares	F	p-value
Intercept	373972.67	1	373972.67	1351.98	0.000
Species	9655.94	2	4827.97	17.45	0.000
CrownHeight	117170.31	1	117170.31	423.59	0.000
Species:CrownHeight	886.04	2	443.02	1.60	0.207
Error	24618.44	89	276.61		
Total	757613.04	95			

There is no significant interaction between the predictive variable and the covariate (p = 0.207). Moreover, Levene's test fails to reject the hypothesis of equality of variances between groups (p = 0.254). The regression slopes between the three groups are similar (Fig. 3, main text).

4. Enamel extension rates at the different tooth thirds

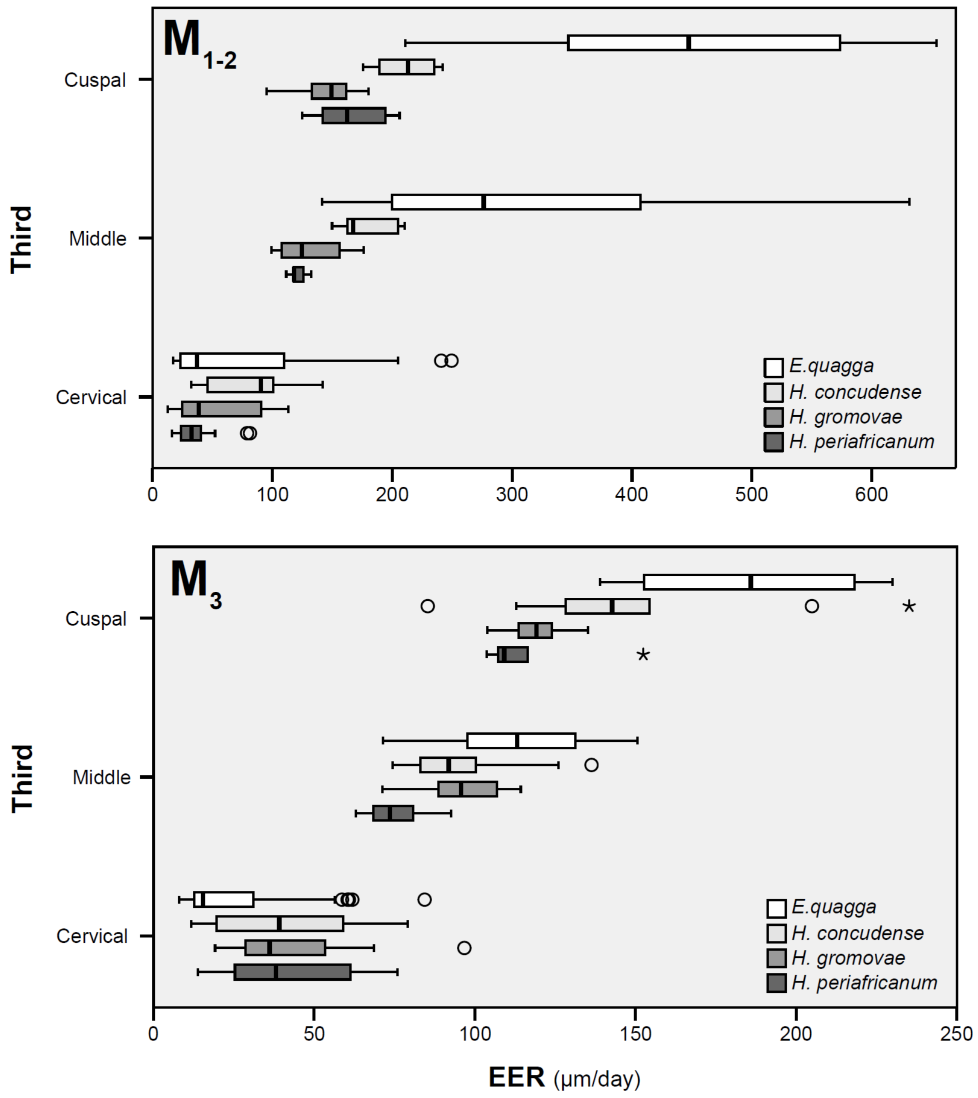

Figure S4. Enamel extension rate (EER) box-plots for each species considering three different thirds of the enamel band. Note the different scales of the x-axis for the first/second molar compared to that of the third molar.

5. Tooth type growth curves

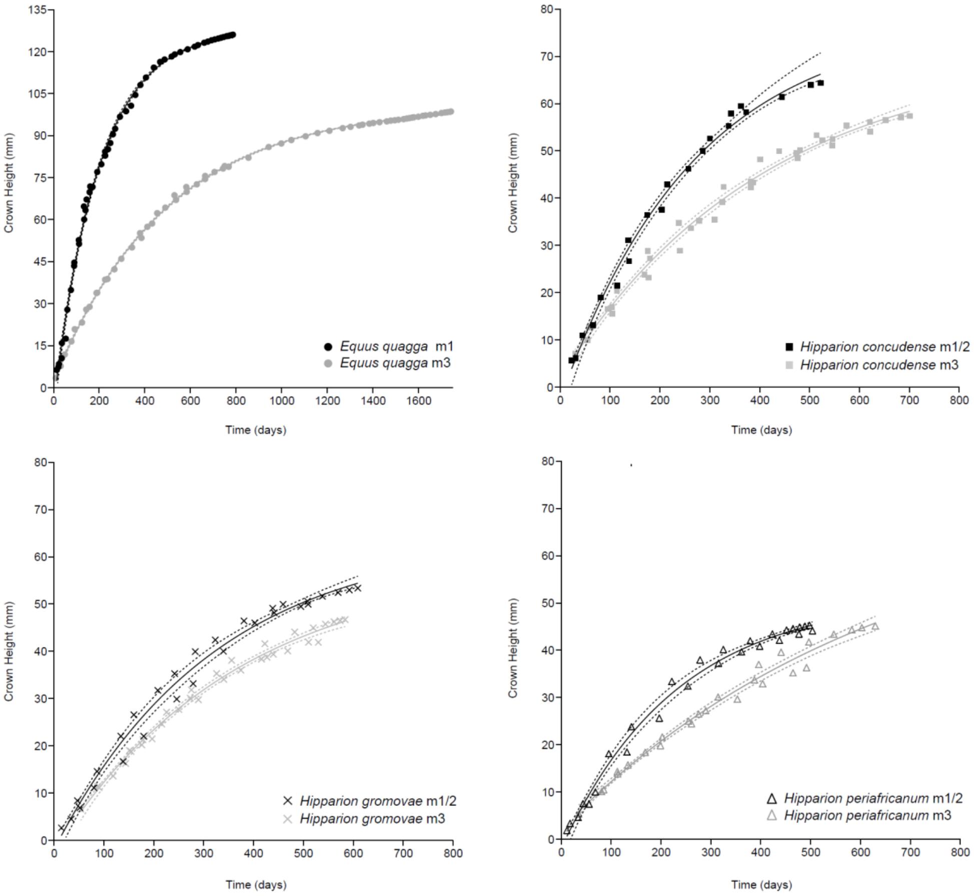

Figure S5. Molar growth curves fitted to von Bertalanffy growth models. The reconstructed growth curve of the first/second molar (black) and the third molar (grey) of each species is represented in each plot. Higher growth rates can be inferred in the first/second molars compared to the third molars. 95 % confidence intervals represented as dashed lines.

6. Enamel thickness

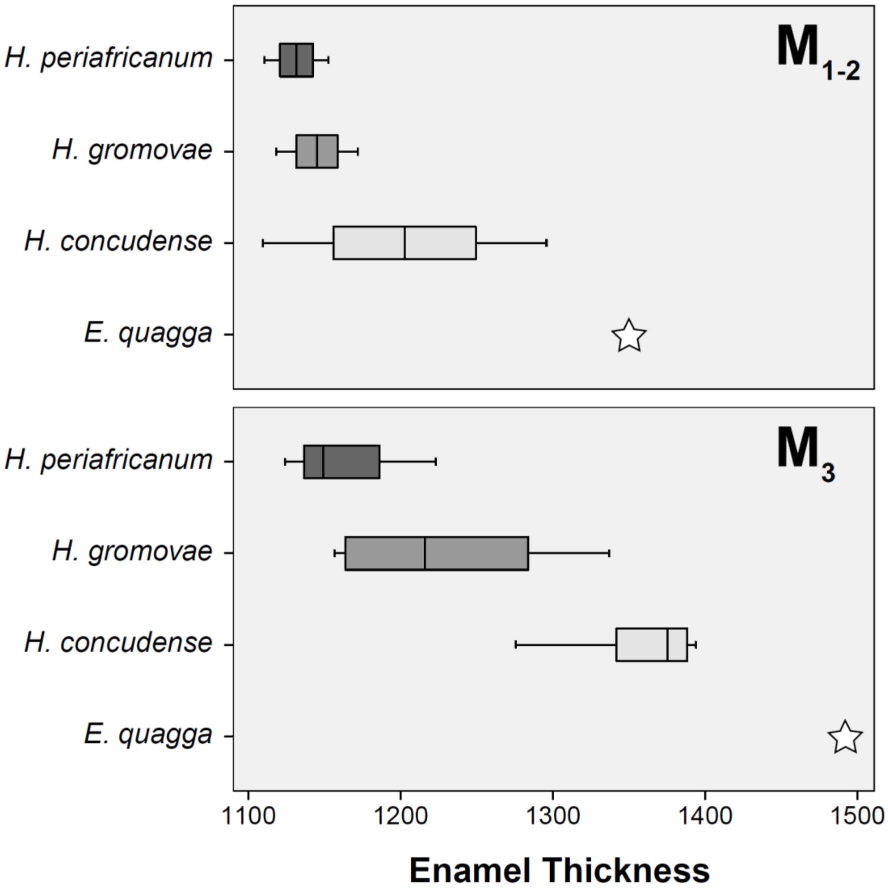

Figure S6. Box-plots showing the enamel thickness measures of all molars analyzed. Because the measures were performed 1 cm above the root, we only included from the *Equus quagga* sample those moderately worn molars with identifiable morphological roots.

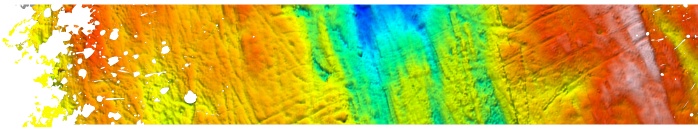

Chapter 6

Feeding Strategies of Circum-Mediterranean Hipparionins during the Late Miocene: Exploring Dietary Preferences Related to Size through Dental Microwear Analysis

Article sent to ***Palaeontologia Electronica*** and currently under review (MS 990).
Some comments and changes proposed on the first-round review have already been incorporated to this version.

Chapter 6

Feeding Strategies of Circum-Mediterranean Hipparionins during the Late Miocene: Exploring Dietary Preferences Related to Size through Dental Microwear Analysis

Guillem Orlandi-Oliveras[1], Meike Köhler[1,2], Julien Clavel[3], Robert S. Scott[4],
Serdar Mayda[5], Tanju Kaya[6], Gildas Merceron[7]

[1] Institut Català de Paleontologia Miquel Crusafont (ICP), Edifici Z, carrer de les Columnes s/n., Campus de la Universitat Autònoma de Barcelona, 08193 Bellaterra (Barcelona), Spain. e-mail: guillem.orlandi@icp.cat

[2] Institut Català de Recerca i Estudis Avançats (ICREA), passeig Lluís Companys 23, 08010 Barcelona, Spain. e-mail: meike.kohler@icp.cat

[3] Life Sciences Department, Natural History Museum, Cromwell Road, SW7 5BD London, United Kingdom. e-mail: j.clavel@nhm.ac.uk

[4] Department of Anthropology and Center for Human Evolutionary Studies, Rutgers,
The State University of New Jersey, New Jersey 08901 New Brunswick, USA. e-mail: robertsc@scarletmail.rutgers.edu

[5] Department of Biology, Faculty of Science, Ege University, Bornova 35100, Izmir, Turkey. e-mail: serdar.mayda@ege.edu.tr

[6] Natural History Museum, Ege University, Bornova 35100, Izmir, Turkey. e-mail: tanju.kaya@ege.edu.tr

[7] Laboratoire Paléontologie Évolution Paléoécosystèmes Paléoprimatologie, UMR 7262, Bâtiment B35 TSA 51106, 86073 Poitiers Cedex9, France. e-mail: gildas.merceron@univ-poitiers.fr

Abstract

The adaptive radiation of hipparionins after their Old World dispersal was linked with a trend towards smaller body sizes. The appearance of these small-sized forms has usually been associated to more open environments and grazing diets. A recent approach, moreover, highlights the role of life history modifications related to habitat conditions as triggers of their size shifts. Here, we test the relationship between hipparionin size and diet, further exploring feeding and habitat preferences in relation to size through time and space. We analyzed dental microwear textures of different-sized hipparionins from Vallesian and Turolian circum-Mediterranean localities. Our results show that hipparionins were mainly mixed-feeders, and that there was no general link between body size and diet. However, in the western Mediterranean, we identified broader feeding spectra in smaller forms and more specialized grazing diets in larger ones. In contrast, the eastern Mediterranean hipparionins do not show this differentiation. Contra with the notion of more open habitats eastwards, we detected a larger browsing component in eastern hipparionin diets. The consumption by extant equids of more woody browse during the dry season, leads us to propose a greater seasonality as a possible cause. Another interpretation might involve the presence of more millimetric grit in the eastern opener habitats. We also found that sympatric hipparionins have similar feeding habits, and their diets appear to be influenced by the local environment. Finally, we suggest that the hipparionin small size resulted from different adaptations to local environments rather than to a generalized and common pattern of size modification due to a shared ecological shift.

Keywords: hipparion; Equidae; diet; body size; late Miocene; dental microwear texture analysis

6.1. Introduction

The living Equidae are today represented by only few species from one genus that chiefly graze and inhabit open habitats (Bauer et al., 1994; Moehlman, 2002). However, in the past the Equidae exhibited much greater taxonomic richness (MacFadden, 1992, 2005; Woodburne and MacFadden, 1982) and a broader spectrum of dietary adaptations (MacFadden et al., 1999; Semprebon et al., 2016; Tütken et al., 2013) more comparable to modern African bovids (Gagnon and Chew, 2000). Similarly, extinct equids occupied more habitat types than their extant relatives (MacFadden, 1992; Semprebon et al., 2016) and showed a broader range of body sizes (Alberdi et al., 1995; Gould and MacFadden, 2004; MacFadden, 1992).

Hipparionins are an equid tribe that was especially diverse during the late Miocene, when it dominated many of the mammal assemblages from the Holarctic realm (Bernor et al., 1996; Woodburne, 1989). These three-toed horses radiated soon after their first dispersal from North America to the Old World (Bernor et al., 1996, 2003; Cantalapiedra et al., 2017; Scott et al., 2003; Woodburne, 1989). Consequently, sympatric and morphologically diverse species are found in western and eastern Mediterranean regions already during the beginning of the Vallesian (Forsten, 1997; Koufos, 2016; Scott et al., 2003) [European Land Mammal Age, 11.2–8.9 Ma (Hilgen et al., 2012)]. Although the hipparionins from circum-Mediterranean regions underwent an important taxonomic and morphological diversification (Bernor et al., 1990b, 1996; Forsten, 1968), in central Europe the specific diversity was much lower (Bernor et al., 1990a; Forsten, 1978a). It is during the Turolian [European Land Mammal Age, 8.9–5.3 Ma (Hilgen et al., 2012)], however, that the Old World hipparionin horses reached their highest taxonomic and ecological diversity (Bernor et al., 1990a, 1996). This diversification is marked by an increase in the range of body sizes, especially towards smaller sizes (Bernor et al., 1996; Ortiz-Jaureguizar and Alberdi, 2003). The "*Cremohipparion* clade" (sensu Bernor et al., 1996), for instance, diversified along two opposite trajectories; leading to the appearance of a lineage characterized by large-sized horses (e.g., *Cremohipparion proboscideum*) and to the appearance of other forms that decreased in body size (e.g., *Cremohipparion matthewi*) (Bernor et al., 1996, 2016). Those hipparionins that decreased in body size may have evolved the small size independently (Bernor and Tobien, 1989; Woodburne and MacFadden, 1982). Hence, contrary to the commonly described phyletic size increase in Equidae, size decrease processes took place numerous times during their evolutionary history (Gould and MacFadden, 2004; MacFadden, 1992).

The shift towards smaller size in some hipparionins, together with their diversification, has been associated with increasing climate seasonality and its repercussions on floral communities (Bernor et al., 1990a, 1996; Saarinen, 2009). Accordingly, some authors have suggested that the small-sized hipparionins dwelt in more open habitats (Bernor et al., 1996; Saarinen, 2009) and were adapted to graze on less nutritious xerophytic forage (Forsten, 1968, 1978b). On the other hand, other authors have argued that these forms were adapted to more closed and forested areas (Ortiz-Jaureguizar and Alberdi, 2003) like extant "smaller zebras" (Alberdi et al., 1995). Recently, these size diminution trends have been associated with shifts in adult mortality regimes in some cases, and resource availability in others (Orlandi-Oliveras et al., 2018). These are two scenarios that can also be indirectly linked to changes in habitat structure.

Animal body size is related to many physiological and ecological factors (Calder, 1984; Palkovacs, 2003; Peters, 1983). One of the central variables determining body size is growth rate, which in turn is strongly affected by the environmental effects on food availability and foraging risk (Dmitriew, 2011). Hence, the items consumed by an animal do not only depend on the availability and quality of the available resources, but also on the competitive pressure and predation risk associated with the exploitation of these resources (Brown, 1988). In turn, these factors all depend on habitat type and structure. A general relationship can thus be described for body mass, diet, and habitat in extant African ungulates: large-sized species tend to inhabit open areas and graze on abundant low quality food, while smaller taxa generally browse on less abundant high quality items in closed habitats (Bell, 1971; Case, 1979; Gagnon and Chew, 2000; Hopcraft et al., 2010; Jarman, 1974). Case (1979) enumerates these examples, among many others, to illustrate this tendency: the Cape buffalo (*Syncerus caffer caffer*) grazes and inhabits savanna landscapes, while the smaller forest buffalo (*Syncerus caffer nanus*) dwells in more closed habitats; the pygmy hippopotamus (*Hexaprotodon liberiensis*) of 235 kg (Jones et al 2009) forages in aquatic masses of forested areas, while the much larger *Hippopotamus amphibius* of 1536 kg (Jones et al 2009) grazes near open savanna lakes.

It was long assumed that hipparionins were mostly open savanna grazers due to their high-crowned teeth (MacFadden and Hulbert, 1988; Matthew, 1926; Stebbins, 1981; Stirton, 1947). Because of that, their arrival to the Old World was tentatively linked to the spread of grasslands (Gabunia and Chochieva, 1982; MacFadden, 1992), a thesis no longer supported by more recent studies on hipparionin diets (Hayek et al., 1992; Kaiser, 2003; Tütken et al., 2013) and by evidence of grassland presence predating their appearance (Strömberg, 2006; Strömberg et al., 2007). In stark contrast, reconstructions of hipparionin paleobiology indicate more diverse dietary niches than grazing (Hayek et al., 1992; MacFadden et al., 1999; Merceron et al., 2016a, 2007; Tütken et al., 2013). For instance, an opportunistic mixed-feeder strategy in a wide range of habitats has been suggested (Kaiser, 2003; Tütken et al., 2013). While some studies have not identified significant feeding differences between sympatric hipparionin species (Clavel et al., 2012; Rey et al., 2013; Solounias et al., 2010), others detected dietary niche-partitioning between taxa (MacFadden et al., 1999; Merceron et al., 2016a). Similarly, life history strategies have also been found to differ between hipparionins of different sizes (Orlandi-Oliveras et al., 2018, 2019). Although hipparionin dietary preferences have been extensively studied from a paleoenvironmental point of view, the relationship between their size and diet has not yet been explored. Due to 1) the long-time interval of hipparionin presence in the Old World, 2) their wide geographical distribution, and 3) their broad range of body sizes, hipparionins constitute a good model for exploring size related niche partitioning with respect to habitat and feeding preferences across closely-related ungulates.

Microwear analysis has proven to be a powerful tool for tracking differences in diet in both extant and extinct species (Calandra and Merceron, 2016; DeSantis, 2016; Martin et al., 2018; Scott et al., 2005; Walker et al., 1978). During mastication, processed matter produces a characteristic microwear signature on wear facets likely related to the foods' physical and mechanical properties and the presence of phytoliths or grit in the food items (Lucas et al., 2014; Madden, 2014; Merceron et al., 2016b; Rabenold and Pearson, 2011; Ramdarshan et al., 2016, 2017; Schulz et al., 2013; Winkler et al., 2019; Xia et al., 2015). It is therefore possible to infer, through the study of the dental microwear texture, properties and types of foods consumed by an animal during the last days or weeks (Teaford and Oyen, 1989; Teaford et al., 2017). Comparative studies across a range of taxonomic groups consistently find empirical relationships between diet and dental microwear textures [e.g., Scott, R.S. et al. (2012) in primates, Schubert et al. (2010) in carnivorans, Scott, J.R (2012) in bovids, etc.]. Using dental microwear texture analysis, researchers have tracked animal's dietary strategies, revealed their feeding plasticity, identified cases of niche partitioning (Merceron et al., 2010a; Rivals et al., 2007; Ungar et al., 2007), and made inferences on the habitat in which they might have dwelt (Merceron et al., 2005a, 2016a). The scans obtained from Dental Microwear Texture Analysis (DMTA) can be quantified repeatably, limiting the risks for intra and inter-observer errors (DeSantis et al., 2013; Scott et al., 2005, 2006; Ungar et al., 2003). Using this method, we obtain some distinct variables that typify the dental microwear texture: the measure of change in roughness with scale (complexity), the measure of orientation concentration of surface roughness (anisotropy), and the variation of complexity within the surface (heterogeneity of complexity) (Scott et al., 2005, 2006). The consumption of tough food—such as mature grasses—tend to produce high anisotropic textures, whereas the processing of harder and more brittle items—such as woody browse—results in textures of lower anisotropy indices and high complexities. Generalists and mixed-feeders consume diverse types of resources with varying mechanical properties, which it appears to increase the heterogeneity of the texture complexity.

In previous studies, the hipparionin size differences have been explored from a life history approach by means of bone and dental histology analysis (Orlandi-Oliveras et al., 2018, 2019). In this work, we aim to evaluate the scaling relationship between ecological preferences (diet) and hipparionin body size, and how it has changed through time and space during the late Miocene.

The present study, hence, might help to test the interpretations on hipparionin paleobiology obtained from previous life history inferences. For this purpose, we use DMTA in different-sized hipparionins from Vallesian and Turolian sites located on eastern and western Mediterranean basins, with special interest on sympatric taxa. Our results will help to understand the dietary preferences of the hipparionins of diverse size classes, and to explore the changes they undergone from Vallesian to Turolian in different areas of their distribution range.

6.2. Material and methods

6.2.1. Sample and Study Area

The fossil specimens come from 20 late Miocene fossil sites of circum-Mediterranean basins (Figure 6.1). We have focused on localities that yielded large hipparionin assemblages and with those exhibiting a high hipparionin size diversity. We predominantly sampled the more diverse Turolian fossil sites. Far from being homogeneous, eastern Mediterranean faunas show some dissimilarities during most part of the Turolian (Kostopoulos, 2009; Koufos and Vlachou, 2016). We divided, hence, the eastern Mediterranean Turolian sample in the western Anatolian (Samos island and continental western Anatolia) and the Balkans bioprovinces (continental Greece and Bulgaria). Vallesian hipparionins come from western Mediterranean and from the Balkans, while Turolian forms come from the three bioprovinces studied (see Appendix 1 for detailed information).

Figure 6.1.
Geographic distribution of the localities from western Mediterranean (circles), Balkans (stars), and western Anatolian (squares) basins. Dashed contours depicting the areas with Vallesian localities sampled. 1. Vallès-Penedès Basin (Santiga, Can Llobateres, Can Poncic); 2. Teruel Basin (Concud, El Arquillo); 3. Cabriel Basin (Venta del Moro); 4. Axios Valley (Pentalophos, Ravin de la Pluie, Ravin des Zouaves-5 and Dytiko sites); 5. Thessaly (Perivolaki); 6. Mesta Valley (Hadjidimovo); 7. Chalkidiki Peninsula (Nikiti-1 and Nikiti-2); 8. Biga Peninsula (Gülpınar); 9. Muğla Yatağan Basin (Şerefköy-2); 10. Samos Island (Mytilinii-A, Mytilinii-B).

Here we decided to use the broad sense of the genus *Hipparion* because of the lack of cranial material available for some of the analyzed taxa, which hinders their unequivocal determination within the proposed supraspecific groupings (Bernor et al., 1996). We organized the eastern Mediterranean hipparionin taxa following the morphotypes defined by Vlachou (2013). We grouped the western Mediterrenan hipparionins considering size morphotypes, which follow specific differences, due to the general lack of complete cranial material.

6.2.2. Microwear Data Acquisition

The sample studied comprises 372 teeth from a wide range of hipparionin populations (Table 6.1; Appendix 2). We discarded unworn and completely worn teeth together with those showing marked taphonomical alterations. We preferably selected second upper or lower molars, although in some cases we also analyzed first/third molars and third/fourth premolars as variations in DMT along the tooth row are not significant (Ramdarshan et al., 2017). Following standard procedures, the occlusal surfaces of the teeth were cleaned using acetone-soaked cotton swabs to remove dust particles and glue. Afterwards, dental replicas were made using a polyvinyl siloxane silicone of medium consistency (ISO 4823, President Regular Body, Coltène-Whaledent). These molds were scanned with the "TRIDENT" Leica DCM8 white-light confocal profilometer (PALEVOPRIM lab CNRS University of Poitiers, France) with a 100× lens (numerical aperture = 0.90; working distance = 0.9 mm). We scanned preferentially the lingual facets of paracone and buccal facets of protoconid, but metacone and hypoconid were selected when the former showed alterations. The lateral resolution (x,y) of the scans was set to 0.129 µm and the vertical spacing to less than 0.002 µm. Once scanned, the surfaces were saved as .plµ files by LeicaScan software (Leica Microsystems) and imported for processing to LeicaMap following procedures shown in Merceron et al. (2016a). A 200 × 200 µm area was extracted and saved as a .sur file. All the specimens were scanned and processed at PALEVOPRIM (CNRS and University of Poitiers, France). Photo-simulations of the surfaces analyzed are available at the Appendix 3.

6.2.3. Dental Microwear Texture Variables and Statistical Analyses

The surfaces were processed using Toothfrax and Sfrax software (Surfract, http://www.surfract.com) applying Scale Sensitive Fractal Analysis (SSFA) and following the standard procedures detailed in Scott et al. (2006). SSFA generates a set of Dental Microwear Texture (DMT) parameters that quantify the enamel surface. These are described in Scott et al. (2006, 2005). In the present study, we focused on the ones that better reflect surface textural attributes correlated to diet: complexity (area scale fractal complexity, *Asfc*), anisotropy (exact proportion of length scale anisotropy of relief, *epLsar*), heterogeneity (heterogeneity of area scale

Table 6.1.
Descriptive statistics of each DMT parameter for all the hipparionin populations included in the present study. Mean body mass (BM) and the mean values of the textural parameters are also shown for each hipparionin group. *Asfc* = complexity, *epLsar* = anisotropy, *HAsfc* = heterogeneity of complexity calculated with a 64 cells mesh, *Tfv* = textural fill volume, N = sample size, sem = standard error of the mean.

Age	Bioprovince	hipparionin group	Size class	Locality	mean BM (kg)	N	mean *Asfc*	sem *Asfc*	mean *epLsar*	sem *epLsar*	mean *Hasfc*	sem *Hasfc*	mean *Tfv* (μm²)	sem *Tfv* (μm²)
Vallesian	Western Mediterranean	?*primigenium* small	Small	Santiga	154^{d}	13	2.00	0.34	3.28	0.51	0.605	0.052	48995	2309
		primigenium	Large	Can Llobateres	194^{d}	47	2.22	0.12	3.43	0.31	0.432	0.017	42658	1430
				Can Poncic	205^{d}	11	1.50	0.22	3.69	0.54	0.485	0.028	43019	1683
				All	**200**	**58**	**2.09**	**0.11**	**3.48**	**0.27**	**0.442**	**0.015**	**42726**	**1196**
	Balkans	*macedonicum*	Small	Axios Vallesian sites^{a}	103^{e}	4	2.96	0.56	3.30	0.49	0.426	0.082	46358	5055
				Nikiti-1	81^{e}	2	1.86	0.16	3.13	0.49	0.388	0.061	51683	444
				All	**92**	**6**	**2.59**	**0.43**	**3.25**	**0.34**	**0.414**	**0.055**	**48133**	**3390**
		primigenium	Large	Axios Vallesian sites^{a}	167^{e}	12	2.78	0.46	3.88	0.60	0.388	0.022	43898	2136
				Nikiti-1	214^{e}	2	2.12	0.43	2.64	1.51	0.510	0.008	42243	8015
				All	**191**	**14**	**2.68**	**0.40**	**3.70**	**0.55**	**0.405**	**0.022**	**43662**	**2010**
Turolian	Western Mediterranean	*periafricanum*	Small	El Arquillo	31^{d}	17	2.30	0.45	2.89	0.31	0.579	0.080	43353	1868
		gromovae	Small	El Arquillo	84^{f}	34	1.80	0.16	3.56	0.28	0.488	0.029	42824	1545
		cf. *matthewi*	Large	Venta del Moro	124^{g}	20	1.17	0.13	4.81	0.42	0.434	0.024	46778	2079
		concudense	Large	Concud	178^{g}	24	1.16	0.09	5.39	0.38	0.431	0.026	43961	2193
		primigenium	Large	El Arquillo	192^{f}	5	1.78	0.54	4.35	1.05	0.361	0.037	43050	4220
	Balkans	*macedonicum*	Small	Nikiti-2	76^{e}	17	1.95	0.15	5.35	0.44	0.412	0.020	42982	1855
				Ravin des Zouaves-5	71^{e}	11	2.75	0.20	4.10	0.68	0.475	0.047	41073	2247
				Perivolaki	73^{e}	11	2.72	0.45	2.69	0.44	0.467	0.063	43848	2025
				Dytiko sites^{b}	62^{e}	6	2.38	0.46	2.65	0.67	0.480	0.049	50561	2518
				All	**71**	**45**	**2.39**	**0.15**	**4.03**	**0.32**	**0.450**	**0.021**	**43738**	**1124**
		dietrichi	Large	Nikiti-2	113^{e}	4	1.74	0.22	5.40	1.03	0.454	0.048	40964	3888
				Perivolaki	127^{e}	6	3.37	0.77	2.53	0.41	0.472	0.042	44124	2455
				Dytiko sites^{b}	144^{e}	21	1.99	0.18	3.91	0.42	0.503	0.037	41592	2649
				All	**128**	**31**	**2.22**	**0.21**	**3.84**	**0.35**	**0.491**	**0.027**	**42001**	**1896**

(Table continues next page)

Table 6.1.
Continuation.

Age	Bioprovince	hipparionin group	Size class	Locality	mean BM (kg)	N	mean *Asfc*	sem *Asfc*	mean *epLsar*	sem *epLsar*	mean *Hasfc*	sem *Hasfc*	mean *Tfv* (μm²)	sem *Tfv* (μm²)
Turolian	Balkans	*proboscideum*	Large	Ravin des Zouaves-5	202^{e}	1	2.00	-	5.44	-	0.356	-	27397	-
				Hadjidimovo	183^{d}	18	2.29	0.19	4.21	0.48	0.585	0.038	38219	2153
				Perivolaki	165^{e}	1	2.11	-	3.27	-	0.454	-	55049	-
				All	**183**	**20**	**2.27**	**0.17**	**4.23**	**0.43**	**0.567**	**0.036**	**38519**	**2187**
		primigenium	Large	Hadjidimovo	256^{d}	17	2.08	0.18	4.28	0.51	0.620	0.056	42308	1859
	Western Anatolia	*macedonicum*	Small	Gülpınar	81^{d}	7	2.39	0.84	4.25	0.82	0.629	0.044	47139	3881
				Şerefköy-2	83^{d}	17	2.16	0.19	3.90	0.39	0.379	0.031	41791	2002
				Samos new Collection^{c}	108^{e}	3	1.95	0.81	3.29	0.62	0.546	0.058	34852	7100
				All	**91**	**27**	**2.20**	**0.25**	**3.92**	**0.32**	**0.462**	**0.031**	**42407**	**1833**
		dietrichi	Large	Gülpınar	161^{d}	10	1.86	0.27	4.04	0.43	0.584	0.056	44344	1751
				Samos new Collection^{c}	201^{e}	3	1.79	0.31	2.73	0.50	0.452	0.043	38931	2359
				All	**181**	**13**	**1.85**	**0.22**	**3.74**	**0.37**	**0.553**	**0.046**	**43095**	**1554**
		proboscideum	Large	Şerefköy-2	201^{d}	19	2.01	0.16	3.88	0.44	0.432	0.018	42361	2169
				Samos new Collection^{c}	238^{e}	9	1.41	0.12	4.08	0.86	0.409	0.017	34554	3009
				All	**220**	**28**	**1.82**	**0.12**	**3.95**	**0.40**	**0.425**	**0.013**	**39852**	**1866**

Fossil sites of Pentalophos and Ravin de la Pluie (a); Dytiko-1, Dytiko-2 and Dytiko-3 (b); Mytilinii A and Mytilinii B (c). Mean body mass estimations were based on metapodial measures and were calculated in this study (d) or obtained from: Vlachou (2013) (e), Orlandi-Oliveras et al. (2018) (f) and Pesquero and Alberdi (2012) (g).

fractal complexity, *HAsfc*), and textural fill volume (*Tfv*) (Scott et al., 2006). Here we consider the heterogeneity of complexity over 64 cells per scan, because this setting contributed the most to the variance in our sample (tested via Principal Component Analysis, Appendix 4). Finally, a linear combination of all four dental microwear texture parameters was performed by means of a Principal Component Analysis. The most explicative principal component (PC1) has been used as a proxy of the overall microwear texture, gathering the major variance from the four DMT variables. Unfortunately, because extant equids are mostly grazers, there is no extensive dataset to which compare the DMT of extinct equids with that of extant forms with different diets. Hence, we relied on the framework provided Scott (2012) in which the DMT has been explored in relation to diet in another group of ungulates with much diverse dietary adaptations.

6.2.3.1. Correlation between body size and diet

Body mass estimates have been used as a measure of body size (Damuth and MacFadden, 1990). We compiled from the literature body mass estimations based on metapodial measures (Orlandi-Oliveras et al., 2018; Pesquero and Alberdi, 2012; Vlachou, 2013), and calculated our own estimations using published data (Clavel et al., 2012; Forsten and Kaya, 1995) and own measures (Appendix 5). Calculations were performed using equations from Scott (1990) and Eisenmann and Sondaar (1998). We tested the link between the hipparionin size and their dietary preferences using linear least squares regressions: mean body mass estimates per population were correlated to our obtained dietary proxies [i.e., each DMT variable and the calculated principal component (PC1)].

6.2.3.2. Dietary differences between hipparionin populations

While considering the size differences, we have further explored the dietary diversity shown among hipparionins through time and space. In this regard, eastern and western Mediterranean hipparionins were differentiated, divided depending on the age of the fossil association (Vallesian/Turolian), and separated by their size category. Our smallest "work unit" was hipparionin population, which we defined as each group present in a specific fossil locality. The mean body masses of the sampled populations range from 31 kg (*periafricanum* group from El Arquillo) to more than 250 kg (*primigenium* group from Hadjidimovo) (Table 6.1). We used a 100 kg threshold to establish two body size categories, dividing the large to medium-sized hipparionins (> 100 kg), and the small-sized ones (< 100 kg). Despite surpassing the 100 kg threshold, we included into the small group the medium-sized *Hipparion* sp. from the western Mediterranean early Vallesian (Forsten, 1997) (154 kg), the *Hipparion macedonicum* from the Axios Valley Vallesian (103 kg), and the *H.* cf. *matthewi* from Samos (108 kg), by considering the larger body masses of their sympatric taxa (Table 6.1), and that these groups represent the smallest forms present in their associations (Appendix 1). Thus, the body mass of the large members from the eastern Mediterranean ranges from 281 kg to 113 kg, while in the small taxa range from 108 kg to 62 kg. In the western Mediterranean, the body mass of the large hipparioins goes from 205 kg to 124 kg, and from 154 kg (84 kg, excluding the early Vallesian form) to 31 kg in the small members.

To explore the variation on the microwear signal related to regional, chronological, and body size factors, a first set of analyses based on three-way ANOVAs were performed for each DMT parameter. Post-hoc pairwise comparisons tests, the Tukey's Honest Significant Differences test (HSD) and the less conservative Fisher's Least Significant Differences test (LSD), were then used in tandem to identify the source of variation. These parametric procedures were applied to rank-transformed variables for approximating distribution free (e.g., non-parametric) tests (Conover and Iman, 1981). Facing unbalanced factorial designs, here we used Type II sums of squares (SS) because it has been proved to be more powerful than Type III SS and does not depend on the arbitrary order of the model terms (Langsrud, 2003). Because marginality principle applies to multifactorial ANOVA designs (Langsrud, 2003; Nelder, 1977), the significance of the main effects was only interpreted when the interaction term was insignificant.

Moreover, a second set of analyses consisting in three-way nested ANOVAs were performed to explore in more detail the hipparionin dietary regimes during the Turolian, when this clade achieved its higher taxonomic and size diversity. Here, we tested for differences on the dental microwear textures between the three bioprovinces surveyed (western Mediterranean, Balkans and western Anatolia) and the hipparionin groups present within these areas (section 6.2.1; Appendix 1), while also considering the localities in which these groups are present. Differences were tested on the four DMT variables and on our calculated PC1. Again, HSD and LSD were used as post-hoc tests, and all the variables were rank-transformed prior to the analyses. A significance level of $\alpha = 0.05$ has been used for all tests.

6.3. Results

6.3.1. Relationship between Hipparionin Diet and Size

The first principal component (PC1) built with the four DMT variables, and considered as a more direct dietary proxy, gathered 34.6% of the total variance (Table 6.2). The variance of this PC1 is chiefly explained by complexity (*Asfc*, 45.2%), anisotropy (*epLsar*; 28.5%), and heterogeneity of complexity (*HAsfc*; 26.3%), whereas textural filled volume (*Tfv*) accounts for less than the 0.1% of it. Anisotropy is positively correlated with this principal component, while *Asfc, HAsfc* and *Tfv* are negatively correlated. Hence, higher PC1 values are linked to less complex enamel surfaces, which in turn are more anisotropic and homogeneous, and have smaller microwear features. The regressions of this PC1 and the four microwear textural parameters with the hipparionin body mass show no significant correlation (Table 6.3; Appendix 6). Thus, there is no general relationship between the microwear signal and the hipparionin body mass when all our sample is considered. However, some significant correlations are detected when separating the three bioprovinces. Heterogeneity of complexity is negatively correlated with hipparionin mass in western Mediterranean ($p < 0.01$), while it is positively correlated in the Balkans sample ($p < 0.01$) (Table 6.3 ; Appendix 6). Moreover, the PC1 is positively correlated with the hipparionin body mass in the western Mediterranean area ($p = 0.03$). In all cases, there is a high dispersion of the data—with R^2 always below 0.05 (Table 6.3)—because the dependent variables (DMT parameters) show high variability as individual data are considered, whereas the independent variable (mass) is represented by mean values per each population.

Table 6.2.
Results of the Principal Component Analysis performed with the four DMT variables. Percentage of variance explained by the principal component and contribution of each variable to the principal components are shown. r: correlation coefficient between the DMT variables and the principal components; r^2: proportion of variance of the principal component explained by each variable.

			Asfc		*epLsar*		*HAsfc*		*Tfv*	
Component	% of variance	cumulative % of variance	r	r^2	r	r^2	r	r^2	r	r^2
PC1	34.58	34.58	-0.672	0.452	0.534	0.285	-0.513	0.263	-0.023	0.001
PC2	25.16	59.73	0.083	0.007	0.138	0.019	-0.010	0.000	0.987	0.974
PC3	23.26	83.00	-0.023	0.001	0.673	0.453	0.735	0.540	-0.084	0.007
PC4	17.00	100	-0.735	0.540	-0.493	0.243	0.444	0.197	0.135	0.018

Table 6.3.
Summary of the linear regressions of the DMT parameters and the calculated principal component (PC1) against body mass. Graphs available at Appendix 6.

	Asfc		*epLsar*		*HAsfc*		*Tfv*		PC1	
Summary Linear Regressions	p-value	R2	p-value	R^2	p-value	R^2	p-value	R^2	p-value	R^2
All Data	0.084	0.008	0.185	0.005	0.901	<0.001	0.087	0.008	0.116	0.007
Western Mediterranean	0.601	0.002	0.125	0.014	**0.006**	0.044	0.889	<0.001	0.028	0.028
Balkans	0.328	0.007	0.591	0.002	**<0.001**	0.010	0.121	0.018	0.449	0.004
Western Anatolia	0.121	0.036	0.990	<0.001	0.526	0.006	0.169	0.029	0.204	0.024

6.3.2. Spatial and Temporal Dietary Variations Related to Hipparionin Size

In our first model we test whether three factors—geological age, geographic region, and body size—contribute to the variance of the dental microwear texture and might have influenced the hipparionin diet. Our results confirm that these three factors affect the dental microwear texture, being in many cases involved in significant interactions (Table 6.4). Hence, changes in the dental microwear textures due to one of these factors follow different directions depending on a second factor. We detect a significant decrease on the complexity parameter from the Vallesian to the Turolian in the large hipparionins, but not for smaller ones (Appendix 7.1), which maintain high levels of complexity during the Turolian (Figure 6.2). Moreover, complexity is generally higher in the eastern hipparionins compared to the western groups (Figure 6.2, 6.3). Anisotropy, on the other hand, increases from Vallesian to Turolian in both regions (Table 6.4; Figure 6.2). In the western Mediterranean, the small-sized hipparionins show significantly lower anisotropy values than the larger forms, while in the east the means between both size groups are similar (Figure 6.2; Appendix 7.2). The western Mediterranean small hipparionins have also higher values of heterogeneity of complexity than the large-sized forms from the same region. In the eastern Mediterranean, we detect the opposite trend, since large-sized species show higher *HAsfc* than the smaller ones (Figure 6.3.3; Appendix 7.3). Heterogeneity of complexity tend to increase from the Vallesian to the Turolian in hipparionins from eastern basins, while it does not vary in the western area (Figure 6.3.3; Appendix 7.4). Finally, the textural fill volume of the small Vallesian forms is higher than that of the larger Vallesian ones, a trend that is not followed during the Turolian (Figure 6.3.4; Appendix 7.5).

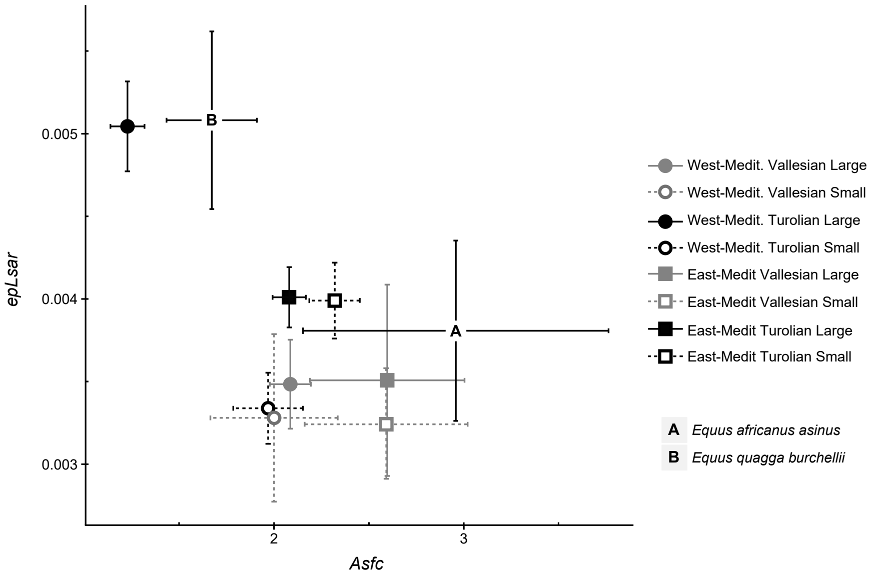

Figure 6.2.
Bivariate plot showing the mean and the standard error of the mean for the complexity (*Asfc*) and anisotropy (*epLsar*) variables. The symbol type (circle/square) represents the region, the filling of the symbol differentiates between hipparionin size types, and the color if they are from Vallesian (grey) or Turolian (black) assemblages. Extant wild *Equus africanus asinus* (A) and *Equus quagga burchelli* (B) are included for comparison.

Table 6.4.
ANOVA results for rank-transformed textural variables. Significant differences highlighted in bold.

	Asfc				*epLsar*				*HAsfc*				*Tfv*			
Source of Variance	df	SS	F	p-value	df	SS	F	p-value	df	SS	F	p-value	df	SS	F	p-value
Age	1	295805	30.229	**< 0.001**	1	151118	13.777	**< 0.001**	1	2	0.000	0.990	1	2482	0.220	0.639
Region	1	506330	51.743	**< 0.001**	1	8926	0.814	0.368	1	2396	0.221	0.639	1	31786	2.820	0.094
Size	1	92512	9.454	**0.002**	1	78955	7.198	**0.008**	1	306	0.028	0.867	1	32824	2.912	0.089
Age x Region	1	22074	2.256	0.134	1	17151	1.564	0.212	1	113296	10.432	**0.001**	1	16282	1.444	0.230
Age x Size	1	80214	8.197	**0.004**	1	29078	2.651	0.104	1	27647	2.546	0.111	1	75853	6.729	**0.010**
Region x Size	1	32516	3.323	0.069	1	110058	10.034	**0.002**	1	160919	14.818	**< 0.001**	1	29595	2.625	0.106
Error	365	3571703			365	4003657			365	3963924			365	4114613		

df: degree of freedom; SS: Sum of Square; F: F-statistic

Table 6.5.
Nested ANOVA results for rank-transformed textural variables and PC1 of Turolian taxa. Significant differences highlighted in bold.

	Asfc				*epLsar*				*HAsfc*				*Tfv*				*PC1*			
Source of Variance	df	SS	F	p-value	df	SS	F	p-value	df	SS	F	p-value	df	SS	F	p-value	df	SS	F	p-value
Bioprovince	2	297866	29.200	**< 0.001**	2	5116	0.435	0.648	2	35666	3.132	**0.045**	2	27124	2.129	0.121	2	125488	11.502	**< 0.001**
Group (Bioprovince)	9	137469	2.995	**0.002**	9	162174	3.065	**0.002**	9	185064	3.611	**< 0.001**	9	50479	0.881	0.543	9	199755	4.069	**< 0.001**
Locality (Group)	11	97747	1.742	0.065	11	164959	2.551	**0.004**	11	159116	2.540	**0.005**	11	128135	1.829	**0.050**	11	116326	1.939	**0.035**
Error	258	1315898			258	1516729			258	1469134			258	1643242			258	1407411		

df: degree of freedom; SS: Sum of Square; F: F-statistic

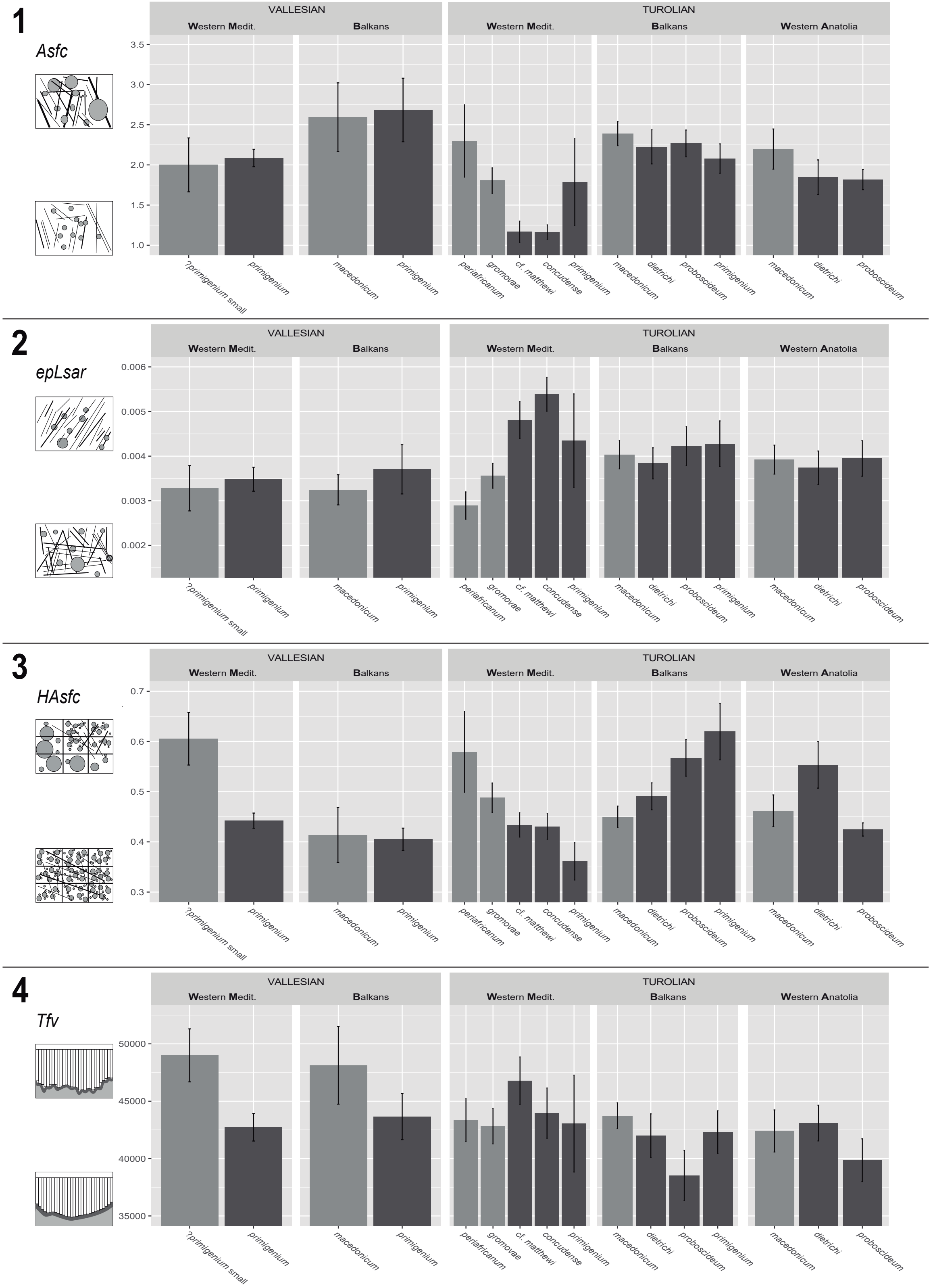

Figure 6.3.
Bar charts with the mean and the standard error of the mean of the four DMT variables considered for each hipparionin group. Small-sized hipparionins depicted in light grey and larger ones in dark grey.

6.3.3. Hipparionin Diets during the Turolian

Nested ANOVAs on the more diverse Turolian sample show that the microwear patterns differ between hipparionin groups within the same bioprovince, and between the hipparionin populations within the same group (Table 6.5). Moreover, differences on the *Asfc* and *HAsfc* parameters between the three bioprovinces are detected. In this regard, complexity values are generally higher in the Balkans than in western Anatolia, while western Mediterranean hipparionins show the lowest complexities (Appendix 8.1). Differences in heterogeneity of complexity are only significant between the Balkan sample and the less heterogeneous microwear signatures of the western Mediterranean hipparionins (Appendix 8.2).

Turolian hipparionin groups significantly differ in all parameters but *Tfv* (Table 6.5). The most notable differences are found between two large-sized groups from the western Mediterranean (*concudense* and cf. *matthewi*) and the rest (Figures 6.3, 6.4; Appendix 8.3). Their dental microwear textures are less complex and tend to be more anisotropic and homogeneous than in other hipparionins (Table 6.1; Figure 6.3; Appendix 8.3), showing, hence, higher PC1 scores (Figure 6.4). The general higher complexity values of the Balkans hipparionins are also detected in the inter-group comparisons, since some groups (e.g., *macedonicum* and *proboscideum*) show minor *Asfc* differences compared to other forms from western Anatolia and the western Mediterranean (Figure 6.3.1; Appendix 8.3). Other significant differences are found between the large-sized *proboscideum* and *primigenium* groups from the Balkans compared to other hipparionins that have lower heterogeneity values (Figure 6.3.3; Appendix 8.3). These inter-group dissimilarities apart, the locality from which the samples came from is also an important factor affecting the variance of our sample (Table 6.5). Focusing on the groups present in more than one locality, pairwise comparisons between fossil sites show that there are minor differences in DMT parameters between populations (Appendices 8.4–8.7). Most of these dissimilarities are caused by the high *epLsar* values of Nikiti-2 *macedonicum* and *dietrichi* morphotypes in comparison with other populations from the same groups; together with the higher *HAsfc* values from Gülpınar and Hadjidimovo hipparionins (Table 6.1; Appendices 8.4–8.7). On the other hand, when considering the localities with sympatric taxa, no significant differences are found among forms coexisting on the same fossil site (Appendices 8.8–8.15). Only some minor variations are detected inside El Arquillo locality, with higher heterogeneity values in the small-sized *periafricanum* and *gromovae* hipparionins compared to that of the larger *primigenium* group (Figure 6.3.3; Appendix 8.15).

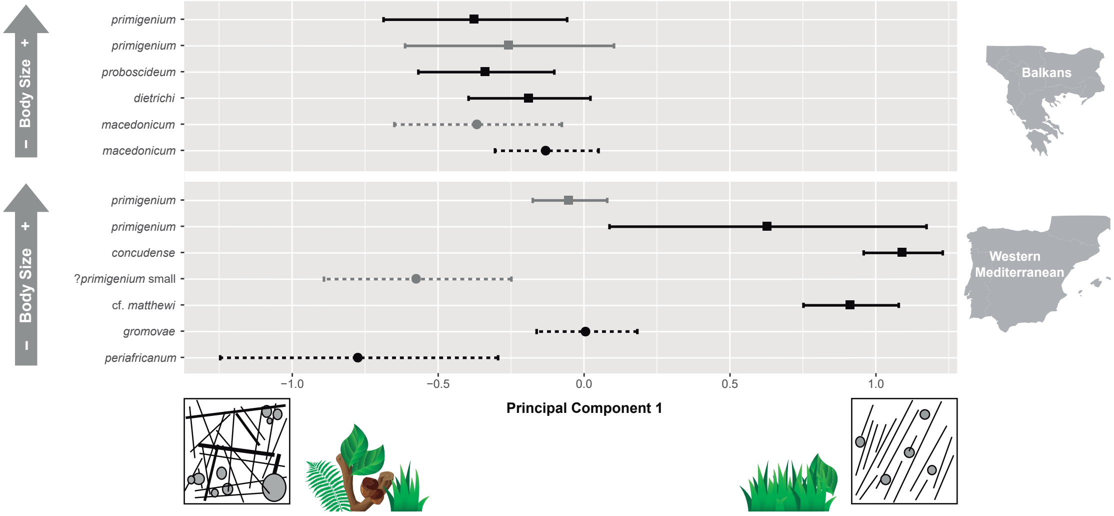

Figure 6.4.
Mean values and confidence intervals (2× standard error of the mean) of the microwear Principal Component 1 for each hipparionin group. Dashed lines used for small-sized groups and continuous for large-sized. Grey color represents Vallesian hipparionins and black color the Turolian hipparionins.

6.4. Discussion

6.4.1. Paleoecology of Hipparionins in Relation to Their Size

In this study, we have investigated the relationship between body size and diet in hipparionin horses. The linkage between body size and dietary strategy is still debated in extant ungulates (Codron et al., 2007; De Iongh et al., 2011). Contrary to previous interpretations (Bell, 1971; Gagnon and Chew, 2000; Jarman, 1974), more recent studies failed to detect a correlation between body mass and diet type in extant African herbivores (Codron et al., 2007), and even between their body mass and the quality of the forage they ingest (De Iongh et al., 2011). A lack of association between size and diet have also been found in Pleistocene ungulates (Saarinen et al., 2016) and in Eocene brontotheres (Mihlbachler and Solounias, 2002). Similarly, our results show that there is no evidence to support a general link between hipparionin size and their dietary preferences at a global scale. However, at a regional scale we still detect 1) an effect of size on the dental microwear texture and 2) a coupling between the hipparionin body size and the heterogeneity of complexity of their dental microwear textures. This later tendency, however, follows opposite directions: in the Balkans the small hipparionins were less generalists than the larger species, while western Mediterranean small forms fed on wider spectra of preferred items. Moreover, the small hipparionins from the western Mediterranean consumed less tough items than the larger taxa, a trend not found in the eastern groups. Accordingly, there is a significant decrease in the grazing behavior related to the size decrease in the western Mediterranean, but not in the other bioprovinces. These biogeographical differences within size groups, strengthen the idea of no general correlation between diet and hipparionin size.

Paleoenvironmental inferences should preferably be done based on the dietary habits of a broad range of ungulates rather than from the diets of a reduced group of them. Nevertheless, the opportunistic feeding habits of hipparionins (Tütken et al., 2013), and the fact that their dietary strategies are related to the available vegetation and, thus, to the habitat properties (Kaiser, 2003), allows us to get a broad idea of the environment in which these hipparionins might have dwelt. Hence, considering the absence of a global relationship between size and diet, we suggest that there should be no general correspondence between hipparionin size and their habitat preferences. The habitat structure, thus, might have not directly affected their body size. Other physiological, ecological, and life history factors may have had a significant influence on the size decrease trends undergone by some hipparionins (Orlandi-Oliveras et al., 2018) and other equids (Saarinen et al., 2016). At a regional scale, however, western Mediterranean small taxa seem to be related to wider dietary spectra and, during the Turolian, to more browsing diets compared to that of their larger counterparts. Therefore, we infer that these smaller hipparionins probably preferred more heterogeneous and somewhat denser habitats. Small eastern Mediterranean hipparionins, on the other hand, have similar microwear textures to those of the larger species, suggesting that they might have occupied comparable niches.

6.4.2. Temporal and Biogeographical Differences in Hipparionin Diets

The study of the dietary strategies of the circum-Mediterranean hipparionins further allows us to compare their feeding preferences and potential habitats through time and space. From Vallesian to Turolian, a general trend of increasing seasonality and habitat opening has been suggested in all the Mediterranean area (Fortelius et al., 1996). These changes have been linked to an increase of xerophytic vegetation and the development of open landscapes with a rich herbaceous layer that includes grasses (Agustí et al., 2003; Jiménez-Moreno et al., 2007). The xerophytic foliage with thicker epidermis and grasses at least available seasonally may have contributed to the observed higher anisotropy observed in Turolian forms. In the eastern Mediterranean, besides, hipparionins generally differed from Vallesian to Turolian by the broadening of their diets, which were already based on mixed-feeding strategies. This dietary niche expansion suggests the prevalence of mosaic habitats that allow the exploitation of food resources with diverse physical properties. Recent isotopic studies did not detect a major climate nor habitat change during the Vallesian-Turolian transition in this area (Merceron et al., 2013; Rey et al., 2013), but only a slight decrease in the precipitation regime (Rey et al., 2013). Wider seasonal variations and more perturbations during the Turolian, however, could have enhanced the presence of heterogeneous landscapes with grasses, bushes and shrubs (Merceron et al., 2016a, 2005a; but see Denk, 2016), that would have provided a high variety of resources. This diversity might have favored the coexistence of diverse hipparionin taxa which do not strongly differ in dietary strategies (Solounias et al., 2010).

Broadly, the main differences between regions lie in the different patterns observed through the hipparionin size range (see section 6.4.1), and the more complex dental microwear textures of eastern hipparionins compared to western forms. Moreover, compared to western Mediterranean hipparionins, the Balkans groups have dental microwear textures suggesting broader diets that include items of harder nature, a dietary regime compatible with a more mixed-feeding strategy.

During the late Miocene, the eastern Mediterranean is typically supposed to be more arid and less wooded than the western realm, based on the comparison of the fossil mammal assemblages (Bonis et al., 1992; Koufos, 2006), and to other proxies that point to the open character of the eastern habitats (Ioakim and Koufos, 2009; Koufos et al., 2009; Merceron et al., 2005a, 2010b, 2016a; Rey et al., 2013; Strömberg et al., 2007). Hence, the eastern Mediterranean biotope has mainly been characterized by an open dry savanna with a rich layer of grasses and with some bushes and shrubs (Koufos et al., 2009; Merceron et al., 2005a, 2016a), although other proxies suggest the existence of more densely wooded areas (Denk, 2016; Denk et al., 2018; Solounias et al., 2010). In this context, we might expect more grazing feeding strategies in the eastern Mediterranean taxa compared to western ones. On the contrary, the large hipparionins from the Turolian western Mediterranean are the species that grazed more, while eastern hipparionins have microwear textures consistent with the consumption of harder items (higher DMT complexity) of diverse physical properties. We interpret this as a consequence of seasonal dry conditions given the open character of the eastern Mediterranean habitats and that late Miocene environments were arguably subject to significant precipitation shifts (Merceron et al., 2005b, 2013). During the dry seasons, extant African ungulates widen their dietary niches thus following less strict grazing diets (De Iongh et al., 2011). Accordingly, extant equids tend to include higher quantity of harder woody browse in their diets during periods of low food availability due to drought (Estes, 1991; Moehlman, 2002). In this regard, the lower selective behavior and higher intake rates of the hindgut fermenters (Janis, 2008) can facilitate the broadening of their diets and compensate for the resource fluctuations. Studies on fossil mammals coping with instable or limited resource supplies also point towards an expansion of the dietary regimes and the inclusion of more browse material (Smith and DeSantis, 2018; Winkler et al., 2013). This increase in the browsing behavior during the dry season can be related to seasonal depletion of herbaceous monocotyledons due to their lower water competitive capacity compared to bushes and shrubs whose roots go deeper in soil (Donzelli et al., 2013; February et al., 2013; Hipondoka et al., 2003; Wang et al., 2010). On the other hand, more humid conditions near lakes and floodplains can support a richer layer of herbaceous vegetation (Rodgers, 1982), which is more present in the diets of our large western Mediterranean hipparionins. Indeed, the populations that show a stronger grazing signal (*Hipparion concudense* from Concud, and *Hipparion* cf. *matthewi* from Venta del Moro) come from fossil associations developed on lacustrine environments (Montoya et al., 2006; Pesquero et al., 2013). Hipparionin obligate grazers, hence, were rather rare and probably inhabited somewhat humid environments and/or faced seasonal migrations. Similarly, the extant zebra species that graze more (*Equus quagga* and *Equus zebra*) are in turn those which undergo larger migrations and are more water-dependent (Bell, 1971; Estes, 1991; Moehlman, 2002).

Besides the physical properties of the food and its phytolith content, the dental wear of ungulate teeth has been related to the action of exogenous particles of grit and dust (Lucas et al., 2014; Madden, 2014; Sanson et al., 2007). The exact role of these particles on the microwear signature is an issue still debated, although recent studies have highlighted the fact that its presence do not significantly alter the dietary signal of the DMT (Burgman et al., 2016; Merceron et al., 2016b). In this sense, while the inclusion of micrometric dust has shown to not increase the complexity of the microwear texture (Merceron et al., 2016b), larger sand particles as millimetric grit could have an impact on it through the generation of large pits (Solounias and Semprebon, 2002), so arguably increasing complexity (Calandra and Merceron, 2016; Hedberg and DeSantis, 2017). Hence, one alternative interpretation to the higher complexity of the DMTs of the eastern Mediterranean hipparionins could be the presence of more micrometric grit in the eastern open environments compared to those of the western Mediterranean.

The dietary reconstructions proposed here potentially reflect the last weekly to monthly preferences, due to the nature of the dental microwear studies (Teaford and Oyen, 1989; Teaford et al., 2017). On the other hand, long-term feeding strategies might be better inferred from mesowear and isotopic analyses, which can provide other comparative proxies for diet and overcome possible caveats as the effect of exogenous grit. Although the short-term nature of microwear studies could represent a limitation, particularly on behalf of the paleoenvironmental reconstruction, the advantage of the DMTA methodology resides in the possibility of tracking at a finer scale the feeding plasticity of taxa, while helping to identify cases of niche partitioning (Calandra and Merceron, 2016). In this regard, our DMT results are key to understand the ecology of the sympatric different-sized hipparionins from different areas and ages. Future paleoenvironmental studies comparing both regions might require the study of diverse ungulate groups, together with the inclusion of isotopic and/or mesowear data that complements the information obtained from the microwear texture.

6.4.3. Diets of Hipparionin Groups and Populations

Previous studies have suggested a mixed-feeding and opportunistic dietary strategy in the *primigenium* hipparionins from the central European Vallesian (Kaiser, 2003; Tütken et al., 2013). Similarly, we show that the Vallesian forms analyzed here were intermediate feeders. Within each region, the coexisting different-sized Vallesian hipparionins did not strongly differ in their diet, except for the broader dietary spectra of the small western Mediterranean forms. In this case, they followed a more generalist diet than the larger hipparionins of the same area, including a wider range of preferred items in a weekly basis. On the other hand, the *primigenium* and the *macedonicum* hipparionins from the eastern Mediterranean show similar dietary preferences, as also suggested from isotopic studies (Rey et al., 2013). Compared between regions, the dental microwear textures of large sized *primigenium* hipparionins are more complex in the eastern than in the western Mediterranean, consistent with the general pattern observed comparing both areas (see section 6.4.2). However, this contrasts with a previous mesowear study that suggests a more browsing diet in the western Mediterranean *primigenium* forms compared to those of the east (Scott et al., 2013). This disagreement can be related to the distinct time scales addressed with the meso- and the microwear studies (Calandra and Merceron, 2016). On one hand, the mesowear signal might illustrate the long-term feeding preferences of the hipparionins due to closer habitats in the west and opener habitats in the east (Koufos, 2006; Scott et al., 2013). On the other hand, our shorter term dental microwear results might reveal the seasonal addition of more woody browse due to a stronger seasonal depletion of monocot resources in the eastern Mediterranean.

When we focus on the much diverse Turolian hipparionin assemblages, the greatest differences are found when comparing the large-sized western hipparionins with the others. As mentioned before, western Mediterranean *H. concudense* and *H.* cf. *matthewi* mainly fed on grasses, while the other hipparionins followed more mixed-feeding strategies and incorporated more browse in their diets. The Turolian *primigenium* group from the western Mediterranean could also have followed a somewhat grazing strategy. However, the small sample hinders a more reliable interpretation. Further comparisons are not possible since no other dental wear studies on Turolian western Mediterranean hipparionins have hitherto been done. The smaller hipparionins from this region, on the other hand, were generalist mixed-feeders that fed on a higher percentage of browse than other western hipparionins. In the eastern Mediterranean, and especially in the Balkans bioprovince, the hipparionins show again more complex microwear textures, which we have mainly related to the higher consumption of browse during seasonal dry phases (section 6.4.2). In this regard, the Balkans' *macedonicum* group included in their diet—besides grasses—more quantity of hard browse material in comparison to other western Mediterranean and western Anatolian hipparionins. This group, however, fed on a narrow range of items on a daily basis, thus suggesting a seasonal mixed-feeding strategy rather than a "meal-by-meal" one (Solounias and Semprebon, 2002).

Previous dietary reconstructions of eastern Mediterranean Turolian hipparionins have mainly inferred grazing diets (Hayek et al., 1992; Koufos et al., 2009; Solounias et al., 2010). Our results rather point to more intermediate feeding preferences both in a daily or in a seasonal basis. Similar mixed-feeding diets have also been suggested within the *proboscideum* group (Hayek et al., 1992; Solounias et al., 2010), while other authors indicate a more grazing tendency for this group (Clavel et al., 2012; Koufos et al., 2009). In our sample, although being mixed-feeders, the *proboscideum* hipparionins from the western Anatolia represent the forms that grazed more of the eastern Mediterranean. On the contrary, the Balkan *proboscideum* show a clear "meal-by-meal" generalist feeding behavior. The *dietrichi* and *macedonicum* hipparionins, on the other hand, do not differ in diet between the two eastern bioprovinces. In the case of the *dietrichi* group, our inferred mixed-feeding strategy agrees with previous interpretations based on material from Samos (Koufos et al., 2009), but contrasts with those that suggest a clear grazing diet (Hayek et al., 1992; Solounias et al., 2010). Our results also point to intermediate feeding preferences in the *macedonicum* hipparionins, in contrast to previously reported grazing diets (Hayek et al., 1992; Koufos et al., 2006; Solounias et al., 2010). Merceron et al. (2016a) also detected variable grazing and even mixed-feeding within the *dietrichi* and *macedonicum* groups; a pattern that they related to the inclusion of more browse during dry seasons. This last interpretation can be supported by our results pointing to intermediate feeding preferences but with narrow daily/weekly dietary spectra.

Local populations within each hipparionin group also show some differences in their microwear textures. For example, the *macedonicum* and *dietrichi* hipparionins from Nikiti-2 grazed more than their analogues from Perivolaki. To a lesser extent, the *macedonicum* hipparionins from Nikiti-2 consumed higher proportion of grasses than those from the localities of Ravin des Zouaves-5 and Dytiko. Additionally, broader dietary preferences have been detected in the *macedonicum* group from Gülpınar, and in the *proboscideum* and *primigenium* hipparionins from Hadjidimovo in comparison to their counterparts from other sites. Comparable dietary variations within the same hipparionin group present in different localities have already been identified (Kaiser, 2003). These differences illustrate the influence of the local environments; like the possible presence of a richer herbaceous layer including monocots in Nikiti-2, as well as a more diverse habitat structure or higher intra- or inter-specific competition levels in Gülpınar and Hadjidimovo sites. In agreement with this pattern, we find a quite homogeneous dental microwear texture within each fossil site, with no significant differences between hipparionin groups coexisting on the same locality. We therefore suggest that the taxa present in one area exploited similar resources and, hence, that there was no strong niche partitioning. The same low degree of dietary differentiation has also been found in previous studies on hipparionin diets (Clavel et al., 2012; Koufos et al., 2006; Solounias et al., 2010), in other extinct perissodactyls (Mihlbachler and Solounias, 2002), and even in extant ungulate assemblages (De Iongh et al., 2011). The presence of various hipparionin groups with no clear niche differentiation can therefore be explained by: 1) the wide mixed-feeding strategies that allow them to consume a large variety of resources, and 2) the size differences that might favor the exploitation of different herbaceous strata (Koufos et al., 2006) in a diverse and rich environment (Solounias et al., 2010). The coexistence in Hadjidimovo of two large hipparionins that show some of the broadest dietary spectra of our sample (higher *HAsfc*), supports the hypothesis of an expansion of the dietary preferences due to competition rather than a niche differentiation strategy. In our sample, however, we have also detected some minor differences that may suggest a case of niche differentiation within El Arquillo fossil site from the western Mediterranean area. Here, the smallest hipparionins follow a more browse dominated generalist diet compared to the larger *primigenium* group. Surprisingly, the larger and more grazing taxon from this site has lower-crowned teeth, while the smaller and more mixed-feeders *periafricanum* and *gromovae* hipparionins show the highest hypsodonty index of the western Mediterranean Turolian (Pesquero, 2003).

6.4.4. Hypsodonty and Hipparionin Diets

Despite their hypsodont teeth, most of the hipparionin groups analyzed here have shown to be intermediate feeders. The same lack of correspondence between the hipparionin high-crowned teeth and a strict grazing diet have been discussed in various studies dealing with dental wear and isotopes (Hayek et al., 1992; MacFadden et al., 1999; Solounias et al., 2010; Tütken et al., 2013). MacFadden et al. (1999), initially proposed that the increased tooth height appeared once within the clade and that this condition was retained despite the following shifts in the dietary strategies. This interpretation, however, fails to explain the observed hypsodonty increase through time in many hipparionin groups (Alberdi, 1989). Alternatively, other authors emphasized that hipparionin hypsodont teeth represent an adaptation to flexible dietary habits (Kaiser, 2003; Tütken et al., 2013). In agreement with this interpretation, our results show that most of the hypsodont hipparionins had mixed-feeding strategies in a daily or a seasonal basis. This feeding flexibility might have represented an advantageous trait during the climatic shifts occurred during the late Miocene (Tütken et al., 2013), since herbivores dealing with instable resource supplies tend to expand their dietary breaths (Winkler et al., 2013).

Besides allowing to switch between a grazing or browsing diet depending on the resource availability, higher-crowned teeth might also promote the achieving of a longer life span (Carranza et al., 2004; Jordana et al., 2012; Veiberg et al., 2007), which is linked to a general slower life history (Stearns, 1992). Indeed, as well as by the diet quality, the wear degree has shown to be influenced by the optimal timing of tooth use in relation to the schedule of growth and reproduction through life (Pérez-Barbería et al., 2015). More hypsodont teeth, then, can be related to a higher resource assignation to the soma maintenance rather than to current performance, a life history strategy which is in turn coupled to longer reproductive lifespans (Carranza et al., 2008; Veiberg et al., 2007). Enamel folding complexity on the occlusal surface, moreover, might have also played an important role in the efficiency of the hipparionin tooth durability (Famoso and Davis, 2016); while in the *Equus* genus dental functionality is chiefly maintained by means of increased crown heights due to the extension of the crown formation time (Nacarino-Meneses et al., 2017; Orlandi-Oliveras et al., 2019). The relationship between life history and dental development (Smith, 1991, 2000), together with the inferred slow molar formation and relatively late eruption of hipparionins' molars (Orlandi-Oliveras et al., 2019), make us interpret the lack of linkage between hypsodonty and diet in hipparionins as possible evidence of the role of life history in the evolution of tooth hypsodonty within this group.

6.4.5. Size Decrease Trends

The decrease in hipparionin size has mainly been related to an adaptation to open landscapes (Bernor et al., 1996; Forsten, 1997; Saarinen, 2009) and to feeding on plants of increasing xerophytism (Forsten, 1968, 1978b). On the other hand, Ortiz-Jaureguizar and Alberdi (2003) suggested more closed-habitat affinities for the small hipparionins. Here, however, we do not find a common dietary pattern shared between the small-sized hipparionins of Vallesian and Turolian assemblages from the circum-Mediterranean regions. In consequence, we interpret that the size differences were not directly promoted by a common dietary or habitat shift but might instead represent independent adaptations that otherwise led to similar size decrease tendencies.

The small and large-sized groups from the eastern Mediterranean did not follow contrasting dietary regimes during the Vallesian and the Turolian. This suggests that the cause or causes triggering the small-sized hipparionin appearance were not directly related to dietary differences. Otherwise, it lends support to the idea that shifts in other factors probably underlay these changes [e.g., mortality regimes shifts (Orlandi-Oliveras et al., 2018)]. In the western Mediterranean Vallesian, the main detected dietary difference resides in the more generalist diets followed by the smaller hipparionins. The smaller form, hence, probably dwelt in more heterogeneous habitats (Forsten, 1997). The sharpest dietary dissimilarities between size groups, however, are found in the western Mediterranean Turolian. Nowadays, the large size of extant grazing plain zebras allows them to go through the seasonal migrations following the grasses fluxes (Moehlman, 2002). In the western Mediterranean, likewise, larger-sized hipparionins were the taxa with the stronger grazing tendencies, and they might arguably undergo seasonal migrations when the resources in monocotyledonous were depleted. The smaller and more hypsodont species, on the other hand, followed browse-dominated mixed-feeding strategies; probably exploiting the available resources in somewhat closer habitats, and broadening the spectrum of ingested items during seasons of lower resource availability. In this regard, bone and dental paleohistological studies have pointed towards relative slower life histories in these more hypsodont small-sized forms in comparison to larger hipparionins from the western Mediterranean Turolian (Orlandi-Oliveras et al., 2018, 2019). Similarly, extant roe deer populations of less productive environments are smaller, more hypsodont, and more longer-lived than larger-sized roe deer populations inhabiting highly productive environments (Veiberg et al., 2007).

6.5. Summary

The dental microwear textures of the northern circum-Mediterranean hipparionins mainly point towards mixed-feeding strategies. Some exceptions are present, since large-sized forms of the Turolian western Mediterranean grazed more than the rest. When considering all the hipparionins analyzed, we do not find a common relationship between their dietary preferences and their size. Despite this lack of general correlation, the western Mediterranean large-sized forms tended to have narrower dietary breadths further associated to a higher percentage of grassy consumption in comparison to smaller hipparionins. On the other hand, the different-sized hipparionins from the eastern bioprovinces follow similar intermediate feeding strategies, including both browse and grasses in their diets (in some cases in a more seasonal basis and others in a more daily-weekly basis). Although we did not reconstruct the paleoenvironmental conditions from the sole diet of hipparionins, their opportunistic feeding adaptations provided some evidence of the habitat in which they might have dwelt. In this regard, the lack of correspondence between diet and size contrasted with the common belief that hipparionin size decrease was related to habitat openness.

The broad comparison between Vallesian and Turolian hipparionin assemblages from different areas also allowed us to detect some general spatiotemporal differences regarding the hipparionin feeding strategies. The inclusion of tough items in their diets tended to increase from Vallesian to Turolian; in the eastern Mediterranean, and a further widening of the dietary strategies is also detected. This could reflect a general increase in plant xerophytism, and the presence of more heterogeneous environments in the eastern Mediterranean late Miocene. More solid paleoenvironmental inferences, however, should be based on dietary reconstructions of more diverse ungulate assemblages (adding other dietary proxies as isotopes and mesowear) and the study of macrobotanical and palynological remains. When comparing the eastern and western Mediterranean regions, we find significant higher complexity values in the eastern forms, and specially on the Balkans. One possible interpretation to this observation is the presence of higher levels of millimetric grit eastwards. However, considering previous studies comparing both areas (Bonis et al., 1992; Koufos, 2006), we relate this to the presence of more dry seasonal episodes (Merceron et al., 2016a, 2005a) and the consumption of harder woody browse by eastern hipparionins. Similarly, extant equids (Estes, 1991; Moehlman, 2002) and other ungulates (De Iongh et al., 2011) include higher proportion of browse during the dry seasons in savanna and more arid environments.

In some cases, the diet of the hipparionin groups differ between the fossil sites surveyed, probably reflecting the season at which most of the specimens died and the influence of local conditions. Accordingly, coexisting hipparionins show no differences on the dental microwear patterns, thus suggesting no strong dietary niche partitioning over the traditional grazing-browsing couple. Alternatively, the segregation might have existed among the frame of mixed-feeders and browsers (exploiting different resources but with similar mechanical properties). The general mixed-feeding strategy inferred in most of the hypsodont hipparionin groups shows no support to the assumption of grazing diets due to high hypsodonty indices. Hypsodonty within the group, hence, might have been influenced by its role on dietary flexibility (Tütken et al., 2013) and life history (Veiberg et al., 2007). Finally, the different ecologies shown by the small-sized hipparionins make us conclude that the size decrease trends were probably achieved independently rather than related to a common habitat shift.

6.6. Acknowledgements

We would like to thank M. Fernández and X. Aymerich for the molding of the material from the ICP (Institut Català de Paleontologia). G.O-O. acknowledges the help received from F. Martin (PALEVOPRIM) during the obtainment of the DMT parameters and the posterior analyses. We further thank to D. Kostopoulos (Aristotle University of Thessaloniki) for his comments on the earlier versions of this manuscript. The editor Yasuyuki Nakamura and two reviewers including Juha Saarinen are acknowledged for their helpful comments which improved the manuscript. Funding for this study was provided by the Spanish Ministry of Economy and Competitiveness (MINECO) (PI: M.K., CGL2015-63777) and the CERCA Program, Generalitat de Catalunya. R.S.S., T.K., S.M., and G.M. were granted through a "Wenner-Gren International Collaborative Research Grant" (PIs: R.S. Scott and T. Kaya) to collect most of the Vallesian and Turolian equid dental molds from the eastern Mediterranean. We would like to thank to Ege University Natural History Museum authorities to give access to study the related materials from Şerefköy and Gülpınar localities. M.K. and G.O-O. are part of a research group recognized without funding by AGAUR (2017 SGR 960). G.O-O. was supported by a FI-DGR 2016 grant (2016FI_B00202) awarded by AGAUR (Generalitat de Catalunya) and held an Erasmus + fellowship during his stay in the PALEVOPRIM laboratory (CNRS and University of Poitiers). The grant SYNTHESIS ES-TAF-1846 for the stay of J.C. at the MNCN of Madrid is also acknowledged.

6.7. References

Agustí, J., Sanz de Siria, A., and Garcés, M. 2003. Explaining the end of the hominoid experiment in Europe. *Journal of Human Evolution*, 45:145–153. https://doi.org/10.1016/S0047-2484(03)00091-5

Alberdi, M.T. 1989. A review of Old World hipparionine horses, p. 234-261. In Prothero, D.R. and Schoch, R.M. (eds.), *The Evolution of Perissodactyls*. Oxford University Press, New York.

Alberdi, M.T., Prado, J.L., and Ortiz-Jaureguizar, E. 1995. Patterns of body size changes in fossil and living Equini (Perissodactyla). *Biological Journal of the Linnean Society*, 54:349–370. https://doi.org/10.1111/j.1095-8312.1995.tb01042.x

Bauer, I.E., McMorrow J., and Yalden, D.W. 1994. The historic ranges of three equid species in north-east Africa: a quantitative comparison of environmental tolerances. *Journal of Biogeography,* 21:169-182. https://doi.org/10.2307/2845470

Bell, R.H.V. 1971. A grazing ecosystem in the Serengeti. *Scientific American,* 225: 86-93. https://doi.org/10.2307/24922780

Bernor, R.L., Koufos, G.D., Woodburne, M.O., and Fortelius, M. 1996. The evolutionary history and biochronology of European and Southwest Asian Late Miocene and Pliocene hipparionine horses, p. 307-338. In Bernor, R.L., Fahlbusch, V., and Mittmann, H.-W. (eds.), *The Evolution of Western Eurasian Neogene Mammal Faunas*. Columbia University Press, New York.

Bernor, R.L., Kovar-Eder, J., Suc, J.-P., and Tobien, H. 1990a. A contribution to the evolutionary history of European Late Miocene age hipparionines (Mammalia: Equidae). *Paléobiologie Continentale,* 17:291–309. https://doi.org/10.1017/CBO9781107415324.004

Bernor, R.L., Mirzaie Ataabadi, M., Meshida, K., and Wolf, D., 2016. The Maragheh hipparions, late Miocene of Azarbaijan, Iran. *Palaeobiodiversity and Palaeoenvironments*, 96:453–488. https://doi.org/10.1007/s12549-016-0235-2

Bernor, R.L., Scott, R.S., Fortelius, M., Kappelman J., and Sen, S. 2003. Equidae (Perissodactyla), p. 220–281. In Fortelius, M., Kappelman, J., Sen, S., and Bernor, R.L. (eds.), *The Geology and Paleontology of the Miocene Sinap Formation, Turkey*. Columbia University Press.

Bernor, R.L., and Tobien, H. 1989. Two small species of *Cremohipparion* (Equidae, Mamm.) from Samos, Greece. *Mitteilungen der Bayerischen Staatssammlung för Paläontologie und Historische Geologie*, 29:207–226.

Bernor, R.L., Tobien, H., and Woodburne, M.O. 1990b. Patterns of Old World hipparionine evolutionary diversification and biogeographic extension, p. 263–319. In: Lindsay, E.H., Fahlbusch, V., and Mein, P. (eds.), *European Neogene Mammal Chronology*. Plenum Press, New York. https://doi.org/10.1007/978-1-4899-2513-8_18

Bonis, L. de, Bouvrain, G., Geraads, D., and Koufos, G.D. 1992. Diversity and paleoecology of Greek late Miocene mammalian faunas. *Palaeogeography, Palaeoclimatology, Palaeoecology*, 91:99–121. https://doi.org/10.1016/0031-0182(92)90035-4

Brown, J.S. 1988. Patch use as an indicator of habitat preference, predation risk, and competition. *Behavioral Ecology and Sociobiology,* 22:37–47. https://doi.org/10.1007/BF00395696

Burgman, J.H.E., Leichliter, J., Avenant, N.L. and Ungar, P.S. 2016. Dental microwear of sympatric rodent species sampled across habitats in southern Africa: Implications for environmental influence. *Integrative Zoology*, 11:111–127. https://doi.org/10.1111/1749-4877.12188

Calandra, I. and Merceron, G. 2016. Dental microwear texture analysis in mammalian ecology. *Mammal Review*, 46:215-218. https://doi.org/10.1111/mam.12063

Calder, W.A. 1984. *Size, Function, and Life History*. Harvard University Press, Cambridge. https://doi.org/10.2307/4086807

Cantalapiedra, J.L., Prado, J.L., Hernández Fernández, M., and Alberdi, M.T. 2017. Decoupled ecomorphological evolution and diversification in Neogene-Quaternary horses. *Science*, 355:627–630. https://doi.org/10.1126/science.aag1772

Carranza, J., Alarcos, S., Sánchez-Prieto, C.B., Valencia, J., and Mateos, C. 2004. Disposable-soma senescence mediated by sexual selection in an ungulate. *Nature,* 432:215–218. https://doi.org/10.1038/nature03004

Carranza, J., Mateos, C., Alarcos, S., Sánchez-Prieto, C.B., and Valencia, J. 2008. Sex-specific strategies of dentine depletion in red deer. *Biological Journal of the Linnean Society*, 93:487–497. https://doi.org/10.1111/j.1095-8312.2007.00903.x

Case, T.J. 1979. Optimal body size and an animal's diet. *Acta Biotheoretica,* 28: 54–69. https://doi.org/10.1007/BF00054680

Clavel, J., Merceron, G., Hristova, L., Spassov, N., Kovachev, D., and Escarguel, G. 2012. On *Mesopithecus* habitat: Insights from late Miocene fossil vertebrate localities of Bulgaria. *Journal of Human Evolution,* 63:162–179. https://doi.org/10.1016/j.jhevol.2012.04.007

Codron, D., Lee-Thorp, J.A., Sponheimer, M., Codron, J., De Ruiter, D., and Brink, J.S. 2007. Significance of diet type and diet quality for ecological diversity of African ungulates. *Journal of Animal Ecology,* 76:526–537. https://doi.org/10.1111/j.1365-2656.2007.01222.x

Conover, W.J. and Iman, R.L. 1981. Rank transformations as a bridge between parametric and nonparametric statistics. *The American Statistician,* 35:124-129. https://doi.org/10.2307/2683975

Damuth, J.D. and MacFadden, B.J. 1990. *Body Size in Mammalian Paleobiology : Estimation and Biological Implications*. Cambridge University Press.

De Iongh, H.H., De Jong, C.B., Van Goethem, J., Klop, E., Brunsting, A.M.H., Loth, P.E., and Prins, H.H.T. 2011. Resource partitioning among African savanna herbivores in North Cameroon: The importance of diet composition, food quality and body mass. *Journal of Tropical Ecology*, 27:503–513. https://doi.org/10.1017/S0266467411000307

Denk, T. 2016. Palaeoecological interpretation of the late Miocene landscapes and vegetation of northern Greece: A comment to Merceron et al., 2016 (Geobios 49, 135–146), p. 423–431. In Koufos, G.D and Kostopoulos D.S. (eds.), *Palaeontology of the upper Miocene vertebrate localities of Nikiti (Chalkidiki Peninsula, Macedonia, Greece). Geobios,* 49. https://doi.org/10.1016/j.geobios.2016.06.009

Denk, T., Zohner, C.M., Grimm, G.W., and Renner, S.S. 2018. Plant fossils reveal major biomes occupied by the late Miocene Old-World Pikermian fauna. *Nature Ecology and Evolution,* 2:1864–1870. https://doi.org/10.1038/s41559-018-0695-z

DeSantis, L.R.G. 2016. Dental microwear textures: Reconstructing diets of fossil mammals. *Surface Topography: Metrology and Properties,* 4:023002. https://doi.org/10.1088/2051-672X/4/2/023002

DeSantis, L.R.G., Scott, J.R., Schubert, B.W., Donohue, S.L., McCray, B.M., Van Stolk, C.A., Winburn, A.A., Greshko, M.A., and O'Hara, M.C. 2013. Direct comparisons of 2D and 3D dental microwear proxies in extant herbivorous and carnivorous mammals. *PLoS ONE*, 8:e71428. https://doi.org/10.1371/journal.pone.0071428

Dmitriew, C.M. 2011. The evolution of growth trajectories: what limits growth rate? *Biological Reviews*, 86:97–116. https://doi.org/10.1111/j.1469-185X.2010.00136.x

Donzelli, D., De Michele, C., and Scholes, R.J. 2013. Competition between trees and grasses for both soil water and mineral nitrogen in dry savannas. *Journal of Theoretical Biology,* 332:181–190. https://doi.org/10.1016/j.jtbi.2013.04.003

Eisenmann, V. and Sondaar, P.Y. 1998. Pliocene vertebrate locality of Çalta, Ankara, Turkey. 7. *Hipparion*. *Geodiversitas*, 20:409–439.

Estes, R. 1991. *The Behavior Guide to African Mammals: Including Hoofed Mammals*, *Carnivores, Primates*. University of California Press, Berkeley.

Famoso, N.A. and Davis, E.B. 2016. On the relationship between enamel band complexity and occlusal surface area in Equids (Mammalia, Perissodactyla). *PeerJ,* 4:e2181. https://doi.org/10.7717/peerj.2181

February, E.C., Higgins, S.I., Bond, W.J., and Swemmer, L. 2013. Influence of competition and rainfall manipulation on the growth responses of savanna trees and grasses. *Ecology,* 94:1155–1164. https://doi.org/10.1890/12-0540.1

Forsten, A. 1968. Revision of the palearctic *Hipparion*. Acta Zoologica Fennica, 119:1-134.

Forsten, A. 1978a. *Hipparion primigenium* (v. Meyer, 1829), an early three-toed horse. *Annales Zoologici Fennici* ,15:298–313.

Forsten, A. 1978b. *Hipparion* and possible Iberian-North African Neogene connections. *Annales Zoologici Fennici* , 15:294–297.

Forsten, A. 1997. *Hipparion* from Santiga (Spain) and its biostratigraphic significance. *Paleontologia i Evolució*, 30-31:77–82.

Forsten, A. and Kaya, T. 1995. The hipparions (Mammalia, Equidae) from Gülpinar (Canakkale, Turkey). *Paläontologische Zeitschrift*, 69:491–501. https://doi.org/10.1007/BF02987809

Fortelius, M., Werdelin, L., Andrews, P., Bernor, R.L., Gentry, A., Humphrey, L., Mittmann, H.W., and Viranta, S. 1996. Provinciality, diversity, turnover and paleoecology in land mammal faunas of the later Miocene of Western Eurasia, p. 414-448. In Bernor, R.L., Fahlbusch, V., and Mittmann, H.-W. *The Evolution of Western Eurasian Neogene Mammal Faunas*. Columbia University Press. https://doi.org/10.1017/S0031182016000445

Gabunia, L.K. and Chochieva, K.I. 1982. Co-evolution of the *Hipparion* fauna and vegetation in the Paratethys region. *Evolutionary Theory*, 6:1–13.

Gagnon, M. and Chew, A.E. 2000. Dietary preferences in extant African Bovidae. *Journal of Mammalogy,*. 81:490–511. https://doi.org/10.1644/1545-1542(2000)081<0490:DPIEAB>2.0.CO;2

Gould, G.C. and MacFadden, B.J. 2004. Gigantism, dwarfism, and Cope's Rule: "nothing in evolution makes sense without a phylogeny". *Bulletin of the American Museum of Natural History,* 285:219–237. https://doi.org/10.1206/0003-0090(2004)285<0219:C>2.0.CO;2

Hayek, L.-A.C., Bernor, R.L., Solounias, N., and Steigerwald, P. 1992. Preliminary studies of hipparionine horse diet as measured by tooth microwear. *Annales Zoologici Fennici,* 28: 187–200.

Hedberg, C. and DeSantis, L.R.G. 2017. Dental microwear texture analysis of extant koalas: clarifying causal agents of microwear. *Journal of Zoology*, 301:206–214. https://doi.org/10.1111/jzo.12413

Hilgen, F.J., Lourens, L.J., van Dam, J., Beu, A.G., Boyes, A.F., Cooper, R.A., Krijgsman, W., Ogg, J.G., Piller, W.E., and Wilson, D.S. 2012. The Neogene Period, p. 923-978. In Gradstein, F.M., Ogg, J.G., Schmitz, M., and Ogg, G. (eds.), *The Geologic Time Scale 2012*. https://doi.org/10.1016/B978-0-444-59425-9.00029-9

Hipondoka, M.H., Aranibar, J., Chirara, C., Lihavha, M., and Macko, S. 2003. Vertical distribution of grass and tree roots in arid ecosystems of Southern Africa: niche differentiation or competition? *Journal of Arid Environments,* 54:319–325. https://doi.org/10.1006/JARE.2002.1093

Hopcraft, J.G.C., Olff, H., and Sinclair, A.R.E. 2010. Herbivores, resources and risks: alternating regulation along primary environmental gradients in savannas. *Trends in Ecology and Evolution,* 25:119–128. https://doi.org/10.1016/j.tree.2009.08.001

Ioakim, C. and Koufos, G.D. 2009. Palynology, p. 27-35. In Koufos, G.D. and Nage, D. (eds.), *The late Miocene Mammal Faunas of the Mytilinii Basin, Samos Island, Greece: New Collection. Beiträge zur Paläontologie,* 31.

Janis, C.M. 2008. An evolutionary history of browsing and grazing ungulates, p. 21-45. In: Gordon, I.J. and Prins, H.H.T. (eds.), *The Ecology of Browsing and Grazing. Ecological Studies.* Springer, Berlin, Heidelberg. https://doi.org/10.1007/978-3-540-72422-3_2

Jarman, P.J. 1974. The social organisation of antelope in relation to their ecology. *Behaviour,* 48:215–267. https://doi.org/10.2307/4533573

Jiménez-Moreno, G., Popescu, S.M., Ivanov, D., and Suc, J.-P. 2007. Neogene flora, vegetation and climate dynamics in southeastern Europe and the northeastern Mediterranean, p. 503-516. In Willians, W., Haywood, A.M., Gregory, F.J., and Schmidt, D.N. (eds.), *Deep-Time Perspectives on Climate Change: Marrying the Signal from Computer Models and Biological Proxies.* The Micropalaeontological Society, London. https://doi.org/1747-602X/07/$15.00

Jordana, X., Marín-Moratalla, N., DeMiguel, D., Kaiser, T.M., and Köhler, M. 2012. Evidence of correlated evolution of hypsodonty and exceptional longevity in endemic insular mammals. *Proceedings of the Royal Society B: Biological Sciences*, 279:3339–3346. https://doi.org/10.1098/rspb.2012.0689

Kaiser, T.M. 2003. The dietary regimes of two contemporaneous populations of *Hippotherium primigenium* (Perissodactyla, Equidae) from the Vallesian (Upper Miocene) of Southern Germany. *Palaeogeography, Palaeoclimatology, Palaeoecology,* 198:381–402. https://doi.org/10.1016/S0031-0182(03)00480-2

Kostopoulos, D.S. 2009. The Pikermian Event: Temporal and spatial resolution of the Turolian large mammal fauna in SE Europe. *Palaeogeography, Palaeoclimatology, Palaeoecology,* 274:82–95. https://doi.org/10.1016/j.palaeo.2008.12.020

Koufos, G.D. 2006. Palaeoecology and chronology of the Vallesian (late Miocene) in the Eastern Mediterranean region. *Palaeogeography, Palaeoclimatology, Palaeoecology,* 234:127–145. https://doi.org/10.1016/j.palaeo.2005.01.014

Koufos, G.D. 2016. *Hipparion macedonicum* revisited: New data on evolution of hipparionine horses from the Late Miocene of Greece. *Acta Palaeontologica Polonica,* 61:519–536. https://doi.org/10.4202/app.00169.2015

Koufos, G.D., Kostopoulos, D.S., and Merceron, G. 2009. Palaeoecology – Palaeobiogeography, p.409-430. In Koufos, G.D. and Nagel, D. (eds.), *The late Miocene Mammal Faunas of the Mytilinii Basin, Samos Island, Greece: new collection. Beiträge zur Paläontologie*, 31.

Koufos, G.D., Merceron, G., Kostopoulos, D.S., Vlachou T.D., and Sylvestrou, I.A. 2006. Palaeoecology and Palaeobiogeography, p. 201-221. In Koufos, G.D. (ed.), *The late Miocene Vertebrate Locality of Perivolaki, Thessaly, Greece. Palaeontographica Abteilung A,* 276.

Koufos, G.D. and Vlachou, T.D. 2016. Equidae, p. 85-118. In Koufos G.D. and Kostopoulos, D.S. (eds.), *Palaeontology of the Upper Miocene Vertebrate Localities of Nikiti (Chalkidiki Peninsula, Macedonia, Greece).Geobios*, 49. https://doi.org/10.1016/j.geobios.2016.01.001

Langsrud, Ø. 2003. ANOVA for unbalanced data: Use Type II instead of Type III sums of squares. *Statistics and Computing,* 13:163–167. https://doi.org/10.1023/A:1023260610025

Lucas, P.W., Casteren, A. van, Al-Fadhalah, K., Almusallam, A.S., Henry, A.G., Michael, S., Watzke, J., Reed, D.A., Diekwisch, T.G.H., Strait, D.S. and Atkins, A.G. 2014. The role of dust, grit and phytoliths in tooth wear. *Annales Zoologici Fennici,* 51:143–152. https://doi.org/10.5735/086.051.0215

MacFadden, B.J. 1992. *Fossil Horses : Systematics, Paleobiology, and Evolution of the Family Equidae*. Cambridge University Press, New York.

MacFadden, B.J. 2005. Fossil Horses--Evidence for Evolution. *Science* (80-.). 307:1728–730. https://doi.org/10.1126/science.1105458

MacFadden, B.J. and Hulbert, R.C. 1988. Explosive speciation at the base of the adaptive radiation of Miocene grazing horses. *Nature*, 336:466–468. https://doi.org/10.1038/336466a0

MacFadden, B.J., Solounias, N., and Cerling, T.E. 1999. Ancient diets, ecology, and extinction of 5-million-year-old horses from Florida. *Science,* 283:824–827. https://doi.org/10.1126/science.283.5403.824

Madden, R.H. 2014. *Hypsodonty in Mammals: Evolution, Geomorphology and the Role of Earth Surface Processes, Hypsodonty in Mammals: Evolution, Geomorphology and the Role of Earth Surface Processes.* Cambridge University Press, Cambridge.

Martin, F., Plastiras, C.-A., Merceron, G., Souron, A., and Boisserie, J.-R. 2018. Dietary niches of terrestrial cercopithecines from the Plio-Pleistocene Shungura Formation, Ethiopia: evidence from Dental Microwear Texture Analysis. *Scientific Reports,* 8:14052. https://doi.org/10.1038/s41598-018-32092-z

Matthew, W.D. 1926. The evolution of the horse: a record and its interpretation. *The Quaterly Review of Biology*, 1:139–185. https://doi.org/10.2307/2808222

Merceron, G., Bonis, L. de, Viriot, L., and Blondel, C. 2005a. Dental microwear of fossil bovids from northern Greece: Paleoenvironmental conditions in the eastern Mediterranean during the Messinian. *Palaeogeography, Palaeoclimatology, Palaeoecology,* 217:173–185. https://doi.org/10.1016/j.palaeo.2004.11.019

Merceron, G., Bonis, L. de, Viriot, L., and Blondel, C. 2005b. Dental microwear of the late Miocene bovids of northern Greece: Vallesian/Turolian environmental changes and disappearance of *Ouranopithecus macedoniensis* ? *Bulletin de la Societe Geologique de France,* 176:475–484. https://doi.org/10.2113/176.5.475

Merceron, G., Escarguel, G., Angibault, J.M., and Verheyden-Tixier, H. 2010a. Can dental microwear textures record inter-individual dietary variations? *PLoS One*, 5:e9542. https://doi.org/10.1371/journal.pone.0009542

Merceron, G., Kaiser, T.M., Kostopoulos, D.S., and Schulz, E. 2010b. Ruminant diets and the Miocene extinction of European great apes. *Proceedings of the Royal Society B: Biological Sciences*, 277:3105–3112. https://doi.org/10.1098/rspb.2010.0523

Merceron, G., Kostopoulos, D.S., Bonis, L. de, Fourel, F., Koufos, G.D., Lécuyer, C., and Martineau, F. 2013. Stable isotope ecology of Miocene bovids from Northern Greece and the ape/monkey turnover in the Balkans. *Journal of Human Evolution,* 65:185–198. https://doi.org/10.1016/j.jhevol.2013.05.003

Merceron, G., Novello, A., and Scott, R.S. 2016a. Paleoenvironments inferred from phytoliths and Dental Microwear Texture Analyses of meso-herbivores, p. 135-146. In Koufos, G.D, and Kostopoulos D.S. (eds.), *Palaeontology of the upper Miocene vertebrate localities of Nikiti (Chalkidiki Peninsula, Macedonia, Greece). Geobios* 49. https://doi.org/10.1016/j.geobios.2016.01.004

Merceron, G., Ramdarshan, A., Blondel, C., Boisserie, J.-R., Brunetière, N., Francisco, A., Gautier, D., Milhet, X., Novello, A., and Pret, D. 2016b. Untangling the environmental from the dietary: Dust does not matter. *Proceedings of the Royal Society B: Biological Sciences,* 283:20161032. https://doi.org/10.1098/rspb.2016.1032

Merceron, G., Schulz, E., Kordos, L., and Kaiser, T.M. 2007. Paleoenvironment of *Dryopithecus brancoi* at Rudabánya, Hungary: evidence from dental meso- and micro-wear analyses of large vegetarian mammals. *Journal of Human Evolution*, 53:331–349. https://doi.org/10.1016/j.jhevol.2007.04.008

Mihlbachler, M.C., and Solounias, N. 2002. Body size, dental microwear, and brontothere diets through the Eocene. *Journal of Vertebrate Paleontology*, 22:88A.

Moehlman, P.D. 2002. *Equids: Zebras, Asses, and Horses: Status Survey and Conservation Action Plan*. IUCN/SSC Equid Specialist Group, IUCN, Gland, Switzerland and Cambridge, UK.

Montoya, P., Morales, J., Robles, F., Abella, J., Benavent, J. V, Marín, M. D., and Ruiz Sánchez, F.J. 2006. Las nuevas excavaciones (1995-2006) en el yacimiento del Mioceno final de Venta del Moro, Valencia. *Estudios Geológicos*, 62:313–326.

Nacarino-Meneses, C., Jordana, X., Orlandi-Oliveras, G., and Köhler, M. 2017. Reconstructing molar growth from enamel histology in extant and extinct *Equus*. *Scientific Reports*, 7:15965. https://doi.org/10.1038/s41598-017-16227-2

Nelder, J.A. 1977. A Reformulation of Linear Models. *Journal of the Royal Statistical Society. Series A (General)*, 140:48. https://doi.org/10.2307/2344517

Orlandi-Oliveras, G., Nacarino-Meneses, C., and Köhler, M. 2019. Dental histology of late Miocene hipparionins compared with extant *Equus*, and its implications for Equidae life history. *Palaeogeography, Palaeoclimatology, Palaeoecology,* 528:133-146. https://doi.org/10.1016/j.palaeo.2019.04.016

Orlandi-Oliveras, G., Nacarino-Meneses, C., Koufos, G.D., and Köhler, M. 2018. Bone histology provides insights into the life history mechanisms underlying dwarfing in hipparionins. *Scientific Reports*, 8:17203. https://doi.org/10.1038/s41598-018-35347-x

Ortiz-Jaureguizar, E. and Alberdi, M.T. 2003. El patrón de cambios en la masa corporal de los Hipparionini (Perissodactyla, Equidae) de la Península Ibérica durante el Mioceno superior-Plioceno superior. *Coloquios de Paleontología*, 1:499–509.

Palkovacs, E.P. 2003. Explaining adaptive shifts in body size on islands: a life history approach. *Oikos,* 103:37–44. https://doi.org/10.1034/j.1600-0706.2003.12502.x

Pérez-Barbería, F.J., Carranza, J., and Sánchez-Prieto, C. 2015. Wear fast, die young: More worn teeth and shorter lives in Iberian compared to Scottish red deer. *PLoS One,* 10:e0134788. https://doi.org/10.1371/journal.pone.0134788

Pesquero, M.D. 2003. *Hipparion* del Turoliense superior de Las Casiones (Fosa de Teruel). *Coloquios de Paleontología,* Volumen Ex:511–548.

Pesquero, M.D. and Alberdi, M.T. 2012. New evidence of conspecificity between *Hipparion primigenium melendezi* Alberdi, 1974 from Los Valles de Fuentidueña (Segovia) and *Hipparion concudense concudense* Pirlot, 1956 from Concud (Teruel) Spain. *Estudios Geológicos,* 68:247–260. https://doi.org/10.3989/egeol.40499.152

Pesquero, M.D., Alcalá, L., and Fernández-Jalvo, Y. 2013. Taphonomy of the reference Miocene vertebrate mammal site of Cerro de la Garita, Spain. *Lethaia*, 46:378–398. https://doi.org/10.1111/let.12016

Peters, R.H. 1983. *The Ecological Implications of Body Size. Cambridge Studies in Ecology*. Cambridge University Press, Cambridge. https://doi.org/10.1017/CBO9780511608551

Rabenold, D. and Pearson, O.M. 2011. Abrasive, silica phytoliths and the evolution of thick molar enamel in primates, with implications for the diet of *Paranthropus boisei*. *PLoS One,* 6:e28379. https://doi.org/10.1371/journal.pone.0028379

Ramdarshan, A., Blondel, C., Brunetière, N., Francisco, A., Gautier, D., Surault, J., and Merceron, G. 2016. Seeds, browse, and tooth wear: a sheep perspective. *Ecology and Evolution,* 6:5559–5569. https://doi.org/10.1002/ece3.2241

Ramdarshan, A., Blondel, C., Gautier, D., Surault, J., and Merceron, G. 2017. Overcoming sampling issues in dental tribology: Insights from an experimentation on sheep. *Palaeontologia Electronica* 19353:1–19. https://doi.org/10.26879/762

Rey, K., Amiot, R., Lécuyer, C., Koufos, G.D., Martineau, F., Fourel, F., Kostopoulos, D.S., and Merceron, G. 2013. Late Miocene climatic and environmental variations in northern Greece inferred from stable isotope compositions (δ18O, δ13C) of equid teeth apatite. *Palaeogeography, Palaeoclimatology, Palaeoecology*, 388:48–57. https://doi.org/10.1016/j.palaeo.2013.07.021

Rivals, F., Solounias, N., and Mihlbachler, M.C. 2007. Evidence for geographic variation in the diets of late Pleistocene and early Holocene *Bison* in North America, and differences from the diets of recent *Bison*. *Quaternary Research,* 68:338–346. https://doi.org/10.1016/j.yqres.2007.07.012

Rodgers, W.A. 1982. The decline of large mammal populations on the Lake Rukwa grasslands, Tanzania. *African Journal of Ecology,* 20:13–22. https://doi.org/10.1111/j.1365-2028.1982.tb01078.x

Saarinen, J.J. 2009. *Body mass patterns of Eurasian Miocene large land mammals and their connections to environment and climate*. Unpublished Master's Thesis, University of Helsinki, Finland.

Saarinen, J.J., Eronen, J., Fortelius, M., Seppä, H., and Lister, A.M. 2016. Patterns of diet and body mass of large ungulates from the Pleistocene of Western Europe, and their relation to vegetation. *Palaeontologia Electronica*, 19:1–58. https://doi.org/10.26879/443

Sanson, G.D., Kerr, S.A. and Gross, K.A. 2007. Do silica phytoliths really wear mammalian teeth? *Journal of Archaeological Science*, 34:526–531. https://doi.org/10.1016/j.jas.2006.06.009

Schubert, B.W., Ungar, P.S., and DeSantis, L.R.G. 2010. Carnassial microwear and dietary behaviour in large carnivorans. *Journal of Zoology*, 280:257–263. https://doi.org/10.1111/j.1469-7998.2009.00656.x

Schulz, E., Piotrowski, V., Clauss, M., Mau, M., Merceron, G., and Kaiser, T.M. 2013. Dietary abrasiveness is associated with variability of microwear and dental surface texture in rabbits. *PLoS One,* 8:e56167. https://doi.org/10.1371/journal.pone.0056167

Scott, J.R. 2012. Dental microwear texture analysis of extant African Bovidae. *Mammalia,* 76:157–174. https://doi.org/10.1515/mammalia-2011-0083

Scott, K.M. 1990. Postcranial dimensions of ungulates as predictors of body mass, p. 301-335. In Damuth, J. and Macfadden, B.J. (eds.), *Body Size in Mammalian Paleobiology: Estimation and Biological Implications*. Cambridge University Press, Cambridge.

Scott, R.S., Clavel, J., DeMiguel, D., Kaya, T., Kostopoulos, D.S., Mayda, S., and Merceron, G. 2013. Ecology of european hipparionines and the diversity of late Miocene hominids in western Eurasia, p. 262. *14th RCMN Congress Neogene to Quaternary Geological Evolution of Mediterranean, Paratethys and Black Sea*. Istanbul, Turkey.

Scott, R.S., Fortelius, M., Huttunen, K., and Armour-Chelu, M. 2003. Abundance of "*Hipparion*," p. 380-397. In Fortelius, M., Kappelman, J., Sen, S., and Bernor, R.L. (eds.), *The Geology and Paleontology of the Miocene Sinap Formation, Turkey*. Columbia University Press.

Scott, R.S., Teaford, M.F., and Ungar, P.S. 2012. Dental microwear texture and anthropoid diets. *American Journal of Physical Anthropology,* 147:551–579. https://doi.org/10.1002/ajpa.22007

Scott, R.S., Ungar, P.S., Bergstrom, T.S., Brown, C.A., Childs, B.E., Teaford, M.F., and Walker, A. 2006. Dental microwear texture analysis: technical considerations. *Journal of Human Evolution,* 51:339–349. https://doi.org/10.1016/j.jhevol.2006.04.006

Scott, R.S., Ungar, P.S., Bergstrom, T.S., Brown, C.A., Grine, F.E., Teaford, M.F., and Walker, A. 2005. Dental microwear texture analysis shows within-species diet variability in fossil hominins. *Nature,* 436:693–695. https://doi.org/10.1038/nature03822

Semprebon, G.M., Rivals, F., Solounias, N., and Hulbert, R.C. 2016. Paleodietary reconstruction of fossil horses from the Eocene through Pleistocene of North America *Palaeogeography, Palaeoclimatology, Palaeoecology*, 442:110–127. https://doi.org/10.1016/j.palaeo.2015.11.004

Smith, B.H. 2000. 'Schultz's Rule' and the evolution of tooth emergence and replacement patterns in primates and ungulates, p. 212-228. In Teaford, M.F., Meredith Smith, M., and Ferguson, M.W.J. (eds.), *Development, Function and Evolution of Teeth*. Cambridge University Press, Cambridge. https://doi.org/10.1017/CBO9780511542626.015

Smith, B.H. 1991. Dental development and the evolution of life history in Hominidae. *American Journal of Physical Anthropology,* 86:157–174. https://doi.org/10.1002/ajpa.1330860206

Smith, G.J. and DeSantis, L.R.G. 2018. Dietary ecology of Pleistocene mammoths and mastodons as inferred from dental microwear textures. *Palaeogeography, Palaeoclimatology, Palaeoecology*, 492:10–25. https://doi.org/10.1016/j.palaeo.2017.11.024

Solounias, N., Rivals, F., and Semprebon, G.M. 2010. Dietary interpretation and paleoecology of herbivores from Pikermi and Samos (late Miocene of Greece). *Paleobiology,* 36:113–136. https://doi.org/10.1666/0094-8373-36.1.113

Solounias, N. and Semprebon, G.M. 2002. Advances in the reconstruction of ungulate ecomorphology with application to early fossil equids. *American Museum Novitates,* 3366:1–49. https://doi.org/10.1206/0003-0082(2002)366<0001:AITROU>2.0.CO;2

Stearns, S.C. 1992. *The Evolution of Life Histories*. Oxford University Press, New York.

Stebbins, G.L. 1981. Coevolution of Grasses and Herbivores. *Annals of the Missouri Botanical Garden,* 68:75-86. https://doi.org/10.1103/PhysRev.34.227

Stirton, R.A. 1947. Observations on evolutionary rates in hypsodonty. *Evolution,* 1:32–41. https://doi.org/10.1111/j.1558-5646.1947.tb02711.x

Strömberg, C.A.E. 2006. Evolution of hypsodonty in equids: testing a hypothesis of adaptation. *Paleobiology,* 32:236–258. https://doi.org/10.1666/0094-8373(2006)32[236:EOHIET]2.0.CO;2

Strömberg, C.A.E., Werdelin, L., Friis, E.M., and Saraç, G. 2007. The spread of grass-dominated habitats in Turkey and surrounding areas during the Cenozoic: Phytolith evidence. *Palaeogeography, Palaeoclimatology, Palaeoecology,* 250:18–49. https://doi.org/10.1016/j.palaeo.2007.02.012

Teaford, M.F. and Oyen, O.J. 1989. In vivo and in vitro turnover in dental microwear. *American Journal of Physical Anthropology,* 80:447-467 https://doi.org/10.1002/ajpa.1330800405

Teaford, M.F., Ungar, P.S., Taylor, A.B., Ross, C.F., and Vinyard, C.J. 2017. In vivo rates of dental microwear formation in laboratory primates fed different food items. *Biosurface and Biotribology*, 3:166–173. https://doi.org/10.1016/J.BSBT.2017.11.005

Tütken, T., Kaiser, T.M., Vennemann, T., and Merceron, G. 2013. Opportunistic feeding strategy for the earliest old world hypsodont equids: evidence from stable isotope and dental wear proxies. *PLoS One,* 8:e74463. https://doi.org/10.1371/journal.pone.0074463

Ungar, P.S., Brown, C.A., Bergstrom, T.S., and Walker, A. 2003. Quantification of dental microwear by tandem scanning confocal microscopy and scale-sensitive fractal analyses. *Scanning,* 25:185–193. https://doi.org/10.1002/sca.4950250405

Ungar, P.S., Merceron, G., and Scott, R.S. 2007. Dental microwear texture analysis of Varswater bovids and early Pliocene paleoenvironments of Langebaanweg, Western Cape Province, South Africa. *Journal of Mammalian Evolution,* 14:163–181. https://doi.org/10.1007/s10914-007-9050-x

Veiberg, V., Mysterud, A., Gaillard, J.M., Delorme, D., Van Laere, G., and Klein, F. 2007. Bigger teeth for longer life? Longevity and molar height in two roe deer populations. *Biology Letters,* 3:268–270. https://doi.org/10.1098/rsbl.2006.0610

Vlachou, T.D. 2013. *Palaeontological, Biostratigraphical and Palaeoecological Study of the Greek Hipparions*. PhD Thesis. Aristotle University of Thessaloniki, Greece. (in Greek with English summary).

Walker, A., Hoeck, H.N., and Perez, L. 1978. Microwear of mammalian teeth as an indicator of diet. *Science,* 201:908–910. https://doi.org/10.1126/science.684415

Wang, L., D'Odorico, P., Ries, L., and Macko, S.A. 2010. Patterns and implications of plant-soil δ13C and δ15N values in African savanna ecosystems. *Quaternary Research*, 73:77–83. https://doi.org/10.1016/j.yqres.2008.11.004

Winkler, D.E., Schulz-Kornas, E., Kaiser, T.M., De Cuyper, A., Clauss, M., and Tütken, T. 2019. Forage silica and water content control dental surface texture in guinea pigs and provide implications for dietary reconstruction. *Proceedings of the National Academy of Sciences of the United States of America,* 116:1325–1330. https://doi.org/10.1073/pnas.1814081116

Winkler, D.E., van den Hoek Ostende, L.W., Schulz, E., Calandra, I., Gailer, J.P., Landwehr, C., and Kaiser, T.M. 2013. Dietary divergence in space and time - Lessons from the dwarf-goat *Myotragus balearicus* (Pleisto-Holocene, Mallorca, Spain). *Mammalian Biology,* 78:430–437. https://doi.org/10.1016/j.mambio.2013.08.003

Woodburne, M.O. 1989. *Hipparion* horses: a pattern of endemic evolution and intercontinental dispersal, p.197-233. In Prothero, D.R. and Schoch, R.M. (eds.), *The Evolution of Perissodactyls*. Oxford University Press, New York.

Woodburne, M.O. and MacFadden, B.J. 1982. A reappraisal of the systematics, biogeography, and evolution of fossil horses. *Paleobiology*, 8:315–327. https://doi.org/10.1017/S0094837300007077

Xia, J., Zheng, J., Huang, D., Tian, Z.R., Chen, L., Zhou, Z., Ungar, P.S., and Qian, L. 2015. New model to explain tooth wear with implications for microwear formation and diet reconstruction. *Proceedings of the National Academy of Sciences of the United States of America*, 112:10669–72. https://doi.org/10.1073/pnas.1509491112

Appendix 1. Information on the hipparionin sample

Appendix 1.1. Western Mediterranean

The Vallesian hipparionins from the western Mediterranean area come from the fossil sites of Can Llobateres, Can Poncic and Santiga. All three localities are situated on the Vallès-Penedès Basin (northeastern Iberian Peninsula) (Fig. 6.1, main text) and are placed on medial to distal facies of alluvial origin (Casanovas-Vilar et al., 2014). The classical fossil site of Can Llobateres registers the early/late Vallesian (MN9/MN10) transition and has been divided into two different levels with estimated ages of 9.72 Ma and 9.65 Ma, respectively (Casanovas-Vilar et al., 2011). Both Can Poncic and Santiga were dated on the early Vallesian with an estimated age of 10.4 to 9.9 Ma (Casanovas-Vilar et al., 2011). Based on a Vallesian hipparionin cranium of the Vallès-Penedès, Pirlot (1956) established the species *Hipparion catalaunicum*. Thereafter, Vallesian hipparionins from this basin have been generally assigned to this taxon. The similarities between this form with the central European *Hipparion primigenium* (= *Hippotherium primigenium* sensu Bernor et al., 1996) (Forsten, 1968; Woodburne and Bernor, 1980) have led some authors to include it within the *H. primigenium* species (Alberdi, 1974; Forsten, 1968; Tomàs et al., 2010), and differentiate it at subspecific level (Alberdi, 1974; Tomàs et al., 2010). The presence of one single large species have been proposed in Can Poncic and Can Llobateres (Scott et al., 2013). We consider both populations to pertain to the *H. primigenium catalaunicum* subspecies following Tomàs et al. (2010). In Santiga, however, it is evident that at least two species are present, an abundant medium-sized to small hipparionin and a much rarer large one (Forsten, 1997). Although unnamed, the small/medium-sized hipparionin from Santiga represent a different taxon compared to larger Vallesian forms, although it might also be related to the *primigenium* group. Here we refer to this form as *Hipparion* sp. (?*primigenium* small). Due to the lack of dentognathic material of the large species from Santiga, we only analyze the microwear texture of the small hipparionin from this site.

The Turolian material from this area come from the localities of Concud, El Arquillo and Venta del Moro. The classical fossil sites from Concud and El Arquillo are located in the Teruel Basin (central eastern Iberian Peninsula), and Venta del Moro in the Cabriel Basin (central eastern Iberian Peninsula) (Fig. 6.1, main text). Both Concud and Venta del Moro sites were formed in marginal lacustrine environments with abundant vegetation (Montoya et al., 2006; Pesquero et al., 2013). The locality of Concud (MN12) has an estimated age of 7.2–7.1 Ma, while El Arquillo and Venta del Moro are dated on the MN13 with estimated ages of 6.2 Ma (van Dam et al., 2001) and 5.8–5.5 Ma (Opdyke et al., 1997), respectively. Recently, however, a magnetostratigraphic study by Gibert et al. 2013 dated Venta del Moro at 6.23 Ma. Still, El Arquillo site is deemed to be older because of the absence of *Paraethomys miocaenicus*, similarly to Las Casiones, which was dated at 6.33

Ma (van Dam, 1997; van Dam et al., 2006). During the middle Turolian (MN12) the most common species was *Hipparion concudense,* a medium to large sized hipparionin [178 kg (Pesquero and Alberdi, 2012)] that is very abundant in Concud (Pesquero and Alberdi, 2012). On the other hand, at least three different sized hipparionins inhabited the Teruel Basin during the late Turolian (MN13). The three sympatric taxa identified in El Arquillo have been referred to *Hipparion periafricanum*, *Hipparion gromovae,* and *H. primigenium truyolsi* (Alberdi, 1974). The two dwarf hipparionins of this site, *H. periafricanum* and *H. gromovae,* are the smallest members of this clade in the Iberian Peninsula (Ortiz-Jaureguizar and Alberdi, 2003; Pesquero, 2003). *H. primigenium truyolsi,* on the other hand, was much larger (Ortiz-Jaureguizar and Alberdi, 2003). An association of three sympatric forms has also been reported in the Venta del Moro. Morphometric comparisons of the most common hipparionin from this site has allowed its assignment to the species *Hipparion matthewi* (Pesquero et al., 2007), which is also present in eastern Mediterranean basins. This identification, however, has recently been questioned (Koufos, 2016b; Koufos and Vlachou, 2016), so here we decided to refer this medium-sized hipparionin as *H.* cf. *matthewi* and to differentiate it from the eastern Mediterranean forms. Pesquero et al. (2007), based on the material from Venta del Moro, also proposed the synonymy of *H. gromovae* and *H. matthewi*. Because we are interested in testing dietary differences related to size, the body mass differences between *H. gromovae* from El Arquillo (84 kg) and *H.* cf. *matthewi* from Venta del Moro (123 kg) (Table 6.1, main text), together with the lack of cranial traits to compare, make us consider both populations two different sets of data. Besides *H.* cf. *matthewi,* there are two other hipparionins present in Venta del Moro: a much rarer large form determined as *H. primigenium,* and a probable smaller subspecies of *H.* cf. *matthewi* (Pesquero et al., 2007). Due to the scarcity of remains assigned to these two last forms, here we only analyze the microwear texture of the medium-sized *H.* cf. *matthewi* from Venta del Moro. All the hipparionin teeth and mandibles from western Mediterranean sites are stored at the collections of the Institut Català de Paleontologia Miquel Crusafont (ICP), Barcelona, and of the Museo Nacional de Ciencias Naturales (MNCN), Madrid.

Appendix 1.2. Balkans

The Vallesian hipparionins pertain to the localities of Ravin de la Pluie and Pentalophos from the Axios Valley (southeastern Balkan Peninsula), and to Nikiti-1, which is located in the Chalkidiki Peninsula (southeastern Balkan Peninsula) (Fig. 6.1, main text). Ravin de la Pluie was dated to the lower part of the late Vallesian (MN10) with an estimated age of ~9.3 Ma based on a combination of biochronological and paleomagnetostratigraphical data (Koufos, 2006a; Sen et al., 2000). Nikiti-1 is correlated based on its mammalian assemblage to the upper part of the late Vallesian with an estimated age ranging from 9.3 to 8.7 Ma (Koufos, 2006b, 2016a). Pentalophos' chronology is not clear, although its faunal association indicates that it could be slightly older than Ravin de la Pluie (Koufos, 2013, 2006a, 2006b). Following Vlachou (2013), two hipparionin morphotypes were present in Macedonia during the Vallesian: the small *macedonicum* and the large *primigenium* morphotype. The material of the small *macedonicum* morphotype has been assigned to the *Hipparion macedonicum* species, while the larger hipparionins of the *primigenium* morphotype have been referred to *Hipparion* aff. *giganteum* in Nikiti-1, and to *Hipparion* cf. *sebastopolitanum* in Pentalophos and Ravin de la Pluie (Koufos et al., 2016; Vlachou, 2013).

Numerous Turolian localities have yielded rich hipparionin assemblages in the Balkan region. The Turolian sample analyzed here comes from the localities of Nikiti-2, Ravin des Zouaves-5, Hadjidimovo, Perivolaki and Dytiko. The oldest fossil site is Nikiti-2 (Chalkidiki Peninsula) (Fig. 6.1, main text), dated to the early Turolian (MN11) with an age comprised between 8.7–8.2 Ma (Koufos, 2016a). Four different hipparionins are recognized here: two small taxa of the *macedonicum* morphotype (*Hipparion sithonis* and *H. macedonicum*), a larger form that pertains to the *dietrichi* morphotype (*Hipparion philippus*), and a rare and large hipparionin of the *proboscideum* group identified as *Hipparion* cf. *proboscideum* (Koufos and Vlachou, 2016; Vlachou, 2013). Ravin des Zouaves-5 (Axios Valley) is also an early Turolian site (MN11) dated at ~8.2 Ma (Koufos, 2006b). In this locality, the species *H. macedonicum*, *H. proboscideum* and *H. philippus* have been recognized (Vlachou, 2013; Koufos and Vlachou, 2016), together with one form pertaining to the *proboscideum* group (Vlachou, 2013). From this site, we analyzed mainly specimens of *H. macedonicum* due to their availability. Hadjidimovo locality (Mesta Valley, central Balkan Peninsula) (Fig. 6.1, main text) was dated between the early-middle Turolian (MN11–MN12) with an estimated age of ~7.5 Ma (Spassov, 2002). Three species have been identified, although the major bulk of the material corresponds to the two large species *Hipparion mediterraneum* (*proboscideum* morphotype sensu Vlachou, 2013) and *Hipparion brachypus* (*primigenium* morphotype sensu Vlachou, 2013) (Hristova, 2009), which are the species herein analyzed. We also sampled the hipparionins from Perivolaki (Thessaly, southeastern Balkan Peninsula) (Fig. 6.1, main text), a site dated on the upper middle Turolian (MN12) with an estimated age of 7.3–7.1 Ma (Koufos, 2006a, 2006b). In Perivolaki, three different species are found: *H. macedonicum, H. philippus* and *H. proboscideum*; forming a similar association than other early and middle Turolian sites from the Axios Valley. Finally, the youngest locality is represented by the three Dytiko sites (DKO, DTK, DIT; Axios Valley) (Fig. 6.1, main text), which were dated to the late Turolian (MN13) (Koufos, 2006b). Three hipparionin taxa are identified in the Dytiko faunal assemblage: the large *Hipparion* aff. *platygenys* (*dietrichi* morphotype sensu Vlachou, 2013), the small *Hipparion* cf. *macedonicum,* and a medium-sized rare form resembling to *Hipparion moldavicum* and tentatively assigned to the *proboscideum* morphotype (Vlachou, 2013). Because of the scarcity of some of the material from the species mentioned, we did not consider for analysis the *proboscideum* group from Nikiti-2 nor from the Dytiko sites, and only include one specimen from Ravin des Zouaves-5. The fossil material analyzed here from Hadjidimovo is stored at the Asenovgrad Museum (a division of the National Museum of Natural History of Sofia, Bulgaria) and the specimens from the Greek localities come from the Laboratory of Geology and Paleontology, Aristotle University of Thessaloniki, Greece.

Appendix 1.3. Western Anatolia

The Turolian hipparionins from the western Anatolian bioprovince come from the localities of Şerefköy-2, Gülpınar and the Samos new collections. The specimens from Samos pertain to the MTLA/B sites found in the Adrianos ravine during the recent excavations (Mytilinii Basin, Samos Island) (Fig. 6.1, main text), which were dated on the late middle Turolian (~7.1 Ma) (Koufos et al., 2009; Vlachou and Koufos, 2009). At least five hipparionin taxa pertaining to four different morphotypes are present there: *H.* cf. *matthewi* (*macedonicum* morphotype), *Hipparion* aff. *forstenae* (*proboscideum* morphotype), *H.* cf. *proboscideum* (*proboscideum* morphotype), *H. dietrichi* (*dietrichi* morphotype) and *H. brachypus* (*primigenium* morphotype) (Vlachou, 2013; Vlachou and Koufos, 2009). In the Anatolian Peninsula, the locality of Şerefköy-2 (Muğla Yatağan Basin, western Anatolia) (Fig. 6.1, main text) has been referred to the middle Turolian (MN12) based on its fossil mammal assemblage (Kaya et al., 2012). Four to five different hipparionin forms might be present in this site, a rare and large species similar to *H. brachypus,* two medium hipparionins broadly referred as *Hipparion*, and two small forms only identified as belonging to the *Cremohipparion* group (sensu Bernor et al., 1996) (Kaya et al., 2012). The medium-sized hipparionins show similarities to *H. mediterraneum* specimens (Kaya et al., 2012). In consequence, we included here the medium sized forms to the *proboscideum* group. We further relate the small hipparionins of Şerefköy-2 to the species *H. matthewi*, as it has been done with the majority of the small-sized forms from eastern Mediterranean basins (Koufos, 2016b), thus including them to the *macedonicum* group defined by Vlachou (2013). Finally, Gülpınar fossil site is located on the Biga Peninsula (northwestern Anatolia) (Fig. 6.1, main text) and corresponds to a sedimentary sequence of fluvial origin dated on early-middle Turolian (MN11–MN12) (Forsten and Kaya, 1995; Koufos et al., 2018). Three different forms have been distinguished in Gülpınar. The smallest hipparionin has been identified as *H.* cf. *matthewi* (*macedonicum* morphotype) and the medium-sized form show affinities to *H. dietrichi* from the classic Samos quarries (Forsten and Kaya, 1995). Due to these similarities, here we include this form to the *dietrichi* group defined by Vlachou (2013). The larger hipparionin remains from Gülpınar have not been determined. We did not analyze the dental microwear textures of the largest taxon—usually related to *H. brachypus* (Kaya et al., 2012; Vlachou and Koufos, 2009)—from the western Anatolian fossil sites due to its scarcity. The material from Samos is stored at the Paleontological Museum of Mytilinii, Samos, Greece, and the material from continental Anatolian sites at the Natural History Museum of Ege University of Izmir, Turkey.

Appendix 1.4. References

Alberdi, M.T. 1974. Las "faunas de *Hipparion*" de los yacimientos españoles. *Estudios Geológicos*, 30:189–212.

Bernor, R.L., Koufos, G.D., Woodburne, M.O., and Fortelius, M. 1996. The evolutionary history and biochronology of European and Southwest Asian Late Miocene and Pliocene hipparionine horses, p. 307-338. In Bernor, R.L., Fahlbusch, V., and Mittmann, H.-W. (eds.), *The Evolution of Western Eurasian Neogene Mammal Faunas*. Columbia University Press, New York.

Casanovas-Vilar, I., Alba, D.M., Garcés, M., Robles, J.M., and Moyà-Solà, S. 2011. Updated chronology for the Miocene hominoid radiation in Western Eurasia. *Proceedings of the National Academy of Sciences of the United States of America*, 108:5554–9. https://doi.org/10.1073/pnas.1018562108

Casanovas-Vilar, I., Van den Hoek Ostende, L.W., Furió, M., and Madern, P.A. 2014. The range and extent of the Vallesian Crisis (Late Miocene): New prospects based on the micromammal record from the Vallès-Penedès basin (Catalonia, Spain). *Journal of Iberian Geology*, 40:29–48. https://doi.org/10.5209/rev_JIGE.2014.v40.n1.44086

Forsten, A. 1968. Revision of the palearctic *Hipparion*. *Acta Zoologica Fennica*, 119:1-134.

Forsten, A. 1997. *Hipparion* from Santiga (Spain) and its biostratigraphic significance. *Paleontologia i Evolució*, 30-31:77–82.

Forsten, A. and Kaya, T. 1995. The hipparions (Mammalia, Equidae) from Gülpinar (Canakkale, Turkey). *Paläontologische Zeitschrift*, 69:491–501. https://doi.org/10.1007/BF02987809

Gibert, L., Scott, R., G., Montoya, P., Ruiz-Sánchez, J.F., Morales, J., Luque, L., Abella, J. and Lería, M. 2013. Evidence for an African-Iberian mammal dispersal during the pre-evaporitic Messinian. Geology, 41:691–694. https://doi.org/10.1130/g34164.1

Hristova, L. 2009. Ontogeny and variability in the cheek region of hipparions from the late Miocene locality of Hadzhidimovo-1, southwest Bulgaria. *Rivista Italiana di Paleontologia e Stratigrafia*, 115:125-132. https://doi.org/10.13130/2039-4942/5924

Kaya, T., Mayda, S., Kostopoulos, D.S., Alcicek, M.C., Merceron, G., Tan, A., Karakutuk, S., Giesler, A.K., and Scott, R.S. 2012. Şerefköy-2, a new Late Miocene mammal locality from the Yataĝan Formation, Muĝla, SW Turkey. *Comptes Rendus – Palevol,*11:5–12. https://doi.org/10.1016/j.crpv.2011.09.001

Koufos, G.D. 2006a. Palaeoecology and chronology of the Vallesian (late Miocene) in the Eastern Mediterranean region. *Palaeogeography, Palaeoclimatology, Palaeoecology*, 234:127–145. https://doi.org/10.1016/j.palaeo.2005.01.014

Koufos, G.D. 2006b. The Neogene mammal localities of Greece: Faunas, chronology and biostratigraphy. *Hellenic Journal of Geosciences*, 41:183–214.

Koufos, G.D. 2013. Neogene mammal biostratigraphy and chronology of Greece, p. 595-621. In Wang, X., Flynn, L.J., and Fortelius, M. (eds.), *Fossil Mammals of Asia—Neogene Biostratigraphy and Chronology.* Columbia University Press, New York.

Koufos, G.D. 2016a. History, stratigraphy and fossiliferous sites, p. 3-10. In Koufos G.D. and Kostopoulos, D.S. (eds.), *Palaeontology of the Upper Miocene Vertebrate Localities of Nikiti (Chalkidiki Peninsula, Macedonia, Greece).Geobios*, 49. https://doi.org/10.1016/j.geobios.2016.01

Koufos, G.D. 2016b. *Hipparion macedonicum* revisited: New data on evolution of hipparionine horses from the Late Miocene of Greece. *Acta Palaeontologica Polonica*, 61:519–536. https://doi.org/10.4202/app.00169.2015

Koufos, G.D., Kostopoulos, D.S., and Merceron, G. 2009. Palaeoecology – Palaeobiogeography, p. 409-430. In Koufos, G.D. and Nagel, D. (eds.), *The late Miocene Mammal Faunas of the Mytilinii Basin, Samos Island, Greece: new collection. Beiträge zur Paläontologie*, 31.

Koufos, G.D., Kostopoulos, D.S., and Vlachou, T.D. 2016. Revision of the Nikiti 1 (NKT) fauna with description of new material, p. 11-22. In Koufos G.D. and Kostopoulos, D.S. (eds.), *Palaeontology of the Upper Miocene Vertebrate Localities of Nikiti (Chalkidiki Peninsula, Macedonia, Greece).Geobios*, 49. https://doi.org/10.1016/j.geobios.2016.01.006,

Koufos, G.D., Mayda, S., and Kaya, T. 2018. New carnivoran remains from the Late Miocene of Turkey. *Paläontologische Zeitschrift,* 92:131–162. https://doi.org/10.1007/s12542-017-0376-2

Koufos, G.D., Vlachou, T.D., 2016. Equidae, p. 85–118. In Koufos G.D. and Kostopoulos, D.S. (eds.), *Palaeontology of the Upper Miocene Vertebrate Localities of Nikiti (Chalkidiki Peninsula, Macedonia, Greece).Geobios*, 49. https://doi.org/10.1016/j.geobios.2016.01.001

Montoya, P., Morales, J., Robles, F., Abella, J., Benavent, J. V, Marín, M. D., and Ruiz Sánchez, F.J. 2006. Las nuevas excavaciones (1995-2006) en el yacimiento del Mioceno final de Venta del Moro, Valencia. *Estudios Geológicos*, 62:313–326.

Opdyke, N., Mein, P., Lindsay, E., Perez-Gonzales, A., Moissenet, E., and Norton, V.L. 1997. Continental deposits, magnetostratigraphy and vertebrate paleontology, late Neogene of eastern Spain. *Palaeogeography, Palaeoclimatology, Palaeoecology*, 133:129–148. https://doi.org/10.1016/S0031-0182(97)00080-1

Ortiz-Jaureguizar, E. and Alberdi, M.T. 2003. El patrón de cambios en la masa corporal de los Hipparionini (Perissodactyla, Equidae) de la Península Ibérica durante el Mioceno superior-Plioceno superior. *Coloquios de Paleontología*, 1:499–509.

Pesquero, M.D. 2003. *Hipparion* del Turoliense superior de Las Casiones (Fosa de Teruel). Coloquios de Paleontología, Volumen Ex:511–548.

Pesquero, M.D. and Alberdi, M.T. 2012. New evidence of conspecificity between *Hipparion primigenium melendezi* Alberdi, 1974 from Los Valles de Fuentidueña (Segovia) and *Hipparion concudense concudense* Pirlot, 1956 from Concud (Teruel) Spain. Estud. Geológicos 68:247–260. https://doi.org/10.3989/egeol.40499.152

Pesquero, M.D., Alberdi, M.T., and Montoya, P. 2007. *Hipparion* (Equidae, Mammalia) from Venta del Moro (Valencia Province, Spain). *Neues Jahrbuch für Geologie und Paläontologie – Abhandlungen*, 243:273–297. https://doi.org/10.1127/0077-7749/2007/0243-0273

Pesquero, M.D., Alcalá, L., and Fernández-Jalvo, Y. 2013. Taphonomy of the reference Miocene vertebrate mammal site of Cerro de la Garita, Spain. *Lethaia* 46:378–398. https://doi.org/10.1111/let.12016

Pirlot, P.L. 1956. *Les Formes Européennes du genre* Hipparion. Consejo Superior de Investigaciones Científicas, Barcelona.

Scott, R.S., Clavel, J., DeMiguel, D., Kaya, T., Kostopoulos, D.S., Mayda, S., and Merceron, G. 2013. Ecology of european hipparionines and the diversity of late Miocene hominids in western Eurasia, p. 262. *14th RCMN Congress Neogene to Quaternary Geological Evolution of Mediterranean, Paratethys and Black Sea*. Istanbul, Turkey.

Sen, S., Kondopoulou, D., and de Bonis, L. 2000. Magnetostratigraphy of Late Miocene continental deposits of the Lower Axios valley, Macedonia, *Geological Society of Greece. Special Publications,* 9:197-206.

Spassov, N. 2002. The Turolian megafauna of west Bulgaria and the character of the Late Miocene "Pikermian biome". *Bollettino della Società Paleontologica Italiana*, 41:69–81.

Tomàs, M., Alba, D.M., Sanisidro, Ó., and Bolet, A. 2010. Los perisodáctilos del Mioceno superior de la autovía orbital de Barcelona B-40, tramo Olesa de Montserrat - Viladecavalls (Cuenca del Vallès-Penedès). *Cidaris,* 30:317–323.

van Dam, J. 1997. The small mammals from the Upper Miocene of the Teruel-Alfambra region (Spain): paleobiology and paleoclimatic reconstructions. Geologica Ultraiectina. Universiteit Utrecht.

van Dam, J., Abdul Aziz, H., Álvarez Sierra, M.A., Hilgen, F.J., Van Den Hoek Ostende, L.W., Lourens, L.J., Mein, P., Van Der Meulen, A.J., and Pelaez-Campomanes, P., 2006. Long-period astronomical forcing of mammal turnover. Nature, 443:687–691. https://doi.org/10.1038/nature05163

van Dam, J.A., Alcalá, L., Zarza, A.A., Calvo, J.P., Garcés, M., and Krijgsman, W. 2001. The upper Miocene mammal record from the Teruel-Alfambra region (Spain). The MN system and continental stage/age concepts discussed. *Journal of Vertebrate Paleontology*, 21:367–385. https://doi.org/10.1671/0272-410.1671/0272-4634(2001)021[0367:TUMMRF]2.0.CO;2

Vlachou, T.D. 2013. *Palaeontological, Biostratigraphical and Palaeoecological Study of the Greek Hipparions*. PhD Thesis. Aristotle University of Thessaloniki, Greece. (in Greek with English summary).

Vlachou, T.D. and Koufos, G.D. 2009. Equidae, p. 207–281 In Koufos, G.D. and Nagel, D. (eds.), *The late Miocene Mammal Faunas of the Mytilinii Basin, Samos Island, Greece: new collection. Beiträge zur Paläontologie*, 31.

Woodburne, M.O. and Bernor, R.L. 1980. On superspecific groups of some Old World hipparionine horses. *Journal of Paleontology*, 54:1319–1348.

Appendix 2. Raw data of all the hipparionin sample analyzed (attached separately as a .xls): https://data.mendeley.com/datasets/np65bh8tgw/draft?a=ead03d9e-6f2a-4bf8-b2b7-9821cb1f8d45

Appendix 3. Photosimulations of the microwear surfaces (attached separately as a .pdf): https://data.mendeley.com/datasets/np65bh8tgw/draft?a=ead03d9e-6f2a-4bf8-b2b7-9821cb1f8d45

Appendix 4. Results of the Principal Component Analysis of the heterogeneity settings

Results of the Principal Component Analysis performed with the ten settings used to calculate *HAsfc* (4, 9, 16, 25, 36, 49, 64, 81, 100, and 121 cells). Percentage of variance explained by the principal component and the contribution of each setting to the principal components are shown.

		% contribution to the variance of the principal components									
Component	% of variance	H4	H9	H16	H25	H36	H49	H64	H81	H100	H121
PC1	84.31	5.11	8.26	9.87	10.69	11.06	11.09	11.15	10.99	10.89	10.89
PC2	7.88	60.94	15.86	3.57	0.02	0.62	2.46	2.68	4.66	5.18	4.03

Appendix 5. Metapodial measures and body mass estimations (attached .xls file): https://data.mendeley.com/datasets/np65bh8tgw/draft?a=ead03d9e-6f2a-4bf8-b2b7-9821cb1f8d45

Appendix 6. Linear regressions on DMT parameters versus body mass

Appendix 6.1. Linear regressions of microwear textural parameters and the calculated principal component against body mass for all hipparionins. Correlation statistics included in each graph.

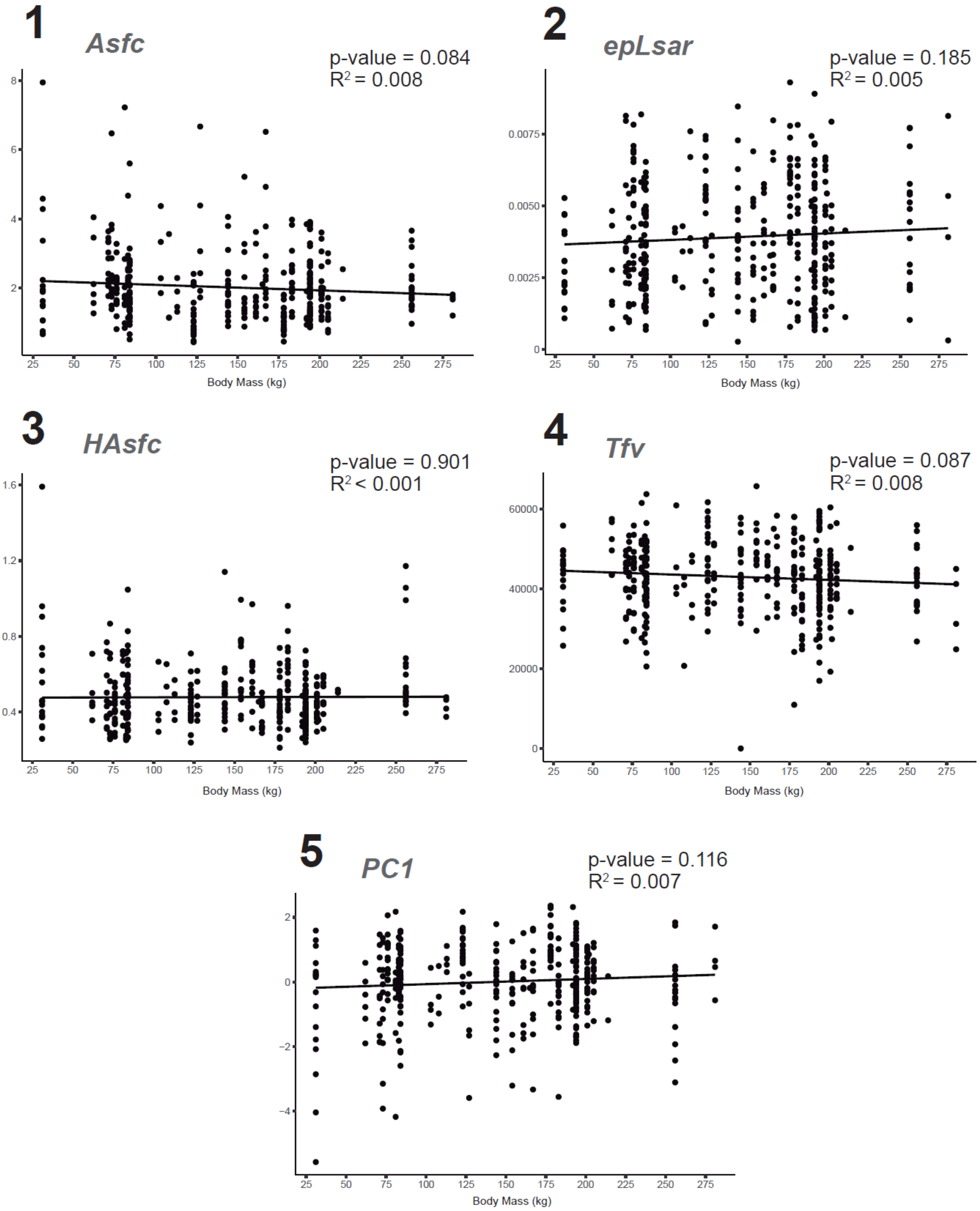

Appendix 6.2. Linear regressions of microwear textural parameters and the calculated principal component against body mass for western Mediterranean hipparionins. Correlation statistics included in each graph.

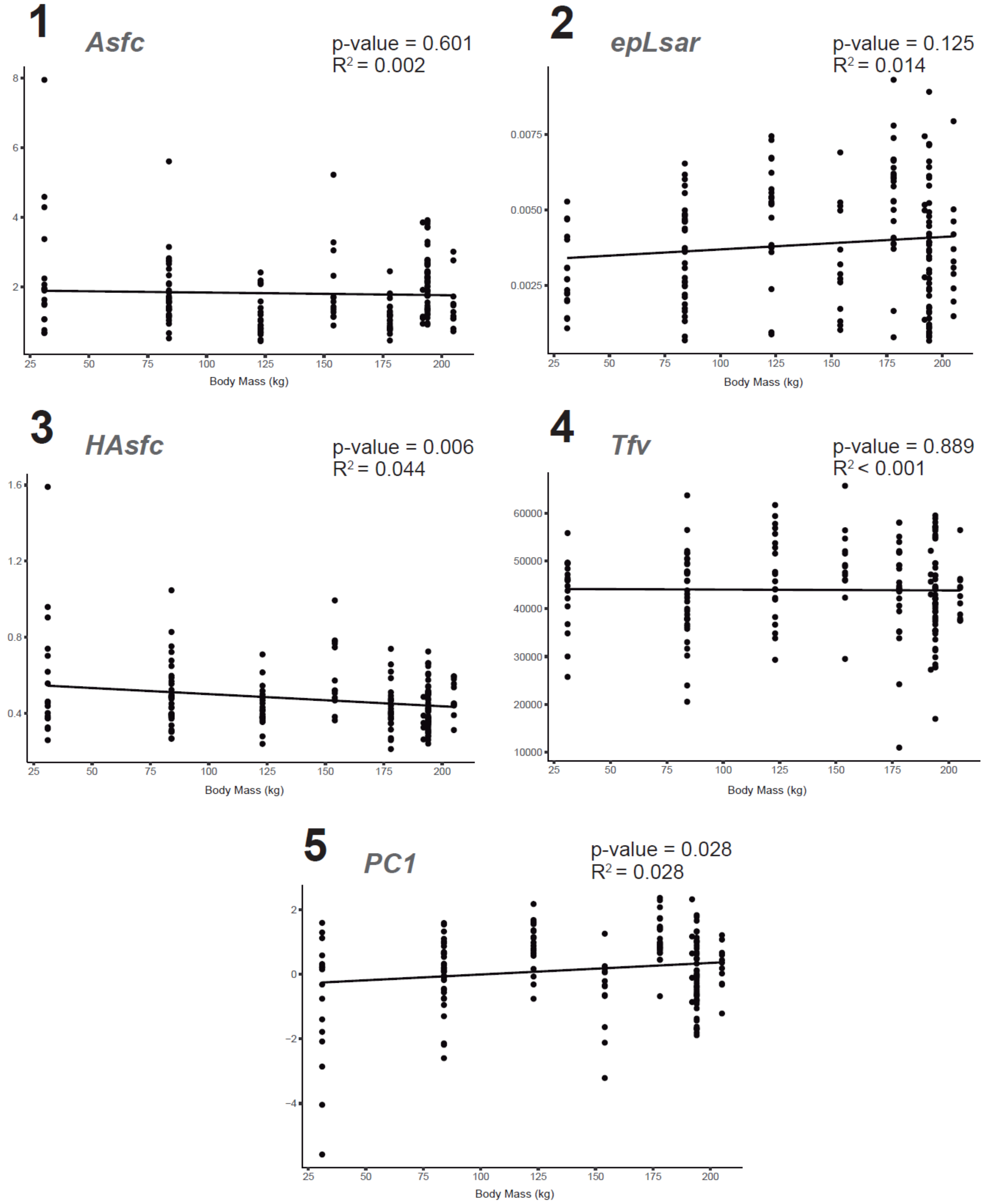

Appendix 6.3. Linear regressions of microwear textural parameters and the calculated principal component against body mass for hipparionins from the Balkans. Correlation statistics included in each graph.

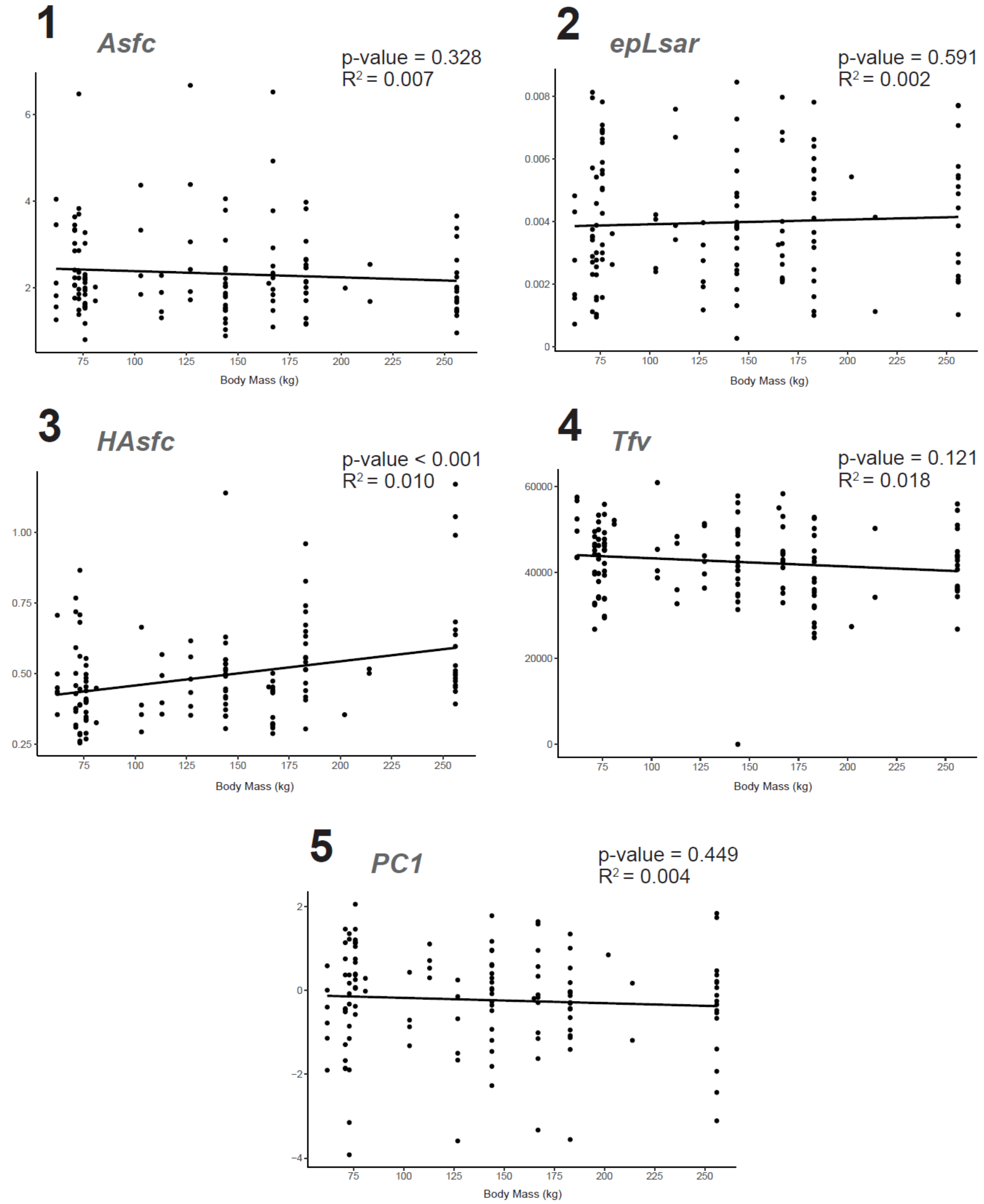

Appendix 6.4. Linear regressions of microwear textural parameters and the calculated principal component against body mass for western Anatolian hipparionins. Correlation statistics included in each graph.

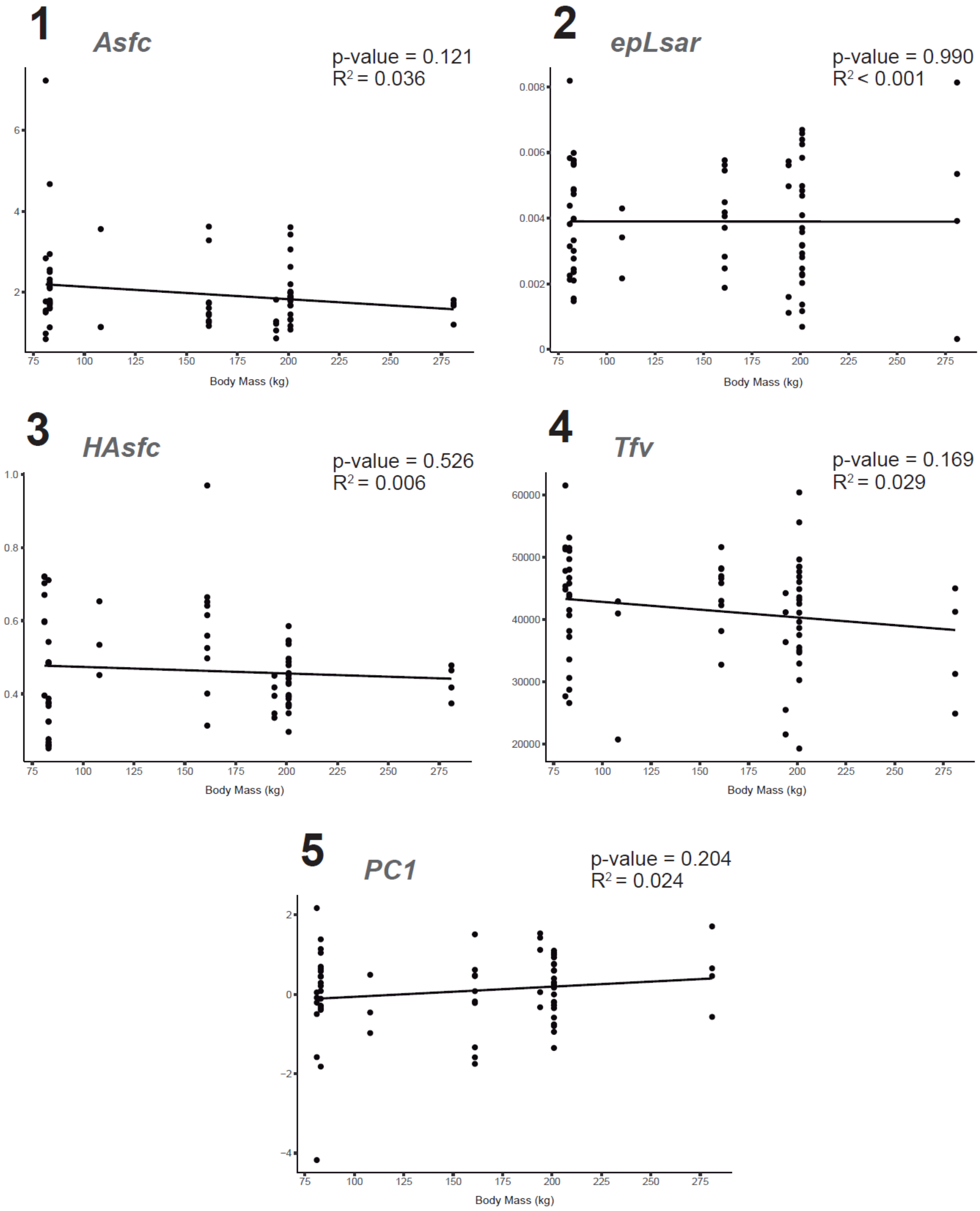

Appendix 7. Post-hoc pairwise comparisons with all hipparionin data

Appendix 7.1. Post-hoc tests on Age-Size interaction considering ranked complexity (*Asfc*) parameter. P-values from HSD test are depicted above the grey diagonal and those from LSD are under it. Significant p-values represented in bold.

Asfc		**Vallesian**		**Turolian**	
Age x Size		**Small**	**Large**	**Small**	**Large**
Vallesian	Small		0.901	0.999	0.509
	Large	0.490		0.768	**0.002**
Turolian	Small	0.889	0.334		**0.012**
	Large	0.167	**< 0.001**	**0.002**	

Appendix 7.2. Post-hoc tests on Region-Size interaction considering ranked anisotropy (*epLsar*) parameter. P-values from HSD test are depicted above the grey diagonal and those from LSD are under it. Significant p-values represented in bold.

epLsar		**Western Mediterranean**		**Eastern Mediterranean**	
Region x Size		**Small**	**Large**	**Small**	**Large**
Western Mediterranean	Small		**0.028**	0.266	0.156
	Large	**0.005**		0.801	0.806
Eastern Mediterranean	Small	0.070	0.365		0.999
	Large	**0.037**	0.370	0.911	

Appendix 7.3. Post-hoc on Region-Size interaction considering ranked *HAsfc*. HSD test p-values shown above the diagonal and LSD under it. Significant p-values in bold.

HAsfc		**Western Mediterranean**		**Eastern Mediterranean**	
Region x Size		**Small**	**Large**	**Small**	**Large**
Western Mediterranean	Small		**0.013**	0.059	0.992
	Large	**0.003**		0.981	**0.006**
Eastern Mediterranean	Small	**0.012**	0.701		**0.044**
	Large	0.780	**0.001**	**0.009**	

Appendix 7.4. Post-hoc on Age-Region interaction considering ranked *HAsfc*. HSD test p-values shown above the diagonal and LSD under it. Significant p-values in bold.

HAsfc		**Western Mediterranean**		**Eastern Mediterranean**	
Age x Region		**Vallesian**	**Turolian**	**Vallesian**	**Turolian**
Western Mediterranean	Vallesian		0.899	0.242	0.877
	Turolian	0.488		0.441	0.322
Eastern Mediterranean	Vallesian	0.062	0.136		0.069
	Turolian	0.455	0.089	**0.015**	

Appendix 7.5. Post-hoc on Age-Size interaction considering ranked *Tfv*. HSD test p-values shown above the diagonal and LSD under it. Significant p-values in bold.

Tfv		**Vallesian**		**Turolian**	
Age x Size		**Small**	**Large**	**Small**	**Large**
Vallesian	Small		**0.029**	0.059	**0.017**
	Large	**0.006**		0.912	1.000
Turolian	Small	**0.012**	0.509		0.847
	Large	**0.003**	0.999	0.415	

Appendix 8. Post-hoc pairwise comparisons with Turolian hipparionin data

Appendix 8.1. Post-hoc tests on ranked complexity (*Asfc*). P-values from HSD test are depicted above the grey diagonal and those from LSD are under it. Significant p values represented in bold.

BIOPROVINCE	Western Mediterranean	Balkans	Western Anatolia
Western Mediterranean		**< 0.001**	**0.001**
Balkans	**< 0.001**		**0.011**
Western Anatolia	**< 0.001**	**0.004**	

Appendix 8.2. Post-hoc tests on ranked heterogeneity of complexity (*HAsfc*). P-values from HSD test are depicted above the grey diagonal and those from LSD are under it. Significant p-values represented in bold.

BIOPROVINCE	Western Mediterranean	Balkans	Western Anatolia
Western Mediterranean		**0.049**	0.935
Balkans	**0.019**		0.189
Western Anatolia	0.727	0.081	

Appendix 8.3. Summary of post-hoc tests on ranked parameters showing significant differences between the Turolian hipparionin groups. Significant differences between groups obtained from HSD test are depicted above the grey diagonal and those from LSD are under it.

Bioprovince		West Mediterranean					Balkans				Western Anatolia		
Turolian hipparionin groups		*periafricanum*	*gromovae*	cf. *matthewi*	*concudense*	*primigenium*	*macedonicum*	*dietrichi*	*proboscideum*	*primigenium*	*macedonicum*	*dietrichi*	*proboscideum*
Western Mediterranean	*periafricanum*			*epLsar*	*Asfc, epLsar, PC1*								
	gromovae				*Asfc, epLsar, PC1*		*Asfc*						
	cf. *matthewi*	*Asfc, epLsar, PC1*	*Asfc, epLsar, PC1*				*Asfc*	*Asfc*	*Asfc, PC1*	*Asfc, PC1*	*Asfc, PC1*		*Asfc*
	concudense	*Asfc, epLsar, PC1*	*Asfc, epLsar, PC1*				*Asfc, PC1*	*Asfc, PC1*	*Asfc, PC1*	*Asfc, HAsfc, PC1*	*Asfc, PC1*	*PC1*	*Asfc, PC1*
	primigenium	*HAsfc*	*HAsfc*							*HAsfc*			
Balkans	*macedonicum*	*Asfc, epLsar*	*Asfc,*	*Asfc, PC1*	*Asfc, epLsar, PC1*	*Asfc,*				*HAsfc*			
	dietrichi		*Asfc,*	*Asfc, epLsar, PC1*	*Asfc, epLsar, PC1*	*HAsfc,*							
	proboscideum	*epLsar, PC1*	*Asfc, HAsfc, PC1*	*Asfc, HAsfc, PC1*	*Asfc, epLsar, HAsfc, PC1*	*Asfc, HAsfc, PC1*	*HAsfc, PC1*	*PC1*					*HAsf*
	primigenium	*epLsar*	*HAsfc*	*Asfc, HAsfc, PC1*	*Asfc, epLsar, HAsfc, PC1*	*HAsfc*	*HAsfc*	*HAsfc*					*HAsfc*
Western Anatolia	*macedonicum*			*Asfc, PC1*	*Asfc, epLsar, PC1*				*HAsfc*	*HAsfc*			
	dietrichi			*Asfc, HAsfc, PC1*	*Asfc, epLsar, HAsfc, PC1*	*HAsfc*	*Asfc, HAsfc*		*Asfc*		*HAsfc*		
	proboscideum	*epLsar*		*Asfc, PC1*	*Asfc, epLsar, PC1*		*Asfc*		*Asfc, HAsfc, PC1*	*HAsfc*		*HAsfc*	

Appendix 8.4. Summary of post-hoc tests on parameters showing significant differences between localities. Here represented the results from pairwise comparisons between localities with hipparionins of the *macedonicum* group. Significant differences obtained from the HSD test are above the grey diagonal and those from LSD are under it.

***macedonicum* group**		**Balkans**				**Western Anatolia**		
	Locality	**NIK**	**RZO**	**PER**	**DTK**	**GLP**	**MYSE**	**MTLA/B**
Balkans	Nikiti-2 (NIK)			*epLsar*				
	Ravin des Zouaves-5 (RZO)	*epLsar*						
	Perivolaki (PER)	*epLsar, PC1*						
	Dytiko (DTK)	*epLsar, PC1*	*Tfv*					
Western Anatolia	Gülpınar (GLP)	*HAsfc, PC1*	*HAsfc*	*HAsfc*			*HAsfc*	
	Şerefköy-2 (MYSE)	*epLsar*			*Tfv*	*HAsfc*		
	Samos (MTLA/B)				*Tfv*		*HAsfc*	

Appendix 8.5. Summary of post-hoc tests on parameters showing significant differences between localities. Here represented the results from pairwise comparisons between localities with hipparionins of the *dietrichi* group. Significant differences obtained from the HSD test are above the grey diagonal and those from LSD are under it.

***dietrichi* group**		**Balkans**			**Western Anatolia**	
	Locality	**NIK**	**PER**	**DTK**	**GLP**	**MTLA/B**
Balkans	Nikiti-2 (NIK)					
	Perivolaki (PER)	*epLsar, PC1*				
	Dytiko (DTK)					
Western Anatolia	Gülpınar (GLP)					
	Samos (MTLA/B)	*epLsar*				

Appendix 8.6. Summary of post-hoc tests on parameters showing significant differences between localities. Here represented the results from pairwise comparisons between localities with hipparionins of the *proboscideum* group. Significant differences obtained from the HSD test are above the grey diagonal and those from LSD are under it.

proboscideum group		**Balkans**			**Western Anatolia**	
	Locality	**RZO**	**PER**	**HD**	**MYSE**	**MTLA/B**
Balkans	Ravin des Zouaves-5 (RZO)					
	Perivolaki (PER)	*Tfv*				
	Hadjidimovo (HD)					
Western Anatolia	Şerefköy-2 (MYSE)			*HAsfc*		
	Samos (MTLA/B)		*Tfv, PC1*	*HAsfc, PC1*	*Tfv*	

Appendix 8.7. Summary of post-hoc tests on parameters showing significant differences between localities. Here represented the results from pairwise comparisons between localities with hipparionins of the *primigenium* group. Significant differences obtained from the HSD test are above the grey diagonal and those from LSD are under it.

***primigenium* group**		**Western Mediterranean**	**Balkans**
Locality		**ARQ**	**HD**
Western Mediterranean	El Arquillo (ARQ)	HSD test →	
Balkans	Hadjidimovo (HD)	*HAsfc*	← LSD test

Appendix 8.8. Results of the post-hoc tests from pairwise comparisons between hipparionin groups from Nikiti-2 locality. Significant p-values represented in bold.

Nikiti-2 (NIK)	***macedonicum***	***dietrichi***
macedonicum	HSD test →	*Asfc:* - *epLSar:* 1.000 *HAsfc:* 1.000 *Tfv:* 1.000 *PC1:* 1.000
dietrichi	*Asfc:* - *epLSar:* 0.968 *HAsfc:* 0.480 *Tfv:* 0.667 *PC1:* 0.811	← LSD test

Appendix 8.9. Results of the post-hoc tests from pairwise comparisons between hipparionin groups from Perivolaki locality. Significant p-values represented in bold.

Perivolaki (PER)	***macedonicum***	***dietrichi***	***proboscideum***
macedonicum	HSD test →	*Asfc:* - *epLSar:* 1.000 *HAsfc:* 1.000 *Tfv:* 1.000 *PC1:* 1.000	*Asfc:* - *epLSar:* 1.000 *HAsfc:* 1.000 *Tfv:* 1.000 *PC1:* 1.000
dietrichi	*Asfc:* - *epLSar:* 0.813 *HAsfc:* 0.569 *Tfv:* 0.997 *PC1:* 0.389		*Asfc:* - *epLSar:* 1.000 *HAsfc:* 1.000 *Tfv:* 1.000 *PC1:* 1.000
proboscideum	*Asfc:* - *epLSar:* 0.744 *HAsfc:* 0.779 *Tfv:* 0.184 *PC1:* 0.203	*Asfc:* - *epLSar:* 0.669 *HAsfc:* 0.997 *Tfv:* 0.198 *PC1:* 0.408	← LSD test

Appendix 8.10. Results of the post-hoc tests from pairwise comparisons between hipparionin groups from Hadjidimovo locality. Significant p-values represented in bold.

Hadjidimovo (HD)	***proboscideum***	***primigenium***
proboscideum	HSD test →	*Asfc*: - *epLSar:* 1.000 *HAsfc*: 1.000 *Tfv*: 1.000 *PC1:* 1.000
primigenium	*Asfc*: - *epLSar:* 0.970 *HAsfc*: 0.990 *Tfv*: 0.257 *PC1:* 0.187	← LSD test

Appendix 8.11. Results of the post-hoc tests from pairwise comparisons between hipparionin groups from Dytiko locality. Significant p-values represented in bold.

Dytiko (DTK)	***macedonicum***	***dietrichi***
macedonicum	HSD test →	*Asfc*: - *epLSar:* 0.998 *HAsfc*: 1.000 *Tfv*: 0.913 *PC1:* 1.000
dietrichi	*Asfc*: - *epLSar:* 0.144 *HAsfc*: 0.806 *Tfv*: **0.040** *PC1:* 0.323	← LSD test

Appendix 8.12. Results of the post-hoc tests from pairwise comparisons between hipparionin groups from Gülpınar locality. Significant p-values represented in bold.

Gülpınar (GLP)	***macedonicum***	***dietrichi***
macedonicum	HSD test →	*Asfc*: - *epLSar:* 1.000 *HAsfc*: 1.000 *Tfv*: 1.000 *PC1:* 1.000
dietrichi	*Asfc*: - *epLSar:* 0.991 *HAsfc*: 0.448 *Tfv*: 0.444 *PC1:* 0.516	← LSD test

Appendix 8.13. Results of the post-hoc tests from pairwise comparisons between hipparionin groups from Samos new collections. Significant p-values represented in bold.

Samos (MTLA/B)	*macedonicum*	*dietrichi*	*proboscideum*
macedonicum	HSD →	*Asfc:* - *epLSar:* 1.000 *HAsfc:* 1.000 *Tfv:* 1.000 *PC1:* 1.000	*Asfc:* - *epLSar:* 1.000 *HAsfc:* 0.971 *Tfv:* 1.000 *PC1:* 0.995
dietrichi	*Asfc:* - *epLSar:* 0.663 *HAsfc:* 0.353 *Tfv:* 0.850 *PC1:* 0.691		*Asfc:* - *epLSar:* 1.000 *HAsfc:* 1.000 *Tfv:* 1.000 *PC1:* 1.000
proboscideum	*Asfc:* - *epLSar:* 0.475 *HAsfc:* 0.066 *Tfv:* 0.902 *PC1:* 0.111	*Asfc:* - *epLSar:* 0.213 *HAsfc:* 0.479 *Tfv:* 0.723 *PC1:* 0.267	← LSD

Appendix 8.14. Results of the post-hoc tests from pairwise comparisons between hipparionin groups from Şerefköy-2 locality. Significant p-values represented in bold.

Şerefköy-2 (MYSE)	*macedonicum*	*proboscideum*
macedonicum	HSD test →	*Asfc:* - *epLSar:* 1.000 *HAsfc:* 0.997 *Tfv:* 1.000 *PC1:* 1.000
proboscideum	*Asfc:* - *epLSar:* 0.972 *HAsfc:* 0.124 *Tfv:* 0.881 *PC1:* 0.659	← LSD test

Appendix 8.15. Results of the post-hoc tests from pairwise comparisons between hipparionin groups from El Arquillo locality. Significant p-values represented in bold.

El Arquillo (ARQ)	***periafricanum***	***gromovae***	***primigenium***
periafricanum	HSD →	*Asfc*: - *epLSar*: 1.000 *HAsfc*: 1.000 *Tfv*: 1.000 *PC1*: 1.000	*Asfc*: - *epLSar*: 0.995 *HAsfc*: 0.840 *Tfv*: 1.000 *PC1*: 1.000
gromovae	*Asfc*: - *epLSar*: 0.175 *HAsfc*: 0.645 *Tfv*: 0.779 *PC1*: 0.743		*Asfc*: - *epLSar*: 1.000 *HAsfc*: 0.909 *Tfv*: 0.985 *PC1*: 1.000
primigenium	*Asfc*: - *epLSar*: 0.112 *HAsfc*: **0.027** *Tfv*: 0.970 *PC1*: 0.604	*Asfc*: - *epLSar*: 0.397 *HAsfc*: **0.039** *Tfv*: 0.830 *PC1*: 0.450	← LSD

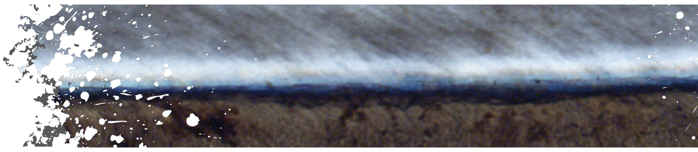

Chapter 7

General Discussion

Chapter 7
General Discussion

This PhD thesis has focused on exploring the life history (LH) and ecology of hipparionin horses that inhabited the circum-Mediterranean area during the late Miocene. Its underlying aim was to shed light on the trend of decreasing body size occurring in this group within the framework of life history theory (LHT). In order to do this, bone and dental tissues were analyzed and the dental microwear textures quantified among different hipparionin populations. The paleohistological results that were obtained allowed the reconstruction of the growth pattern of skeletal (Chapter 4) and dental (Chapter 5) elements of different-sized hipparionin forms. Based on previous histological studies on extant equids (Nacarino-Meneses et al., 2016b, 2017; Nacarino-Meneses and Köhler, 2018), and the inclusion of comparative *Equus* material, key LH information has been extracted from the paleohistological data (Chapters 4 and 5). Thereafter, the reconstruction of the dietary preferences of some hipparionin populations and their relation to body size (Chapter 6) have given clues to the environments in which these circum-Mediterranean hipparionins dwelt. The ecological interpretations obtained through the reconstructed growth strategies (Chapters 4 and 5) applying an LH predictive model (Palkovacs, 2003) have then been contrasted with the inferred ecological preferences of various hipparionin groups (Chapter 6). In the following chapter, I provide an overview of the main findings presented in this thesis, interpret the results in light of previous studies, and focus on how and why some hipparionin lineages underwent reductions in body size. To the best of my knowledge, this is the first time that data from paleohistological and dental wear analyses have been integrated into a study on shifts in body size in continental taxa from an LHT perspective.

7.1. Bone and Dental Histology in Hipparionins

7.1.1. Metapodial Growth

Thanks to the application of long bone histology in living taxa (Castanet et al., 2004; García-Martínez et al., 2011; Köhler et al., 2012; Marín-Moratalla et al., 2013; Nacarino-Meneses et al., 2016ab; Calderón et al., 2019), the LHs of extinct mammals can be inferred through the study of their fossilized bone microstructure (Köhler and Moyà-Solà, 2009; Martinez-Maza et al., 2014; Amson et al., 2015; Kolb et al., 2015; Moncunill-Solé et al., 2016; Nacarino-Meneses and Orlandi-Oliveras, 2019). Therefore, in order to reconstruct the growth patterns and make inferences on the LHs, bone histology has been analyzed and compared in the metapodials of eastern Mediterranean hipparionins with both small (*macedonicum* morphotype) and large body sizes (*primigenium* and *dietrichi* morphotypes), together with that of a western Mediterranean small form (*H. gromovae*) and a larger one (*H. primigenium truyolsi*). Although Horner et al. (1999) discouraged the use of metapodials for the reconstruction of growth patterns in dinosaurs, recent work has supported its value in both extant (Nacarino-Meneses et al., 2016b) and extinct (Martinez-Maza et al., 2014) equids. Our observations on hipparionin metapodial histology (Chapter 4) agree with these more recent studies, as metapodials do not show a major process of medullary resorption nor do they show an intense remodeling that could potentially erase the growth record.

The rate at which bone is deposited is reflected by the type of bone tissue and its vascular arrangement (de Margerie et al., 2002, 2004). In a previous study, Martinez-Maza et al. (2014) described the metapodial microstructure of a medium to large-sized hipparionin as being composed of a fibrolamellar complex (FLC) with longitudinal primary osteons arranged in circular rows, such as can be seen in both living and fossil *Equus* species (Stover et al., 1992; Sander and Andrássy, 2006; Cuijpers and Lauwerier, 2008; Nacarino-Meneses et al., 2016b; Nacarino-Meneses and Orlandi-Oliveras, 2019). All the hipparionin groups analyzed here conform to this pattern, with only few of the specimens showing local variations of the vascular orientation in parts of their cortex (Fig. 1B and 1C in Chapter 4), which could be linked to minor differences in the rate of bone deposition (de Margerie et al., 2004). In most of the metapodials, we also identified a change in the vascularity and in the amount of parallel fibered component at the innermost cortex (Fig. 1A in Chapter 4). We related this observation to a non-cyclical growth mark signaling the moment of birth (neonatal line), as recently described in extant asses and zebras (Nacarino-Meneses and Köhler, 2018). The identification of this mark provided us with a rough estimate of the size at birth and a time-zero point for the reconstruction of the growth curves through skeletochronology (Lee et al., 2013). The metapodial radial growth in hipparionins was then properly adjusted to sigmoidal logistic curves (Zullinger et al., 1984; Lee et al., 2013) (Fig. 5 in Chapter 4), such as in the case of some dinosaurian long bones (Bybee et al., 2006; Lee and O'Connor, 2013). The curve fitting allowed us to quantitatively assess characteristic growth parameters and bone growth rates (Table 1 in Chapter 4).

Although neonates in some dwarfed insular mammals have been shown to be smaller than predicted from allometry (Köhler, 2010), our analyses revealed that size at birth in hipparionins was proportional to the adult size (Fig. 4A in Chapter 4). Moreover, the growth rate during the first year of growth was allometrically related to the final asymptotic size in the analyzed taxa (Fig. 4B in Chapter 4). This means that metapodials of larger hipparionins start to grow proportionally larger and relatively faster than in the case of the dwarfed forms; something that conforms to the scaling predictions (Case, 1978; Calder, 1984). Similarly, higher bone growth rates in larger forms have been identified from bone histology in cervids (Amson et al., 2015; Kolb et al., 2015) and also among extant wild equids and domestic horse breeds in the course of the research for this thesis (Suppl. Fig. S3 in Chapter 4).

In addition to the growth rate, the time span devoted to growth also determines the size of the adult (Roff, 2002). In this regard, the occurrence of slow-growing lamellar tissue in the outermost periosteum (external fundamental system, EFS) has typically been related to the finalization of bone growth (skeletal maturity) (Cormack, 1987; Woodward et al., 2013). Thus, counting the cyclical growth marks (CGMs) deposited before the EFS is supposed to indicate the annual growth cycles that occurred before maturity attainment (Woodward et al., 2013). In most metapodials of *H. concudense,* Martinez-Maza et al. (2014) identified two CGMs within their cortex, and in *Equus hemionus*, Nacarino-Meneses et al. (2016b) reported two CGMs in the metapodials of a mare, but three in those of a stallion. On the other hand, Nacarino-Meneses and Orlandi-Oliveras (2019) have found more than four CGMs in the metapodial cortexes of some of the largest equid representatives (*Equus mosbachensis* and *Equus steinheimensis*). In our sample, we observed that all the metapodials continued to grow after the first growth cycle, and that another CGM is subsequently deposited before the formation of the EFS (Fig. 2 and 3 in Chapter 4). In the *H. gromovae* metapodials, however, we identified three or more CGMs before the appearance of the EFS (Fig 2D and 3D in Chapter 4), while in some specimens of the *macedonicum* morphotype the second CGM is deposited near the periosteum (Fig. 2C and 3E in Chapter 4). This narrower growth zone suggests an earlier maturity (Chinsamy and Valenzuela, 2008) in the *macedonicum* hipparionins, whereas in *H. gromovae* the higher number of CGMs in the cortex suggests an extended growth period.

Nevertheless, the interpretation of the occurrence of EFS in mammalian bone is complex. Generally, its deposition is linked to epiphyseal fusion and, thus, to reaching skeletal maturity (Kolb et al., 2015; Calderón et al., 2019). Some authors, moreover, have related EFS formation in certain elements (i.e., femurs) to the onset of the reproductive maturity (Marín-Moratalla et al., 2013;

Jordana et al., 2016; Nacarino-Meneses et al., 2016b). Research in close-related, extant species is therefore essential for correctly interpreting how the growth and LH of an extinct organism is recorded in the microstructure of a specific bone (Woodward et al., 2013). In this regard, Nacarino-Meneses et al. (2016b) noted that the EFS deposition in equid metapodials is not directly related to any LH event; rather, the significant decrease in the bone radial growth signals epiphyseal closure and, thus, the end of the longitudinal growth of the bone. In contrast with other bones that keep growing for longer periods, such as femurs (Silver, 1969), metapodials merely provide a relative age of growth cessation instead of the absolute age at which the organism attains physiological or reproductive maturity. This idea is further supported by the earlier metapodial maturity estimated in *H. gromovae* (after approximately 2 ½ years, see Chapter 4) in comparison with the later maturity inferred from the third molar eruption (at the third year, see Chapter 5). In this thesis, this relative maturity considered within the context of body size has allowed us to examine whether differences in equid size were coupled with shifts in growth strategies.

In extant hemiones, although the metapodials of a male exhibited three CGMs before the EFS deposition and two in a female, the significant decrease in growth rate (relative maturity) occurred in both cases in the second year of life (Nacarino-Meneses et al., 2016b). Similarly, metapodials of zebras and large Middle Pleistocene equids tend to show this growth rate drop in the second year after birth (Nacarino-Meneses and Orlandi-Oliveras, 2019). In this dissertation, the growth curves of hipparionin metapodials (Fig. 5 in Chapter 4) and the logistic growth parameters (Table 1 in Chapter 4) have helped to compare the growth trajectories of the different groups. Our results have indicated that the metapodials of the larger eastern Mediterranean morphs (*primigenium* and *dietrichi*) approached their final size and showed a significant decrease in growth rate well after their second year, later than those of the smaller form (*macedonicum*). The small metapodials of *H. gromovae* from the western Mediterranean follow a similar growth trajectory to those of the eastern large *primigenium* and *dietrichi* hipparionins; hence, reducing their growth rate later than the *macedonicum* group and the single *H. primigenium truyolsi* specimen (Fig. 5 in Chapter 4). Consequently, and in line with what was observed when counting the CGMs, the two dwarf groups had different growth strategies: while *H. gromovae* matured relatively late considering its size, the *macedonicum* form had a faster LH characterized by earlier maturity attainment. Moreover, considering the studies on the metapodial growth in extant equids (Nacarino-Meneses et al., 2016b; Nacarino-Meneses and Orlandi-Oliveras, 2019), our results suggest that some hipparionins matured relatively late, or at a comparable moment with larger *Equus* species. Finer LH reconstructions can be performed in the future based on the histology of fossilized femurs, helping to contrast or support the inferences obtained from metapodial growth.

7.1.2. Dental Growth

The study of tooth growth through dental histology is also increasingly applied to reconstructing the LH of mammalian taxa (Schwartz et al., 2002; Dean, 2006; Dirks and Bowman, 2007; Dirks et al., 2009; Hogg and Walker, 2011; Jordana and Köhler, 2011) due to the close relationship between LH and the rate and timing of the formation and eruption of teeth (Smith, 2000; Jordana et al., 2014; Veitschegger and Sánchez-Villagra, 2016; Hogg, 2018). Therefore, in order to make inferences on the hipparionins' LHs, their enamel histology has been explored here in lower molars from western Mediterranean hipparionins with large (*H. concudense*) and small body sizes (*H. gromovae* and *H. periafricanum*), and in an extant equid (*E. quagga*) for comparison. To my knowledge, this is the first time that dental formation has been analyzed and directly compared in two distinct sets of teeth (first/second molars and third molars) in a non-primate group. The tooth growth has hence been characterized for each species during the immature stage (m1/m2 formation) and during the period close to maturity attainment (m3 formation). Moreover, this has allowed us to estimate the timing of two key LH events, as the eruption of the first and the third molars are respectively linked to weaning and age at maturity (Smith, 1994, 2000; Dean, 2006).

7.1.2.1. Enamel Formation

In order to calculate the parameters that describe enamel growth, dental histology studies rely on the identification of periodic incremental markings (Smith, 2006). As it is not possible to directly test the periodicity of marks found in the enamel of fossil taxa, the understanding of the enamel histology on extant analogs becomes essential. In general, research that is based on this method has mostly been focused on low-crowned primate teeth (see review in Smith, 2008), from where incremental features have been extensively characterized (Dean, 2006; Smith, 2006). On the other hand, the histological study of tooth formation in high-crowned ungulates has been overlooked, until some recent studies have started to address it (e.g., Iinuma et al., 2004; Jordana and Köhler, 2011; Kierdorf et al., 2014; Nacarino-Meneses et al., 2017). In this dissertation, the recognition of the incremental features and their periodicity in the hipparionins' enamel was based on the comparison with the patterns observed in other ungulates (Kierdorf et al., 2013) and particularly in extant equids (Nacarino-Meneses et al., 2017; Chapter 5). In lines with these previous studies, laminations of circadian-periodicity (Kierdorf et al., 2013) have been identified as the main incremental features localized in the enamel of hipparionin horses.

Enamel Daily Secretion Rate

The recognition of these daily laminations has allowed us to quantify the amount of enamel secreted per day by each ameloblast (DSR) in both tooth types of the four analyzed species. The first preliminary study addressing this issue in equids reported DSR estimates of 5 µm/day in horse molars (Hoppe et al., 2004), whereas other studies indicated DSRs comprised of between 10–18 µm/day in equids and other ungulates (Iinuma et al., 2004; Kierdorf et al., 2013; Nacarino-Meneses et al., 2017). Our mean DSR values of around 15 µm/day (Table 2 in Chapter 5) are in stark contrast with the preliminary estimates of Hoppe et al. (2004), but are in line with those studies that indicated higher DSRs.

We related the low previous estimates to the misidentification of sub-daily features with those of daily nature, as first stated by Kierdorf et al. (2013). They also found differences in the DSR from the inner to the outer enamel regions (Smith, 2008; Kierdorf et al., 2013), although other studies failed to detect them on extant equids (Nacarino-Meneses et al., 2017). Unfortunately, it was not possible to perform the same number of DSR measurements in the different tooth portions because of the uneven observation of laminations along the length and width of the enamel bands. Therefore, because of the arguable variation on the DSR between the tooth and enamel portions, caution should be taken when interpreting the minor DSR differences reported here.

The significance of the DSR parameter is still not fully understood (Dirks et al., 2012; Jordana et al., 2014; Kierdorf et al., 2014; Nacarino-Meneses et al., 2017). Following the interpretations of Jordana et al. (2014), greater DSRs are related to higher hypsodonty indices. Accordingly, we found significantly higher DSRs in the more hypsodont *Equus* molars compared to the hipparionin ones, and higher DSR values on the hipparionins' m1/m2s in comparison to the less hypsodont m3s (Table 1 and 2 in Chapter 5). However, the differences in hypsodonty have been shown to be more influenced by the ameloblast secretory lifespan and the overall crown formation time than to the DSR parameter (Nacarino-Meneses et al., 2017; Witzel et al., 2018), as also seem to occur with the differences on the enamel band thickness reported here (Table 2 and Suppl Fig. S6 in Chapter 5). We then proposed that the lower DSRs could also be influenced by a depleted tissue deposition because of its formation at a late ontogenetic stage, as in the case of the hipparionins' m3 (Domingo et al., 2018). This idea is supported by the progressive DSR decrease through the enamel band of the *Equus* third molar (Table 2 in Chapter 5) during its extensive formation (1750 days, Table 3 in Chapter 5). Thereafter, we suggested that the DSR differences might be the result of the interplay of many factors, such as the moment of formation, phylogeny (Dirks et al., 2012), enamel thickness (Kierdorf et al., 2014), and the height and morphology of the tooth (Jordana et al., 2014). Further studies with a strict sampling protocol and the inclusion of species with more accused differences could shed more light on the exact significance of this parameter.

Growth in Height and Eruption

The other parameter that characterizes enamel formation is the enamel extension rate (EER), which describes the speed at which the tooth increases in height (Hogg, 2018). In general, most studies have explored equid tooth growth through the measurement of teeth in skeletonized mandibles or radiographies (e.g., Dixon and Copeland, 1993; Hoppe et al., 2004; Bendrey et al., 2015). Recently, dental formation of extant equids has been more accurately reconstructed through dental histology (Nacarino-Meneses et al., 2017), like in the case of caprines' teeth formation (Jordana and Köhler, 2011; Kierdorf et al., 2012; Witzel et al., 2018). In hipparionins, the identification of isotopic seasonal cycles in their enamel has previously allowed to obtain broad estimates of tooth growth rates (35–40 mm/year, = 96–110 µm/day) (Sharp and Cerling, 1998; Van Dam and Reichart, 2009), which reasonably resemble the EER values we reported in this group (Table 2 in Chapter 5). In view of our results, however, we questioned the significance of a general mean for the extension rate, since this parameter has been shown to linearly decrease from the beginning of the cuspal formation to the end of cervical enamel deposition (Fig. 3 in Chapter 5).

Similarly, a decline in the rate of enamel extension has been reported in some dental histological studies performed on ungulates (Dirks et al., 2009; Jordana and Köhler, 2011; Kierdorf et al., 2013; Nacarino-Meneses et al., 2017; Witzel et al., 2018) and other mammalian clades such as primates (Shellis, 1984; Guatelli-Steinberg et al., 2012) and proboscideans (Dirks et al., 2012). In our sample, the progressive EER decrease reflects the described nonlinear growth pattern of equid molars (Bendrey et al., 2015; Nacarino-Meneses et al., 2017). Concretely, the growth of equid molars has been adjusted here to sigmoidal von Bertalanffy curves (Fig. 4 in Chapter 5), which resemble the sigmoidal logistic equations (Zullinger et al., 1984) we used to model the metapodial growth of hipparionins (Fig. 5 in Chapter 4).

Differences in the growth rate between tooth types have been reported in previous works on primate dental histology (Smith et al., 2007, 2010). Our results also found differences in ungulates' tooth types, since faster EERs have been identified in the m1/m2s compared to the m3s (Table 2 and Suppl. Fig. S5 in Chapter 5). These observations suggested to us that higher EERs are probably influenced by (i) the need to form the enamel layer in a short period of time for its eruption (Kierdorf et al., 2014) and by (ii) the fast juvenile somatic growth during tooth development. Therefore, we have interpreted the higher EERs of the m1/m2s as a result of their earlier formation and the need to erupt faster in comparison to the m3s (Hoppe et al., 2004; Domingo et al., 2018). The role of growth hormones (GH and IGF-1) in the differentiation and proliferation of odontogenic cells (Young, 1995; Symons and Seymour, 2000), together with the existence of a common endogenous rhythm that links bone and tooth formation (Bromage et al., 2009, 2016), further support this relationship between the EER and the ontogenetic growth.

In this context, the lower EERs of hipparionin molars (and especially of the small forms) (Table 2 and Fig. 3 in Chapter 5), could suggest a delayed onset in their formation and a later eruption time, which is characteristic of mammals with slower paces of life (Smith, 2000). Indeed, a link between lower EERs and traits indicative of slower LHs have already been identified in other groups such as primates and bovids (Hogg and Walker, 2011; Jordana et al., 2014; Hogg, 2018). Accordingly, the supposed relationship between EER and eruption time is upheld here by the earlier eruption of the fast-growing m1 of *Equus* (~230 days) compared to the m1/m2s of hipparionins (~300 days in *H. concudense*, ~350 days in *H. gromovae* and *H. periafricanum*) (Fig. 4 in Chapter 5). These eruption data further point to a slower LH in hipparionins and in the dwarf forms due to the existing correlation between the first molar eruption and the organisms' LH (Smith, 1989; Veitschegger and Sánchez-Villagra, 2016). The same interpretations have been drawn from the m3 eruption, as this trait represents a marker of somatic adulthood (Engström et al., 1983; Dean, 2006), and occurred at the same time in the four species (~500 days) (Fig. 4 in Chapter 5) despite the marked size differences.

Once molar eruption occurs, the complete lack of a rooting system in extant equids' molars (Easley et al., 2005) (see Suppl. Fig. S1 in Chapter 5) implies that they continue to grow in height while also starting to wear down (Nacarino-Meneses et al., 2017). From the reconstructed growth curves, we corroborated the fact that the molars of extant equids show this prolonged growth, whereas hipparionin molars keep growing at a slower rate and for a shorter time, and without considerably increasing the crown height after eruption (Fig. 4 in Chapter 5). This confirms our idea that a single hipparionin tooth registers most of its growth, allowing the estimation of a reliable CFT. By contrast, *Equus* molars keep growing when wear has already erased a significant part of the cuspal enamel, thereby requiring the use of composites for the estimation of CFTs (Nacarino-Meneses et al., 2017).

In previous dental histology studies, longer CFTs in later-formed third molars compared to other teeth have been reported (Shellis, 1984; Smith et al., 2007; Jordana and Köhler, 2011). Similarly, our estimated CFTs within each species tend to be longer in the m3 compared to m1/m2 (Table 3 in Chapter 5), probably because of the slower growth rates of the former. In addition, we found that hipparionin molars had longer CFTs than less hypsodont bovids (Jordana and Köhler, 2011; Kierdorf et al., 2012), but shorter than the ones obtained from the *Equus* "composites" (Table 3 in Chapter 5). This trend confirms that more hypsodont teeth are mainly formed through extended CFTs, as recently suggested (Nacarino-Meneses et al., 2017; Witzel et al., 2018). The prolonged formation time in *Equus* molars, and thus higher hypsodonty, might then compensate for their earlier eruption and, as a consequence, their earlier exposure to wear.

7.2. Life History Inferences

7.2.1. Hipparionin Life History Compared to Extant Equids

Because of the coupling between body size and LH (Millar and Zammuto, 1983; Calder, 1984), Miocene horses are generally thought to have faster paces of life than extant equids as these are commonly larger (Van Valen, 1964; MacFadden, 1992; Martinez-Maza et al., 2014). This interpretation has been supported by the earlier maturities and shorter potential lifespans inferred for some fossil taxa in a few population dynamic studies (Kurtén, 1953; Van Valen, 1964; Hulbert, 1982) (see section 1.3.2.1). These demographic studies relied on the identification of discrete dental wear classes—assumed to represent annual stages (Hulbert, 1982)—and were based on age determination models (eruption and wear) for extant species. Hence, the generally lower crowned molars of hipparionins led to the proposal of shorter potential lifespans in comparison to the more hypsodont extant equids (MacFadden, 1992). Nevertheless, some of the assumptions of these demographic studies have recently been challenged, as there are differences between *Equus* and hipparionins on (i) the eruption sequence (Domingo et al., 2018), (ii) the eruption timing (see previous section), and (iii) the dental wear rate. Actually, dental wear rate was most likely lower in hipparionins due to their mixed-feeding diets (Chapter 6) and their higher enamel band complexities that increase dental durability (Famoso and Davis, 2016).

Indeed, the presumed rapid LH of hipparionins has been directly questioned in a recent study that analyzed hipparionin molar eruption in view of Schultz's Rule (Domingo et al., 2018) (see section 1.3.2.2). In this study, the authors identified a late m3 eruption relative to premolars that suggests that decidual teeth lost functionality (p4 replaced the dp4) when the jaw had not yet grown enough to accommodate the m3, a characteristic of slow-growing organisms (Smith, 2000). In contrast, *Equus*' third molar tends to erupt earlier than the fourth premolar (Smuts, 1974), and in many specialized ruminants it erupts even before the other permanent premolars (Smith, 2000). In accordance with Schultz's Rule, ruminants and living equids have been proposed to have relatively fast LHs (Sibly and Brown, 2007), as well as, in all probability, some lineages of notoungulates that erupted all molars before the replacement premolars (Gomes Rodrigues et al., 2017). In contrast, a bovid with an extended life span [*Myotragus balearicus* (Köhler and Moyà-Solà, 2009)] shows a later eruption of the third molar (Jordana et al., 2013) compared to other caprines (Silver, 1969; Pérez-Barberia and Mutuberria, 1996).

Nevertheless, recent studies have questioned the usefulness of Schultz's Rule, and have placed more emphasis on the impact of phylogeny on the pattern of tooth eruption (Veitschegger and Sánchez-Villagra, 2016; Monson and Hlusko, 2018). The fact that one trait is "phylogenetically conserved", however, does not necessarily invalidate its relationship with the organism's ecology, as the evolution of a trait is driven by ecological pressures (Westoby et al., 1995; McNab, 2015). Mandibular development and molar emergence, as well as somatic growth, are regulated by growth hormones (growth hormone and its mediator insulin-like growth factor I) (Pirinen, 1995; Vandeberg et al., 2004; Litsas, 2015; Bartke, 2017), which might be the mechanistic link between the eruption pattern and the organisms' pace of growth. Indeed, the LH proxies inferred from molar eruption schedules are in good agreement with predictions from Shultz's Rule: taxa with an earlier m3 eruption compared to premolars (suggesting a fast LH on the basis of Shultz's Rule) show an advanced eruption of the first molar—a good indicator of a fast LH (Smith, 1989; Veitschegger and Sánchez-Villagra, 2016), as in the case of extant equids and some notoungulates (Gomes Rodrigues et al., 2017; Chapter 5). Interestingly, this pattern (advanced m1 eruption and m3 appearing before the p4) is also coupled with delayed root formation in both of the aforementioned groups (Gomes Rodrigues et al., 2017; Nacarino-Meneses et al., 2017), which could represent an adaptation to the increased dental wear caused by the early exposal of molars and the rapid early somatic growth (characteristic of a fast LH) that imply an increased food intake (Veiberg et al., 2007a).

In fact, the results presented in this thesis challenge the idea that hipparionins generally have faster LHs compared to larger living equids. Firstly, metapodial histology suggests that most hipparionins reached relative maturity at a similar or later age than larger *Equus* species (see section 7.1.1), although we would expect a more advanced maturity due to their smaller size (Calder, 1984). Secondly, the lower EERs found in hipparionin molars (Fig. 3 in Chapter 5) are indicative of slower LHs, as supported by previous studies that linked low EERs to later ages of foraging independence (Hogg and Walker, 2011; Hogg, 2018) and a later onset of reproduction (Jordana et al., 2014). Finally, data on the molar eruption timing have illustrated the similar or later occurrences of two LH events in hipparionins compared to *Equus*, as weaning and skeletal maturity ages can be respectively inferred from the eruption of the m1 (Smith, 1991b) and the m3 (Engström et al., 1983; Dean, 2006) (Table 4 in Chapter 5). Then, if we assume that all equids have a similar molar formation onset, the hipparionins studied through dental histology would have been weaned around 100 days later than *Equus*, at one year after birth. Adult skeletal maturity, on the other hand, might have taken place at a similar age in the three hipparionins and the extant *Equus*, three years after birth (see section 4.3 in Chapter 5). These similar or later timings contrast with what we would expect from the coupling of LH and size (Peters, 1983; Calder, 1984) and are suggestive of a relative slower LH for hipparionin horses compared to extant equids.

7.2.2. Small-sized Hipparionins

To the best of my knowledge, no other studies have directly addressed LH differences with regard to body size in hipparionin horses. However, when relating the general phyletic increase in equid body size to longer potential lifespans, MacFadden (1992) had already raised questions about the LH changes that might have occurred in lineages experiencing dwarfing trends (see section 1.3.2.1). He speculated that the dwarf *Pseudhipparion simpsoni* might have maintained the arguably longer lifespan of its ancestors and thus an increased lifetime reproduction (MacFadden, 1992). In this thesis, the results on bone and dental histology point to distinct LHs on the different-sized hipparionins analyzed. From the estimated relative maturity of the small-sized hipparionin from the western Mediterranean (*H. gromovae*), we inferred a slower LH strategy than was expected for its size (Chapter 4). Moreover, the lower EERs also led us to propose a slower LH in this species and in the even smaller *H. periafricanum* in comparison to the larger hipparionin and its probable ancestor, *H. concudense* (Alberdi, 1972) (Chapter 5). The reconstruction of molar eruption timing and its relationship with LH events further supports this inference—as shown in Fig. 7.1A, weaning probably took place later than predicted from scaling in both dwarfed species, as it also occurs in the case of maturity attainment (Fig. 7.1B). It is worth mentioning that the ages of m3 eruption (proxy for skeletal maturity) have been plotted here with data on the age at first reproduction (Fig. 7.1B) because most datasets lack values for somatic maturity. However, I am assuming that (i) hipparionins may have reached sexual maturity when they stopped growing, due to the trade-off between growth-reproduction (Stearns, 1992), and (ii) that they reproduced shortly after becoming sexually mature.

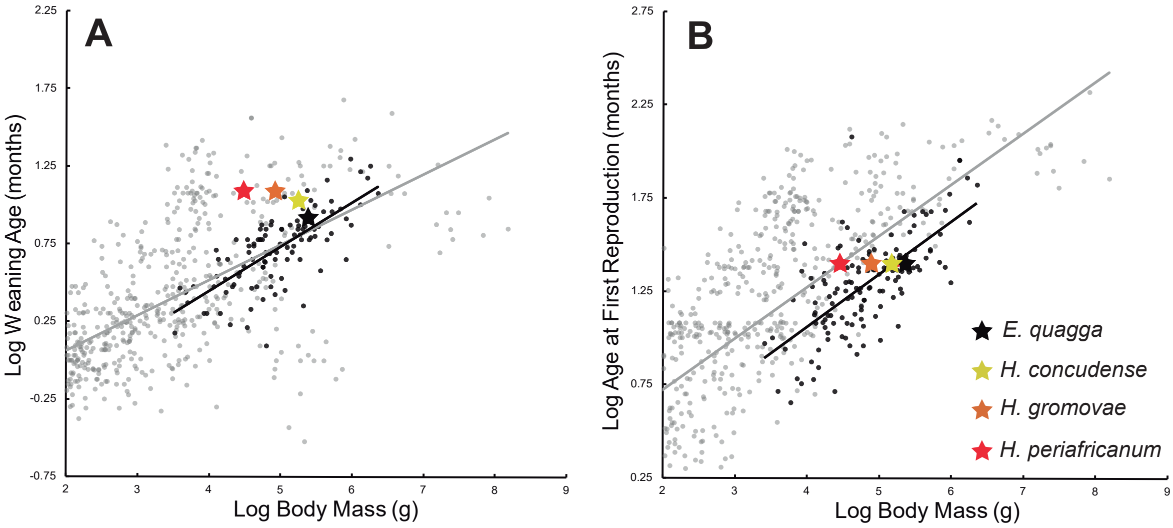

Figure 7.1.
Allometries for weaning (A) and age at first reproduction (B) based on data from the mammalian LH database published in Ernest (2003). The black color highlights the regression line for perissodactyls and artiodactyls. Weaning and maturity ages inferred in this thesis from molar eruption are indicated with stars. Note that the stars in B actually indicate the ages at skeletal maturity and not the age at first reproduction. Hipparionin body masses were taken from Table 6.1 of Chapter 6.

The small-sized hipparionins from the eastern Mediterranean (*macedonicum* morphotype), on the other hand, have shown to advance their relative maturity attainment compared to larger forms, which point toward a shift to a faster LH in this group (Chapter 4). Interestingly, the larger *H. primigenium truyolsi* from the western Mediterranean reached relative maturity around the same time as *macedonicum* hipparionins (Fig. 5 in Chapter 4), despite the striking differences in size. We were cautious, however, regarding the interpretations of this result owing to the limited sample size and the high presence of remodeling on the single *H. primigenium truyolsi* specimen. The occurrence of this earlier maturation in a large-sized taxon, and of the slower LH in dwarfed taxa, suggest that there are other factors besides body size that are acting on the LHs, which are related to the environmental conditions and the organisms' ecology (Stearns, 1992; Sibly and Brown, 2007).

7.3. Ecological Interpretations

Resource availability and extrinsic mortality are the two principal ecological agents that shape LHs (Law, 1979; Promislow and Harvey, 1990; Stearns, 1992). A higher extrinsic mortality due to increased predation selects for an advanced maturity (faster LH), as that warrants reproduction before an early death (Gadgil and Bossert, 1970; Reznick et al., 1996; Gaillard et al., 2000). On the other hand, a later maturity is favored under low predation levels (Stearns, 1992) because of the benefits of reproducing late: fecundity increases with the size of the progenitor, and juvenile mortality decreases with the age and size of the progenitor (Stearns and Koella, 1986; Palkovacs, 2003). In the context of resource limitations, delayed maturation can also help to increase juvenile survival, which has shown to be significantly affected by resource constraints (Skogland, 1985; Choquenot, 1991; Gaillard et al., 2000). Indeed, the best strategy under conditions of low resource availability is to invest more energy to soma maintenance in detriment of growth and reproduction (slower LH), thus favoring survival (Holliday, 1989). Moreover, under a scenario of low resource availability (e.g., low habitat productivity), growth rate is constrained due to the necessity of spending more energy to obtain food (Palkovacs, 2003). Besides habitat productivity, density-dependence is another important aspect influencing the levels of available resources (Skogland, 1983; Choquenot, 1991), which can influence ungulates' LHs (Gaillard et al., 2000).

Because the rate and duration of growth determine the organism body size, the adaptive changes in maturity attainment and growth rate may lead to changes in adult body size (Palkovacs, 2003). Smaller sizes can be as a result of the outcome of (i) lowered growth rates, due to resource limitation (e.g., Long et al., 2019), (ii) or of the shortening of the growth period because of advanced maturity (e.g., Stearns et al., 2000). In contrast, larger body sizes are reached through an extended growth period or increased growth rates (Roff, 2002). Dwarfing trends, however, have also shown to be occasionally coupled to delayed maturities (Skogland, 1983; Köhler and

Moyà-Solà, 2009; Jordana and Köhler, 2011) because the direction of the size shift depends on the magnitude and relative importance of the changes in the mortality regime and the availability of resources (Palkovacs, 2003). All these LH responses to ecological variation are first expressed through phenotypic plasticity (Stearns and Koella, 1986) and are later selected and assimilated genetically in the population (Lande, 2015). Afterwards, the characteristic LH strategy will be maintained distinct and stable in as far as it remains optimal under the prevailing environmental conditions (Promislow and Harvey, 1990).

7.3.1. Life History Differences Between Hipparionins and Extant Equids

Despite the similar or advanced timing of LH events in hipparionin horses and extant equids (section 7.2.1)—implying a shorter or comparable timespan to grow— *Equus* species generally reach larger body sizes. Therefore, faster somatic growth in *Equus* compared to hipparionins must necessarily be involved. Similarly, differences in growth rate seem to account for the body size differences observed between domestic horse breeds (Strand et al., 2007; Heck et al., 2017), and between extant *Equus* species and significantly larger Pleistocene forms (Nacarino-Meneses and Orlandi-Oliveras, 2019). In this regard, abundant food supplies have been shown to favor higher somatic growth rates (Marín-Moratalla et al., 2013; Woodward et al., 2014; Nacarino-Meneses et al., 2016a), and animals under these conditions tend to increase in body mass and advance breeding (reviewed in Boutin, 1990). The availability of resources is thus likely to be the underlying cause of the observed differences.

It is hypothesized, therefore, that extant equids may rely on a more abundant and/or nutritious type of vegetation than most hipparionins. Indeed, the graminaceous plants that compose much of the *Equus* diet (Nowak, 1999) tend to lack the secondary metabolites, while forbs and browse species produce more defense compounds that make them less nutritious (Harborne, 1988; Duncan and Poppi, 2008). Hipparionins, which had more opportunistic diets and include a higher proportion of browse (Tütken et al., 2013; Chapter 6), might then have had a poorer source of energy to sustain high somatic growth rates and rapid development. In accordance with the proposed hypothesis, it has been suggested that hipparionins were probably more mixed feeders, while the Equini might have consumed mainly grasses in the North American ecosystems in which both groups co-occurred (Shotwell, 1961; Forsten, 1989). In the case of the hipparionin populations for which we have inferred stronger grazing strategies, i.e., those from Concud and Venta del Moro (Fig. 6.4 in Chapter 6), the paleoenvironmental data indicate that they were dwelling in wetlands near lacustrine areas (Montoya et al., 2006; Pesquero et al., 2013). In these habitats, grasses were probably not as abundant as in they are in modern-day savannas and steppes since monocots may have been mostly confined to the shores of lakes; whereas more closed or mixed landscapes probably occupied the lake surroundings (DeMiguel et al., 2018).

Aside from the quantity and quality of the primary producers, the available food for an ungulate also depends on its population density (Wolverton et al., 2009) and that of other competitors. Hence, both resource productivity and population density have been shown to influence body size in extant ungulates (Klein, 1965; Klein and Strandgaard, 1972). In this regard, Saarinen et al. (2016) recently proposed that higher intraspecific competition due to high population densities was the cause of the smaller body size of some *Equus ferus* populations from the European Pleistocene. Thus, in hipparionin horses, the lower resource availability could have also been related to higher competence levels due to the presence of sympatric hipparionin taxa in most assemblages, or to higher population densities of the same species. The wide dietary spectra observed for some hipparionin populations (Chapter 6) might support this interpretation since ungulates tend to expand their feeding preferences under density-dependent resource limitation (Skogland, 1988; Freeland and Choquenot, 1990; Winkler et al., 2013). Conversely, in extant faunal associations, only one equid species tends to occur (Janis, 2008). In this case, competition with other ungulates is avoided through the exploitation of the more abundant, less digestible, and more abrasive plants (Janis et al., 1994) from which equids can feed thanks to their different craniodental morphology and digestive strategy compared to ruminants (Janis, 1976).

7.3.2. Dwarfing in Hipparionins

The main objective of this thesis has been to elucidate the processes and causes that led some hipparionin groups to undergo a decrease in body size. The mechanistic basis and evolutionary factors that underlie the organisms' size shifts in continental settings are still poorly understood. Islands, however, represent natural laboratories from which evolutionary patterns can be studied and can subsequently be applied in the mainland. In general, it has been thought that shifts in body sizes in insular organisms are the result of direct selection for larger or smaller sizes (reviewed in Palkovacs, 2003) and that the accompanying changes in LH are simply an effect of allometry (Calder, 1984). LHT, however, offers a more general explanation for the body size shifts in insular organisms (see section 1.2.1). Body size modifications can be merely a byproduct of natural selection acting on the LH traits to which body size is sensitive (Palkovacs, 2003). Thus, based on Palkovacs' (2003) model for body size evolution on islands, this thesis aims to unravel whether the hipparionin dwarfing trends were related to differences in predation pressures (extrinsic mortality) or to resource availability. The contrasting growth strategies identified in the dwarfed hipparionins from the eastern and the western Mediterranean (see section 7.2.2), suggest that two different selective agents triggered two distinct adaptive mechanisms that, conversely, led to a similar phenotypic outcome (small size).

In the case of the *macedonicum* group from the eastern Mediterranean, we inferred that higher extrinsic mortality—due to predation—selected for a faster LH resulting in an associated decrease in body size. This higher mortality rate likely affected adult survival, since population growth rates in ungulates are more sensitive to changes in this parameter than to variations in juvenile survival (Gaillard et al., 2000; Gaillard and Yoccoz, 2003). An alternative interpretation of direct selection for smaller body size to avoid dietary competition (a niche partitioning hypothesis) is preliminary discarded here in view of the similar foraging preferences of the sympatric differently sized hipparionins from the eastern Mediterranean (Chapter 6). However, dietary segregation could have occurred through the exploitation of different food items but with similar mechanical properties (thereby producing similar dental microwear textures).

On the other hand, the reduced growth rates, relatively delayed maturities, and slower LHs of the western Mediterranean dwarfs (*H. gromovae* and *H. periafricanum*) have been interpreted here as a response to low resource availability, as it is the main selective pressure influencing the organisms' growth rate (Stearns, 1992; Palkovacs, 2003). In this context of constrained growth, a delayed maturity arises from (i) the extension of the growth period to reaching the proper condition for reproduction (Stearns and Koella, 1986; Berrigan and Koella, 1994) and/or from (ii) the postponement of breeding in favor of survival and maintenance (Holliday, 1989). Additionally, later maturation leads to more experienced and larger progenitors (Sand, 1996; Gaillard et al., 2000) that may help to counterbalance the probable higher rate of juvenile mortality due to resource limitations (Skogland, 1985; Choquenot, 1991; Gaillard and Yoccoz, 2003). The lower resource availability inferred from growth rate could have been caused by either lower habitat productivity, density-dependent food limitations (Wolverton et al., 2009), or both.

Accordingly, individuals from extant ungulate populations living in less productive habitats exhibit smaller body sizes and traits indicative of slower LHs (longer lifespans) than those inhabiting more productive areas (Veiberg et al., 2007b). Likewise, ungulate populations affected by density-dependent resource constraints have also shown to be composed of smaller individuals with delayed maturities (Skogland, 1983; Choquenot, 1991) and later weaning ages (extended lactation times) (Skogland, 1983) as observed in the dwarf western Mediterranean hipparionins (Fig. 7.1A).

7.3.2.1. Environmental Setting and Inferences on the Ecology of Different-sized Hipparionins

Because the selective pressures acting on LHs are exerted by the biotic and abiotic environment (Stearns, 1992), we considered the paleoenvironmental reconstructions of the eastern and western Mediterranean in order to explore the occurrence of the factors driving hipparionin dwarfing (i.e., higher extrinsic mortality and lower resources, see Chapter 4). Additionally, the ecological interpretations inferred from LH analysis were examined by reconstructing the foraging ecology of hipparionins from both regions using dental wear analysis (Chapter 6). Our results on hipparionin DMTs indicated that most hipparionins were mixed feeders (Fig. 6.4 in Chapter 6), which contrasts with the classic interpretation that characterize them as grazing zebras inhabiting grassland plains (Matthew, 1926; Stebbins, 1981; Gabunia and Chochieva, 1982), but reinforce the idea of their wide dietary flexibility (Kaiser, 2003; Tütken et al., 2013). Moreover, although the dietary preferences of a sole group of ungulates do not directly indicate the habitat type, the opportunistic diets of the hipparionins have given us clues as to habitat composition (Kaiser, 2003) due to the necessary association between grazing diets and the presence of grasses, and between browsing diets and the presence of woody cover (Ungar et al., 2007; Schulz et al., 2010).

The Eastern Mediterranean

The eastern Mediterranean landscapes during the late Miocene were likely more open than those of the western part, and would have mostly consisted of savannas and shrubland (Bonis et al., 1992a, 1999; Fortelius et al., 1996, 2006; Merceron et al., 2005, 2016a; Strömberg et al., 2007; Costeur and Legendre, 2008; but see Denk et al., 2018). For ungulates, more open environments such as these are richer in resources than more closed and forested ones (Fischhoff et al., 2007; Godvik et al., 2009; Thaker et al., 2010), which tend to support lower quantities and quality of forage (Mysterud and Ostbye, 1999). However, in comparison to the shelter provided by covered areas, opener habitats are riskier for ungulates (Fortin et al., 2005; Hernández and Laundré, 2007; Godvik et al., 2009) since predators can more easily detect their prey and have fewer obstacles when attacking (see review in Mysterud and Ostbye, 1999). In this context, the high predation pressures that triggered the earlier maturity of the *macedonicum* hipparionins could have been caused by the diverse carnivore associations occurring in the more open eastern Mediterranean environments (Koufos and Konidaris, 2011). The existence in this region of rich hipparionin assemblages with no strong DMT differences (so low dietary partitioning) neither in general (Appendix 8.3 of Chapter 6) nor within each locality (Appendices 8.8 to 8.14 in Chapter 6), also point to the presence of highly productive open habitats with diverse and abundant resources. Hence, the different-sized hipparionin forms present in this area could live sympatrically, broadening their dietary preferences as a function of the exploitable primary resources and of intra/interspecific competition.

In addition to the presence of a grassy layer in the eastern Mediterranean landscapes (Merceron et al., 2007; Strömberg et al., 2007), our DMTA data further indicate the existence of bushy and shrubby vegetation because of the mixed-feeding diets of the eastern hipparionins (Fig. 6.2 and 6.4 in Chapter 6). Indeed, our results do not attest the inclusion of more grasses in the diet of the eastern Mediterranean hipparionins compared to the western forms—due to the higher DMT complexities of the former (Fig. 6.3.1 in Chapter 6)—as would be expected due to the more open habitats eastwards. We interpreted this as the consequence of hipparionins consuming a higher proportion of woody browse during seasonal depletions of monocots. A similar browsing behavior has been reported in extant equids during drought periods (common in open environments) (Estes, 1991; Moehlman, 2002), which constrain the growth of grasses due to their lower water competitive capacity compared to bushes and shrubs (Hipondoka et al., 2003; Wang et al., 2010). As a consequence, extant ungulates that only feed on grasses are generally confined to wetlands, or alternatively they are subject to seasonal migrations (discussed in Merceron et al., 2016a). An alternative interpretation involves the arguable presence of millimetric grit in the open landscapes of the eastern Mediterranean. To date, the role and effect of exogenous grit, and of the silica phytoliths in the microwear signature, is a contentious issue (Lucas et al., 2014; Merceron et al., 2016b; Sanson et al., 2017). In this regard, the incorporation by ungulates of micrometric dust has been shown to not significantly alter the DMT complexities (Merceron et al., 2016b; Ramdarshan et al., 2016) and, more importantly, to not obscure the DMT differences between dietary classes (Burgman et al., 2016; Merceron et al., 2016b). However, the processing of larger sand particles (millimetric grit) might form large pits on the enamel surface (Solounias and Semprebon, 2002) that increase the DMT complexity (Calandra and Merceron, 2016; Hedberg and DeSantis, 2017). Thus, an arguably higher presence of grit in the east—due to drier and more open habitats—could be hindering the direct comparison between the diets of hipparionins from the eastern and the western Mediterranean. A future multi-proxy study which includes mesowear and isotopic analyses may help to shed light on this comparison.

The Western Mediterranean

In the western side of the Mediterranean, the landscapes during the late Miocene were generally more forested than those of the eastern part (Bonis et al., 1992b; Koufos, 2006). Along with occasional open habitats, the presence of xeric woodlands and forested areas in Iberia (Hernández Fernández et al., 2006; Domingo et al., 2013; DeMiguel et al., 2018) could have provided increased cover (Mysterud and Ostbye, 1999; Godvik et al., 2009) to some of the hipparionins that were analyzed. Therefore, considering the LH reconstructions discussed here (section 7.2.2), the western Mediterranean dwarf hipparionins dwelt in the more densely covered areas, where they were less exposed to the present predators (Salesa et al., 2012) (lower predation pressures) but had lower availability of resources due to the shading effect of trees (Mysterud and Ostbye, 1999). Therefore, their slower LHs were triggered by the lower resource availability caused by them living in more secure but less productive closed environments. In a similar way, Macho and Williamson (2002) recognized that among African bovids, smaller taxa tend to occupy more forested habitats and have longer gestation periods (slower LHs) than expected for their size.

These interpretations on the ecology of the smaller hipparionins from the western Mediterranean are supported by our results on the DMTA. We have found that, contrary to the similar diets of the eastern hipparionins, the diets of the western smaller-sized forms generally differ to those of the larger ones by the inclusion of a higher proportion of browse and of items of diverse physical properties (Fig. 6.4 in Chapter 6). Specifically, while the larger Turolian hipparionins from this area fed mainly on grasses, *H. gromovae* and *H. periafricanum* had a more varied browse-dominated diet (Fig. 6.2 and 6.4 in Chapter 6) that endorsess their occupation of denser habitats with more woody cover. This trend of relating smaller forms to more closed habitats, and larger hipparionins to more open ones, conforms to the model of body size changes in the Equini proposed by Alberdi et al. (1995) and later applied to Iberian hipparionins by Ortiz-Jaureguizar and Alberdi (2003). In agreement with this, Kaiser et al. (2003) also found that in a German fossil locality the smaller hipparionin was a browser that was more adapted to closed habitats compared to the larger species present in the same site.

In addition, the greater inclusion of hard ligneous material and the broader diets of the western Mediterranean dwarfs could also point to a dietary expansion favored by the low availability of resources. In a similar way, extant ungulates under resource limited conditions feed on a wider range of lower quality food, which increases their tooth wear and constrains their somatic growth rate, leading to smaller adult body sizes (Skogland, 1988; Veiberg et al., 2007b). This could explain, for example, that the aforementioned hipparionins have higher hypsodonty indices compared to larger-sized forms (Pesquero, 2003) that otherwise fed mainly on grasses (e.g., *H. concudense*) (Fig. 6.4 in Chapter 6). Seasonal variability in climate and resource productivity is overcome by large ungulates through migration to other foraging areas (Sinclair and Norton-Griffiths, 1979), as that allows them to increase resource availability and reduce its variations (Georgiadis et al., 2003). Migratory behavior, therefore, represents another tactic to maximize fitness, and thus should be considered when characterizing an organism's LH strategy (Southwood, 1988). In this context, it is hypothesized that the grazing larger hipparionins from the Iberian Peninsula arguably underwent seasonal migrations following fluxes in grass production, whereas the smaller forms would have seasonally expanded their diets and exploited the fewer available resources.

To see whether these hipparionin populations did indeed undergo seasonal migrations or remained in the same area, a promising topic to address in the future would be to explore the variations on the strontium isotopic ratio ($^{87}Sr/^{86}Sr$) of their enamel. As this ratio varies with differences in the underlying bedrock (Gosz and Moore, 1989), its analysis on the enamel of large mammals has been shown to help tracking migratory movements (e.g., Hoppe et al., 1999). The presented data on enamel growth (Chapter 5), together with that of the hipparionin dietary preferences (Chapter 6), can then help to interpret at a finer level the results of this eventual isotopic study as well as others that address isotopic variations on hipparionin enamel—a proxy widely used for paleoecological inferences (e.g., Nelson, 2005; Domingo et al., 2009; Van Dam and Reichart, 2009). Future work will benefit in particular from the growth reconstruction of the third molar of both extant and extinct equids (Chapter 5), as this tooth is preferred for isotopic analysis due to its longer formation times (Table 3 in Chapter 5) and to the fact that its isotopic signal is not affected by the consumption of mother's milk (Bryant et al., 1994).

In summary, the results of this thesis have evidenced that different ecological settings led to convergent decreases in body size in hipparionins from both sides of the Mediterranean. Previously, other studies proposed a general link between forested biomes and the presence of smaller hipparionins (Ortiz-Jaureguizar and Alberdi, 2003), in contrast with others that considered the smaller forms to be more adapted to open habitats (Bernor et al.,1996). Based on a body size evolution model rooted in LHT (Palkovacs, 2003), the results of this thesis suggest that high predation pressures typical of open landscapes indeed triggered the dwarfing of some eastern Mediterranean hipparionins. On the other hand, it has also been inferred here that lower resource availability was the cause of the small body size of some hipparionins from the western Mediterranean, as was also advocated by Forsten (1968, 1978a). Moreover, as suggested from the reconstructed LHs and dietary preferences, these dwarf hipparionins likely dwelt in more densely covered habitats compared to larger forms, in accordance with the interpretation of Ortiz-Jaureguizar and Alberdi (2003). This thesis, based on the study of the LH and foraging ecology of extinct taxa by means of paleohistology and dental wear, sets a precedent for the understanding of shifts in body size and the ecological factors underlying them.

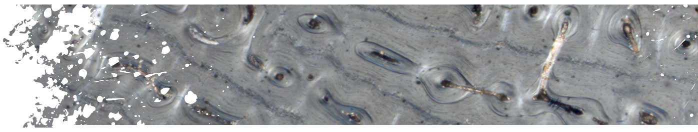

Chapter 8

Conclusions

Chapter 8
Conclusions

I. Hipparionin metapodials show a similar arrangement of bone tissues and vascularity to that described in extant equids. Their cortex is mostly formed by a fibrolamellar complex with longitudinal primary osteons oriented in circular rows, and with some occasional circular and radial canals. The neonatal line previously observed in the limb bones of zebras and asses has been found within the innermost cortex of hipparionin metapodials. Because of the low resorption of the metapodial medullary cavity, the neonatal line has been identified in mature specimens, distinguished here by the deposition of slow-growing lamellar bone in the periosteal surface. This fact has allowed the reconstruction of the entire metapodial growth, which properly fits a logistic growth curve.

II. The metapodial size at birth and its growth rate during the first year of life are functions of the final size of the metapodia in the analyzed hipparionin taxa. The marked reduction in the rate of bone deposition, which indicates the attainment of a relative maturity, occurs earlier in the eastern Mediterranean small hipparionins (*macedonicum* group) than in the larger morphotypes (*primigenium* and *dietrichi*). The metapodials of the western Mediterranean dwarf hipparionin (*H. gromovae*) show an extended growth period, indicating a relatively late maturity for its size.

III. The main incremental markings identified in the hipparionin enamel are laminations analogous to the daily increments found in other ungulates. This finding has allowed us to determinate that the amount of enamel secreted per day (DSR) in hipparionin molars was approximately 15 µm/day, which is akin to the rates reported for ungulates in more recent studies. Differences in this parameter have been detected among the species analyzed, but particularly between *Hipparion* and *Equus* because of the higher enamel secretion values of the latter. Numerous factors are playing a role in the rate of enamel secretion, as the observed DSR differences have not been shown to be directly related to hypsodonty or differences in enamel thickness. Future studies with rigorous sampling protocols and a more heterogeneous sample will help to identify the factors involved.

IV. The rate of increase in tooth height (EER) decreases linearly from the first-formed cuspal area to the cervical enamel due to the nonlinear growth trajectory of equid molar development. Taking into account this intra-tooth variability in EERs, it has been shown that *Equus*' molars are formed at higher rates than those of hipparionins, and that the molars of a large western Mediterranean hipparionin grew faster in height than those of the dwarf taxa from the same region.

V. The higher DSRs and EERs of the first/second molars compared to the later-formed third molars suggest that the timing of tooth formation/eruption and the tooth growth rates are correlated. Therefore, this could indicate an earlier formation and eruption of the fast-growing molars of extant equids compared to those of hipparionins. In accordance, the first molar in *Equus* has been shown to erupt earlier than the hipparionins' first/second molars, and the slower-growing m1/m2s of *H. periafricanum* and *H. gromovae* likely erupted later than those of the larger *H. concudense*. The m3s, on the other hand, erupt at the third year of life in all the analyzed taxa despite the marked differences in body size. Although *Equus* molars show similar or earlier eruption timings to those of hipparionins, they extend their growth over a much longer time period, thus becoming more hypsodont.

VI. The LH proxies obtained from bone and dental histology debunk previous postulations on the faster LH of hipparionins compared to *Equus*, which were based on their generally smaller size and less hypsodont molars. Moreover, the dwarf hipparionins from the western Mediterranean must have followed slower LHs than expected for their size, as evidenced by (i) the late relative maturity of *H. gromovae*'s metapodials and (ii) the estimated late weaning age (~one year old) and maturity age (~three years old) of *H. gromovae* and *H. periafricanum*. Conversely, the eastern Mediterranean small-sized forms show an advanced relative maturity and thus a faster LH in comparison to the larger morphotypes.

VII. Based on the predictive LHT model of Palkovacs (2003), it has been inferred that a higher extrinsic mortality was the selective pressure that triggered the earlier maturity of the *macedonicum* group, indirectly leading to dwarfing. On the other hand, lower resource availability led to the decrease in size of the western Mediterranean dwarfs, as evidenced by their slower LHs. Similarly, this thesis has hypothesized that the LH differences between *Equus* and hipparionins could have been related to resource availability, either due to differences in the quantity/quality of forage, in the intra/interspecific competition levels, or both.

VIII. Differences in landscape composition between the eastern and the western Mediterranean might account for the contrasting ecological scenarios implied to drive dwarfing in hipparionins. The results suggest that a higher extrinsic mortality arose in the open environments around eastern Mediterranean in the late Miocene, which were richer in forage but riskier for ungulates as they were exposed to higher levels of predation. The dwarf hipparionins from the western Mediterranean, by contrast, likely dwelt in more secure but less forage-rich forested habitats.

IX. The analysis of DMTs revealed that most hipparionin groups were mixed feeders. In the eastern Mediterranean, the different-sized forms had similar dietary habits (and arguably also habitat preferences), which supports the hypothesis of the presence of resource-rich environments. The DMTs of eastern Mediterranean hipparionins tend to be more complex than those of the western ones, which has been related to a higher consumption of browse during seasonal droughts or, alternatively, to feeding in open habitats with vegetation containing more particles of millimetric grit.

X. The dietary strategies of the western Mediterranean hipparionins were more differentiated. The smaller forms had broader diets and included a larger proportion of ligneous browse while larger hipparionins grazed almost exclusively. This pattern suggests that the dwarfed hipparionins dwelt in more densely covered areas and/or had more opportunistic diets prompted by an environment with low resource availability.

XI. This thesis evidences, for the first time, that the process and mechanisms behind dwarfing are neither universal nor uniform but depend on the ecological context. Accordingly, the dwarfed eastern and western Mediterranean hipparionins did not follow the same LH strategies, and probably did not even dwell in similar habitats. Future studies based on multi-proxy data will provide more information on the paleoenvironmental settings inhabited by the different-sized hipparionins.

Chapter 9

References

Chapter 9

References

Adler GH, Levins R. 1994. The island syndrome in rodent populations. *The Quarterly Review of Biology* 69, 473–490.

Agustí J, Sanz de Siria A, Garcés M. 2003. Explaining the end of the hominoid experiment in Europe. *Journal of Human Evolution* 45, 145–153.

Alberdi MT. 1972. *El género* Hipparion *en España. Nuevas formas en Castilla y Andalucía, Revisión e Historia Evolutiva.* Universidad Complutense de Madrid.

Alberdi MT. 1974. Las "faunas de *Hipparion*" de los yacimientos españoles. *Estudios Geológicos* 30, 189–212.

Alberdi MT. 1978. El género *Hipparion* en la provincia de Teruel (España). *Teruel: Revista del Instituto de Estudios Turolenses* 60, 33–48.

Alberdi MT. 1986. The Pliocene species of *Hipparion* and their biostratigraphical meanings. *Geobios* 19, 517–522.

Alberdi MT. 1989. A review of Old World hipparionine horses. In: Prothero DR, Schoch RM (Eds.), *The Evolution of Perissodactyls*. Oxford University Press, New York, 234–261.

Alberdi MT, Alcalá L. 1989. El género *Hipparion* en la fosa de Alfambra-Teruel. *Paleontologia i Evolució* 23, 105–109.

Alberdi MT, Ortiz-Jaureguizar E, Prado JL. 1998. A quantitative review of European stenonoid horses. *Journal of Paleontology* 72, 371–387.

Alberdi MT, Prado JL, Ortiz-Jaureguizar E. 1995. Patterns of body size changes in fossil and living Equini (Perissodactyla). *Biological Journal of the Linnean Society* 54, 349–370.

Amprino R. 1947. La structure du tissu osseux enviasagée comme expression de différences dans la vitesse de l'accroissement. *Archives de Biologie* 58, 315–330.

Amson E, Kolb C, Scheyer TM, Sánchez-Villagra MR. 2015. Growth and life history of Middle Miocene deer (Mammalia, Cervidae) based on bone histology. *Comptes Rendus - Palevol* 14, 637–645.

Athanassiou A. 2018. A Villafranchian *Hipparion*-Bearing Mammal Fauna from Sésklo (E. Thessaly, Greece): implications for the Question of *Hipparion–Equus* Sympatry in Europe. *Quaternary* 1, 12.

Azzaroli A. 1992. Ascent and decline of monodactyle equids: a case for prehistoric overkill. *Annales Zoologici Fennici* 28, 151–163.

Bartke A. 2017. Somatic growth, aging, and longevity. *npj Aging and Mechanisms of Disease* 3, 14.

Bendrey R, Vella D, Zazzo A, Balasse M, Lepetz S. 2015. Exponentially decreasing tooth growth rate in horse teeth: implications for isotopic analyses. *Archaeometry* 57, 1104–1124.

Bernor RL, Göhlich UB, Harzhauser M, Semprebon GM. 2017. The Pannonian C hipparions from the Vienna Basin. *Palaeogeography, Palaeoclimatology, Palaeoecology* 476, 28–41.

Bernor RL, Koufos GD, Woodburne MO, Fortelius M. 1996. The evolutionary history and biochronology of European and Southwest Asian Late Miocene and Pliocene hipparionine horses. In: Bernor RL, Fahlbusch V, Mittmann H-W (Eds.), *The Evolution of Western Eurasian Neogene Mammal Faunas*. Columbia University Press, New York, 307–338.

Bernor RL, Kovar-Eder J, Lipscomb D, Rögl F, Sen S, Tobien H. 1988. Systematic, stratigraphic, and paleoenvironmental contexts of first-appearing *Hipparion* in the Vienna Basin, Austria. *Journal of Vertebrate Paleontology* 8, 427–452.

Bernor RL, Kovar-Eder J, Suc JP, Tobien H. 1990a. A contribution to the evolutionary history of European Late Miocene age hipparionines (Mammalia: Equidae). *Paléobiologie Continentale,* 17, 291–309.

Bernor RL, Lipscomb D. 1991. The systematic position of "*Plesiohipparion*" aff. *huangheense* (Equidae, Hipparionini) from Gülyazi, Turkey. *Mitteilung der Bayerischen Staatssammlung für Paläontologie und historische Geologie* 31, 107–123.

Bernor RL, Lipscomb D. 1995. A consideration of Old World hipparionine horse phylogeny and global abiotic processes. In: Vrba E, Denton GH, Partridge TC, Burckle LH (Eds.), *Paleoclimate and Evolution, with Emphasis on Human Origins*. Yale University Press, New Haven, 164–177.

Bernor RL, Mirzaie Ataabadi M, Meshida K, Wolf D. 2016. The Maragheh hipparions, late Miocene of Azarbaijan, Iran. *Palaeobiodiversity and Palaeoenvironments* 96, 453–488.

Bernor RL, Scott RS, Fortelius M, Kappelman J, Sen S. 2003. Equidae (Perissodactyla). In: Fortelius M, Kappelman J, Sen S, Bernor RL (Eds.), *The Geology and Paleontology of the Miocene Sinap Formation, Turkey*. Columbia University Press, 220–281.

Bernor RL, Sen S. 2017. The Early Pliocene *Plesiohipparion* and *Proboscidipparion* (Equidae, Hipparionini) from Çalta, Turkey (Ruscinian Age, c. 4.0 Ma). *Geodiversitas* 39, 285–314.

Bernor RL, Sun B. 2015. Morphology through ontogeny of Chinese *Proboscidipparion* and *Plesiohipparion* and observations on their Eurasian and African relatives. *Vertebrata Palasiatica* 53, 73–92.

Bernor RL, Tobien H. 1989. Two small species of *Cremohipparion* (Equidae, Mamm.) from Samos, Greece. *Mitteilungen der Bayerischen Staatssammlung för Paläontologie und Historische Geologie* 29, 207–226.

Bernor RL, Tobien H, Woodburne MO. 1990b. Patterns of Old World hipparionine evolutionary diversification and biogeographic extension. In: Lindsay EH, Fahlbusch V, Mein P (Eds.), *European Neogene Mammal Chronology*. Plenum Press, New York, 263–319.

Berrigan D, Koella JC. 1994. The evolution of reaction norms: simple models for age and size at maturity. *Journal of Evolutionary Biology* 7, 549–566.

Beynon AD, Dean MC, Leakey MG, Reid DJ, Walker A. 1998. Comparative dental development and microstructure of *Proconsul* teeth from Rusinga Island, Kenya. *Journal of Human Evolution* 35, 163–209.

Bonis L de, Bouvrain G, Geraads D, Koufos GD. 1992a. Diversity and paleoecology of Greek late Miocene mammalian faunas. *Palaeogeography, Palaeoclimatology, Palaeoecology* 91, 99–121.

Bonis L de, Bouvrain G, Geraads D, Koufos GD. 1992b. Multivariate study of late Cenozoic mammalian faunal compositions and paleoecology. *Paleontologia i Evolució* 24, 93–101.

Bonis L de, Bouvrain G, Koufos GD. 1999. Palaeoenvironments of late Miocene primate localities in Macedonia, Greece. In: Agustí J, Rook L, Andrews P (Eds.), *Hominoid Evolution and Climatic Change in Europe: Vol.1, The Evolution of Neogene Terrestrial Ecosystems in Europe*. Cambridge University Press.

Boutin S. 1990. Food supplementation experiments with terrestrial vertebrates: patterns, problems, and the future. *Canadian Journal of Zoology* 68, 203–220.

Braendle C, Heyland A, Flatt T. 2011. Integrating mechanistic and evolutionary analysis of life history variation. In: Flatt T, Heyland A (Eds.), *Mechanisms of Life History Evolution. The Genetics and Physiology of Life History Traits and Trade-Offs*. Oxford University Press, Oxford, 3–10.

Bromage TG. 1991. Enamel incremental periodicity in the pig-tailed macque: a polychrome fluorescent labeling study of dental hard tissues. *American Journal of Physical Anthropology* 86, 205–214.

Bromage TG, Dirks W, Erdjument-Bromage H, Huck M, Kulmer O, Oner R, Sandrock O, Schrenk F. 2002. A life history and climate change solution to the evolution and extinction of insular dwarfs: a Cypriot experience. In: *Waldren, W.H., Ensenyat, J.A. (Eds.) World Islands in Prehistory. International Insular Investigations, V Deià Conference of Prehistory.* Archaeopress, Oxford, 420–427.

Bromage TG, Goldman HM, McFarlin SC, Warshaw J, Boyde A, Riggs CM. 2003. Circularly polarized light standards for investigations of collagen fiber orientation in bone. *Anatomical Record - Part B New Anatomist* 274, 157–168.

Bromage TG, Idaghdour Y, Lacruz RS, Crenshaw TD, Ovsiy O, Rotter B, Hoffmeier K, Schrenk F. 2016. The swine plasma metabolome chronicles "many days" biological timing and functions linked to growth. *PLoS ONE* 11, 1–19.

Bromage TG, Lacruz RS, Hogg RT, Goldman HM, McFarlin SC, Warshaw J, Dirks W, Perez-Ochoa A, Smolyar I, Enlow DH, Boyde A. 2009. Lamellar bone is an incremental tissue reconciling enamel rhythms, body size, and organismal life history. *Calcified Tissue International* 84, 388–404.

Bromage TG, Werning S. 2013. Image standardization in paleohistology. In: Padian K, Lamm E-T (Eds.), *Bone Histology of Fossil Tetrapods - Advancing Methods, Analysis, and Interpretation*. University of California Press, Berkeley, 161–175.

Brown JH, Marquet PA, Taper ML. 1993. Evolution of body size: consequences of an energetic definition of fitness. *The American Naturalist* 142, 573–584.

Brown JH, Sibly RM. 2006. Life-history evolution under a production constraint. *Proceedings of the National Academy of Sciences* 103, 17595–17599.

Bryant JD, Luz B, Froelich PN. 1994. Oxygen isotopic composition of fossil horse tooth phosphate as a record of continental paleoclimate. *Palaeogeography, Palaeoclimatology, Palaeoecology* 107, 303–316.

Burgman JHE, Leichliter J, Avenant NL, Ungar PS. 2016. Dental microwear of sympatric rodent species sampled across habitats in southern Africa: implications for environmental influence. *Integrative Zoology* 11, 111–127.

Bybee PJ, Lee AH, Lamm E-T. 2006. Sizing the Jurassic theropod dinosaur *Allosaurus*: assessing growth strategy and evolution of ontogenetic scaling of limbs. *Journal of Morphology* 267, 347–359.

Calandra I, Merceron G. 2016. Dental microwear texture analysis in mammalian ecology. *Mammal Review* 46, 215-228.

Calder WA. 1984. *Size, Function, and Life History*. Harvard University Press, Cambridge.

Calderón T, DeMiguel D, Arnold W, Stalder G, Köhler M. 2019. Calibration of life history traits with epiphyseal closure, dental eruption and bone histology in captive and wild red deer. *Journal of Anatomy* 235, 205-216.

Cantalapiedra JL, Prado JL, Hernández Fernández M, Alberdi MT. 2017. Decoupled ecomorphological evolution and diversification in Neogene-Quaternary horses. *Science* 355, 627–630.

Casanovas-Vilar I, Alba DM, Garcés M, Robles JM, Moyà-Solà S. 2011. Updated chronology for the Miocene hominoid radiation in Western Eurasia. *Proceedings of the National Academy of Sciences of the United States of America* 108, 5554–5559.

Case TJ. 1978. A general explanation for insular body size trends in terrestrial vertebrates. *Ecology* 59, 1–18.

Case TJ. **1979**. Optimal body size and an animal's diet. *Acta Biotheoretica* 28, 54–69.

Castanet J. **2006**. Time recording in bone microstructures of endothermic animals; functional relationships. *Comptes Rendus - Palevol* 5, 629–636.

Castanet J, Croci S, Aujard F, Perret M, Cubo J, de Margerie E. **2004**. Lines of arrested growth in bone and age estimation in a small primate: *Microcebus murinus*. *Journal of Zoology* 263, 31–39.

Castanet J, Francillon-Vieillot H, Meunier FJ, de Ricqlès AJ. **1993**. Bone and individual aging. In: *Bone Volume 7 Bone Growth*. CRC Press, Boca Raton, 245–283.

Castanet J, Rogers KC, Cubo J, Boisard J-J. **2000**. Periosteal bone growth rates in extant ratites (ostriche and emu). Implications for assessing growth in dinosaurs. *Comptes Rendus de l'Academie des sciences. Serie III, Sciences de la vie* 323, 543–550.

Cerling TE, Harris JM. **1999**. Carbon isotope fractionation between diet and bioapatite in ungulate mammals and implications for ecological and paleoecological studies. *Oecologia* 120, 347–363.

Cerling TE, Harris JM, MacFadden BJ, Leakey MG, Quade J, Eisenmann V, Ehleringer JR. **1997**. Global vegetation change through the Miocene/Pliocene boundary. *Nature* 389, 153–158.

Charlesworth B. **1994**. *Evolution in Age-Structured Populations*. Cambridge University Press, Cambridge.

Chinsamy-Turan A. **2005**. *The Microstructure of Dinosaur Bone*. The Johns Hopkins University Press, Baltimore and London.

Chinsamy A, Chiappe LM, Dodson P. **1995**. Mesozoic avian bone microstructure: physiological implications. *Paleobiology* 21, 561–574.

Chinsamy A, Valenzuela N. **2008**. Skeletochronology of the endangered side-neck turtles *Podocnemis expansa*. *South African Journal of Science* 104, 311–314.

Choquenot D. **1991**. Density-dependent growth, body condition, and demography in feral donkeys: testing the food hypothesis. *Ecology* 72, 805–813.

Christol J de. **1832**. Description d'*Hipparion*. *Annales des Sciences et de l'Industrie du Midi de France* 1, 180–181.

Churcher CS. **1993**. *Equus grevyi*. *Mammalian Species* 423, 1–9.

Clavel J, Merceron G, Hristova L, Spassov N, Kovachev D, Escarguel G. **2012**. On *Mesopithecus* habitat: insights from late Miocene fossil vertebrate localities of Bulgaria. *Journal of Human Evolution* 63, 162–179.

Clementz MT. **2012**. New insight from old bones: stable isotope analysis of fossil mammals. *Journal of Mammalogy* 93, 368–380.

Cody ML. **1966**. A general theory of clutch size. *Evolution* 20, 174–184.

Conover WJ, Iman RL. 1981. Rank transformations as a bridge between parametric and nonparametric statistics. *The American Statistician* 35, 124-129.

Cormack D. 1987. *Ham's Histology*. Lippincott Williams & Wilkins, Philadelphia.

Costeur L, Legendre S. 2008. Spatial and temporal variation in European Neogene large mammals diversity. *Palaeogeography, Palaeoclimatology, Palaeoecology* 261, 127–144.

Cubo J, Le Roy N, Martinez-Maza C, Montes L. 2012. Paleohistological estimation of bone growth rate in extinct archosaurs. *Paleobiology* 38, 335–349.

Cuijpers S, Lauwerier RCGM. 2008. Differentiating between bone fragments from horses and cattle: a histological identification method for archaeology. *Environmental Archaeology* 13, 165–179.

Currey JD. 2002. *Bones. Structure and Mechanics*. Princeton University Press, Princeton and Oxford.

Currey JD. 2003. The many adaptations of bone. *Journal of Biomechanics* 36, 1487–1495.

Curry KA. 1999. Ontogenetic histology of *Apatosaurus* (Dinosauria: Sauropoda): new insights on growth rates and longevity. *Journal of Vertebrate Paleontology*.

D'Ambrosia ARD, Clyde WC, Fricke HC, Gingerich PD, Abels HA. 2017. Repetitive mammalian dwarfing during ancient greenhouse warming events. *Science Advances* 3, 1–19.

Damuth JD, Janis CM. 2011. On the relationship between hypsodonty and feeding ecology in ungulate mammals, and its utility in palaeoecology. *Biological Reviews* 86, 733–758.

Damuth JD, MacFadden BJ. 1990. *Body Size in Mammalian Paleobiology : Estimation and Biological Implications*. Cambridge University Press.

Dauphin Y, Williams CT. 2004. Diagenetic trends of dental tissues. *Comptes Rendus - Palevol* 3, 583–590.

de Jong G. 2006. Covariances between traits deriving from successive allocations of a resource. *Functional Ecology* 7, 75–83.

de Margerie E, Cubo J, Castanet J. 2002. Bone typology and growth rate: testing and quantifying "Amprino's rule" in the mallard (*Anas platyrhynchos*). *Comptes Rendus - Biologies* 325, 221–230.

de Margerie E, Robin J-P, Verrier D, Cubo J, Groscolas R, Castanet J. 2004. Assessing a relationship between bone microstructure and growth rate: a fluorescent labelling study in the king penguin chick (*Aptenodytes patagonicus*). *The Journal of experimental biology* 207, 869–79.

de Ricqlès AJ, Meunier FJ, Castanet J, Francillon-Vieillot H. 1991. Comparative microstructure of bone. In: Hall BK (Ed.), *Bone Volume 3: Bone Matrix and Bone Specific Products*. CRC Press, Boca Raton, 1–78.

Dean MC. 2000. Incremental markings in enamel and dentine: what they can tell us about the way teeth grow. In: Teaford MF, Meredith Smith M, Ferguson MWJ (Eds.), *Development, Function and Evolution of Teeth*. Cambridge University Press, Cambridge, 119–130.

Dean MC. 2006. Tooth microstructure tracks the pace of human life-history evolution. *Proceedings. Biological sciences / The Royal Society* 273, 2799–2808.

Dean MC, Leakey MG, Reid DJ, Schrenk F, Schwartz GT, Stringer C, Walker A. 2001. Growth processes in teeth distinguish modern humans from *Homo erectus* and earlier hominins. *Nature* 414, 628–631.

DeMiguel D, Azanza B, Morales J. 2018. Regional impacts of global climate change: a local humid phase in central Iberia in a late Miocene drying world. *Palaeontology* 62, 77-92.

Denk T, Zohner CM, Grimm GW, Renner SS. 2018. Plant fossils reveal major biomes occupied by the late Miocene Old-World Pikermian fauna. *Nature Ecology and Evolution* 2, 1864–1870.

DeSantis LRG. 2016. Dental microwear textures: reconstructing diets of fossil mammals. *Surface Topography: Metrology and Properties* 4, 023002.

DeSantis LRG, Scott JR, Schubert BW, Donohue SL, McCray BM, Van Stolk CA, Winburn AA, Greshko MA, O'Hara MC. 2013. Direct comparisons of 2D and 3D dental microwear proxies in extant herbivorous and carnivorous mammals. *PLoS ONE* 8, e71428.

Dirks W, Anemone RL, Holroyd PA, Reid DJ, Walton P. 2009. Phylogeny, life history and the timing of molar crown formation in two archaic ungulates, *Meniscotherium* and *Phenacodus* (Mammalia, 'Condylarthra'). *Frontiers of Oral Biology* 13, 3–8.

Dirks W, Bowman JE. 2007. Life history theory and dental development in four species of catarrhine primates. *Journal of Human Evolution* 53, 309–320.

Dirks W, Bromage TG, Agenbroad LD. 2012. The duration and rate of molar plate formation in *Palaeoloxodon cypriotes* and *Mammuthus columbi* from dental histology. *Quaternary International* 255, 79–85.

Dixon PM, Copeland AN. 1993. The radiological appearance of mandibular cheek teeth in ponies of different ages. *Equine Veterinary Education* 5, 317–323.

Domingo L, Grimes ST, Domingo MS, Alberdi MT. 2009. Paleoenvironmental conditions in the Spanish Miocene-Pliocene boundary: isotopic analyses of *Hipparion* dental enamel. *Naturwissenschaften* 96, 503–511.

Domingo L, Koch PL, Hernández Fernández M, Fox DL, Domingo MS, Alberdi MT. 2013. Late Neogene and Early Quaternary paleoenvironmental and paleoclimatic conditions in southwestern Europe: isotopic analyses on mammalian taxa. *PLoS ONE* 8, e63739.

Domingo MS, Cantero E, García-Real I, Chamorro Sancho MJ, Martín Perea DM, Alberdi MT, Morales J. 2018. First radiological study of a complete dental ontogeny sequence of an extinct equid: implications for equidae life history and taphonomy. *Scientific Reports* 8, 8507.

Duncan AJ, Poppi DP. 2008. Nutritional ecology of grazing and browsing ruminants. In: Gordon IJ, Prins HHT (Eds.), *The Ecology of Browsing and Grazing. Ecological Studies*. Springer, Berlin, Heidelberg, Berlin, Heidelberg, 89–116.

Easley J, Dixon PM, Schumacher J. 2005. *Equine Dentistry*, Third. ed. Elsevier Saunders.

Ehleringer JR, Cerling TE, Helliker BR. 1997. C_4 photosynthesis, atmospheric CO_2, and climate. *Oecologia* 112, 285–299.

Eisenberg JF. 1990. The behavioral/ecological significance of body size in the Mammalia. In: Damuth J, Macfadden BJ (Eds.), *Body Size in Mammalian Paleobiology: Estimation and Biological Implications*. Cambridge University Press, Cambridge, 25–37.

Eisenmann V. 1980. Caractères spécifiques et problèmes taxonomiques relatifs à certains hipparions africains. In: Leakey RE, Ogot BA (Eds.), *Proceedings of the 8th Panafrican Congress of Prehistory and Quaternay Studies*. Nairobi, 77–81.

Eisenmann V. 1985. Les Equidés des gisements de la vallée de l'Omo en Ethiopie. In: Coppens Y, Howell FC (Eds.), *Les Faunes Plio-Pléistocène de La Basse Vallée de l'Omo (Ethiopie). Tome 1: PCahiers de Paléontologie, Travaux de Paléontologie Est-Africaine*. CNRS, Paris, 13–65.

Eisenmann V. 1995. What metapodial morphometry has to say about some Miocene hipparions. In: Vrba ES, Denton GH, Partridge T, Burckle LH (Eds.), *Paleoclimate and Evolution, with Emphasis on Human Origins*. New Haven and London, 149–164.

Eisenmann V. 2003. Gigantic horses. In: Petculescu A, Ştiuca E (Eds.), *Advances in Vertebrate Paleontology = Progrés Dans La Paléontologie Des Vertébrates : Hen to Panta*. Romanian Academy "Emil Racoviţă" Institute of Speleology, Bucharest, 31–40.

Eisenmann V, Alberdi MT, De Giuli C, Staesche U. 1988. Studying fossil horses. *Collected papers after the "New York International* Hipparion *Conference, 1981."*

Eisenmann V, Sondaar PY. 1989. Hipparions and the Mio-Pliocene boundary. *Bollettino della Società Paleontologica Italiana* 28, 217–226.

Eisenmann V, Sondaar PY. 1998. Pliocene vertebrate locality of Çalta, Ankara, Turkey. 7. *Hipparion*. *Geodiversitas* 20, 409–439.

Eisenmann V, Sondaar PY, Alberdi MT, De Giuli C. 1987. Is horse phylogeny becoming a playfield in the game of theoretical evolution? *Journal of Vertebrate Paleontology* 7, 224–229.

Engström C, Engström H, Sagne S. 1983. Lower third molar development in relation to skeletal maturity and chronological age. *The Angle Orthodontist* 53, 97–106.

Enlow DH. 1962. A study of the post-natal growth and remodeling of bone. *American Journal of Anatomy* 110, 79–101.

Enlow DH, Brown SO. 1958. A comparative histological study of fossil and recent bone tissues. Part III. *The Texas Journal of Science* 10, 187–230.

Erickson GM, Curry KA, Yerby SA. 2001. Dinosaurian growth patterns and rapid avian growth rates. *Nature* 412, 429–433.

Erickson GM, Makovicky PJ, Currie PJ, Norell MA, Yerby SA, Brochu CA. 2004. Gigantism and comparative life-history parameters of tyrannosaurid dinosaurs. *Nature* 430, 772–775.

Ernest SKM. 2003. Life history characteristics of placental nonvolant mammals. *Ecology* 84, 3402–3402.

Estes R. 1991. *The Behavior Guide to African Mammals: Including Hoofed Mammals, Carnivores, Primates*. University of California Press, Berkeley.

Fahlbusch V. 1976. Report on the International Symposium on mammalian stratigraphy of the European Tertiary (München, April 11-14, 1975). *Newsletters on Stratigraphy* 5, 160–167.

Fischhoff IR, Sundaresan SR, Cordingley J, Rubenstein DI. 2007. Habitat use and movements of plains zebra (*Equus burchelli*) in response to predation danger from lions. *Behavioral Ecology* 18, 725–729.

Fitzgerald CM. 1998. Do enamel microstructures have regular time dependency? Conclusions from the literature and a large-scale study. *Journal of Human Evolution* 35, 371–386.

Fitzgerald CM, Rose JC. 2008. Reading between the lines: dental development and subadult age assessment using the microstructural growth markers of teeth. In: *Biological Anthropology of the Human Skeleton: Second Edition*. John Wiley & Sons, Inc., Hoboken, NJ, USA, 237–263.

Flatt T, Heyland A. 2011. *Mechanisms of Life History Evolution : The Genetics and Physiology of Life History Traits and Trade-Offs*. Oxford University Press, Oxford.

Forsten A. 1968. Revision of the palearctic *Hipparion*. *Acta Zoologica Fennica* 119, 1–134.

Forsten A. 1978a. *Hipparion* and possible Iberian-North African Neogene connections. *Annales Zoologici Fennici* 15, 294–297.

Forsten A. 1978b. *Hipparion primigenium* (v. Meyer, 1829), an early three-toed horse. *Annales Zoologici Fennici* 15, 298–313.

Forsten A. 1983. The preorbital fossa as a taxonomic character in some Old World *Hipparion*. *Journal of Paleontology* 57, 686–704.

Forsten A. 1988. Middle Pleistocene replacement of stenonid horses by caballoid horses - ecological implications. *Palaeogeography, Palaeoclimatology, Palaeoecology* 65, 23–33.

Forsten A. 1989. Horse diversity through the ages. *Biological Reviews* 64, 279–304.

Forsten A. 1991. Size decrease in Pleistocene-Holocene true or caballoid horses of Europe. *Mammalia* 55, 407–420.

Forsten A. 1997. *Hipparion* from Santiga (Spain) and its biostratigraphic significance. *Paleontologia i Evolució* 30, 77–82.

Forsten A, Kaya T. 1995. The hipparions (Mammalia, Equidae) from Gülpinar (Canakkale, Turkey). *Paläontologische Zeitschrift* 69, 491–501.

Fortelius M, Eronen J, Liu L, Pushkina D, Tesakov A, Vislobokova I, Zhang Z. 2006. Late Miocene and Pliocene large land mammals and climatic changes in Eurasia. *Palaeogeography, Palaeoclimatology, Palaeoecology* 238, 219–227.

Fortelius M, Solounias N. 2000. Functional characterization of ungulate molars using the abrasion-attrition wear gradient: a new method for reconstructing paleodiets. *American Museum Novitates* 3301, 1–36.

Fortelius M, Werdelin L, Andrews P, Bernor RL, Gentry A, Humphrey L, Mittmann HW, Viranta S. 1996. Provinciality, diversity, turnover and paleoecology in land mammal faunas of the later Miocene of Western Eurasia. In: Bernor RL, Fahlbusch V, Mittmann H-W (Eds.), *The Evolution of Western Eurasian Neogene Mammal Faunas*. Columbia University Press, 414–448.

Fortin D, Beyer HL, Boyce MS, Smith DW, Mao JS, Ecology S, May N. 2005. Wolves influence elk movements: behavior shapes a trophic cascade in Yellowstone National Park. *Ecology* 86, 1320–1330.

Foster JB. 1964. Evolution of mammals on islands. *Nature* 202, 234–235.

Francillon-Vieillot H, de Buffrénil V, Castanet J, Géraudie J, Meunier FJ, Sire JY, Zylberberg L, de Ricqlès AJ. 1990. Microstructure and mineralization of vertebrate skeletal tissues. In: Carter JC (Ed.), *Skeletal Biomineralization: Patterns, Processes and Evolutionary Trends*. Van Nostrand Reinhold, New York, 471–530.

Franzen JL. 2010. *The Rise of Horses: 55 Million Years of Evolution*. Johns Hopkins University Press, Baltimore.

Freeland WJ, Choquenot D. 1990. Determinants of herbivore carrying capacity: plants, nutrients, and *Equus asinus* in northern Australia. *Ecology* 71, 589–597.

Froehlich DJ. 2002. Quo vadis eohippus? The systematics and taxonomy of the early Eocene equids (Perissodactyla). *Zoological Journal of the Linnean Society* 134, 141–256.

Gabunia LK, Chochieva KI. 1982. Co-evolution of the *Hipparion* fauna and vegetation in the Paratethys region. *Evolutionary Theory* 6, 1–13.

Gadgil M, Bossert WH. 1970. Life historical consequences of natural selection. *American Naturalist*.

Gagnon M, Chew AE. 2000. Dietary preferences in extant African Bovidae. *Journal of Mammalogy* 81, 490–511.

Gaillard JM, Festa-Bianchet M, Yoccoz NG, Loison A, Toïgo C. 2000. Temporal variation in fitness components and population dynamics of large herbivores. *Annual Review of Ecology and Systematics* 31, 367–393.

Gaillard JM, Pontier D, Allainé D, Lebreton JD, Trouvilliez J, Clobert J. 2006. An analysis of demographic tactics in birds and mammals. *Oikos* 56, 59.

Gaillard JM, Yoccoz NG. 2003. Temporal variation in survival of mammals: a case of environmental canalization? *Ecology* 84, 3294–3306.

Garcés M, Agustí J, Cabrera L, Parés JM. 1996. Magnetostratigraphy of the Vallesian (late Miocene) in the Vallès-Penedès Basin (northeast Spain). *Earth and Planetary Science Letters* 142, 381–396.

Garcés M, Cabrera L, Agustí J, Maria Parés J. 1997. Old World first appearance datum of "*Hipparion*" horses: late Miocene large-mammal dispersal and global events. *Geology* 25, 19.

García-Martínez R, Marín-Moratalla N, Jordana X, Köhler M. 2011. The ontogeny of bone growth in two species of dormice: reconstructing life history traits. *Comptes Rendus - Palevol* 10, 489–498.

Georgiadis N, Hack M, Turpin K. 2003. The influence of rainfall on zebra population dynamics: Implications for management. *Journal of Applied Ecology* 40, 125–136.

Godfrey LR, Samonds KE, Jungers WL, Sutherland MR. 2001. Teeth, brains, and primate life histories. *American Journal of Physical Anthropology* 114, 192–214.

Godvik IMR, Loe LE, Vik JO, Veiberg V, Langvatn R, Mysterud A. 2009. Temporal scales, trade-offs, and functional responses in red deer habitat selection. *Ecology* 90, 699–710.

Gomes Rodrigues H, Herrel A, Billet G. 2017. Ontogenetic and life history trait changes associated with convergent ecological specializations in extinct ungulate mammals. *Proceedings of the National Academy of Sciences* 114, 1069–1074.

Gosz JR, Moore DI. 1989. Strontium isotope studies of atmospheric inputs to forested watersheds in New Mexico. *Biogeochemistry* 8, 115–134.

Gould GC, MacFadden BJ. 2004. Gigantism, dwarfism, and Cope's Rule: "nothing in evolution makes sense without a phylogeny." *Bulletin of the American Museum of Natural History* 285, 219–237.

Gould SJ. 1966. Allometry and size in ontogeny and phylogeny. *Biological Reviews* 41, 587–638.

Gould SJ. 1987. Life's little joke. *Natural history* 96, 16–24.

Grubb P. 1981. *Equus burchelli*. *Mammalian Species* 157, 1-9.

Guatelli-Steinberg D, Floyd BA, Dean MC, Reid DJ. 2012. Enamel extension rate patterns in modern human teeth: two approaches designed to establish an integrated comparative context for fossil primates. *Journal of Human Evolution* 63, 475–486.

Guthrie RD. 2003. Rapid body size decline in Alaskan Pleistocene horses before extinction. *Nature* 426, 169–171.

Hammer Ø, Harper DAT a. T, Ryan PD. 2001. PAST: paleontological statistics software package for education and data analysis. *Palaeontologia Electronica* 4, 1–9.

Harborne JB. 1988. *Introduction to Ecological Biochemistry*. Academic Press, London.

Harvati K, Frost SR. 2007. Dental eruption sequences in fossil colobines and the evolution of primate life histories. *International Journal of Primatology* 28, 705–728.

Hayek L-AC, Bernor RL, Solounias N, Steigerwald P. 1992. Preliminary studies of hipparionine horse diet as measured by tooth microwear. *Annales Zoologici Fennici* 28, 187–200.

Heck L, Clauss M, Sánchez-Villagra MR. 2017. Gestation length variation in domesticated horses and its relation to breed and body size diversity. *Mammalian Biology* 84, 44–51.

Hedberg C, DeSantis LRG. 2017. Dental microwear texture analysis of extant koalas: clarifying causal agents of microwear. *Journal of Zoology* 301, 206–214.

Hernández Fernández M, Alberdi MT, Azanza B, Montoya P, Morales J, Nieto M, Pelaez-Campomanes P. 2006. Identification problems of arid environments in the Neogene-Quaternary mammal record of Spain. *Journal of Arid Environments* 66, 585–608.

Hernández L, Laundré JW. 2007. Foraging in the 'landscape of fear' and its implications for habitat use and diet quality of elk *Cervus elaphus* and bison *Bison bison*. *Wildlife Biology* 11, 215–220.

Hillson S. 2005. *Teeth*. Cambridge University Press.

Hipondoka MH., Aranibar J., Chirara C, Lihavha M, Macko S. 2003. Vertical distribution of grass and tree roots in arid ecosystems of Southern Africa: niche differentiation or competition? *Journal of Arid Environments* 54, 319–325.

Hogg RT. 2018. Permanent record: The use of dental and bone microstructure to assess life history evolution and ecology. In: Delson E, Sargis EJ (Eds.), *Vertebrate Paleobiology and Paleoanthropology*. Springer, Cham, 75–98.

Hogg RT, Walker RS. 2011. Life-history correlates of enamel microstructure in cebidae (platyrrhini, primates). *Anatomical Record* 294, 2193–2206.

Holliday R. 1989. Food, reproduction and longevity: is the extended lifespan of calorie-restricted animals an evolutionary adaptation? *BioEssays : news and reviews in molecular, cellular and developmental biology* 10, 125–127.

Hoppe KA, Koch PL, Carlson RW, Webb SD. 1999. Tracking mammoths and mastodons: reconstruction of migratory behavior using strontium isotope ratios. *Geology* 27, 439–442.

Hoppe KA, Stover SM, Pascoe JR, Amundson R. 2004. Tooth enamel biomineralization in extant horses: implications for isotopic microsampling. *Palaeogeography, Palaeoclimatology, Palaeoecology* 206, 355–365.

Horner JR, de Ricqlès AJ, Padian K. 1999. Variation in dinosaur skeletochronology indicators: implications for age assessment and physiology. *Paleobiology* 25, 295–304.

Horner JR, de Ricqlès AJ, Padian K. 2000. Long bone histology of the hadrosaurid dinosaur *Maiasaura peeblesorum*: growth dynamics and physiology based on an ontogenetic series of skeletal elements. *Journal of Vertebrate Paleontology* 20, 115–129.

Horner JR, Padian K. 2004. Age and growth dynamics of *Tyrannosaurus rex*. *Proceedings of the Royal Society of London. Series B: Biological Sciences* 271, 1875–1880.

Hristova L. 2009. Ontogeny and variability in the cheek region of hipparions from the late Miocene locality of Hadzhidimovo-1, southwest Bulgaria. *Rivista Italiana di Paleontologia e Stratigrafia* 115, 125-132.

Hulbert RC. 1982. Population dynamics of the three-toed horse *Neohipparion* from the late Miocene of Florida. *Paleobiology* 8, 159–167.

Hulbert RC. **1984**. Paleoecology and population dynamics of the early Miocene (Hemingfordian) horse *Parahippus leonensis* from the Thomas Farm site, Florida. *Journal of Vertebrate Paleontology* 4, 547–558.

Hulbert RC. **1988**. *Cormohipparion* and *Hipparion* (Mammalia, Perissodactyla, Equidae) from the Late Neogene of Florida. *Bulletin of the Florida State Museum, Biological Sciences* 33, 229–338.

Hulbert RC. **1993**. Taxonomic evolution in North American Neogene horses (subfamily Equinae): the rise and fall of an adaptive radiation. *Paleobiology* 19, 216–234.

Hulbert RC, MacFadden BJ. **1991**. Morphological transformation and cladogenesis at the base of the adaptive radiation of Miocene hypsodont horses. *American Museum Novitates* 3000, 1–61.

Huttenlocker AK, Woodward HN, Hall BK. **2013**. The biology of bone. In: Padian K, Lamm E-T (Eds.), *Bone Histology of Fossil Tetrapods - Advancing Methods, Analysis, and Interpretation*. University of California Press, Berkeley, 13–34.

Iinuma YM, Tanaka S, Kawasaki K, Kuwajima T, Nomura H, Suzuki M, Ohtaishi N. **2004**. Dental incremental lines in sika deer (*Cervus nippon*); polarized light and fluorescence microscopy of ground sections. *Journal of Veterinary Medical Science* 66, 665–669.

Ioakim C, Koufos GD. **2009**. Palynology. In: Koufos GD, Nagel D (Eds.), *The Late Miocene Mammal Faunas of the Mytilinii Basin, Samos Island, Greece: New Collection Beiträge Zur Paläontologie* 31, 27–35.

Janis CM. **1976**. The evolutionary strategy of the equidae and the origins of rumen and cecal digestion. *Evolution* 30, 757-774.

Janis CM. **1990**. Correlation of cranial and dental variables with body size in ungulates and macropodoids. In: Damuth J, Macfadden BJ (Eds.), *Body Size in Mammalian Paleobiology: Estimation and Biological Implications*. Cambridge University Press, Cambridge, 255–299.

Janis CM. **2007**. The Horse series. In: Regal B (Ed.), *Icons of Evolution*. Greenwood Press, Wesport, 251–280.

Janis CM. **2008**. An evolutionary history of browsing and grazing ungulates. In: Gordon IJ, Prins HHT (Eds.), *The Ecology of Browsing and Grazing. Ecological Studies*. Springer, Berlin, Heidelberg, 21–45.

Janis CM, Gordon IJ, Illius AW. **1994**. Modelling equid/ruminant competition in the fossil record. *Historical Biology* 8, 15–29.

Jiménez-Moreno G, Fauquette S, Suc JP. **2010**. Miocene to Pliocene vegetation reconstruction and climate estimates in the Iberian Peninsula from pollen data. *Review of Palaeobotany and Palynology* 162, 403–415.

Johnson MR, Geary DH. **2016**. Stable isotope ecology of *Hippotherium* from the Late Miocene Pannonian Basin system. *Palaeogeography, Palaeoclimatology, Palaeoecology* 459, 44–52.

Jónsson H, Schubert M, Seguin-Orlando A, Ginolhac A, Petersen L, Fumagalli M, Albrechtsen A, Petersen B, Korneliussen TS, Vilstrup JT, Lear T, Myka JL, Lundquist J, Miller DC, Alfarhan AH, Alquraishi SA, Al-Rasheid KAS, Stagegaard J, Strauss G, Bertelsen MF, Sicheritz-Ponten T, Antczak DF, Bailey E, Nielsen R, Willerslev E, Orlando L. 2014. Speciation with gene flow in equids despite extensive chromosomal plasticity. *Proceedings of the National Academy of Sciences* 111, 18655–18660.

Jordana X, Köhler M. 2011. Enamel microstructure in the fossil bovid *Myotragus balearicus* (Majorca, Spain): implications for life-history evolution of dwarf mammals in insular ecosystems. *Palaeogeography, Palaeoclimatology, Palaeoecology* 300, 59–66.

Jordana X, Marín-Moratalla N, DeMiguel D, Kaiser TM, Köhler M. 2012. Evidence of correlated evolution of hypsodonty and exceptional longevity in endemic insular mammals. *Proceedings of the Royal Society B: Biological Sciences* 279, 3339–3346.

Jordana X, Marín-Moratalla N, Moncunill-Solé B, Bover P, Alcover JA, Köhler M. 2013. First fossil evidence for the advance of replacement teeth coupled with life history evolution along an anagenetic mammalian lineage. *PLoS ONE* 8, e70743.

Jordana X, Marín-Moratalla N, Moncunill-Solé B, Köhler M. 2014. Ecological and life-history correlates of enamel growth in ruminants (Artiodactyla). *Biological Journal of the Linnean Society* 112, 657–667.

Jordana X, Marín-Moratalla N, Moncunill-Solé B, Nacarino-Meneses C, Köhler M. 2016. Ontogenetic changes in the histological features of zonal bone tissue of ruminants: A quantitative approach. *Comptes Rendus - Palevol* 15, 265–276.

Kaiser TM. 2003. The dietary regimes of two contemporaneous populations of *Hippotherium primigenium* (Perissodactyla, Equidae) from the Vallesian (Upper Miocene) of Southern Germany. *Palaeogeography, Palaeoclimatology, Palaeoecology* 198, 381–402.

Kaiser TM, Bernor RL, Scott RS, Franzen JL, Solounias N. 2003. New interpretations of the systematics and paleoecology of the Dorn-Düerkheim 1 hipparions (Late Miocene, Turolian Age (MN11)), Rheinhessen, Germany. *Senckenbergiana lethaea* 83, 103–134.

Kierdorf H, Breuer F, Richards A, Kierdorf U. 2014. Characterization of enamel incremental markings and crown growth parameters in minipig molars. *Anatomical Record* 297, 1935–1949.

Kierdorf H, Kierdorf U, Frölich K, Witzel C. 2013. Lines of evidence-incremental markings in molar enamel of soay sheep as revealed by a fluorochrome labeling and backscattered electron imaging study. *PLoS ONE* 8, e74597.

Kierdorf H, Witzel C, Upex B, Dobney K, Kierdorf U. 2012. Enamel hypoplasia in molars of sheep and goats, and its relationship to the pattern of tooth crown growth. *Journal of Anatomy* 220, 484–495.

Klein DR. 1965. Ecology of deer range in Alaska. *Ecological Monographs* 35, 259–284.

Klein DR, Strandgaard H. 1972. Factors affecting growth and body size of roe deer. *The Journal of Wildlife Management* 36, 64–79.

Klevezal GA. 1996. *Recording Structures of Mammals: Determination of Age and Reconstruction of Life History*. Balkema, Rotterdam.

Köhler M. 2010. Fast or slow? The evolution of life history traits associated with insular dwarfing. In: Pérez-Mellado V, Ramon, MM (Eds.)*, Islands and Evolution*. Institut Menorquí d'Estudis, 261–280.

Köhler M, Marín-Moratalla N, Jordana X, Aanes R. 2012. Seasonal bone growth and physiology in endotherms shed light on dinosaur physiology. *Nature* 487, 358–361.

Köhler M, Moyà-Solà S. 2009. Physiological and life history strategies of a fossil large mammal in a resource-limited environment. *Proceedings of the National Academy of Sciences of the United States of America* 106, 20354–20358.

Kolb C, Scheyer TM, Lister AM, Azorit C, de Vos J, Schlingemann M, Rössner GE, Monaghan NT, Sánchez-Villagra MR. 2015a. Growth in fossil and extant deer and implications for body size and life history evolution. *BMC Evolutionary Biology* 15, 19.

Kolb C, Scheyer TM, Veitschegger K, Forasiepi AM, Amson E, Van der Geer AA, Van den Hoek Ostende LW, Hayashi S, Sánchez-Villagra MR. 2015b. Mammalian bone palaeohistology: a survey and new data with emphasis on island forms. *PeerJ* 3, e1358.

Koons DN, Metcalf CJE, Tuljapurkar S. 2008. Evolution of delayed reproduction in uncertain environments: a life-history perspective. *The American Naturalist* 172, 797–805.

Kostopoulos DS. 2009. The Pikermian Event: temporal and spatial resolution of the Turolian large mammal fauna in SE Europe. *Palaeogeography, Palaeoclimatology, Palaeoecology* 274, 82–95.

Koufos GD. 1986. Study of the Vallesian hipparions of the lower Axios valley (Macedonia, Greece). *Geobios* 19, 61–85.

Koufos GD. 1987. Study of the Turolian hipparions of the Lower Axios Valley (Macedonia, Greece). 1. Locality «Ravin des Zouaves-5 (RZO). *Geobios* 20, 293–312.

Koufos GD. 2006. Palaeoecology and chronology of the Vallesian (late Miocene) in the Eastern Mediterranean region. *Palaeogeography, Palaeoclimatology, Palaeoecology* 234, 127–145.

Koufos GD. 2013. Neogene mammal biostratigraphy and chronology of Greece. In: Wang X, Flynn LJ, Fortelius M (Eds.), *Fossil Mammals of Asia—Neogene Biostratigraphy and Chronology*. Columbia University Press, New York, 595–621.

Koufos GD. 2016. *Hipparion macedonicum* revisited: new data on evolution of hipparionine horses from the Late Miocene of Greece. *Acta Palaeontologica Polonica* 61, 519–536.

Koufos GD, Konidaris GE. 2011. Late Miocene carnivores of the Greco-Iranian Province: composition, guild structure and palaeoecology. *Palaeogeography, Palaeoclimatology, Palaeoecology* 305, 215–226.

Koufos GD, Kostopoulos DS, Merceron G. **2009**. Palaeoecology - Palaeobiogeography. In: Koufos GD, Nagel D (Eds.), *The Late Miocene Mammal Faunas of the Mytilinii Basin, Samos Island, Greece: New Collection. Beiträge Zur Paläontologie* 31, 409–430.

Koufos GD, Kostopoulos DS, Vlachou TD. **2016**. Revision of the Nikiti 1 (NKT) fauna with description of new material. In: Koufos GD, Kostopoulos DS (Eds.), *Palaeontology of the Upper Miocene Vertebrate Localities of Nikiti (Chalkidiki Peninsula, Macedonia, Greece). Geobios* 49, 11–22.

Koufos GD, Merceron G, Kostopoulos DS, Vlachou TD, Sylvestrou IA. **2006**. Palaeoecology and Palaeobiogeography. In: Koufos GD (Ed.), *The Late Miocene Vertebrate Locality of Perivolaki, Thessaly, Greece. Palaeontographica Abteilung A* 276, 201–221.

Koufos GD, Vlachou TD. **2016**. Equidae. In: Koufos GD, Kostopoulos DS (Eds.), *Palaeontology of the Upper Miocene Vertebrate Localities of Nikiti (Chalkidiki Peninsula, Macedonia, Greece). Geobios* 49, 85–118.

Kurtén B. **1953**. On the variation and population dynamics of fossil and recent mammal populations. *Acta Zoologica Fennica* 76, 1–122.

Lacruz RS, Habelitz S, Wright JT, Paine ML. **2017**. Dental enamel formation and implications for oral health and disease. *Physiological Reviews* 97, 939–993.

Lacruz RS, Hacia JG, Bromage TG, Boyde A, Lei Y, Xu Y, Miller JD, Paine ML, Snead ML. **2012**. The circadian clock modulates enamel development. *Journal of Biological Rhythms* 27, 237–245.

Lamm E-T. **2013**. Preparation and sectioning of specimens. In: Padian K, Lamm E-T (Eds.), *Bone Histology of Fossil Tetrapods - Advancing Methods, Analysis, and Interpretation*. University of California Press, Berkeley, 55–160.

Lande R. **2015**. Evolution of phenotypic plasticity in colonizing species. *Molecular Ecology* 24, 2038–2045.

Law R. **1979**. Optimal life histories under age-specific predation. *The American Naturalist* 114, 399–417.

Lee AH, Huttenlocker AK, Padian K, Woodward HN. **2013**. Analysis of growth rates. In: Padian K, Lamm E-T (Eds.), *Bone Histology of Fossil Tetrapods - Advancing Methods, Analysis, and Interpretation*. University of California Press, Berkeley, 217–251.

Lee AH, O'Connor PM. **2013**. Bone histology confirms determinate growth and small body size in the noasaurid theropod *Masiakasaurus knopfleri*. *Journal of Vertebrate Paleontology* 33, 865–876.

Lindsay EH, Opdyke ND, Johnson NM. **1980**. Pliocene dispersal of the horse *Equus* and late Cenozoic mammalian dispersal events. *Nature* 287, 135–138.

Lindstedt SL, Calder, WA. **1981**. Body size, physiological time, and longevity of homeothermic animals. *The Quarterly Review of Biology* 56, 1–16.

Litsas G. **2015**. Growth hormone and craniofacial tissues. An update. *The Open Dentistry Journal* 9, 1–8.

Lomolino M V. 1985. Body size of mammals on islands: the Island Rule reexamined. *The American Naturalist* 125, 310–316.

Long ES, Courtney KL, Lippert JC, Wall-Scheffler CM. **2019**. Reduced body size of insular black-tailed deer is caused by slowed development. *Oecologia* 189, 675–685.

Lorenzen ED, Nogués-Bravo D, Orlando L, Weinstock J, Binladen J, Marske KA, Ugan A, Borregaard MK, Gilbert MTP, Nielsen R, Ho SYW, Goebel T, Graf KE, Byers D, Stenderup J, Rasmussen M, Campos PF, Leonard JA, Koepfli K-P, Froese D, Zazula GD, Stafford TW, Aaris-Sørensen K, Batra P, Haywood AM, Singarayer JS, Valdes PJ, Boeskorov G, Burns JA, Davydov SP, Haile J, Jenkins DL, Kosintsev P, Kuznetsova T, Lai X, Martin LD, McDonald HG, Mol D, Meldgaard M, Munch K, Stephan E, Sablin M, Sommer RS, Sipko T, Scott E, Suchard MA, Tikhonov A, Willerslev R, Wayne RK, Cooper A, Hofreiter M, Sher A, Shapiro B, Rahbek C, Willerslev E. **2011**. Species-specific responses of Late Quaternary megafauna to climate and humans. *Nature* 479, 359–364.

Lucas PW. **2004**. *Dental Functional Morphology : How Teeth Work*. Cambridge University Press, Cambridge.

Lucas PW, Casteren A van, Al-Fadhalah K, Almusallam AS, Henry AG, Michael S, Watzke J, Reed DA, Diekwisch TGH, Strait DS, Atkins AG. **2014**. The role of dust, grit and phytoliths in tooth wear. *Annales Zoologici Fennici* 51, 143–152.

MacArthur RH, Wilson EO. **1967**. *The Theory of Island Biogeography*. Princeton University Press.

MacFadden BJ. **1984**. Systematics and phylogeny of *Hipparion*, *Neohipparion*, *Nannippus*, and *Cormohipparion* (Mammalia, Equidae) from the Miocene and Pliocene of the New World. *Bulletin of the American Museum of Natural History* 179, 1–196.

MacFadden BJ. **1986**. Fossil horses from "*Eohippus*" (*Hyracotherium*) to *Equus*: scaling, Cope 's Law, and the evolution of body size. *Paleobiology* 12, 355–369.

MacFadden BJ. **1992**. *Fossil Horses : Systematics, Paleobiology, and Evolution of the Family Equidae*. Cambridge University Press, New York.

MacFadden BJ. **2005**. Fossil Horses--Evidence for Evolution. *Science* 307, 1728–1730.

MacFadden BJ, Hulbert RC. **1988**. Explosive speciation at the base of the adaptive radiation of Miocene grazing horses. *Nature* 336, 466–468.

MacFadden BJ, Skinner MF. **1981**. Earliest holarctic hipparion, *Cormohipparion goorisi* n. sp. (Mammalia, Equidae), from the Barstovian (medial Miocene) Texas Gulf Coastal Plain. *Journal of Paleontology* 55, 619–627.

Macho GA, Williamson DK. 2002. The effects of ecology on life history strategies and metabolic disturbances during development: an example from the African bovids. *Biological Journal of the Linnean Society* 75, 271–279.

Marín-Moratalla N, Jordana X, García-Martínez R, Köhler M. 2011. Tracing the evolution of fitness components in fossil bovids under different selective regimes. *Comptes Rendus - Palevol* 10, 469–478.

Marín-Moratalla N, Jordana X, Köhler M. 2013. Bone histology as an approach to providing data on certain key life history traits in mammals: implications for conservation biology. *Mammalian Biology* 78, 422–429.

Marmi J, Casanovas-Vilar I, Robles JM, Moyà-Solà S, Alba DM. 2012. The paleoenvironment of *Hispanopithecus laietanus* as revealed by paleobotanical evidence from the Late Miocene of Can Llobateres 1 (Catalonia, Spain). *Journal of Human Evolution* 62, 412–423.

Marsh OC. 1879. Polydactyl horses, recent and extinct. *American Journal of Science* 102, 499–505.

Martinez-Maza C, Alberdi MT, Nieto-Diaz M, Prado JL. 2014. Life-history traits of the Miocene *Hipparion concudense* (Spain) inferred from bone histological structure. *PLoS ONE* 9, e103708.

Matthew WD. 1926. The evolution of the horse: a record and its interpretation. *The Quaterly Review of Biology* 1, 139–185.

McNab BK. 1990. The physiological significance of body size. In: Damuth J, Macfadden BJ (Eds.), *Body Size in Mammalian Paleobiology: Estimation and Biological Implications*. Cambridge University Press, Cambridge, 11–23.

McNab BK. 2015. Behavioral and ecological factors account for variation in the mass-independent energy expenditures of endotherms. *Journal of Comparative Physiology B* 185, 1–13.

McNaughton SJ, Georgiadis NJ. 1986. Ecology of African grazing and browsing mammals. *Annual Review of Ecology and Systematics* 17, 39–66.

Mein P. 1990. Updating of MN Zones. In: Lindsay EH, Fahlbusch V, Mein P (Eds.), *European Neogene Mammal Chronology*. Plenum Press, New York, 73–90.

Merceron G, Blondel C, Brunet M, Sen S, Solounias N, Viriot L, Heintz E. 2004. The Late Miocene paleoenvironment of Afghanistan as inferred from dental microwear in artiodactyls. *Palaeogeography, Palaeoclimatology, Palaeoecology* 207, 143–163.

Merceron G, Blondel C, Viriot L, Koufos GD, Bonis L de. 2007. Dental microwear analysis of bovids from the Vallesian (late Miocene) of Axios Valley in Greece: reconstruction of the habitat of *Ouranopithecus macedoniensis* (Primates, Hominoidea). *Geodiversitas* 29, 421–433.

Merceron G, Bonis L de, Viriot L, Blondel C. 2005. Dental microwear of fossil bovids from northern Greece: paleoenvironmental conditions in the eastern Mediterranean during the Messinian. *Palaeogeography, Palaeoclimatology, Palaeoecology* 217, 173–185.

Merceron G, Novello A, Scott RS. 2016a. Paleoenvironments inferred from phytoliths and Dental Microwear Texture Analyses of meso-herbivores. In: Koufos GD, Kostopoulos DS (Eds.), *Palaeontology of the Upper Miocene Vertebrate Localities of Nikiti (Chalkidiki Peninsula, Macedonia, Greece). Geobios* 49, 135–146.

Merceron G, Ramdarshan A, Blondel C, Boisserie J-R, Brunetière N, Francisco A, Gautier D, Milhet X, Novello A, Pret D. 2016b. Untangling the environmental from the dietary: dust does not matter. *Proceedings of the Royal Society B: Biological Sciences* 283, 20161032.

Metcalfe JZ, Longstaffe FJ. 2012. Mammoth tooth enamel growth rates inferred from stable isotope analysis and histology. *Quaternary Research* 77, 424–432.

Mihlbachler MC, Rivals F, Solounias N, Semprebon GM. 2011. Dietary change and evolution of horses in North America. *Science* 331, 1178–1181.

Millar JS, Zammuto RM. 1983. Life histories of mammals: an analysis of life tables. *Ecology* 64, 631–635.

Moehlman PD. 2002. *Equids: Zebras, Asses, and Horses: Status Survey and Conservation Action Plan*. IUCN/SSC Equid Specialist Group, IUCN, Gland, Switzerland and Cambridge, UK.

Moncunill-Solé B, Orlandi-Oliveras G, Jordana X, Rook L, Köhler M. 2016. First approach of the life history of *Prolagus apricenicus* (Ochotonidae, Lagomorpha) from Terre Rosse sites (Gargano, Italy) using body mass estimation and paleohistological analysis. *Comptes Rendus - Palevol* 15, 235–245.

Monfort SL, Arthur NP, Wildt DE. 1994. Reproduction in the Przewalski's horse. In: Boyd L, Houpt KA (Eds.), *Przewalski's Horse: The History and Biology of an Endangered Species*. State University of New York Press, Albany, 173–194.

Monson TA, Hlusko LJ. 2018. Breaking the rules: phylogeny, not life history, explains dental eruption sequence in primates. *American Journal of Physical Anthropology* 167, 217–233.

Montes L, Castanet J, Cubo J. 2010. Relationship between bone growth rate and bone tissue organization in amniotes: first test of Amprino's rule in a phylogenetic context. *Animal Biology* 60, 25–41.

Montoya P, Morales J, Robles F, Abella J, Benavent J V, Marín M. D, Ruiz Sánchez FJ. 2006. Las nuevas excavaciones (1995-2006) en el yacimiento del Mioceno final de Venta del Moro, Valencia. *Estudios Geológicos* 62, 313–326.

Mysterud A, Ostbye E. 1999. Cover as a habitat element for temperate ungulates: effects on habitat selection and demography. *Wildlife Society Bulletin* 27, 385–394.

Nacarino-Meneses C. 2018. *Life History Inferences in Extant and Extinct* Equus *from the Histological Analysis of Bone and Enamel Tissues*. Universitat Autònoma de Barcelona.

Nacarino-Meneses C, Jordana X, Köhler M. 2016a. First approach to bone histology and skeletochronology of *Equus hemionus*. *Comptes Rendus - Palevol* 15, 277–287.

Nacarino-Meneses C, Jordana X, Köhler M. 2016b. Histological variability in the limb bones of the Asiatic wild ass and its significance for life history inferences. *PeerJ* 4, e2580.

Nacarino-Meneses C, Jordana X, Orlandi-Oliveras G, Köhler M. 2017. Reconstructing molar growth from enamel histology in extant and extinct *Equus*. *Scientific Reports* 7, 15965.

Nacarino-Meneses C, Köhler M. 2018. Limb bone histology records birth in mammals. *PLoS ONE* 13, e0198511.

Nacarino-Meneses C, Orlandi-Oliveras G. 2019. The life history of European Middle Pleistocene equids: first insights from bone histology. *Historical Biology*.

Nanci A. 2008. *Ten Cate's Oral Histology: Development, Structure, and Function*. Elsevier, St. Louis, Missouri.

Nelson S V. 2005. Paleoseasonality inferred from equid teeth and intra-tooth isotopic variability. *Palaeogeography, Palaeoclimatology, Palaeoecology* 222, 122–144.

Newman HN, Poole DFG. 1993. Dental enamel growth. *Journal of the Royal Society of Medicine* 86, 61.

Nowak R. 1999. *Walker's Mammals of the World*. John Hopkins University Press, Baltimore and London.

Oakenfull EA, Lim HN, Ryder OA. 2000. A survey of equid mitochondrial DNA: implications for the evolution, genetic diversity and conservation of *Equus*. *Conservation Genetics* 1, 341–355.

Orlandi-Oliveras G, Jordana X, Moncunill-Solé B, Köhler M. 2016. Bone histology of the giant fossil dormouse *Hypnomys onicensis* (Gliridae, Rodentia) from Balearic Islands. *Comptes Rendus - Palevol* 15, 247–253.

Orlando L. 2015. Equids. *Current Biology* 25, 973–978.

Orlando L, Ginolhac A, Zhang G, Froese D, Albrechtsen A, Stiller M, Schubert M, Cappellini E, Petersen B, Moltke I, Johnson PLF, Fumagalli M, Vilstrup JT, Raghavan M, Korneliussen TS, Malaspinas A-S, Vogt J, Szklarczyk D, Kelstrup CD, Vinther J, Dolocan A, Stenderup J, Velazquez AM V., Cahill J, Rasmussen M, Wang X, Min J, Zazula GD, Seguin-Orlando A, Mortensen C, Magnussen K, Thompson JF, Weinstock J, Gregersen K, Røed KH, Eisenmann V, Rubin CJ, Miller DC, Antczak DF, Bertelsen MF, Brunak S, Al-Rasheid KAS, Ryder O, Andersson L, Mundy J, Krogh A, Gilbert MTP, Kjær K, Sicheritz-Ponten T, Jensen LJ, Olsen J V., Hofreiter M, Nielsen R, Shapiro B, Wang J, Willerslev E. 2013. Recalibrating *Equus* evolution using the genome sequence of an early Middle Pleistocene horse. *Nature* 499, 74–78.

Ortiz-Jaureguizar E, Alberdi MT. 2003. El patrón de cambios en la masa corporal de los Hipparionini (Perissodactyla, Equidae) de la Península Ibérica durante el Mioceno superior-Plioceno superior. *Coloquios de Paleontología* 1, 499–509.

Padian K. **2013**. Why study the bone microstructure of fossil tetrapods? In: Padian K, Lamm E-T (Eds.), *Bone Histology of Fossil Tetrapods - Advancing Methods, Analysis, and Interpretation*. University of California Press, Berkeley, 1–11.

Padian K, de Ricqlès AJ, Horner JR. **2001**. Dinosaurian growth rates and bird origins. *Nature* 412, 405–408.

Padian K, Lamm E-T. **2013**. *Bone Histology of Fossil Tetrapods : Advancing Methods, Analysis, and Interpretation*. University of California Press, Berkeley.

Palkovacs EP. **2003**. Explaining adaptive shifts in body size on islands: a life history approach. *Oikos* 103, 37–44.

Palombo MR. **2007**. How can endemic proboscideans help us understand the "island rule"? A case study of Mediterranean islands. *Quaternary International* 169–170, 105–124.

Peabody FE. **1961**. Annual growth zones in living and fossil vertebrates. *Journal of Morphology* 108, 11–62.

Pérez-Barberia FJ, Mutuberria G. **1996**. Teeth eruption pattern in Cantabrian chamois *Rupicapra pyrenaica parva*. *Acta Theriologica* 41, 217–221.

Pesquero MD. **2003**. *Hipparion* del Turoliense superior de Las Casiones (Fosa de Teruel). *Coloquios de Paleontología* Volumen Ex, 511–548.

Pesquero MD, Alberdi MT. **2012**. New evidence of conspecificity between *Hipparion primigenium melendezi* Alberdi, 1974 from Los Valles de Fuentidueña (Segovia) and *Hipparion concudense concudense* Pirlot, 1956 from Concud (Teruel) Spain. *Estudios Geológicos* 68, 247–260.

Pesquero MD, Alberdi MT, Alcalá L. **2006**. New species of *Hipparion* from La Roma 2 (Late Vallesian; Teruel, Spain): a study of the morphological and biometric variability of *Hipparion primigenium*. *Journal of Paleontology* 80, 343–356.

Pesquero MD, Alberdi MT, Alcalá L. **2011**. Remains of *Hipparion* (Equidae, Perissodactyla) from Puente Minero (Teruel Province, Spain) and their implications for the systematics of the Turolian Hipparionini. *Palaeontology* 54, 1303–1321.

Pesquero MD, Alberdi MT, Montoya P. **2007**. *Hipparion* (Equidae, Mammalia) from Venta del Moro (Valencia Province, Spain). *Neues Jahrbuch für Geologie und Paläontologie - Abhandlungen* 243, 273–297.

Pesquero MD, Alcalá L, Fernández-Jalvo Y. **2013**. Taphonomy of the reference Miocene vertebrate mammal site of Cerro de la Garita, Spain. *Lethaia* 46, 378–398.

Peters RH. **1983**. *The Ecological Implications of Body Size*, Cambridge Studies in Ecology. Cambridge University Press, Cambridge.

Pianka ER. **1970**. On r- and K-Selection. *The American Naturalist* 104, 592–597.

Pianka ER. **1974**. *Evolutionary Ecology*. Harper& Row, New York.

Pirinen S. **1995**. Endocrine regulation of craniofacial growth. *Acta Odontologica Scandinavica* 53, 179–185.

Pirlot PL. 1956. Les Formes européennes du genre *Hipparion*. *Memorias y Comunicaciones del Instituto Geológico, Diputación Provincial de Barcelona* 14, 1-121.

Pound MJ, Haywood AM, Salzmann U, Riding JB, Lunt DJ, Hunter SJ. 2011. A Tortonian (Late Miocene, 11.61–7.25 Ma) global vegetation reconstruction. *Palaeogeography, Palaeoclimatology, Palaeoecology* 300, 29–45.

Promislow DEL, Harvey PH. 1990. Living fast and dying young: a comparative analysis of life□ history variation among mammals. *Journal of Zoology* 220, 417–437.

Pueyo EL, Muñoz A, Laplana C, Parés JM. 2016. The Last Appearance Datum of *Hipparion* in Western Europe: magnetostratigraphy along the Pliocene–Pleistocene boundary in the Villarroya Basin (northern Spain). *International Journal of Earth Sciences* 105, 2203–2220.

Qiu Z, Weilong H, Zhihui G. 1987. Chinese hipparionines from the Yushe Basin. *Palaeontologica Sinica* 175, 1–250.

Raia P, Barbera C, Conte M. 2003. The fast life of a dwarfed giant. *Evolutionary Ecology* 17, 293–312.

Raia P, Meiri S. 2006. The island rule in large mammals: paleontology meets ecology. *Evolution; international journal of organic evolution* 60, 1731–1742.

Ramdarshan A, Blondel C, Brunetière N, Francisco A, Gautier D, Surault J, Merceron G. 2016. Seeds, browse, and tooth wear: a sheep perspective. *Ecology and Evolution* 6, 5559–5569.

Ramdarshan A, Blondel C, Gautier D, Surault J, Merceron G. 2017. Overcoming sampling issues in dental tribology: insights from an experimentation on sheep. *Palaeontologia Electronica* 19353, 1–19.

Ramirez-Rozzi F V. 1993. Tooth development in East African *Paranthropus*. *Journal of Human Evolution* 24, 429–454.

Read AF, Harvey PH. 1989. Life history differences among the eutherian radiations. *Journal of Zoology* 219, 329–353.

Rey K, Amiot R, Lécuyer C, Koufos GD, Martineau F, Fourel F, Kostopoulos DS, Merceron G. 2013. Late Miocene climatic and environmental variations in northern Greece inferred from stable isotope compositions (δ18O, δ13C) of equid teeth apatite. *Palaeogeography, Palaeoclimatology, Palaeoecology* 388, 48–57.

Reynolds JD. 2003. Life histories and extinction risk. In: Blackburn TM, Gaston KJ (Eds.), *Macroecology: Concepts and Consequences*. Blackwell Publishing Ltd, Oxford, UK, 195–217.

Reznick DN, Bryant MJ, Bashey F. 2002. r- and K-selection revisited: the role of population regulation in life-history evolution. *Ecology*.

Reznick DN, Butler MJ, Rodd FH, Ross P. 1996. Life-history evolution in guppies (*Poecilia reticulata*) 6. differential mortality as a mechanism for natural selection. *Evolution* 50, 1651-1660.

Ricklefs RE. **1967**. A graphical method of fitting equations to growth curves. *Ecology* 48, 978–983.

Ricklefs RE. **2008**. *The Economy of Nature*, 5th ed. Macmillan, New York.

Risnes S. **1998**. Growth tracks in dental enamel. *Journal of Human Evolution* 35, 331–350.

Roff DA. **1992**. *The Evolution of Life Histories : Theory and Analysis*. Chapman & Hall.

Roff DA. **2002**. *Life History Evolution*. Sinauer Associates.

Romano CO, Pesquero MD, Alberdi MT. **2017**. *Hipparion*: los caballos de Batallones. In: Morales J (Ed.), *La Colina de Los Tigres Dientes de Sable: Los Yacimientos Miocenos Del Cerro de Los Batallones (Torrejón de Velasco, Comunidad de Madrid)*. Museo Arqueológico Regional, Comunidad de Madrid, 427–440.

Rook L, Cirilli O, Bernor RL. **2017**. A late occurring "*Hipparion*" from the middle Villafranchian of Montopoli, Italy (Early Pleistocene; MN16b; ca. 2.5 Ma). *Bollettino della Societa Paleontologica Italiana* 56, 333–339.

RStudio Team. **2016**. RStudio: integrated Development for R. *[Online] RStudio, Inc.*, Boston.

Saarinen JJ. **2009**. *Body Mass Patterns of Eurasian Miocene Large Land Mammals and their Connections to Environment and Climate*. University of Helsinki.

Saarinen JJ, Eronen J, Fortelius M, Seppä H, Lister AM. **2016**. Patterns of diet and body mass of large ungulates from the Pleistocene of Western Europe, and their relation to vegetation. *Palaeontologia Electronica* 19, 1–58.

Salesa MJ, Pesquero MD, Siliceo G, Antón M, Alcalá L, Morales J. **2012**. A rich community of Felidae (Mammalia, Carnivora) from the late Miocene (Turolian, MN 13) site of Las Casiones (Villalba Baja, Teruel, Spain). *Journal of Vertebrate Paleontology* 32, 658–676.

Sand H. **1996**. Life history patterns in female moose (*Alces alces*): the relationship between age, body size, fecundity and environmental conditions. *Oecologia* 106, 212–220.

Sander PM, Andrássy P. **2006**. Lines of arrested growth and long bone histology in Pleistocene large mammals from Germany: what do they tell us about dinosaur physiology? *Palaeontographica A* 277, 143–159.

Sander PM, Mateus O, Laven T, Knötschke N. **2006**. Bone histology indicates insular dwarfism in a new Late Jurassic sauropod dinosaur. *Nature* 441, 739–741.

Sanson GD, Kerr S, Read J. **2017**. Dietary exogenous and endogenous abrasives and tooth wear in African buffalo. *Biosurface and Biotribology* 3, 211–223.

Schneider CA, Rasband WS, Eliceiri KW. **2012**. NIH Image to ImageJ: 25 years of image analysis. *Nature methods* 9, 671–675.

Schultz AH. **1935**. Eruption and decay of the permanent teeth in primates. *American Journal of Physical Anthropology* 19, 489–581.

Schulz E, Calandra I, Kaiser TM. **2010**. Applying tribology to teeth of hoofed mammals. *Scanning* 32, 162–182.

Schulz E, Kaiser TM. 2013. Historical distribution, habitat requirements and feeding ecology of the genus *Equus* (Perissodactyla). *Mammal Review* 43, 111–123.

Schulz E, Piotrowski V, Clauss M, Mau M, Merceron G, Kaiser TM. 2013. Dietary abrasiveness is associated with variability of microwear and dental surface texture in rabbits. *PLoS ONE* 8, e56167.

Schwartz GT, Godfrey LR, Mahoney P. 2007. Inferring primate growth, development and life history from dental microstructure: the case of the extinct Malagasy lemur, *Megaladapis*. In: Bailey SE, Hublin J-J (Eds.), *Dental Perspectives on Human Evolution: State of the Art Research in Dental Paleoanthropology*. Springer, Dordrecht, 147–162.

Schwartz GT, Samonds KE, Godfrey LR, Jungers WL, Simons EL. 2002. Dental microstructure and life history in subfossil Malagasy lemurs. *Proceedings of the National Academy of Sciences of the United States of America* 99, 6124–6129.

Scott JR. 2012. Dental microwear texture analysis of extant African Bovidae. *Mammalia* 76, 157–174.

Scott KM. 1990. Postcranial dimensions of ungulates as predictors of body mass. In: Damuth J, Macfadden BJ (Eds.), *Body Size in Mammalian Paleobiology: Estimation and Biological Implications*. Cambridge University Press, Cambridge, 301–335.

Scott RS, Clavel J, DeMiguel D, Kaya T, Kostopoulos DS, Mayda S, Merceron G. 2013. Ecology of European hipparionines and the diversity of late Miocene hominids in Western Eurasia. In: *14th RCMN Congress Neogene to Quaternary Geological Evolution of Mediterranean, Paratethys and Black Sea, Istanbul*, 262.

Scott RS, Maga M. 2005. Paleoecology of the Akkaşdagı hipparions (Mammalia, Equidae), late Miocene of Turkey. In: Sen S (Ed.), *Geology, Mammals and Environments at Akka□ dagı, Late Miocene of Central Anatolia. Geodiversitas* 27, 809–830.

Scott RS, Teaford MF, Ungar PS. 2012. Dental microwear texture and anthropoid diets. *American Journal of Physical Anthropology* 147, 551–579.

Scott RS, Ungar PS, Bergstrom TS, Brown CA, Childs BE, Teaford MF, Walker A. 2006. Dental microwear texture analysis: technical considerations. *Journal of Human Evolution* 51, 339–349.

Scott RS, Ungar PS, Bergstrom TS, Brown CA, Grine FE, Teaford MF, Walker A. 2005. Dental microwear texture analysis shows within-species diet variability in fossil hominins. *Nature* 436, 693–695.

Secord R, Bloch JI, Chester SGB, Boyer DM, Wood AR, Wing SL, Kraus MJ, McInerney FA, Krigbaum J. 2012. Evolution of the earliest horses driven by climate change in the Paleocene-Eocene Thermal Maximum. *Science* 335, 959–962.

Semprebon GM, Rivals F, Solounias N, Hulbert RC. 2016. Paleodietary reconstruction of fossil horses from the Eocene through Pleistocene of North America. *Palaeogeography, Palaeoclimatology, Palaeoecology* 442, 110–127.

Sen S. 1990. *Hipparion* Datum and its Chronologic Evidence in the Mediterranean Area. In: Lindsay EH, Fahlbusch V, Mein P (Eds.), *European Neogene Mammal Chronology*. Plenum Press, New York, 495–505.

Sharp ZD, Cerling TE. 1998. Fossil isotope records of seasonal climate and ecology: straight from the horse's mouth. *Geology* 26, 219–222.

Shellis RP. 1984. Variations in growth of the enamel crown in human teeth and a possible relationship between growth and enamel structure. *Archives of Oral Biology* 29, 697–705.

Shoemaker L, Clauset A. 2014. Body mass evolution and diversification within horses (family Equidae). *Ecology Letters* 17, 211–220.

Shotwell JA. 1961. Late Tertiary biogeography of horses in the northern Great Basin. *Journal of Paleontology* 35, 203–217.

Sibly RM, Brown JH. 2007. Effects of body size and lifestyle on evolution of mammal life histories. *Proceedings of the National Academy of Sciences* 104, 17707–17712.

Silver IA. 1969. The ageing of domestic animals. In: Brothweel D, Higgs E (Eds.), *Science in Archaeology*. New York, 250–268.

Simpson GG. 1951. *Horses. The Story of the Horse Family in the Modern World and Through Sixty Million Years of History.* Oxford University Press, New York.

Simpson GG. 1953. *Major Features of Evolution*. Columbia University Press, New York.

Sinclair ARE, Norton-Griffiths M. 1979. *Serengeti: Dynamics of an Ecosystem*. University of Chicago Press, Chicago, Illinois.

Skinner MF, MacFadden BJ. 1977. *Cormohipparion* n. gen. (Mammalia, Equidae) from the North American Miocene (Barstovian–Clarendonian). *Journal of Paleontology* 51, 912–926.

Skogland T. 1983. The effects of density dependent resource limitation on size of wild reindeer. *Oecologia* 60, 156–168.

Skogland T. 1985. The effects of density-dependent resource limitations on the demography of wild reindeer. *The Journal of Animal Ecology* 54, 359–374.

Skogland T. 1988. Tooth wear by food limitation and its life history consequences in wild reindeer. *Oikos* 51, 238–242.

Smith BH. 1989. Dental development as a measure of life history in primates. *Evolution* 43, 683–688.

Smith BH. 1991a. Age of weaning approximates age of emergence of the first permanent molar in nonhuman primates. *American Journal of Physical Anthropology* 34, 163–164.

Smith BH. 1991b. Dental development and the evolution of life history in Hominidae. *American Journal of Physical Anthropology* 86, 157–174.

Smith BH. **1994**. Sequence of emergence of the permanent teeth in *Macaca*, *Pan*, *Homo*, and *Australopithecus*: its evolutionary significance. *American Journal of Human Biology* 6, 61–76.

Smith BH. **2000**. 'Schultz's Rule' and the evolution of tooth emergence and replacement patterns in primates and ungulates. In: Teaford MF, Meredith Smith M, Ferguson MWJ (Eds.), *Development, Function and Evolution of Teeth*. Cambridge University Press, Cambridge, 212–228.

Smith TM. **2006**. Experimental determination of the periodicity of incremental features in enamel. *Journal of Anatomy* 208, 99–113.

Smith TM. **2008**. Incremental dental development: methods and applications in hominoid evolutionary studies. *Journal of Human Evolution* 54, 205–224.

Smith TM, Reid DJ, Dean MC, Olejniczak AJ, Martin LB. **2007**. Molar development in common chimpanzees (*Pan troglodytes*). *Journal of Human Evolution* 52, 201–216.

Smith TM, Tafforeau P, Reid DJ, Pouech J, Lazzari V, Zermeno JP, Guatelli-Steinberg D, Olejniczak AJ, Hoffman A, Radovcic J, Makaremi M, Toussaint M, Stringer C, Hublin J-J. **2010**. Dental evidence for ontogenetic differences between modern humans and Neanderthals. *Proceedings of the National Academy of Sciences* 107, 20923–20928.

Smuts GL. **1974**. Age determination in Burchell's zebra (*Equus burchelli antiquorum*) from the Kruger National Park. *South African Journal of Wildlife Research* 4, 103–115.

Smuts GL. **1975**. Pre-and postnatal growth phenomena of Burchell's Zebra *Equus burchelli antiquorum*. *Koedoe* 18, 69–102.

Smuts GL. **1976a**. Reproduction in the zebra mare *Equus burchelli antiquorum* from the Kruger National Park. *Koedoe* 19, 89–132.

Smuts GL. **1976b**. Reproduction in the zebra stallion *Equus burchelli antiquorum* from the Kruger National Park South Africa. *Zoologica Africana* 11, 207–220.

Solounias N, Rivals F, Semprebon GM. **2010**. Dietary interpretation and paleoecology of herbivores from Pikermi and Samos (late Miocene of Greece). *Paleobiology* 36, 113–136.

Solounias N, Semprebon GM. **2002**. Advances in the reconstruction of ungulate ecomorphology with application to early fossil equids. *American Museum Novitates* 3366, 1–49.

Solounias N, Teaford MF, Walker A. **1988**. Interpreting the diet of extinct ruminants: the case of a non-browsing giraffid. *Paleobiology* 14, 287–300.

Sondaar PY. **1961**. Les *Hipparion* de l'Aragon meridional. *Estudios Geológicos* 17, 209–305.

Sondaar PY. **1977**. Insularity and its effect on mammal evolution. In: *Major Patterns of Vertebrate Evolution*. Springer US, Boston, 671–707.

Southwood TRE. **1988**. Tactics, strategies and templets. *Oikos* 52, 3–18.

Stanley S. **1973**. An explanation for Cope's Rule. *Evolution* 27, 1–26.

Stearns SC. **1983**. The influence of size and phylogeny on patterns of covariation among life-history traits in the mammals. *Oikos* 41, 173-187.

Stearns SC. **1992**. *The Evolution of Life Histories*. Oxford University Press, New York.

Stearns SC. 2000. Life history evolution: successes, limitations, and prospects. *Naturwissenschaften* 87, 476-486.

Stearns SC, Ackermann M, Doebeli M, Kaiser M. 2000. Experimental evolution of aging, growth, and reproduction in fruitflies. *Proceedings of the National Academy of Sciences* 97, 3309–3313.

Stearns SC, Koella JC. 1986. The evolution of phenotypic plasticity in life-history traits: predictions of reaction norms for age and size at maturity. *Evolution* 40, 893-913.

Stebbins GL. 1981. Coevolution of grasses and herbivores. *Annals of the Missouri Botanical Garden* 68, 75–86.

Steiner CC, Ryder OA. 2011. Molecular phylogeny and evolution of the Perissodactyla. *Zoological Journal of the Linnean Society* 163, 1289–1303.

Stirton RA. 1947. Observations on evolutionary rates in hypsodonty. *Evolution* 1, 32–41.

Stover SM, Pool RR, Martin RB, Morgan JP. 1992. Histological features of the dorsal cortex of the third metacarpal bone mid-diaphysis during postnatal growth in thoroughbred horses. *Journal of anatomy* 181, 455–469.

Strand E, Braathen LC, Hellsten MC, Huse-Olsen L, Bjornsdottir S. 2007. Radiographic closure time of appendicular growth plates in the Icelandic horse. *Acta Veterinaria Scandinavica* 49, 19.

Strömberg CAE, Werdelin L, Friis EM, Saraç G. 2007. The spread of grass-dominated habitats in Turkey and surrounding areas during the Cenozoic: phytolith evidence. *Palaeogeography, Palaeoclimatology, Palaeoecology* 250, 18–49.

Symons AL, Seymour GJ. 2000. A histological study of the effect of growth hormone on odontogenesis in the Lewis dwarf rat. *Archives of Oral Biology* 45, 123–131.

Tacutu R, Thornton D, Johnson E, Budovsky A, Barardo D, Craig T, Diana E, Lehmann G, Toren D, Wang J, Fraifeld VE, De Magalhães JP. 2018. Human ageing genomic resources: new and updated databases. *Nucleic Acids Research* 46, 1083–1090.

Tafforeau P, Bentaleb I, Jaeger J-J, Martin C. 2007. Nature of laminations and mineralization in rhinoceros enamel using histology and X-ray synchrotron microtomography: potential implications for palaeoenvironmental isotopic studies. *Palaeogeography, Palaeoclimatology, Palaeoecology* 246, 206–227.

Teaford MF. 1988. Scanning electron microscope diagnosis of wear patterns versus artifacts on fossil teeth. *Scanning microscopy* 2, 1167–1175.

Teaford MF, Oyen OJ. 1989. In vivo and in vitro turnover in dental microwear. *American Journal of Physical Anthropology* 80, 447–460.

Teaford MF, Ungar PS, Taylor AB, Ross CF, Vinyard CJ. 2017. In vivo rates of dental microwear formation in laboratory primates fed different food items. *Biosurface and Biotribology* 3, 166–173.

Thaker M, Vanak AT, Owen CR, Ogden MB, Slotow R. 2010. Group dynamics of zebra and wildebeest in a woodland savanna: effects of predation risk and habitat density. *PLoS ONE* 5, e12758.

Thesleff I. 1995. Differentiation of ameloblasts and its regulation by epithelial-mesenchymal interactions. In: Robinson C, Kirkham J, Shore R (Eds.), *Dental Enamel, Formation to Destruction*. CRC Press, Boca Raton, 23–57.

Tipple BJ, Pagani M. 2007. The early origins of terrestrial C_4 photosynthesis. *Annual Review of Earth and Planetary Sciences* 35, 435–461.

Tomàs M, Alba DM, Sanisidro Ó, Bolet A. 2010. Los perisodáctilos del Mioceno superior de la autovía orbital de Barcelona B-40, tramo Olesa de Montserrat - Viladecavalls (Cuenca del Vallès-Penedès). *Cidaris* 30, 317–323.

Turner-Walker G, Mays S. 2008. Histological Studies on Ancient Bone. In: *Advances in Human Palaeopathology*. John Wiley & Sons, Ltd, Chichester, 121–146.

Tütken T, Kaiser TM, Vennemann T, Merceron G. 2013. Opportunistic feeding strategy for the earliest Old World hypsodont equids: evidence from stable isotope and dental wear proxies. *PloS ONE* 8, e74463.

Ungar PS. 1996. Dental microwear of European Miocene catarrhines: evidence for diets and tooth use. *Journal of Human Evolution* 31, 335–366.

Ungar PS, Brown CA, Bergstrom TS, Walker A. 2003. Quantification of dental microwear by tandem scanning confocal microscopy and scale-sensitive fractal analyses. *Scanning* 25, 185–193.

Ungar PS, Merceron G, Scott RS. 2007. Dental microwear texture analysis of Varswater bovids and early Pliocene paleoenvironments of Langebaanweg, Western Cape Province, South Africa. *Journal of Mammalian Evolution* 14, 163–181.

Van Dam J. 2006. Geographic and temporal patterns in the late Neogene (12-3 Ma) aridification of Europe: the use of small mammals as paleoprecipitation proxies. *Palaeogeography, Palaeoclimatology, Palaeoecology* 238, 190–218.

Van Dam J, Alcalá L, Zarza AA, Calvo JP, Garcés M, Krijgsman W. 2001. The upper Miocene mammal record from the Teruel-Alfambra region (Spain). The MN system and continental stage/age concepts discussed. *Journal of Vertebrate Paleontology* 21, 367–385.

Van Dam J, Reichart GJ. 2009. Oxygen and carbon isotope signatures in late Neogene horse teeth from Spain and application as temperature and seasonality proxies. *Palaeogeography, Palaeoclimatology, Palaeoecology* 274, 64–81.

Van Valen L. 1964. Age in two fossil horse populations. *Acta Zoologica* 45, 93–106.

Van Valen LM. 1973. Pattern and the balance of nature. *Evolutionary Theory* 1, 31–49.

Vandeberg JR, Buschang PH, Hinton RJ. 2004. Craniofacial growth in growth hormone-deficient rats. *Anatomical Record - Part A Discoveries in Molecular, Cellular, and Evolutionary Biology* 278, 561–570.

Veiberg V, Mysterud A, Bjørkvoll E, Langvatn R, Loe LE, Irvine RJ, Bonenfant C, Couweleers F, Stenseth NC. 2007a. Evidence for a trade-off between early growth and tooth wear in Svalbard reindeer. *Journal of Animal Ecology* 76, 1139–1148.

Veiberg V, Mysterud A, Gaillard JM, Delorme D, Van Laere G, Klein F. 2007b. Bigger teeth for longer life? Longevity and molar height in two roe deer populations. *Biology Letters* 3, 268–270.

Veitschegger K, Sánchez-Villagra MR. 2016. Tooth eruption sequences in cervids and the effect of morphology, life history, and phylogeny. *Journal of Mammalian Evolution* 23, 251–263.

Vlachou TD. 2013. *Palaeontological, Biostratigraphical and Palaeoecological Study of the Greek Hipparions*. Aristotle University of Thessaloniki.

Vlachou TD, Koufos GD. 2009. Equidae. In: Koufos GD, Nagel D (Eds.), *The Late Miocene Mammal Faunas of the Mytilinii Basin, Samos Island, Greece: New Collection. Beiträge Zur Paläontologie* 31, 207–281.

Voorhies MR. 1969. *Taphonomy and Population Dynamics of an Early Pliocene Vertebrate Fauna, Knox County, Nebraska*. University of Wyoming.

Walker A, Hoeck HN, Perez L. 1978. Microwear of mammalian teeth as an indicator of diet. *Science* 201, 908–910.

Wang L, D'Odorico P, Ries L, Macko SA. 2010. Patterns and implications of plant-soil δ13C and δ15N values in African savanna ecosystems. *Quaternary Research* 73, 77–83.

Weiner S, Wagner HD. 1998. The material bone: structure-mechanical function relations. *Annual Review of Materials Science* 28, 271–298.

Westoby M, Leishman MR, Lord JM. 1995. Further remarks on phylogenetic correction. *Journal of Ecoloy* 83, 727–730.

Winkler DE, Schulz E, Calandra I, Gailer JP, Landwehr C, Kaiser TM. 2013. Indications for a dietary change in the extinct Bovid genus *Myotragus* (Plio-Holocene, Mallorca, Spain). *Geobios* 46, 143–150.

Witzel C, Kierdorf U, Frölich K, Kierdorf H. 2018. The pay-off of hypsodonty - timing and dynamics of crown growth and wear in molars of Soay sheep. *BMC Evolutionary Biology* 18, 207.

Wolf D, Semprebon GM, Bernor RL. 2012. New observations on the paleodiet of the late Miocene Höwenegg (Hegau, Germany) *Hippotherium primigenium* (Mammalia, Equidae). *Bollettino della Societa Paleontologica Italiana* 51, 185–191.

Wolverton S, Huston MA, Kennedy JH, Cagle K, Cornelius JD. 2009. Conformation to Bergmann's rule in white-tailed deer can be explained by food availability. *The American Midland Naturalist* 162, 403–417.

Woodburne MO. 1989. *Hipparion* horses: a pattern of endemic evolution and intercontinental dispersal. In: Prothero DR, Schoch RM (Eds.), *The Evolution of Perissodactyls*. Oxford University Press, New York, 197–233.

Woodburne MO. 2007. Phyletic diversification of the *Cormohipparion occidentale* complex (Mammalia; Perissodactyla, Equidae), Late Miocene, North America, and the origin of the Old World *Hippotherium* datum. *Bulletin of the American Museum of Natural History* 306, 1–138.

Woodburne MO. 2009. The early Vallesian vertebrates of Atzelsdorf (Late Miocene, Austria). 9. *Hippotherium* (Mammalia, Equidae). *Annalen des Naturhistorischen Museums in Wien. Serie A* 111, 585–604.

Woodburne MO, Bernor RL. 1980. On superspecific groups of some Old World hipparionine horses. *Journal of Paleontology* 54, 1319–1348.

Woodburne MO, MacFadden BJ. 1982. A reappraisal of the systematics, biogeography, and evolution of fossil horses. *Paleobiology* 8, 315–327.

Woodward HN, Freedman Fowler EA, Farlow JO, Horner JR. 2015. *Maiasaura*, a model organism for extinct vertebrate population biology: a large sample statistical assessment of growth dynamics and survivorship. *Paleobiology* 41, 1–25.

Woodward HN, Horner JR, Farlow JO. 2014. Quantification of intraskeletal histovariability in *Alligator mississippiensis* and implications for vertebrate osteohistology. *PeerJ* 2, e422.

Woodward HN, Padian K, Lee AH. 2013. Skeletochronology. In: Padian K, Lamm E-T (Eds.), *Bone Histology of Fossil Tetrapods - Advancing Methods, Analysis, and Interpretation*. University of California Press, Berkeley, 195–216.

Young WG. 1995. Growth hormone and insulin-like growth factor-I in odontogenesis. *The International Journal of Developmental Biology* 39, 263–272.

Zullinger EM, Ricklefs RE, Redford KH, Mace GM. 1984. Fitting sigmoidal equations to mammalian growth curves. *Journal of Mammalogy* 65, 607–636.

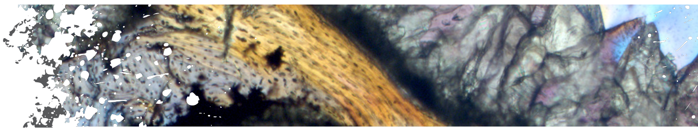

Chapter 10

Agraïments

Chapter 10

Agraïments

Aquesta tesi ha estat realitzada gràcies al programa d'ajudes per a la contractació de personal investigador novell FI-DGR (Agència de Gestió d'Ajuts Universitaris i de Recerca, Generalitat de Catalunya, 2016FI_B00202). El seu desenvolupament també ha estat finançat pel projecte "Evolution of mammalian life history in continental Iberian ecosystems from the Miocene to Pleistocene: correlation with climatic changes*"* (Ministeri d'Economia i Competitivitat, CGL2015-63777) i pel grup de recerca "Paleoecologia i ecologia evolutiva" (Generalitat de Catalunya, 2014-SGR-1207). L'estada al PALEVOPRIM (Laboratoire Paléontologie Evolution Paléoécosystèmes Paléoprimatologie, Université de Poitiers) va estar en part subvencionada pel Programa Erasmus + Doctorat.

En primer lloc, vull agrair a la meva directora, la Dra. Meike Köhler, tot l'esforç i dedicació bolcats en aquesta tesi. Moltes gràcies per haver-me guiat des de la finalització del Grau fins avui, a punt de dipositar la Tesi Doctoral, en la meva tasca com a investigador. Estic agraït per haver-me fet un lloc en el Departament de Paleobiologia Evolutiva de l'Institut Català de Paleontologia (ICP) on he pogut créixer científicament i completar aquesta etapa. En el sentit més acadèmic, vull agrair també a la Dra. Carmen Nacarino-Meneses la seva tasca en l'estudi de la histologia d'èquids actuals, la qual ha servit de referent per estudiar els teixits fossilitzats dels hipparionins, com també el seu suport durant aquests anys de treball. M'agradaria, a més, reconèixer el seu paper com a coautora d'articles que conformen aquesta tesi, conjuntament amb el de la meva directora Dra. Meike Köhler, i el d'altres investigadors d'institucions estrangeres: Dr. George D. Koufos, Dr. Gildas Merceron, Dr. Julien Clavel, Dr. Robert S. Scott, Dr. Serdar Mayda i Dra. Tanju Kaya. A part dels comentaris i correccions dels coautors, vull agrair aquells dels revisors que de forma desinteressada han dedicat un temps per millorar la qualitat dels articles, en especial al Dr. Timothy G. Bromage i al Dr. Juha Saarinen. D'igual manera, també agrair els comentaris dels editors de les revistes: Dr. Howard Falcon-Lang, Dr. Thomas Algeo i Dr. Yasuyuki Nakamura. Als ja mencionats

Dra. Carmen Nacarino-Meneses i Dr. Gildas Merceron, els hi vull donar de nou les gràcies per fer els informes necessaris per a l'obtenció de la Menció de Doctorat Internacional.

M'agradaria mostrar el meu agraïment als investigadors i conservadors a càrrec de les col·leccions paleontològiques i osteològiques d'on prové el material aquí estudiat: Dr. David M. Alba, Dr. Salvador Moyà-Solà, Marta Soteras i Jordi Galindo pel permís d'analitzar fòssils del Museu de l'ICP (i al Manel Méndez per fer-me'ls arribar!), Dr. George D. Koufos i Dr. Dimitris S. Kostopoulos de l'Aristotle University of Thessaloniki, Dr. Javier Quesada del Museu de Ciències Naturals de Barcelona, Dr. Benjamin Lamglait de la Réserve Africaine de Sigean, Dr. Thomas Kaiser del Zoologisches Museum (Universität Hamburg) i Dra. Renate Schafberg del Museum für Haustierkunde (Martin-Luther-Universität Halle-Wittenberg). També agrair al Dr. Gildas Merceron per haver-me donat accés a la col·lecció de motlles dentals del PALEVOPRIM. Per acabar, vull donar gràcies als encarregats de preparar i/o replicar tot aquest material i permetre'n així el seu estudi: Gemma Prats, Luis Gordón i les tècniques de restauració de l'ICP. Però en especial, vull agrair la tasca del Manuel Fernández que gràcies a la seva paciència, interès i destresa ha produït unes excel·lents làmines primes.

De la Universitat Autònoma de Barcelona, vull primerament reconèixer l'ajut durant tots els tràmits acadèmics de la Dra. Assumpció Malgosa com a coordinadora del Programa de Doctorat en Biodiversitat. També vull fer especial menció al Dr. Xavier Jordana per haver-me assessorat durant els primers mesos del doctorat i instruït en l'estudi de la histologia dental. Finalment, donar les gràcies al Dr. Emmanuel Serrano, Dra. Iolanda Álvarez i Dra. Maria Constenla per la seva tasca com a membres del comitè de seguiment de doctorat.

Recordant les visites a l'estranger, vull agrair un altre cop al Gildas el seu paper com a responsable de la meva estada al laboratori PALEVOPRIM. Gràcies per ensenyar-me la tècnica de l'anàlisi de la textura del microdesgast i resoldre els dubtes que m'han anat sorgit. Moltes gràcies també als amics i companys que em van fer sentir un més allí: Christopher, Laurent, Emilie, Jeremie, Baptiste, a l'Auria per totes les llargues converses sense sentit per correu electrònic, i a la Marion i al Florian per haver compartit tantes inquietuds, dubtes i cafès durant aquells tres mesos. Del Florian, a més, reconèixer la seva total disponibilitat i ajut amb les anàlisis de microsdesgast. Voldria també agrair al Dani i a la Flavia pels moments que vam compartir junts per Poitiers. Canviant de banda del Mediterrani (com els hipparionins protagonistes de la tesi), vull donar les gràcies als investigadors de l'Aristotle University of Thessaloniki, Dr. George D. Koufos, Dra. Theodora Vlachou i Dr. Dimitris S. Kostopoulos, per obrir-me les portes del Laboratory of Geology and Palaeontology i ajudar-me amb la identificació dels espècimens. Agrair també a la Krystalia per acollir-me, transportar-me (com a una pizza) i ensenyar-me la ciutat de Tessalònica; i al Ioannis pels dinars plegats i les llargues converses de despatx.

Un apartat especial mereixen totes les persones amb les que he coincidit a l'ICP, aquelles que d'una manera o d'altra m'han ajudat a tirar endavant aquesta tesi. Agrair al Salvador i al David la seva tasca com directors d'aquesta institució. Al Pere, Enric i Josep, per ajudar-me sempre que els he necessitat. A les restauradores, Xènia, Marta, Núria i Marina; per deixar-me tafanejar els fòssils durant les meves visites al pis de dalt. Als investigadors que m'han resolt dubtes i amb els qui he compartit bones estones: la Judit, l'Arnau, el Madu, el Fortu, el Marc, l'Isaac, el Vaqui, la Sole i el Juan. D'aquests, vull agrair també al Madu la confiança depositada en mi durant les seves campanyes d'excavació. Donar gràcies a la Maria, a qui trobo molt a faltar i espero veure aviat, per totes les nostres converses i tes compartits (i els milions d'euros que li dec de la subscripció de Netflix). Encara que no pugui gaudir a diari de la seva companyia, vull agrair totes les rialles que el Raef (amb els seus espectaculars "*tocados*") i el Joan (amb les seves paraules inventades) aportaven al meu dia a dia. També m'agradaria mostrar la meva gratitud a la Pepi i a la Sónia, per la seva tasca i pel somriure i salut que intercanviem cada dia.

Menció especial mereixen, d'igual forma, tots els pre-docs o estudiants amb els qui he compartit moments dins i fora de l'ICP: l'Ale (i la seva cafetera donadora de vida), la Sílvia, el Leonardo (aka el Sorba), el Rafel, la Maria, el Víctor de les hienes i el Víctor dels dinos, el Florian (aka Antoine), la Sharrah, l'Eudald, el Chabi, i el Steven. Agrair al meu alter ego barbut Guillem Pe el seu seriós i relaxant tarannà, juntament amb la seva entera disponibilitat. Destacar també l'ajut que m'han brindat les meves companyes (presents i passades) de departament, la Blanca, la Carmen i la Teresa, per sempre estar allí quan les he necessitat. A la Teresa, vull agrair-li especialment el seu suport durant aquests darrers mesos de tesi. Moltes gràcies per les visites reclamant xocolata i organitzant (i posteriorment recordant) l'escapada al Kruger. Del mateix departament, però situat en les altures, vull donar-li les gràcies al Manu per les calçotades a Castellar. Finalment, dels ja esmentats, m'agradaria reconèixer la tasca del Leonardo per haver fet la imatge de portada (seguint les delirants idees d'un Guillem amb una tesi per finalitzar) i de la Blanca per l'excel·lent maquetació. Segur que em deixo algú, ja que són tants els qui han aportat un gra de sorra en aquesta tesi... Espero que no m'ho tingui en compte, ja que el temps corre i encara he de fer les darreres correccions. De fora de l'ICP, però, no puc oblidar-me de l'Andrea (i les seves fotografies de coloms) ni de l'Isaac (el meu gironí preferit). També, d'entre les esferes de la paleontologia, vull donar gràcies al Juan Benito per totes les nostres conversacions i els nombrosos cops de mà.

D'igual manera, m'agradaria mostrar la meva gratitud a les persones que, lluny dels ambients paleontològics i acadèmics, m'han fet costat durant aquests anys de tesi. Gràcies als meus amics per interessar-se en el que faig i intentar entendre l'objectiu de tot això. Gràcies per considerar-me un expert "gerontòleg", ferm llepador de pedres, i un estudiós dels dits de cavall. D'entre ells, reconèixer l'ajut de l'Albert amb les corbes i funcions matemàtiques, i la seva companyia en passejades “de gos”. Destacar també el Joan, qui sempre s’ha interessat en el desenvolupament de la tesi i ha trobat un moment per revisar textos i donar la seva valuosa opinió. A ell, li vull agrair tot el suport rebut i transmetre-li molta força per al camí que ha decidit emprendre.

A la meva família, a qui tant ha costat entendre en que consistia tot això del doctorat (part de culpa tindré jo i la meva reduïda capacitat comunicativa), m’agradaria agrair-li la seva comprensió i estima. Donar les gràcies (o retreure?) al meu pare per inculcar-me la passió per la paleontologia, i a la meva mare per preocupar-se i preguntar sempre com va tot. Vull també mencionar al meu germà, avis, tiets i cosines pel seu interès i ajut. No puc tancar aquest apartat, però, sense agrair el paper que han tingut els pares de la Vero durant tots aquests anys, moltes gràcies per haver estat família.

Per acabar, vull reservar aquest espai a la Vero, la persona que m’ha acompanyat de més a prop durant tota aquesta etapa. Moltes gràcies per haver-me aconsellat, animat i donat un cop de mà sempre que ho he requerit. Moltíssimes gràcies per creure sempre en mi i les meves capacitats, per haver estat, en els moments més difícils, el suport que necessitava.